

**Characterisation of New Platinum Complexes  
as Possible Intermediates in the  
Methoxycarbonylation of Ethene**



**THE UNIVERSITY  
*of* LIVERPOOL**

Thesis submitted in accordance with the requirements of  
the University of Liverpool for the degree of Doctor in  
Philosophy by Joanna Wołowska

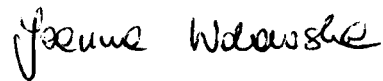
Department of Chemistry

October 2002

## **Declaration**

I declare that, except otherwise stated, the work contained within this thesis in my own research, carried out from October 1999 until September 2002 at the Department of Chemistry, University of Liverpool.

**Signed**

A handwritten signature in black ink, appearing to read 'Joanna Wolowska', written in a cursive style.

Joanna Wolowska

## Abstract

This thesis is concerned with the NMR spectroscopic studies of the mechanistic aspects involved in the methoxycarbonylation of ethene promoted by a catalytic system based on  $[\text{Pt}(\text{d}^{\text{t}}\text{bpx})(\text{dba})]$  and  $\text{RSO}_3\text{H}$  ( $\text{R} = \text{CF}_3, \text{CH}_3$ ).

Chapter one surveys the literature of the reactions between carbon monoxide and ethene, with particular regards to the recent synthesis of polyketones developed by Shell and the synthesis of MeP developed by Lucent International. NMR spectroscopic studies of the catalytic process for the methoxycarbonylation of ethene promoted by  $[\text{Pd}(\text{d}^{\text{t}}\text{bpx})(\text{dba})]$  are described. More recent catalytic mechanistic studies based on a platinum catalyst are illustrated.

Chapter two describes the NMR characterisation of the starting material  $[\text{Pt}(\text{d}^{\text{t}}\text{bpx})(\text{dba})]$  in THF at 293 and 193 K.

Chapter three describes the reactivity of  $[\text{Pt}(\text{d}^{\text{t}}\text{bpx})(\text{dba})]$  with  $\text{RSO}_3\text{H}$  ( $\text{R} = \text{CF}_3, \text{CH}_3$ ) in MeOH.  $[\text{Pt}(\text{d}^{\text{t}}\text{bpx})(\text{dbaH})]^+$  is formed after the addition of either acids, but the products formed from further reaction with  $\text{O}_2$  or BQ, depend on the acid used for the protonation.  $[\text{Pt}(\text{d}^{\text{t}}\text{bpx})\text{H}(\text{MeOH})][\text{CF}_3\text{SO}_3]$  is formed in the  $\text{CF}_3\text{SO}_3\text{H}$ -system, whereas,  $[\text{Pt}(\text{d}^{\text{t}}\text{bpx})(\eta^2\text{-CH}_3\text{SO}_3)][\text{CH}_3\text{SO}_3]$  is formed in the  $\text{CH}_3\text{SO}_3\text{H}$ -system.

Chapter four describes the reactivity of  $[\text{Pt}(\text{d}^{\text{t}}\text{bpx})\text{H}(\text{MeOH})][\text{RSO}_3]$  ( $\text{R} = \text{CF}_3, \text{CH}_3$ ) with  $\text{C}_2\text{H}_4$  at different temperatures in MeOH and in  $\text{CH}_2\text{Cl}_2$ . The main product formed is  $[\text{Pt}(\text{d}^{\text{t}}\text{bpx})(\text{CH}_2\text{CH}_3)]^+$  and its variable temperature dynamic behaviour is analysed.

Chapter five describes the reactivity of  $[\text{Pt}(\text{d}^{\text{t}}\text{bpx})(\text{CH}_2\text{CH}_3)]^+$  with CO.  $[\text{Pt}(\text{d}^{\text{t}}\text{bpx})\text{H}(\text{CO})]^+$  is formed during the reaction of the platinum ethyl complex in MeOH at 293 and 193 K. Two intermediates can be observed in the reaction of  $[\text{Pt}(\text{d}^{\text{t}}\text{bpx})(\text{CH}_2\text{CH}_3)]^+$  with  $^{13}\text{CO}$  in  $\text{CH}_2\text{Cl}_2$ . At 193 K  $[\text{Pt}(\text{d}^{\text{t}}\text{bpx})(\text{C}_2\text{H}_5)(^{13}\text{CO})]^+$  is formed, by warming the same solution to 293 K in the presence of excess CO;  $[\text{Pt}(\text{d}^{\text{t}}\text{bpx})(^{13}\text{C}(\text{O})\text{C}_2\text{H}_5)(^{13}\text{CO})]^+$  is the main product. The reactivity of  $[\text{Pt}(\text{d}^{\text{t}}\text{bpx})(\text{C}_2\text{H}_5)(^{13}\text{CO})]^+$  and  $[\text{Pt}(\text{d}^{\text{t}}\text{bpx})(^{13}\text{C}(\text{O})\text{C}_2\text{H}_5)(^{13}\text{CO})]^+$  with  $\text{PPh}_3$  is illustrated.

Chapter six describes the reactivity and the dynamic behaviour of the main products characterised in the previous chapters at high temperature (293 K–353 K) under  $\text{N}_2$ ,  $\text{C}_2\text{H}_4$ ,  $^{13}\text{CO}$  and the gas mixture  $\text{C}_2\text{H}_4/\text{CO}$  (1/1, 9/1) at high pressure, performed in a sapphire tube and conventional autoclave.

Chapter seven contains general conclusions about the mechanistic aspects of the catalytic process. Some major differences between the platinum and palladium catalysts are described.

# Contents

<b>1. Introduction .....</b>	<b>2</b>
1.1. The reactions between carbon monoxide and ethene.....	2
1.2. The Shell Process .....	4
1.2.1 Formation of Polyketones .....	5
1.2.2 Formation of Methyl Propanoate .....	8
1.3. The Lucite Process .....	9
1.4. Mechanistic studies of the methoxycarbonylation of ethene promoted by the palladium catalyst $[\text{Pd}(\text{d}^t\text{bpx})(\text{dba})]$ .....	10
1.4.1 Formation of $[\text{Pd}(\text{d}^t\text{bpx})\text{H}(\text{MeOH})]^+$ , A .....	11
1.4.2 Formation of $[\text{Pd}(\text{d}^t\text{bpx})(\text{CH}_2\text{CH}_3)]^+$ , B .....	14
1.4.3 Formation of $[\text{Pd}(\text{d}^t\text{bpx})(\text{C}(\text{O})\text{C}_2\text{H}_5)(\text{THF})]^+$ , C <sup>39</sup> .....	15
1.5. Heavier Platinum Metals as Catalysts.....	16
1.5.1 Hydroformylation of olefins .....	17
1.5.2 Platinum(II) complexes as Lewis Acids .....	20
1.6. The aim of this thesis .....	25
1.7. References .....	26
<b>2. Characterisation of <math>[\text{Pt}(\text{d}^t\text{bpx})(\text{dba})]</math> .....</b>	<b>32</b>
2.1. Introduction .....	32
2.2. Characterisation of $[\text{Pt}(\text{d}^t\text{bpx})(\text{dba})]$ , 1 .....	36
2.3. Dynamic NMR studies of $[\text{Pt}(\text{d}^t\text{bpx})(\text{dba})]$ , 1 .....	41
2.4. References .....	44

<b>3.</b>	<b>Reactivity of [Pt(d<sup>4</sup>bpx)(dba)] with acids .....</b>	<b>47</b>
3.1.	The CF <sub>3</sub> SO <sub>3</sub> H-system.....	47
3.1.1.	Protonation of [Pt(d <sup>4</sup> bpx)(dba)], 1 .....	47
3.1.2.	Oxidation of [Pt(d <sup>4</sup> bpx)(dbaH)][CF <sub>3</sub> SO <sub>3</sub> ], 2a.....	51
3.1.3.	On the formation of the platinum hydride complex.....	55
3.1.4.	Crystal structure of [Pt(d <sup>4</sup> bpx)(H <sub>2</sub> O) <sub>2</sub> ][CF <sub>3</sub> SO <sub>3</sub> ] <sub>2</sub> , 4a.....	58
3.2.	The CH <sub>3</sub> SO <sub>3</sub> H-system .....	62
3.2.1.	Protonation of [Pt(d <sup>4</sup> bpx)(dba)], 1 .....	62
3.2.2.	Oxidation of [Pt(d <sup>4</sup> bpx)(dbaH)][CH <sub>3</sub> SO <sub>3</sub> ], 2b.....	63
3.2.3.	Reactivity of [Pt(d <sup>4</sup> bpx)(η <sup>2</sup> -CH <sub>3</sub> SO <sub>3</sub> )][CH <sub>3</sub> SO <sub>3</sub> ], 5b, with water... 70	
3.3.	Conclusions .....	72
3.4.	References .....	74
<b>4.</b>	<b>Reactivity of [Pt(d<sup>4</sup>bpx)H(solvent)][RSO<sub>3</sub>] with C<sub>2</sub>H<sub>4</sub> .....</b>	<b>77</b>
4.1.	Introduction.....	77
4.2.	Reactivity of [Pt(d <sup>4</sup> bpx)H(solvent)][CF <sub>3</sub> SO <sub>3</sub> ], 3a, with C <sub>2</sub> H <sub>4</sub> .....	79
4.3.	The dynamic behaviour of [Pt(d <sup>4</sup> bpx)(CH <sub>2</sub> CH <sub>3</sub> )] <sup>+</sup> , 6a .....	83
4.3.1	Dynamic behaviour of 6a at high temperature (293-353 K).....	84
4.3.2	Dynamic behaviour of 6a at low temperature (293–145 K) .....	89
4.4.	The β-agostic interaction .....	96
4.5.	Formation of [Pt(d <sup>4</sup> bpx)(CH <sub>2</sub> CH <sub>3</sub> )][CH <sub>3</sub> SO <sub>3</sub> ], 4b.....	99
4.6.	Conclusions.....	100
4.7.	References.....	102

<b>5. Reactivity of [Pt(d<sup>4</sup>bpx)(CH<sub>2</sub>CH<sub>3</sub>)][RSO<sub>3</sub>] with CO .....</b>	<b>105</b>
5.1. Introduction.....	105
5.2. Reactivity of [Pt(d <sup>4</sup> bpx)(CH <sub>2</sub> CH <sub>3</sub> )] [CF <sub>3</sub> SO <sub>3</sub> ], 6a, with CO in MeOH at 293 K .....	106
5.3. Reactivity of [Pt(d <sup>4</sup> bpx)(CH <sub>2</sub> CH <sub>3</sub> )] [CH <sub>3</sub> SO <sub>3</sub> ], 6b, with CO in MeOH at 293 K .....	111
5.4. Reactivity of [Pt(d <sup>4</sup> bpx)(CH <sub>2</sub> CH <sub>3</sub> )] [CF <sub>3</sub> SO <sub>3</sub> ], 6a, with CO in CH <sub>2</sub> Cl <sub>2</sub> and THF .....	114
5.4.1 Reactivity of 6a with CO in CH <sub>2</sub> Cl <sub>2</sub> at 193 K and 293 K.....	114
5.4.2 Reactivity of 6a with CO in THF at 193 K and 293 K .....	125
5.5. Reactivity of 9a and 10a with PPh <sub>3</sub> .....	127
5.6. Formation and decomposition of [Pt(d <sup>4</sup> bpx)(C(O)Et)(CO)] <sup>+</sup> , 10a .....	131
5.7. Alcoholysis-step.....	133
5.8. References .....	139

<b>6.</b>	<b>Studies at high temperature and high pressure .....</b>	<b>142</b>
6.1.	Introduction .....	142
6.2.	CF <sub>3</sub> SO <sub>3</sub> H-system .....	142
6.2.1	Stability of [Pt(d <sup>4</sup> bpx)H(solvent)][CF <sub>3</sub> SO <sub>3</sub> ], 3a, under N <sub>2</sub> pressure .	142
6.2.2	Stability of [Pt(d <sup>4</sup> bpx)H( <sup>13</sup> CO)][CF <sub>3</sub> SO <sub>3</sub> ], 3a, under <sup>13</sup> CO and C <sub>2</sub> H <sub>4</sub> pressure .....	144
6.3.	CH <sub>3</sub> SO <sub>3</sub> H-system with addition of H <sub>2</sub> O .....	147
6.3.1	Reactivity under 10 bar of N <sub>2</sub> .....	148
6.3.2	Reactivity under 10 bar of C <sub>2</sub> H <sub>4</sub> .....	149
6.3.3	Reactivity under 7 bar of CO and 10 bar of C <sub>2</sub> H <sub>4</sub> .....	151
6.3.4	Reactivity under 10 bar of gas mixture CO/C <sub>2</sub> H <sub>4</sub> (1/1) .....	153
6.3.5	Reactivity under 10 bar of gas mixture CO/C <sub>2</sub> H <sub>4</sub> (1/9) .....	154
6.4.	CH <sub>3</sub> SO <sub>3</sub> H-system without H <sub>2</sub> O.....	155
6.4.1	Stability of [Pt(d <sup>4</sup> bpx)(η <sup>2</sup> -CH <sub>3</sub> SO <sub>3</sub> )] <sup>+</sup> , 5b, under N <sub>2</sub> pressure .....	156
6.4.2	Reactivity under 10 bar of C <sub>2</sub> H <sub>4</sub> .....	157
6.4.3	Reactivity under 7 bar of <sup>13</sup> CO and 10 bar of C <sub>2</sub> H <sub>4</sub> .....	158
6.4.4	Reactivity under 10 bar of gas mixture CO/C <sub>2</sub> H <sub>4</sub> (1/1) .....	159
6.4.5	Reaction of [Pt(d <sup>4</sup> bpx)(η <sup>2</sup> -CH <sub>3</sub> SO <sub>3</sub> )] <sup>+</sup> 5b with CO, formation of the complex 13b.....	161
6.4.6	Reactivity under 10 bar of gas mixture CO/C <sub>2</sub> H <sub>4</sub> (1/9) .....	167
6.5.	Catalytic experiments carried out in autoclave at Ineos-Acrylics....	168
6.5.1	CH <sub>3</sub> SO <sub>3</sub> H, T = 253 K, P = 10 bar of C <sub>2</sub> H <sub>4</sub> :CO (9:1) gas mixture	168
6.5.2	CF <sub>3</sub> SO <sub>3</sub> H, T = 353 K, P = 10 bar of C <sub>2</sub> H <sub>4</sub> :CO (9:1) gas mixture	169
6.5.3	CF <sub>3</sub> SO <sub>3</sub> H, T = 393 K, P = 10 bar of C <sub>2</sub> H <sub>4</sub> :CO (9:1) gas mixture	170

6.5.4	CH <sub>3</sub> SO <sub>3</sub> H, T = 393 K, P = 10 bar of C <sub>2</sub> H <sub>4</sub> :CO (9:1) gas mixture	171
6.6.	Conclusions .....	172
<b>7.</b>	<b>General conclusions .....</b>	<b>176</b>
7.1.	Platinum catalytic cycle for the methoxycarbonylation of ethene...	176
7.2.	References .....	184
<b>8.</b>	<b>Experimental.....</b>	<b>186</b>
8.1.	General methods and procedures.....	186
8.2.	Experimental for Chapter Two .....	188
8.3.	Experimental for Chapter Three .....	189
8.4.	Experimental for Chapter Four.....	192
8.5.	Experimental for Chapter Five .....	195
8.6.	Experimental for Chapter Six .....	199
8.7.	References .....	201

## Abbreviations

IR	infra-red
NMR	Nuclear Magnetic Resonance
$\delta$	chemical shift
$J$	coupling constant
${}^nJ$	n-bond coupling constant
ppm	parts per million
Hz	Hertz
VT	variable temperature
BQ	benzoquinone
Me	methyl
Et	ethyl
Ph	phenyl
THF	tetrahydrofuran
MeP	methyl propanoate
cod	cycloocta-1,5-diene
dba	dibenzylideneacetone
${}^t\text{bcpx}$	1,2-bis( <i>tert</i> -butylcyclohexylphosphinomethyl)benzene
${}^t\text{b}^t\text{ppx}$	1,2-bis( <i>tert</i> -butyl <i>tert</i> pentylphosphinomethyl)benzene
dbpe	1,2-bis(di-butylphosphino)ethane
dbpp	1,3-bis(di-butylphosphino)propane
${}^t\text{dbpp}$	1,3-bis(di- <i>tert</i> -butylphosphino)propane
${}^t\text{dbpx}$	1,2-bis(di- <i>tert</i> -butylphosphinomethyl)benzene
dcpb	1,4-bis(dicyclohexylphosphino)butane

dcpe	1,2-bis(dicyclohexylphosphino)ethane
dcpp	1,3-bis(dicyclohexylphosphino)propane
dcpx	1,2-bis(dicyclohexylphosphinomethyl)benzene
dppb	1,4-bis(diphenylphosphino)butane
dppe	1,2-bis(diphenylphosphino)ethane
d <sup>i</sup> ppe	1,2-bis(di-isopropylphosphino)ethane
dppm	bis(diphenylphosphino)methane
dppp	1,3-bis(diphenylphosphino)propane
d <sup>i</sup> ppp	1,3-bis(di-isopropylphosphino)propane
dppx	1,2-bis(diphenylphosphinomethyl)benzene
d <sup>i</sup> ppx	1,2-bis(di-isopropylphosphinomethyl)benzene
d <sup>t</sup> ppx	1,2-bis(di-tert-pentylphosphinomethyl)benzene

## List of complexes

$[\text{Pt}(\text{d}^t\text{bpx})(\text{dba})]$	<b>1</b>
$[\text{Pt}(\text{d}^t\text{bpx})(\text{dbaH})][\text{CF}_3\text{SO}_3]$	<b>2a</b>
$[\text{Pt}(\text{d}^t\text{bpx})(\text{dbaH})][\text{CH}_3\text{SO}_3]$	<b>2b</b>
$[\text{Pt}(\text{d}^t\text{bpx})\text{H}(\text{solv})][\text{CF}_3\text{SO}_3]$	<b>3a</b>
$[\text{Pt}(\text{d}^t\text{bpx})\text{H}(\text{solv})][\text{CH}_3\text{SO}_3]$	<b>3b</b>
$[\text{Pt}(\text{d}^t\text{bpx})(\text{H}_2\text{O})_2][\text{CF}_3\text{SO}_3]_2$	<b>4a</b>
$[\text{Pt}(\text{d}^t\text{bpx})(\text{H}_2\text{O})_2][\text{CH}_3\text{SO}_3]_2$	<b>4b</b>
$[\text{Pt}(\text{d}^t\text{bpx})(\eta^2\text{-CH}_3\text{SO}_3)][\text{CH}_3\text{SO}_3]$	<b>5b</b>
$[\text{Pt}(\text{d}^t\text{bpx})(\text{CH}_2\text{CH}_3)[\text{CF}_3\text{SO}_3]$	<b>6a</b>
$[\text{Pt}(\text{d}^t\text{bpx})(\text{CH}_2\text{CH}_3)[\text{CH}_3\text{SO}_3]$	<b>6b</b>
$[\text{Pt}(\text{d}^t\text{bpx})(\eta^2\text{-C}_2\text{H}_4)]$	<b>7</b>
$[\text{Pt}(\text{d}^t\text{bpx})\text{H}(\text{CO})][\text{CF}_3\text{SO}_3]$	<b>8a</b>
$[\text{Pt}(\text{d}^t\text{bpx})\text{H}(\text{CO})][\text{CH}_3\text{SO}_3]$	<b>8b</b>
$[\text{Pt}(\text{d}^t\text{bpx})(\text{C}_2\text{H}_5)(\text{CO})][\text{CF}_3\text{SO}_3]$	<b>9a</b>
$[\text{Pt}(\text{d}^t\text{bpx})(\text{C}(\text{O})\text{C}_2\text{H}_5)(\text{CO})][\text{CF}_3\text{SO}_3]$	<b>10a</b>
$[\text{Pt}(\text{d}^t\text{bpx})(\text{C}(\text{O})\text{C}_2\text{H}_5)(\text{PPh}_3)][\text{CF}_3\text{SO}_3]$	<b>11a</b>
$[\text{Pt}(\text{d}^t\text{bpx})\text{H}(\text{PPh}_3)][\text{CF}_3\text{SO}_3]$	<b>12a</b>

# **Chapter one**

# 1. Introduction

## 1.1. The reactions between carbon monoxide and ethene

The reaction between carbon monoxide and ethene have attracted considerable attention over the last few decades.<sup>1-4</sup> First, ethene and carbon monoxide are quite cheap and readily available monomers. Second, this reaction can give rise to a broad spectrum of products such as high melting thermoplastic polymers, polyketones, or low boiling liquids such as methyl propanoate (MeP). The former materials are very interesting because the CO/C<sub>2</sub>H<sub>4</sub> copolymer has a perfect alternation of CO/C<sub>2</sub>H<sub>4</sub> which provides high mechanical strength, mainly because of its crystallinity.<sup>5</sup> From a different point of view, these polyketones are expected to constitute a new class of photodegradable and biodegradable polymers, because of the relative reactivity of the carbonyl group present in the polymer backbone.<sup>6,7</sup> Finally, because of the ease with which the carbonyl group can be chemically modified, the polyketones serve as good starting materials for other classes of functionalised polymers.<sup>8-10</sup>

Methyl propanoate has attracted interest as a possible intermediate for the production of methyl methacrylate.

The first example of non-alternating CO/C<sub>2</sub>H<sub>4</sub> copolymerisation was reported in the 1940's.<sup>11</sup> A free radical process was used under very drastic conditions (500-1500 bar). The product obtained was a polymer with a low molecular weight containing branched molecular structures and irregular carbon monoxide incorporation.

In 1951 Reppe and Mangin reported the first example of a metal-catalysed process.<sup>12,13</sup> They used the complex  $K_2[Ni(CN)_4]$  in water; as products they obtained low melting oligomers, in addition to diethyl ketone and propionic acid. In the early 1970's, Shryne and Holler succeeded in improving the catalyst by addition of strong acids such as TfOH and TsOH in solvents such as hexafluoroisopropanol.<sup>14,15</sup> With this system, they obtained a polymer with relatively high molecular weight, but the yield of polymer per gram of catalyst was still low. Recently Klabunde has reported a new nickel catalyst, based on a bidentate P-O anionic ligand.<sup>16</sup>

In the same period, rhodium catalysts were investigated, but gave low molecular weight copolymer and also the rates of formation of the products were low.<sup>17,18</sup>

The most successful route to polyketones as well as methyl propanoate has been formed using palladium catalysts. These were discovered by Gouch at ICI in 1967.<sup>19</sup> He used  $[Pd(PR_3)_2Cl_2]$  as catalysts. The disadvantage was that severe conditions were required (250°C, 2000 bar) and yields in gram of polymer/gram of palladium were low. During the following 15 years, only small advances were made in increasing catalyst efficiency.<sup>20,21</sup> For example, Sen reported that cationic bis(triphenylphosphine)palladiumtetrafluoroborate complexes in aprotic solvents such as dichloromethane, produced CO/C<sub>2</sub>H<sub>4</sub> copolymers under very mild conditions.<sup>22</sup> However, the reaction rates were very low as well as the molecular weights. It must be observed that insurmountable processing problems were encountered for the resulting polymers. Extensive crosslinking under melt processing conditions led to a lack of significant thermoplastic properties of the resulting materials and this presented a major obstacle in further developments. At that time it

was concluded that the polymer backbone of polyketones is unstable and that polyketones could not be efficiently produced.

These conclusions proved to be invalid, when in the early 1980's, workers at Shell demonstrated that the polyketone produced using palladium cyanide as the catalyst had an improved melt process ability, after extensive extraction of catalyst residues from the polymers and blending these with other polymers. From these studies, it was suggested that thermoplastic properties were possible and that the polyketone backbone was not inherently unstable in the melt processing conditions. However, catalyst extraction did not offer a viable production option from a technical and economic point of view.

At the same time, it was reported from the research group at Shell in Amsterdam, that cationic palladium complexes containing tertiary phosphines and weakly coordinating anions in MeOH were very efficient catalysts for the synthesis of methyl propanoate from CO and ethene. It was also discovered that experiments using catalysts containing bidentate tertiary phosphine ligands produced high molecular weight polyketones at very high rates, instead of methyl propanoate.<sup>23</sup>

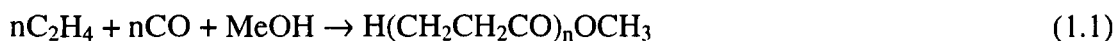
## 1.2. The Shell Process

Until recently, Shell produced these polyketones on an industrial scale, but now the process has been discontinued.<sup>24</sup> The first commercial polymer produced by Shell was a terpolymer of ethene/propene/CO, marketed under the trade name Carilon. A lot of work has been done in order to understand the mechanism of polymer

formation but, at the moment, a detailed understanding of the process awaits elucidation.<sup>3,25,26</sup>

### 1.2.1 Formation of Polyketones

Shell found that the catalyst can be formed *in situ* by mixing a Pd(II) salt, *e.g.* Pd(OAc)<sub>2</sub> with a diphosphine, *e.g.* Ph<sub>2</sub>P(CH<sub>2</sub>)<sub>n</sub>PPh<sub>2</sub> (n = 2-6, Pd/phosphine = 1:1) in MeOH in order to form polyketones, or an excess of PPh<sub>3</sub> if methyl propanoate is the required product; in the latter process, it is essential to carry out the reaction in the presence of an acid (*e.g.* TsOH), (see Equation 1.1)



A typical reaction rate would be *ca.* 10<sup>4</sup> mol of converted ethene (mol of Pd)<sup>-1</sup>h<sup>-1</sup> to give a polymer with an average molecular weight (M<sub>n</sub>) of *ca.* 20000 (dppp/TsOH/MeOH, 65 °C).<sup>3</sup> Under suitable conditions, the catalyst is highly stable and total conversion of more than 10<sup>6</sup> mole of ethene per mole of palladium can be obtained.

Different factors can control both the reaction rate and molecular weight of the product, such as the amount and the nature of the acid, the ligand, the solvent, the temperature, the pressure and composition of gas mixture and the use of particular promoters.

As described above, different ligands can lead to large changes in the nature of the product formed. When monodentate phosphines are used, methyl propanoate is formed, whereas with diphosphine ligands, the polyketones are the main product. Furthermore, varying the nature of the bidentate ligand results in significant changes

in the activity and selectivity of the process. Considering the effect of the chain length,  $n$ , of the diphosphine,  $\text{Ph}_2\text{P}(\text{CH}_2)_n\text{PPh}_2$ , the best results are obtained when  $n = 3$ , whereas both the rate and molecular weight rapidly decrease on either increasing or decreasing the chain length. It has been proposed that the control exerted by the diphosphine is due to its ability to stabilise both square planar and trigonal bipyramidal geometries. The maximum activity is observed for phosphines in which the bite angle (P-Pd-P) enables complexation in both geometries to allow accommodation of both 90 and 120°. <sup>4</sup>

The role of the acid HX is to allow introduction of the anion (see Equation 1.2), and the best results have been formed with weakly coordinating anions.



In some cases, it has been observed that a metal salt of the anion can be used instead of the free acid. Considering the effect of the anion, the reaction rate increases greatly on going from strongly coordinating anion, like chloride, to a weakly or completely non coordinating one, like *p*-toluenesulfonate or tetrafluoroborate. These observations can be explained by a competition between the anion and the monomers for the coordination site of the metal. A weakly coordinating anion favours coordination of the monomer and speeds up the reaction rate. The amount of acid added also plays an important role. In general, the best results are obtained with a significant excess of acid with respect to that required in equation 1.2. <sup>27</sup> It has been proposed, <sup>27</sup> that the effect of excess acid may increase the concentration of  $[\text{Pd-H}]^+$  species as a result of addition of  $\text{H}^+$  to  $\text{Pd}(0)$ , but our work makes this now seem less likely. However, it must be considered that at high acid

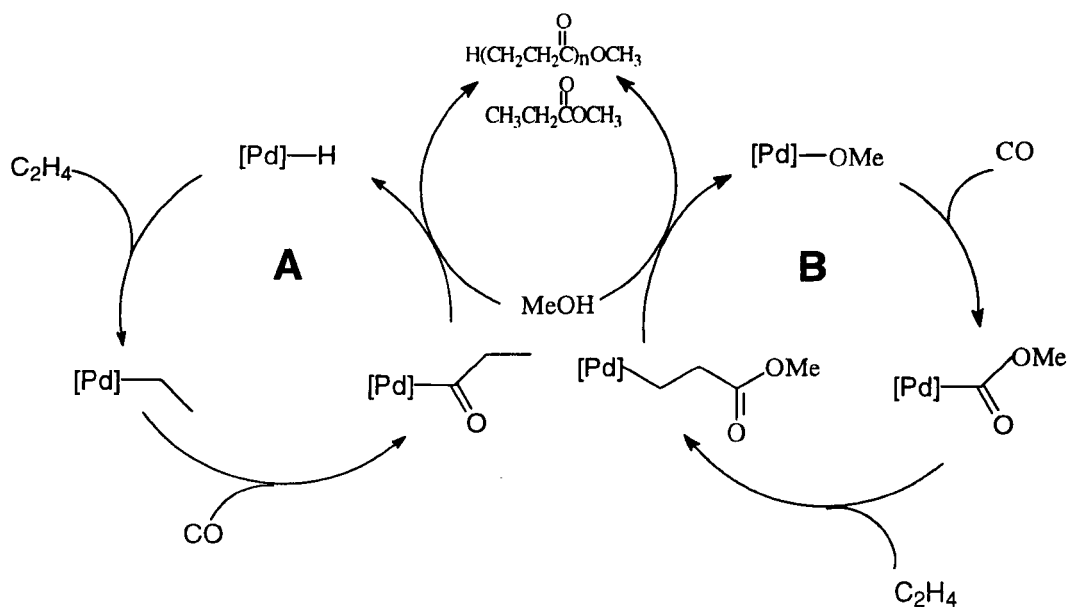
concentration, the acid becomes a poison because the anion can compete with the monomers for the coordination sites of the metal.

The copolymerisation catalysts generally show a higher activity in the presence of added oxidants like quinones. It has been suggested that quinones must cause the participation of large number of active centres and chain lengths are not affected by addition of oxidants.

In both catalytic processes, formation of polyketones and formation of methyl propanoate, two catalytic cycles are possible (see Scheme 1.1).

### Scheme 1.1

*Proposed mechanisms for the formation of polyketones and methyl propanoate*



One cycle is a methoxy cycle, starting from a palladium methoxy species ( $Pd-OMe$ ) and terminating by a protolysis process; the second cycle is a hydride cycle,

which starts with a palladium hydride (Pd-H) complex and terminating by alcoholysis. Each cycle produces a polymer, which contains a keto group and an ester group (keto-ester).

### 1.2.2 Formation of Methyl Propanoate

Previously, the most important effect was the change of selectivity for polyketone *versus* methyl propanoate formation induced on changing from a bidentate to a monodentate phosphine.

The formation of methyl propanoate can be considered a particular case of the polymerisation process, which involves only initiation and termination steps, without the propagation steps (see Equation 1.3)



Indeed, under the conditions used for the synthesis of polyketones, cationic Pd(II) catalysts modified with excess monodentate phosphine and Bronsted acids of weakly coordinating anions, selectively give methyl propanoate with high rates. It has been proposed that the main difference between the behaviour of catalyst containing monodentate and bidentate phosphines is the fact that in the case of bidentate ligands the two phosphorus atoms are always in *cis* position; this allows the growing polymer chain and the vacant fourth coordination site to always be *cis* to each other, which is the most favourable position for insertion.

However, in the case of monodentate ligands it has been proposed that a *trans* orientation is most favourable, for steric reasons and probably because it also avoids the unfavourable situation of a Pd-P bond *trans* to a Pd-C bond. Moreover, because

of the presence of excess ligand, *cis/trans* isomerisation is expected to be rapid.<sup>28,29</sup> Assuming that the hydride cycle occurs (see Scheme 1.1), it is reasonable to assume that both the insertion of ethene into the Pd-H bond and the insertion of CO into a Pd-alkyl can only occur when the reacting ligands are *cis*. Immediately after insertion, *cis/trans* isomerisation occurs, which puts the growing chain *trans* to the vacant fourth coordination site, preventing further monomer insertion

### 1.3. The Lucite Process

Recent patents by Shell<sup>30</sup> and Lucite International (formerly INEOS Acrylics)<sup>31</sup> partially contradict the hypothesis made in Section 1.2, about the relation between the nature of the phosphine and the observed products. In particular, they have reported some examples of tertiary butyl substituted bidentate phosphines, which give methyl propanoate in high yield and selectivity. In the Shell patent, the ligand 1,3-bis(di-*tert*-butylphosphino)propane (d<sup>t</sup>bpp) is used, whereas the Lucite process is based on 1,2-bis(di-*tert*-butylphosphinomethyl)benzene (d<sup>t</sup>bpx).

In the case of the Lucite process, the catalyst is formed *in situ via* the reaction of [Pd(d<sup>t</sup>bpx)(dba)] (dba = *trans,trans*-(PhCH=CH)<sub>2</sub>CO] with CH<sub>3</sub>SO<sub>3</sub>H in MeOH. The resulting catalytic system gives methyl propanoate with a selectivity of 99.98% at the production rate of 50000 mol product (mol Pd)<sup>-1</sup> h<sup>-1</sup> under very mild conditions (353 K and 10 atm of C<sub>2</sub>H<sub>4</sub>/CO).<sup>32</sup> These features make this process very attractive from a commercial point of view since MeP is an attractive precursor for the synthesis of methyl methacrylate.<sup>33</sup> A different catalyst based on Pd(OAc)<sub>2</sub>/PPh<sub>3</sub> (excess)/TsOH gives MeP with a selectivity of 95% at a production rate of only 500 mol product

$(\text{mol Pd})^{-1} \text{ h}^{-1}$ . Other bidentate ligands have been studied for the same process, but it is clear that the best result is obtained using  $d^t\text{bpx}$  as ligand.<sup>34</sup>

Some important recent results,<sup>35,36</sup> together with examination of the structures of diphosphine ligands which promote MeP formation, consider a particular explanation. The suggestion was made first by Tooze<sup>32</sup>, followed by Cole-Hamilton<sup>37</sup>, and it considers that ligands which do not have a very high chelate stabilisation when coordinated in a bidentate mode may be less directing for the formation of polyketone. It was tentatively suggested that this may be related to the *cis-trans* isomerisation thought to be responsible for the production of low molecular weight materials in palladium catalysed methoxycarbonylation using triphenylphosphine as the ligand. They considered the diphosphines  $d^t\text{bpp}$  and  $d^t\text{bpx}$ , which selectively produce MeP and that sometimes coordinate in a unidentate manner.

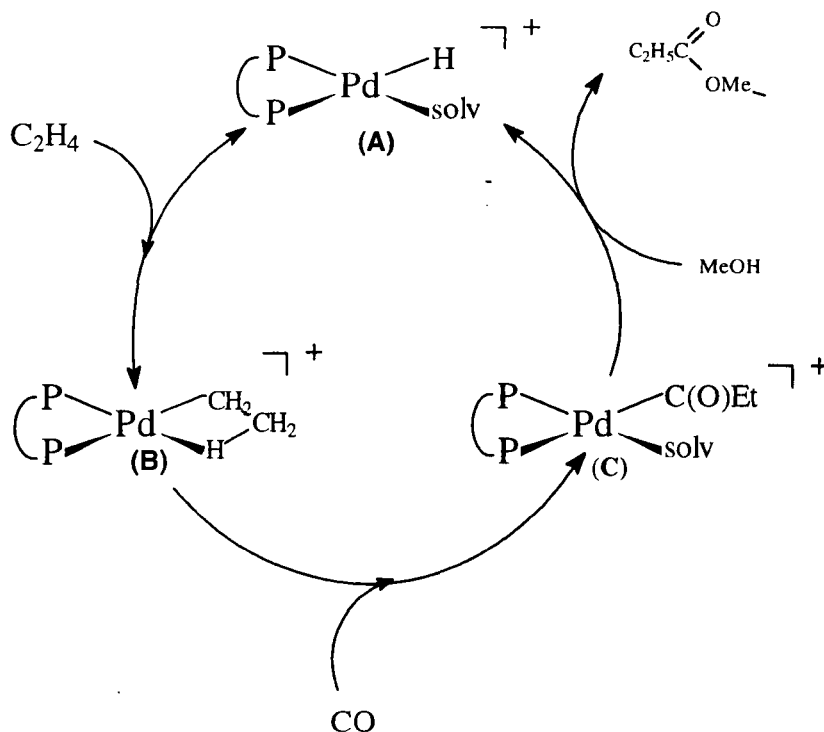
#### **1.4. Mechanistic studies of the methoxycarbonylation of ethene promoted by the palladium catalyst $[\text{Pd}(d^t\text{bpx})(\text{dba})]$ .**

At this point, the question concerning the mechanism for the methoxycarbonylation of ethene remains unresolved and a full understanding of the intermediates involved in the catalytic process become very important.

This section will describe the results of *in situ* spectroscopic studies of the methoxycarbonylation of ethene, which involves the catalyst  $[\text{Pd}(d^t\text{bpx})(\text{dba})]$ .

The first important results of these studies support the fact that the methoxycarbonylation of ethene proceeds *via* a hydride catalytic cycle (see Scheme 1.2).<sup>38</sup>

## Scheme 1.2

*Palladium Hydride Catalytic Cycle*

All the intermediates involved in this catalytic cycle have been fully characterised,<sup>39</sup> and they are  $[\text{Pd}(\text{d}^1\text{bpx})\text{H}(\text{MeOH})]^+$ , **A**,  $[\text{Pd}(\text{d}^1\text{bpx})(\text{CH}_2\text{CH}_3)]^+$ , **B**, and  $[\text{Pd}(\text{d}^1\text{bpx})(\text{C}(\text{O})\text{Et})(\text{solv})]^+$ , **C**. The important point from these studies is that the palladium hydride complex,  $[\text{Pd}(\text{d}^1\text{bpx})\text{H}(\text{MeOH})]^+$ , **A** is a key intermediate in the process.

#### 1.4.1 Formation of $[\text{Pd}(\text{d}^1\text{bpx})\text{H}(\text{MeOH})]^+$ , **A**

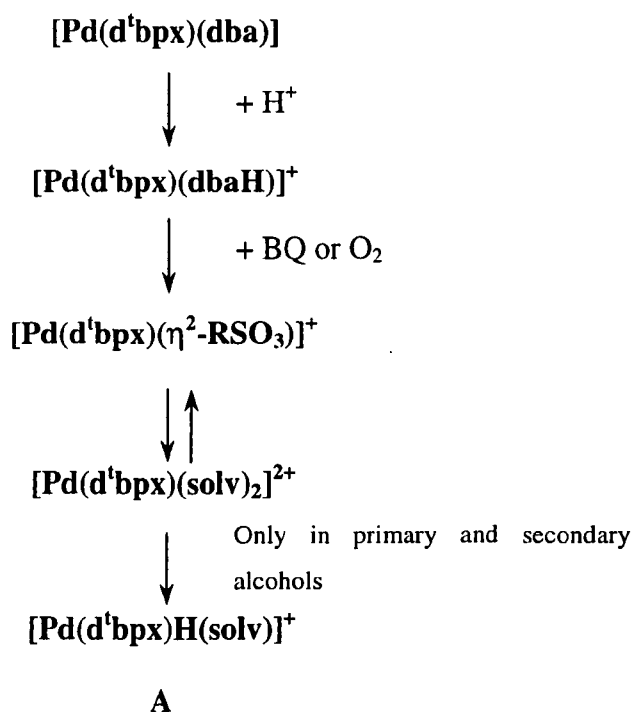
**A** has been fully characterised and it is a rare example of stable palladium hydride, because, usually, these complexes are quite reactive and unstable species,

especially in the presence of labile ligands, such as weakly coordinating solvent molecules.<sup>40</sup>

The formation of the palladium hydride **A** is not a direct process, but takes place in at least four steps (see Scheme 1.3).<sup>41</sup>

### Scheme 1.3

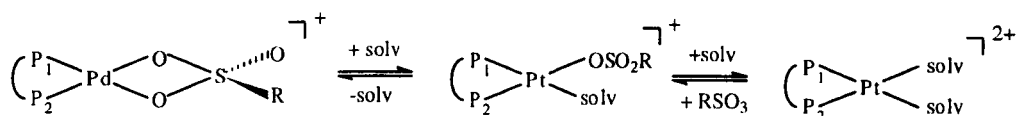
*Formation of the palladium hydride complex, A*



The first reaction is protonation of  $[\text{Pd}(\text{d}^t\text{bpx})(\text{dba})]$  to give  $[\text{Pd}(\text{d}^t\text{bpx})(\text{dbaH})]^+$ . This reaction is irreversible and it is important since it transforms the insoluble compound  $[\text{Pd}(\text{d}^t\text{bpx})(\text{dba})]$  into a soluble species,  $[\text{Pd}(\text{d}^t\text{bpx})(\text{dbaH})]^+$ , which is more easily oxidised by  $\text{O}_2$  or BQ to  $[\text{Pd}(\text{d}^t\text{bpx})(\eta^2\text{-RSO}_3)]^+$  ( $\text{R} = \text{CH}_3$  or  $\text{CF}_3$ ). The third step is the displacement of the coordinated  $\text{RSO}_3^-$  anion and formation of  $[\text{Pd}(\text{d}^t\text{bpx})(\text{solv})_2]^{2+}$ . This step is an equilibrium and its position depends on the

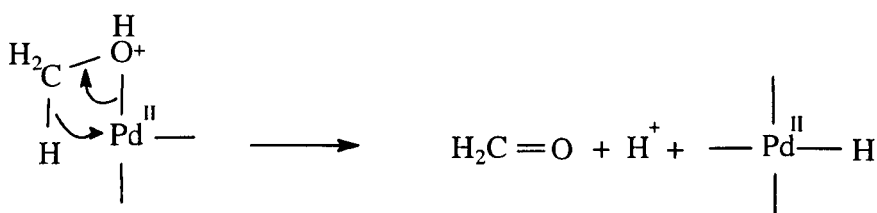
nature of the R-group present on the anion and the solvent used. Polar solvents favour the formation of  $[\text{Pd}(\text{d}^t\text{bpx})(\text{solv})_2]^{2+}$ , whereas basic R-groups shift the equilibrium towards the formation of  $[\text{Pd}(\text{d}^t\text{bpx})(\eta^2\text{-RSO}_3)]^+$ .<sup>41</sup> The replacement of  $\text{RSO}_3^-$  proceeds through two steps (see Scheme 1.4).<sup>42</sup>

Scheme 1.4



First, one molecule of the solvent coordinates to the metal and  $\text{RSO}_3^-$  group changes its coordination mode from  $\eta^2$  to  $\eta^1$ , resulting in the formation of the intermediate  $[\text{Pd}(\text{d}^t\text{bpx})(\eta^1\text{-RSO}_3)(\text{solv})]^+$ . Thus, the bidentate coordinated anion,  $\text{RSO}_3^-$ , loses the extra stabilisation resulting from chelation effect and the monodentate  $\text{RSO}_3^-$  group is easily displaced by the second molecule of solvent. The final step in the hydride formation is a redox process involving the solvent (see Scheme 1.5).<sup>41</sup>

Scheme 1.5

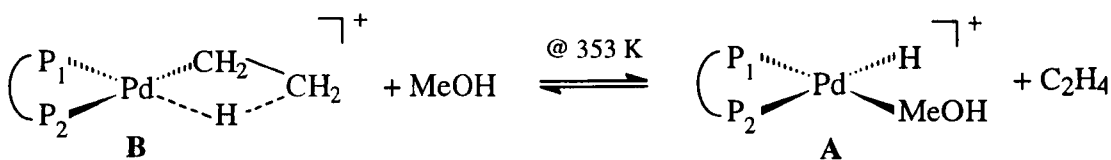


This reaction is irreversible and involves  $\beta$ -hydride elimination from a primary or secondary alcohol coordinated to the palladium. It must be emphasised that the palladium hydride **A** is formed only in primary and secondary alcohols.

#### 1.4.2 Formation of $[\text{Pd}(\text{d}^t\text{bpx})(\text{CH}_2\text{CH}_3)]^+$ , **B**

The second step in the Scheme 1.2 shows that  $[\text{Pd}(\text{d}^t\text{bpx})\text{H}(\text{MeOH})]^+$ , **A**, reacts with ethene to give  $[\text{Pd}(\text{d}^t\text{bpx})(\text{CH}_2\text{CH}_3)]^+$ , **B**. The reaction is immediate and only at 353 K it is possible to observe the reformation of the palladium hydride complex **A** (see Scheme 1.6).

Scheme 1.6



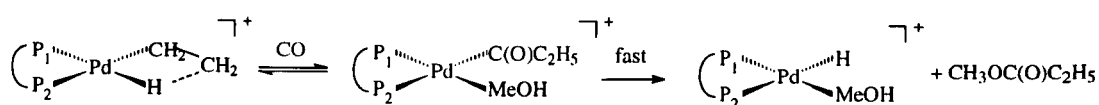
Spencer reported previously the protonation of  $[\text{Pd}(\text{d}^t\text{bpx})(\text{C}_2\text{H}_4)]$  as a possible route for the formation of **B**;<sup>43</sup> unfortunately, no NMR data were reported. However, using mono- $^{13}\text{C}$ -labeled ethene, it was possible to assign unambiguously the two inequivalent carbon resonances.<sup>39</sup> The first reasonable assumption was to assign the fourth coordination site in the palladium ethyl complex **B** to MeOH, but subsequent work shows that the occupancy of the fourth coordination site in **B** is due to a  $\beta$ -C-H interaction.<sup>39</sup> The most important support for a  $\beta$ -agostic formulation of **B**, comes from  $^{13}\text{C}\{^1\text{H}\}$  NMR spectra. In the classical palladium ethyl complex,  $[\text{Pd}(\text{L}-$

$L)(CH_2CH_3)(solv)]^+$ ,<sup>44,45</sup>  $\delta(CH_3) > \delta(CH_2)$ , but for **B**,  $\delta(CH_3) < \delta(CH_2)$ . This reversal of the  $CH_2$  and  $CH_3$  chemical shifts between classical and nonclassical metal-ethyl complexes is found for  $[\overline{Pt(d^t\text{bpx})(CH_2CH_3)}]^+$ , which also contains a  $\beta$ -agostic interaction.<sup>46</sup>

### 1.4.3 Formation of $[\overline{Pd(d^t\text{bpx})(C(O)C_2H_5)(THF)}]^+$ , **C**<sup>39</sup>

$[\overline{Pd(d^t\text{bpx})(CH_2CH_3)}]^+$ , **B**, reacts in MeOH under  $N_2$  atmosphere with 1 equivalent of CO to give  $[Pd(d^t\text{bpx})H(MeOH)]^+$ , **A**, and MeP. This results from the reaction of **B** with CO to give  $[Pd(C(O)C_2H_5)(MeOH)]^+$ , **C**, followed by rapid formation of the final product MeP (see Scheme 1.7). However, this process is too fast to follow by NMR, even at low temperature, thus, to isolate and characterise the acyl complex, the reaction has been performed in non-alcoholic solvents.

Scheme 1.7



$[\overline{Pd(d^t\text{bpx})(CH_2CH_3)}]^+$ , **B**, reacts in THF at low temperature with 1 equivalent of CO, resulting in the formation of a new species which shows two doublets in the  $^{31}P\{^1H\}$  NMR spectrum at 193 K in THF. These NMR data indicate that the new complex contains two *cis* inequivalent phosphorus atoms, which is in agreement with the formulation of  $[\overline{Pd(d^t\text{bpx})(C(O)C_2H_5)(THF)}]^+$ , **C**. To establish unambiguously

the formulation of the complex **C**, NMR measurements of the  $^{13}\text{C}$ -labelled complex with either the  $\text{C}(\text{O})$  and/or  $\text{C}_2\text{H}_5$  groups labelled. From these studies, it is possible to conclude that the NMR data of the isotopomers are consistent with the formulation of  $[\text{Pd}(\text{d}^t\text{bpx})(\text{C}(\text{O})\text{C}_2\text{H}_5)(\text{THF})]^+$ , **C**. In particular, the values for  $^1J(\text{C}-\text{H})$  are as expected for normal  $\text{sp}^3$  carbons and are consistent with the absence of any significant  $\beta$ -agostic interaction. Also, the occupancy of the fourth coordination site in  $[\text{Pd}(\text{d}^t\text{bpx})(\text{C}(\text{O})\text{C}_2\text{H}_5)(\text{THF})]^+$ , **C**, by THF is supported by the large difference in the  $^{31}\text{P}$  chemical shifts at 193 K, when THF is replaced by  $\text{C}_2\text{H}_5\text{CN}$ .

It is possible to conclude that both the formation of  $[\text{Pd}(\text{d}^t\text{bpx})(\text{CH}_2\text{CH}_3)]^+$ , **B**, from  $[\text{Pd}(\text{d}^t\text{bpx})\text{H}(\text{MeOH})]^+$ , **A**, and the formation of  $[\text{Pd}(\text{d}^t\text{bpx})(\text{C}(\text{O})\text{C}_2\text{H}_5)(\text{THF})]^+$ , **C**, are facile equilibria, whereas the methanolysis of **C** is an irreversible process and is the rate determining step. Moreover, it has been observed that the hydride complex **A** is static over all the temperatures studied, whereas the palladium ethyl **B** and the acyl **C** complexes undergo a variety of intramolecular exchanges. In particular, for both the ethyl and the acyl complexes there are exchange processes that make the two phosphorus atoms equivalent, whereas the two phosphorus atoms in the hydride complex are always inequivalent.

## 1.5. Heavier Platinum Metals as Catalysts

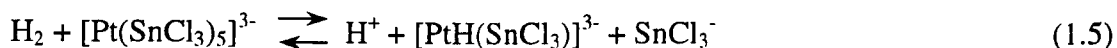
The carbonylation of methanol using rhodium catalysts is a very efficient process and it is interesting that a more efficient/selective homogeneous catalytic reaction could be introduced commercially by BP; this uses Ir as the catalyst and is known as

the CATIVA process.<sup>47</sup> For this reason, it is worthwhile to investigate the catalytic behaviour of platinum *versus* palladium.

Very few industrial processes use platinum complexes as the catalyst in the homogeneous catalytic reactions. This section will illustrate some industrial processes and some mechanistic studies, where platinum is used as the catalyst.

### 1.5.1 Hydroformylation of olefins

A family of catalysts suitable for hydrogenation of C=C in the presence of CO is generated by mixing platinum and tin chloride. The commercially available  $\text{H}_2\text{PtCl}_6$  and  $\text{SnCl}_2$  react in MeOH to form deep red solutions which contain species such as  $[\text{Pt}(\text{SnCl}_3)_5]^{3-}$ .<sup>48</sup> The  $\text{SnCl}_3^-$  ligand is very labile and dissociates to give vacant coordination sites for reaction with  $\text{H}_2$  and with olefins. The ligand also inhibits reduction of the Pt(II) to platinum metal.  $\text{SnCl}_3^-$  appears to be a weak  $\sigma$ -donor and a good  $\pi$ -acceptor like carbon monoxide.<sup>49</sup> In this process, the hydrogen activation occurs by heterolytic cleavage of  $\text{H}_2$  (see Equation 1.5)



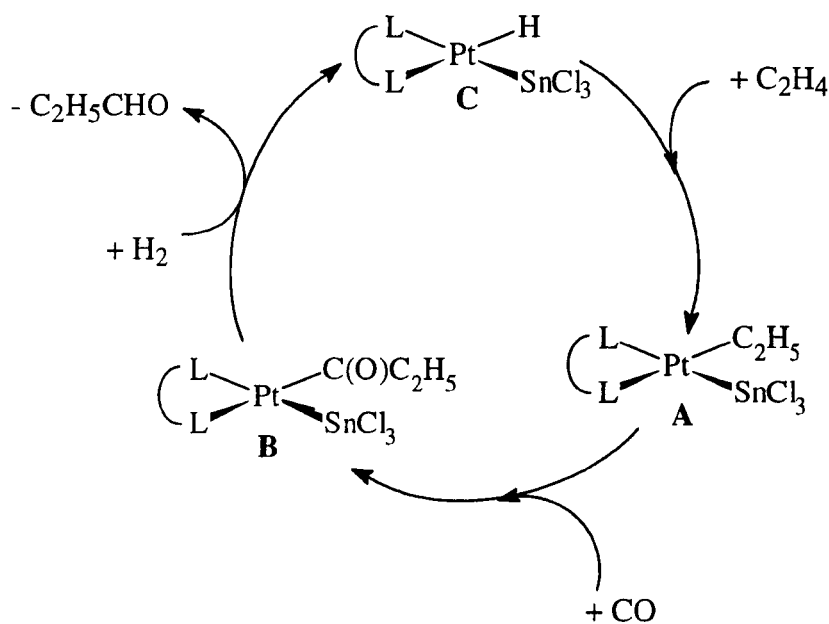
At this stage, the anionic platinum hydride, which can be isolated as a tetraalkylammonium salt, reacts with olefins to give  $[\text{PtR}(\text{SnCl}_3)_4]^{3-}$ .

A similar catalytic system  $[\text{Pt}(\text{PPh}_3)_2\text{Cl}_2]/\text{SnCl}_2$  has been considered in some detail in the hydroformylation of ethene,<sup>50,51</sup> and it was noted that complexes of the type *cis*- $[\text{Pt}(\text{PPh}_3)_2(\text{SnCl}_3)(\text{C}_2\text{H}_5)]$  were involved.

Also the system  $\text{PtCl}_2/\text{chelating diphosphine}/\text{SnCl}_2$  is an efficient catalyst for the hydroformylation of 1-alkenes; in this case, the diphosphine is able to form a seven-

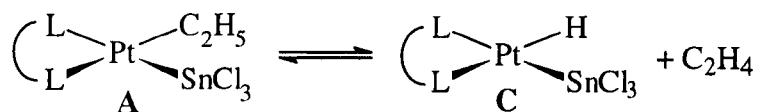
membered ring upon coordination to the metal centre.<sup>52</sup> In particular some detailed mechanistic studies have been reported for the investigation of the reactivity of the system *cis*-[Pt(dppp)(C<sub>2</sub>H<sub>5</sub>)Cl]/SnCl<sub>2</sub> towards CO and hydrogen.<sup>53</sup> From the results reported, the catalytic cycle in Scheme 1.8 represents a reasonable model for this process.

Scheme 1.8



The complex *cis*-[Pt(dppp)(C<sub>2</sub>H<sub>5</sub>)Cl]<sup>54</sup> was found to react with an equimolar amount of SnCl<sub>2</sub> in CH<sub>2</sub>Cl<sub>2</sub> under ethene to give the corresponding trichlorostannate derivative *cis*-[Pt(dppp)(C<sub>2</sub>H<sub>5</sub>)(SnCl<sub>3</sub>)], **A**, whose formation was confirmed by <sup>1</sup>H and <sup>31</sup>P NMR spectroscopy.<sup>53,55</sup> Ethene contributes to the stability of the complex **A** by driving the equilibrium with the complex *cis*-[Pt(dppp)H(SnCl<sub>3</sub>)], **C**, to the left (see Scheme 1.9).

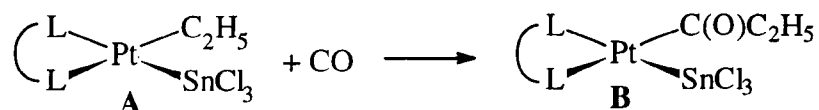
## Scheme 1.9



In the process above, the ethene elimination process probably occurs *via* a  $\beta$ -H elimination reaction.

Carbonylation of the complex **A** at atmospheric pressure gives the acyl complex *cis*-[Pt(dppp)(C(O)C<sub>2</sub>H<sub>5</sub>)(SnCl<sub>3</sub>)], **B** (see Scheme 1.10).<sup>53</sup>

## Scheme 1.10



It has been observed that the reaction reported in Scheme 1.10 is at least 10 times faster than the carbonylation of the complex [Pt(dppp)(C<sub>2</sub>H<sub>5</sub>)Cl], where the stannate ligand is not present.

The acyl complex, *cis*-[Pt(dppp)(C(O)C<sub>2</sub>H<sub>5</sub>)(SnCl<sub>3</sub>)], **B**, undergoes hydrogenolysis to give the corresponding aldehyde and the platinum hydride complex *cis*-[Pt(dppp)H(SnCl<sub>3</sub>)], **C**; in this case, the Pt-SnCl<sub>3</sub> group probably assists with the activation of hydrogen, but the amount of propanal formed was not reported.<sup>53</sup>

## 1.5.2 Platinum(II) complexes as Lewis Acids

In the last decade the square planar complexes of the noble metals have been somehow neglected as Lewis acid catalysts, probably because, being electron rich, they are not an obvious choice. Indeed, the notion of Lewis acidity is already present in the so-called nucleophilic attack,<sup>56</sup> a common process in organometallic chemistry involving molecules such as olefins, carbon monoxide, aldehydes, ketones, once they are coordinated to and activated by metal centres such as Pt(II).

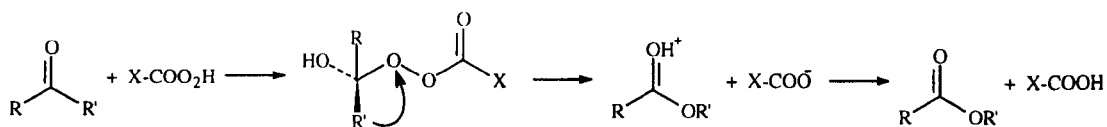
A short review reported by Strukul,<sup>57</sup> on some catalytic proprieties of cationic diphosphine complexes of Pt(II) and Pd(II) has demonstrated the Lewis acidity of these compounds. The results are quite peculiar because those complexes are electron rich  $d^8$  centres modified with electron donating diphosphine ligands, however, they have been shown to carry out some interesting organic transformations in a very efficient manner. It must be noted that these complexes are robust, air stable, easy to handle, water insensitive, square planar species that can be used over a relatively wide range of temperatures and conditions.

The next part of this section will illustrate the behaviour of a variety of cationic diphosphine complexes of Pt(II) as Lewis acid catalysts in organic reactions: the Baeyer-Villiger oxidation of ketones, the acetalisation of aldehydes and ketones, the Diels-Alder reaction.

### *The Baeyer-Villiger oxidation of ketones*

This reaction was first reported over a century ago by Baeyer and Villiger and involves the oxidation of a ketone with a peroxy acid to the corresponding lactone/ester.<sup>58</sup> The reaction proceeds *via* the formation of an intermediate resulting from addition of the peracid to the carbonyl group and migration of one of the substituents on the peroxy oxygen and formation of the product (see Scheme 1.11).<sup>59</sup>

**Scheme 1.11**

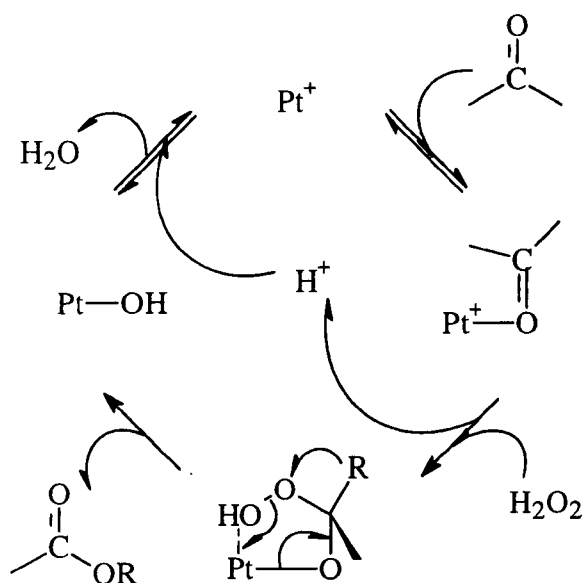


In 1991 Strukul reported the first example of transition metal catalysis, where a complex of Pt(II) was used for the oxidation of a variety of cyclic ketones under mild conditions using commercial 35% hydrogen peroxide as oxidant.<sup>60</sup> The catalyst used was a platinum diphosphine complex  $[\text{Pt}(\text{dppe})(\text{CF}_3)(\text{CH}_2\text{Cl}_2)]^+$  and its stability, in the presence of  $\text{H}_2\text{O}_2$ , was enhanced by the presence of the chelating ligand which prevents dissociation and oxidation of the ligand. This complex could be easily modified with commercially available diphosphines, such as dppp, dppb, and chiral diphosphines. The study of these platinum complexes gave rise to the formulation of the mechanism shown in Scheme 1.12.

Analysing the mechanism in Scheme 1.12, it has been demonstrated that one of the roles of platinum is to increase the electrophilic character of the carbonyl carbon in the ketone, then to behave as a Lewis acid. The other important role of platinum in

the system is to provide an easy pathway for the  $\text{OH}^-$  to leave. The hydroxyl ion is a poor leaving group and for this reason  $\text{H}_2\text{O}_2$  cannot be used as an oxidant in the Baeyer-Villiger oxidation in the absence of a catalyst.

**Scheme 1.12**



After many different studies, it has been observed that the complex  $[\text{Pt}(\text{dppb})(\mu\text{-OH})_2]^{2+}$  is the most active transition metal catalyst known and the only one presently known which can oxidise acyclic ketones with moderate activity.<sup>61</sup>

### *The acetalisation of aldehydes and ketones*

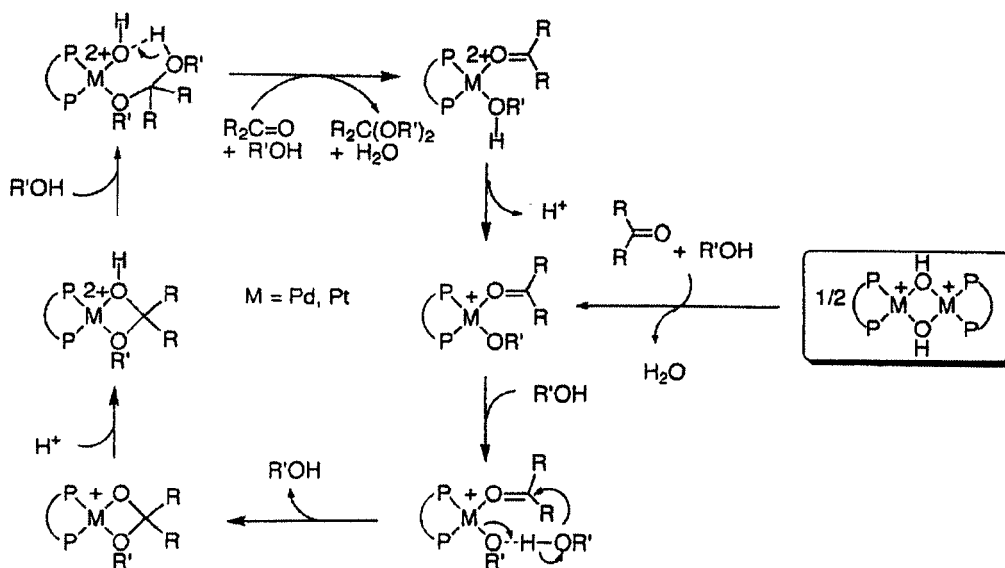
The acetalisation reaction is a process that is used in organic synthesis to protect the carbonyl group of aldehydes and ketones (see Scheme 1.13).<sup>62</sup>

Scheme 1.13



Some years ago, Gorla and Venanzi found that various cationic solvento complexes of Rh(III), Pd(II) and Pt(II) could catalyse the acetalisation of a variety of aldehydes and ketones.<sup>63</sup> The basic requirements necessary to achieve a high catalytic activity were the presence of at least a 2+ positive charge on the complex to ensure a sufficient Lewis acidity and the existence of two adjacent vacant coordination sites in order to have the aldehyde/ketone and alcohol present in *cis* position. Different complexes proved to be very active as catalysts, such as  $[\text{M}(\text{dppe})(\text{H}_2\text{O})_2]^{2+}$  ( $\text{M} = \text{Pt}, \text{Pd}$ ),<sup>63</sup>  $[\text{M}(\text{P-P})(\mu\text{-OH})]_2^{2+}$  ( $\text{M} = \text{Pt}, \text{Pd}$ , P-P = dpmm, dppe, dppp, dppb) (see Scheme 1.14).<sup>64</sup>

Scheme 1.14



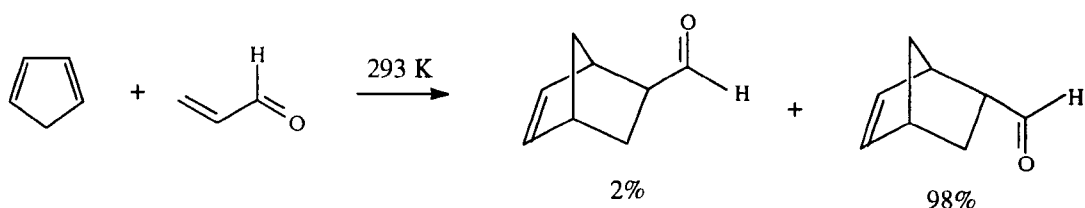
In general, palladium complexes showed a higher activity compared to the corresponding platinum complexes, but they were shown to be more thermally labile, whereas platinum complexes could be used without decomposition even at 353 K to produce good yields of acetals.

### *The Diels-Alder reaction*

The Diels-Alder reaction is a typical Lewis acid catalysed process, which consists of a 4 + 2 cycloaddition between a diene and dienophile.<sup>65</sup>

Some examples in which Pd(II) and Pt(II) complexes have been used to catalyse the asymmetric aldol reaction or asymmetric 1,3-dipolar cycloadditions have recently been reported in the literature.<sup>66</sup> The moderate acidity of the bridging hydroxo complexes  $[M(P-P)(\mu-OH)]_2^{2+}$  ( $M = Pt, Pd$ ) was found to be insufficient to promote the reaction, which generally requires strong Lewis acids as the catalysts. For this reason, the more coordinatively unsaturated, positively charged, diphosphine, bis-solvento complex  $[Pd(dppb)(MeCN)_2]^{2+}$  was found to be very efficient catalyst for the coupling of cyclopentadiene with unsaturated aldehydes (see Scheme 1.15).<sup>67</sup>

**Scheme 1.15**



However, the results on this system are preliminary and more synthetic work will be necessary to optimise the catalytic conditions and better understand the catalytic mechanism.

## 1.6. The aim of this thesis

The previous section has shown how platinum(II) complexes can be used in homogeneous catalysis. In many mechanistic studies, platinum and palladium have been considered together in order to understand the main differences between the two metals. Usually, palladium is more catalytically active but more labile, whereas platinum is more inert and can therefore be used over a wide temperature range. For this reason, a lot of mechanistic studies have been carried out on platinum with a view to gain a better understanding of the catalytic steps of the more active palladium analogue. The mechanistic studies involved in the methoxycarbonylation of ethene promoted by the palladium catalyst elucidated the main intermediates involved in the catalytic cycle. However, there still remains further work to be done in order to completely understand the catalytic mechanism and the objective of this thesis is to understand more about the palladium catalyst and to explore the main differences between the platinum and the palladium systems.

Although catalytic tests have shown that the platinum complex,  $[\text{Pt}(\text{d}^t\text{bpx})(\text{dba})]$ , is very much less active for the methoxycarbonylation of ethene than the palladium analogue, *in situ* spectroscopic studies have been carried out in order to understand the main mechanistic differences between the catalytic activity of the palladium and platinum analogues.

## 1.7. References

- (1) A. Sen *Adv. Polym. Sci.*, **1986**, 73-74, 125.
- (2) A. Sen *Acc. Chem. Res.*, **1993**, 26, 303.
- (3) E. Drent and P.M.H. Budzelaar *Chem. Rev.*, **1996**, 96, 663.
- (4) E. Drent; J.A.M. van Broekhoven; M.J. Doyle *J. Organomet. Chem.*, **1991**, 417, 235.
- (5) Numerous Patents by Shell *U.S. Patent 4,904,744 (1990)*, *Eur. Pat. Appl. 400,719 (1990)*, *Eur. Pat. Appl. 373,725 (1990)*.
- (6) M.Heskins and J.E. Guillet *Macromolecules*, **1970**, 3, 224.
- (7) G.H. Hartley and J.E. Guillet *Macromolecules*, **1986**, 1, 413.
- (8) M.M. Brubaker; D.D. Coffman; H.H. Hoehn *J. Am. Chem. Soc.*, **1952**, 74, 1509.
- (9) A. Sen; Z. Jiang; J.T. Chen *Macromolecules*, **1989**, 22, 2012.
- (10) Z. Jiang and A. Sen *Macromolecules*, **1992**, 25, 880.
- (11) Du Pont; (M.M. Brubacher) *U.S. Patent 2,459,286 (1950)*.
- (12) W. Reppe and A. Mangin *U.S Patent 2,577,208 (1951)*.
- (13) W. Reppe and A. Mangin *Chem. Abstr.*, **1952**, 46, 6143.
- (14) T.M. Shryne and H.V. Holler *U.S. Patent 3,984,388 (1976)*.
- (15) T.M. Shryne and H.V. Holler *Chem. Abstr.*, **1976**, 85, 178219.
- (16) U. Klabunde; T.H. Tulip; D.C. Roe; S.D. Ittel *J. Organomet. Chem.*, **1987**, 334, 141.
- (17) Y. Iwashita and M. Sakaruba *Tetrahedron Lett.*, **1971**, 26, 2409.
- (18) A. Sen and J.S. Brumbaugh *J. Organomet. Chem.*, **1985**, 279, C5.
- (19) A. Gouch *British Pat. 1,081, 304 (1967)*; *Chem. Abstr.*, **1967**, 67, 100569.

- (20) D.M. Fenton *U.S Patent 4,076,911 (1978)*.
- (21) K. Nozaki *U.S Patent 3,835,123 (1974)*.
- (22) A. Sen and T.W. Lai *Organometallics* **1984**, 3, 866.
- (23) E. Drent *Eur. Pat. Appl. 121,965,A2 (1984)*; *Chem. Abstr.*, **1985**, 102, 46423.
- (24) C.E. Ash *J. Mater. Educ.*, **1994**, 16, 1.
- (25) F.C. Rix; M. Brookhart; P.S. Wite *J. Am. Chem. Soc.*, **1996**, 118, 4746.
- (26) C. Bianchini and A. Meli *Coord. Chem. Rev.*, **2002**, 225, 35.
- (27) A. Vavasori and L. Toniolo *J. Mol. Cat. A*, **1996**, 110, 13.
- (28) D.G. Cooper and J. Powell *Can. J. Chem.*, **1973**, 51, 1634.
- (29) D.A. Redfield and J.H. Nelson *Inorg. Chem.*, **1973**, 12, 15.
- (30) J.C.L.J. Suykerbuyk; E. Drent; P.G. Pringle (Shell) *WO 98/427/17*, priority date 26/03/97.
- (31) G.R. Eastham; R.P. Tooze; X.L. Wang; K. Whiston (INEOS/Lucite) *WO 96/19434*, priority date 22/12/94.
- (32) W. Clegg; G. R. Eastham; M. R. J. Elsegood; R. P. Tooze; Wang, X. L.; Whiston, K. W. *Chem. Comm.* **1999**, 1877.
- (33) K. Othmer *Encyclopedia of Chemical Technology*, **1995**, Wiley, New York, 4<sup>th</sup> edn., vol. 16, p.487.
- (34) G.R. Eastham *PhD Thesis*, **1996**, University of Durham.
- (35) S. Doherty; E.G. Robins; J.G. Knight; C.R. Newman; B. Rhodes; P.A. Champkin; W. Clegg *J. Organomet. Chem.*, **2001**, 640, 182.
- (36) J.G. Knight; S. Doherty; A. Harriman; E.G. Robins; M. Betham; G.R. Eastham; R.P. Tooze; M.R.J. Elsegood; P. Champkin; W. Clegg *Organometallics*, **2000**, 19, 4957.

- (37) D.J. Cole-Hamilton and R.A.M. Robertson *in press* **2002**.
- (38) G. R. Eastham; B. T. Heaton; J. A. Iggo; R. P. Tooze; R. Whyman; S. Zacchini *Chem. Comm.*, **2000**, 609.
- (39) W. Clegg; G.R. Eastham; M.R.J. Elsegood; B.T. Heaton; J.A. Iggo; R.P. Tooze; R. Whyman; S. Zacchini *Organometallics*, **2002**, *21*, 1832.
- (40) V.V. Grushin *Chem. Rev.*, **1996**, *96*, 2011.
- (41) W. Clegg; G. R. Eastham; M. R. J. Elsegood; B.T. Heaton; J.A. Iggo; R. P. Tooze; R. Whyman; S. Zacchini *J. Chem. Soc., Dalton Trans.*, **2002**, 3300.
- (42) S. Zacchini *PhD Thesis*, **2001**, University of Liverpool.
- (43) T.M. Conroy-Lewis; L. Mole; A.D. Redhouse; S.A. Listen; J.L. Spencer *Chem. Comm.*, **1991**, 1601.
- (44) K. Osokada; Y. Ozawa; A.J. Yamamoto *J. Chem. Soc., Dalton Trans.*, **1991**, 759.
- (45) D.Drago; P.S. Pregosin *J.Chem. Soc., Dalton Trans.*, **2000**, 3191.
- (46) N. Carr; L. Mole; A. Guy Orpen; J. L. Spencer *J. Chem. Soc.,Dalton Trans.*, **1992**, 2653.
- (47) P.M. Maitlis; A. Haynes; G.J. Sunley; M.J. Howard *J.Chem. Soc., Dalton Trans.*, **1996**, 2187.
- (48) W. Strohmeier; L. Weigelt *Z. Naturforsch.*, **1976**, *31b*, 387.
- (49) G.W. Parshall; S.D. Ittel *Homogeneous Catalysis*, **1992**, Second Ed.,ed. John Wiley & Sons, Inc., section 3.
- (50) A. Scrivanti; A. Berton; L. Toniolo; C. Botteghini *J. Organomet. Chem.*, **1986**, *314*, 369.
- (51) G.K. Anderson; H.C. Clark; J.A. Davies *Organometallics*, **1982**, *1*, 64.

- (52) T. Hayashi; Y. Kawabata; T. Isoyama; I. Ogata *Bull. Chem. Soc. Jpn.*, **1981**, *54*, 3438.
- (53) A. Scrivanti; C. Botteghini; L. Toniolo; A. Berton *J. Organomet. Chem.*, **1988**, *344*, 261.
- (54) D.A. Slack; M.C. Baird *Inorg. Chim. Acta*, **1977**, *24*, 277.
- (55) K.M. Mackay; B.K. Nicholson in G. Wilkinson; F.G.A. Stone and E.W. Able (Eds.) *Comprehensive Organometallic Chemistry*, **1982**, Pergamon Press, Oxford, Vol.6, p.1043.
- (56) J.P. Collman; L.S. Hegeudus; J.R. Norton; R. Finke *Principles and Applications of Organotransition Metal Chemistry*, **1987**, University Science Book, Mill Valley.
- (57) G. Strukul *Topics in Catalysis*, **2002**, *19*, 33.
- (58) A. Baeyer and V. Villiger *Berichte*, **1899**, *32*, 3625.
- (59) R. Criegee *Justus Liebigs Ann. Chem.*, **1948**, *560*, 127.
- (60) M. Del Todesco Frisone; F. Pinna; G. Strukul *Organometallics*, **1993**, *12*, 148.
- (61) R. Gavagnin; M.Cataldo; F. Pinna; G. Strukul *Organometallics*, **1998**, *17*, 661.
- (62) T.W. Green *Protective Groups in Organic Synthesis*, **1981**, (Wiley-Interscience, New York).
- (63) F. Gorla and L.M. Venanzi *Helv. Chim. Acta*, **1990**, *73*, 690.
- (64) M. Cataldo; E. Nieddu; R. Gavagnin; F. Pinna; G. Strukul *J. Mol. Catal. A*, **1999**, *142*, 305.

- (65) W. Carruthers *Cycloadditions Reactions in Organic Chemistry*, **1990**,  
(Pergamon, Oxford).
- (66) O. Fujimura *J. Am. Chem. Soc.*, **1998**, *120*, 10032.
- (67) K. Pignat; J. Vallotto; F. Pinna; G. Strukul *Organometallics*, **2000**, *19*, 5160.

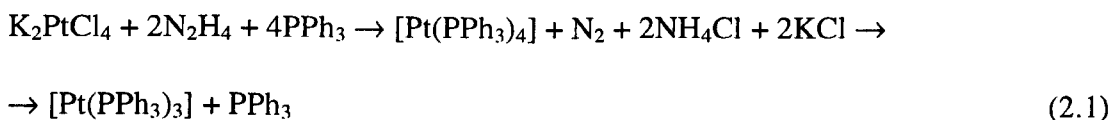
# **Chapter Two**

## 2. Characterisation of [Pt(d<sup>t</sup>bpx)(dba)]

### 2.1. Introduction

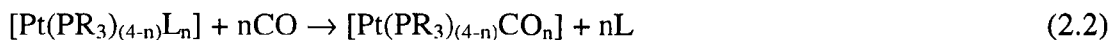
The principal oxidation states of platinum are II and IV, but more recently the chemistry of Pt(0) has been increasingly developed. In most cases, Pt(0) binds to PR<sub>3</sub>, CO, or other π-acid ligands such as η<sup>2</sup>-monoalkene and η<sup>n</sup>-polyene. In particular, platinum π-complexes are used as catalyst precursors in many organic transformations.

The most common monomeric phosphine complex is [Pt(PPh<sub>3</sub>)<sub>3</sub>], which is formed by the reduction of K<sub>2</sub>PtCl<sub>4</sub> with N<sub>2</sub>H<sub>4</sub> in the presence of four equivalents of PPh<sub>3</sub> in ethanol.<sup>1</sup> The product formed is [Pt(PPh<sub>3</sub>)<sub>4</sub>] but it dissociates giving the three coordinate complex [Pt(PPh<sub>3</sub>)<sub>3</sub>]; this behavior is found for most of the [M(PR<sub>3</sub>)<sub>4</sub>] complexes and the dissociation is due to the cone angle of the phosphine and electronic factors.<sup>2,3</sup>

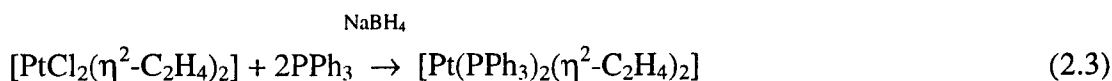


Compounds of platinum and carbon monoxide alone remain accessible only by particular isolation methods. The most stable and common carbonyl platinum(0) complexes contain carbon monoxide and triaryl and trialkyl phosphines. The 16-electrons complex [Pt(PPh<sub>3</sub>)<sub>3</sub>] reacts easily with CO at 193 K to form [Pt(PPh<sub>3</sub>)<sub>3</sub>(CO)], which forms [Pt(CO)<sub>2</sub>(PPh<sub>3</sub>)<sub>2</sub>] at 208 K.<sup>2</sup> Also, the dihydrogen in

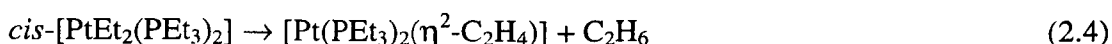
[Pt(PEt<sub>3</sub>)<sub>2</sub>H<sub>2</sub>] is readily displaced by  $\pi$ -acceptor ligands such as carbon monoxide with the formation of the *cis* square planar complex [Pt(PEt<sub>3</sub>)<sub>2</sub>(CO)<sub>2</sub>].<sup>4</sup>



Other important complexes where a  $\pi$ -acid ligand is involved are  $\eta^2$ -monoalkene complexes. They mostly form three-(16 electron) and four-coordinate (18 electron) structures and complexes of the general class [PtL<sub>2</sub>( $\eta^2$ -C<sub>2</sub>H<sub>4</sub>)<sub>2</sub>] (L = a group 15 electron donor) are easily formed. For example, [Pt(PPh<sub>3</sub>)<sub>2</sub>( $\eta^2$ -C<sub>2</sub>H<sub>4</sub>)<sub>2</sub>] is formed by treatment in dichloromethane/ethanol solution of [PtCl<sub>2</sub>( $\eta^2$ -C<sub>2</sub>H<sub>4</sub>)<sub>2</sub>] with NaBH<sub>4</sub> in the presence of PPh<sub>3</sub> and ethene, at ambient pressure.<sup>5</sup>



Sodium naphthalenide is effective in the preparation of the class of complexes [PtL<sub>2</sub>( $\eta$ -C<sub>2</sub>H<sub>4</sub>)<sub>2</sub>] where L = PEt<sub>3</sub>, PPr<sub>3</sub>, PEt<sub>2</sub>Ph, PPh<sub>3</sub>;<sup>6,7</sup> L<sub>2</sub> = dppe,<sup>8</sup> dcpe, dcpp, dcpb.<sup>7</sup> A convenient route to [Pt(PEt<sub>3</sub>)<sub>2</sub>( $\eta^2$ -C<sub>2</sub>H<sub>4</sub>)] is provided by the thermolytic rearrangement of *cis*-[PtEt<sub>2</sub>(PEt<sub>3</sub>)<sub>2</sub>] via  $\beta$ -hydrogen transfer and reductive C-H elimination.<sup>9</sup>



The unconjugated diene derivative of platinum(0) [Pt(cod)<sub>2</sub>] is a very useful precursor to other zerovalent platinum complexes, including those with monoalkenes.<sup>10</sup> [Pt(cod)<sub>2</sub>] can be used to prepare complexes containing both  $\eta^2$ -alkene and phosphine (or other) ligands using the appropriate stoichiometric amount of reagents. A range of [PtL<sub>2</sub>( $\eta^2$ -norbornene)] complexes with bidentate phosphines,

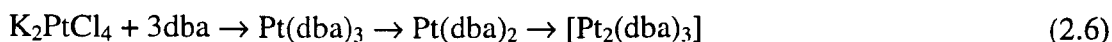
$L_2$ , has been synthesized by reaction of  $[Pt(\eta^2\text{-norbornene})_3]$  with appropriate diphosphines (dcpe, dcpp, dbpe, dbpp).<sup>11</sup> Reactions of  $[Pt(dba)_2]$  with other alkenes should be considered. For example,  $[Pt(dba)_2]$  reacts with equimolar amounts of maleic anhydride and hexa-1,5-diene to form  $[Pt(\eta^2\text{-C}_4\text{H}_2\text{O}_3)(\eta^2, \eta^2\text{-C}_6\text{H}_{10})]$ .<sup>12</sup>

However, the most versatile  $\eta^n$ -polyene complex is  $[Pt(\text{cod})_2]$ . It is formed from  $[Pt(\text{nb})_3]$ , by reduction of  $[PtCl_2(\text{cod})]$  with  $[Li_2(\text{cod})]$ .<sup>13</sup>



This compound is a useful precursor to other platinum(0) derivatives by displacement of both cod ligands. The molecular structure has been determined by X-ray diffractometry and displays a quasi-tetrahedral disposition of the four  $\eta^2$ -alkene groups.<sup>14</sup>

Another important platinum complex containing an olefinic ligand is  $[Pt(\text{dba})_n]$  ( $n = 2$  or  $3$ ) (dba = dibenzylideneacetone). It has been reported in 1971 for the first time following the characterization of  $[Pd(\text{dba})_2]$ .  $[Pt(\text{dba})_2]$  has been prepared by the reaction of  $K_2PtCl_4$  with 3 equivalents of dba in refluxing aqueous ethanol under nitrogen in the presence of sodium acetate. Whereas, the tris-complex,  $Pt(\text{dba})_3$  can be obtained by refluxing the same mixture in the presence of air or oxygen.<sup>15</sup> Subsequent work has suggested that three compounds are present in equilibrium, as shown in equation 2.6:<sup>16</sup>



However, there has been some contradiction concerning the structures of these complexes. Recently, it has been shown that platinum coordinates to dba *via* the  $\pi$ -

olefin group and does not involve coordination of the ketonic group as proposed originally in 1971.<sup>17</sup> The single-crystal X-ray structure has been reported and it shows that the complex adopts an apparent binuclear structure with three bridging dba units, where the second platinum position is only present at 44% of the time. This structure has been confirmed by the <sup>195</sup>Pt NMR spectrum which shows that the two nonequivalent platinum atoms are coupled to each other. This spectrum indicates that only the full occupancy dimer is present in solution.<sup>17</sup>

These dba platinum complexes have been used as starting materials for the preparation of a range of platinum(0) complexes because of the relatively easy displacement of dba by other ligands. Complexes of the type [PtL<sub>2</sub>(dba)] can be prepared by treatment of a toluene solution of [Pt(dba)<sub>2</sub>] with an excess of L ligand (L = PPh<sub>3</sub>, PPh<sub>2</sub>Me, PEt<sub>3</sub>). [Pt(PPh<sub>3</sub>)<sub>2</sub>(dba)] can also be prepared from the reaction of [Pt(PPh<sub>3</sub>)<sub>4</sub>] with an excess of dba.



The formation of [Pt(PPh<sub>3</sub>)<sub>2</sub>(olefin)] has been observed during the reaction of [Pt(dba)<sub>2</sub>] with two equivalents of PPh<sub>3</sub> in the presence of an excess of olefin.<sup>18</sup>

So far, there are only a few other synthetic procedures involving [Pt(dba)<sub>2</sub>] and diphosphines P-P and aminophosphine P-N ligands. [Pt(dba)<sub>2</sub>] reacts with N, N-bis(dicyclohexylphosphinomethyl)methylamine, (Cy<sub>2</sub>PCH<sub>2</sub>)<sub>2</sub>NMe and N, N-bis(diphenylphosphinomethyl)methylamine, (Ph<sub>2</sub>PCH<sub>2</sub>)<sub>2</sub>NMe, to give the complex [Pt(dba){(R<sub>2</sub>PCH<sub>2</sub>)<sub>2</sub>NMe}]. Recently, it has been observed that the dba ligand is firmly attached to the platinum and is not displaced by ligands, such as diphenylacetylene, carbon monoxide, tertiary-t-butyl isocyanide or

diphenylmethylphosphine on reaction overnight at room temperature in benzene solution.<sup>19</sup>

The lack of reports of the reaction of [Pt(dba)<sub>2</sub>] with diphosphine bidentate ligands should be compared with the chemistry of palladium which has been fully described and the role of the ligand in the palladium-catalysis has been studied. Mixtures of [Pd(dba)<sub>2</sub>] with one equivalent of L-L (L-L = dppm, dppe, dppp, dppb and diop) lead to [Pd(L-L)(dba)] complexes via the formation of the complex [Pd(L-L)<sub>2</sub>] which then slowly con-proportionate with unreacted [Pd(dba)<sub>2</sub>] to generate [Pd(L-L)(dba)].<sup>20</sup>

## 2.2. Characterisation of [Pt(d<sup>t</sup>bpx)(dba)], **1**

The complex [Pt(d<sup>t</sup>bpx)(dba)], **1**, (d<sup>t</sup>bpx = 1,2-bis(di-tert-butylphosphinomethyl)benzene) is prepared by the reaction of [Pt(dba)<sub>2</sub>] with one equivalent of d<sup>t</sup>bpx ligand in THF, using a similar procedure to that used for the synthesis of [Pd(d<sup>t</sup>bpx)(dba)]. However, the rates of these two reactions are quite different. In the case of palladium, [Pd(d<sup>t</sup>bpx)(dba)] is quantitatively obtained after a few hours, whereas the formation of the platinum complex **1** occurs after one week at room temperature. This is probably because of the stronger interaction between platinum and the dba ligand, which results in the substitution of the dba ligand being faster in the palladium complex than in the platinum complex **1**.

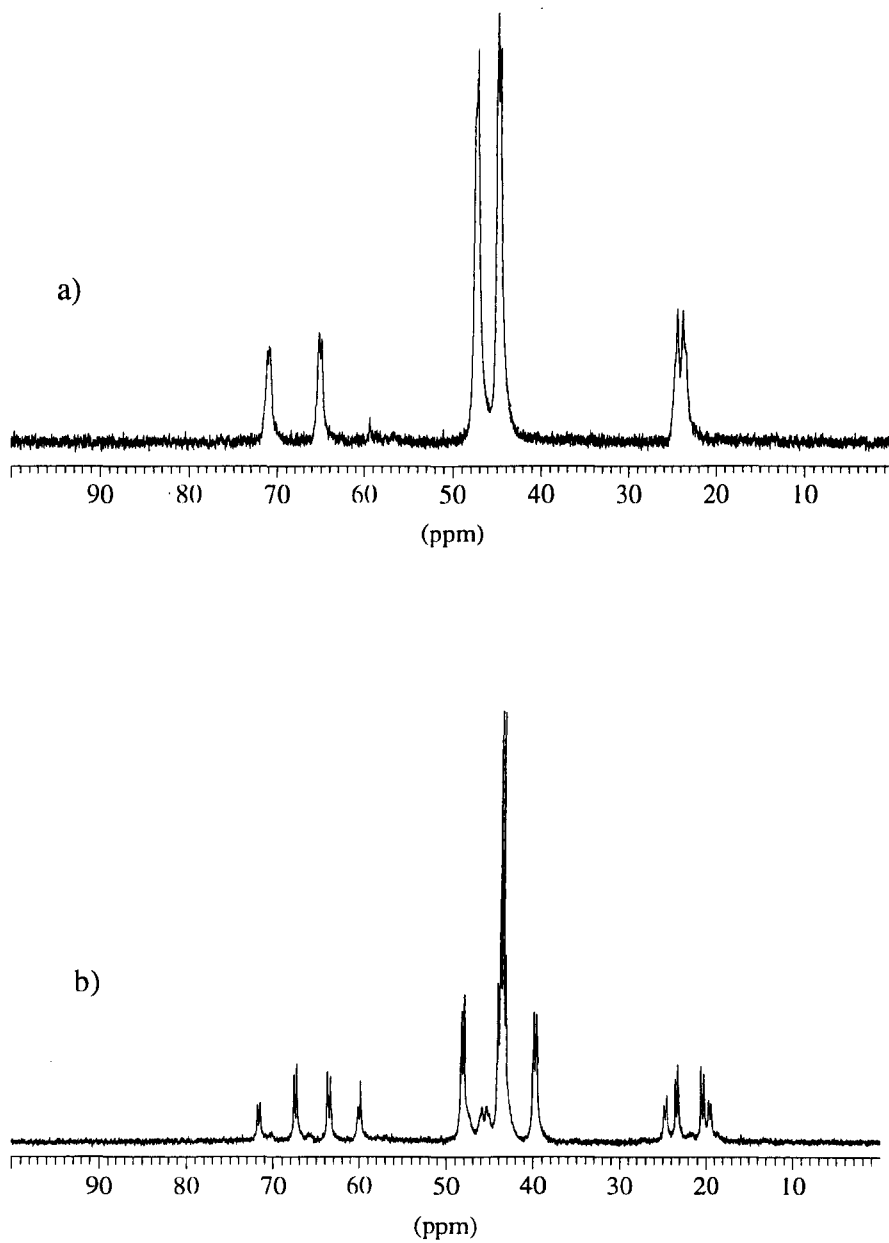
[Pt(d<sup>t</sup>bpx)(dba)], **1**, is not very soluble in methanol; as a result, the characterisation has been done in THF, in which the complex is completely soluble. The <sup>31</sup>P{<sup>1</sup>H} NMR spectrum shows two broad resonances, whereas at 193 K two

different sets of doublets are present (see Figure 2.1). All the resonances of the phosphorus spectrum show platinum satellites, with different phosphorus-platinum coupling constants (see Table 2.1).

Therefore, two main compounds **1A** and **1B** are clearly present in solution at low temperature. The compound **1A** shows a second order NMR spectrum, where the spins are strongly coupled; instead the compound **1B** shows a first order NMR spectrum (see Figure 2.2). Close inspection of the baseline reveals the presence of a minor conformer (at ca. 45 ppm) which gives rise to another AB pattern, second order spectrum. Hence, [Pt(d<sup>t</sup>bpx)(dba)], **1**, can exist in solution as different conformers, due to the different orientations of the dba chain with respect to the plane containing the platinum and the two phosphorus atoms. The broadening of the spectrum on increasing the temperature, clearly indicates the presence of an exchange process between the two main conformers. However, since there are two different resonances in the spectrum at room temperature, the two phosphorus atoms must remain inequivalent during the exchange process. This confirms that the exchange process involves only the movement of the dba chain and the atoms directly coordinated to the platinum-center do not move. The same behavior has been observed in the  $^{195}\text{Pt}\{^1\text{H}\}$  NMR spectrum (see Figure 2.3), which shows only a doublet of doublets at 293 K, whereas at 193 K two different sets of doublet of doublets are present. This means that there must be two different conformers giving rise to two different platinum resonances.

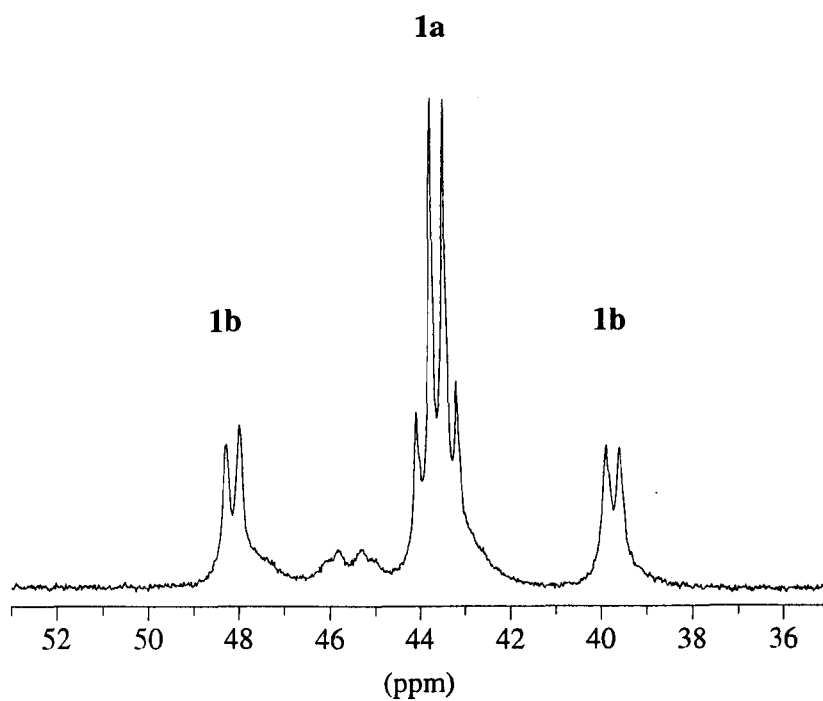
**Figure 2.1**

$^{31}\text{P}\{^1\text{H}\}$  NMR spectra of [Pt(*d*<sup>4</sup>bpx)(dba)], **1**, in THF, (a) 293 K,  
(b) 193 K



**Figure 2.2**

$^{31}\text{P}\{^1\text{H}\}$  NMR spectrum of [Pt(*d'*bpx)(dba)], **1**, in THF at 193 K  
(expansion)

**Table 2.1**

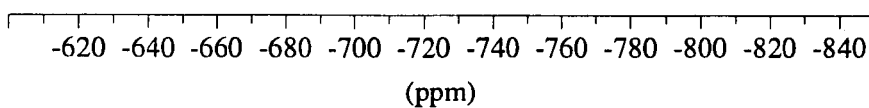
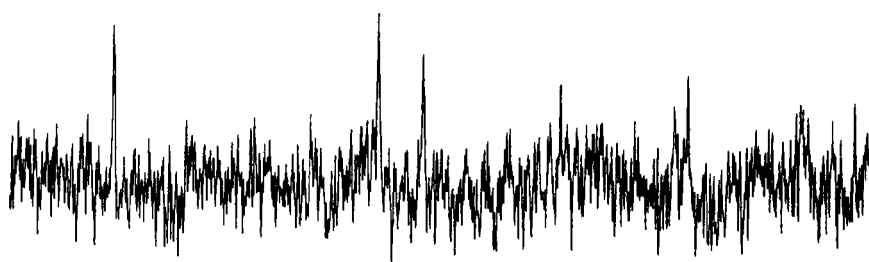
NMR data for the two conformers of [Pt(*d'*bpx)(dba)], **1**,  
at 193 K in THF

	$\delta\text{P}_1$ (ppm)	$\delta\text{P}_2$ (ppm)	$\delta\text{Pt}$ (ppm)	$^2J(\text{P}_1\text{-P}_2)$ (Hz)	$^1J(\text{Pt-P}_1)$ (Hz)	$^1J(\text{Pt-P}_2)$ (Hz)
<b>conf. A</b>	43.9	43.4	737.6	25	3808	3257
<b>conf. B</b>	48.2	39.8	726.7	23	3805	3270

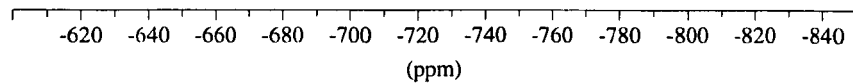
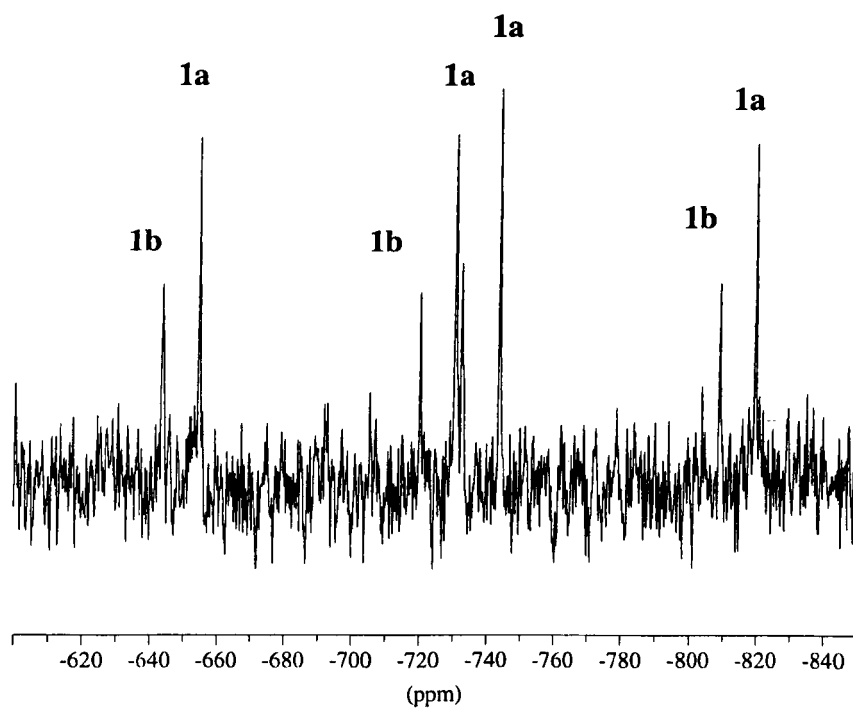
Figure 2.3

$^{195}\text{Pt}\{^1\text{H}\}$  NMR spectra of [Pt(*d*bpx)(dba)], **1**, in THF, (a) 293 K,  
(b) 193 K

a)



b)

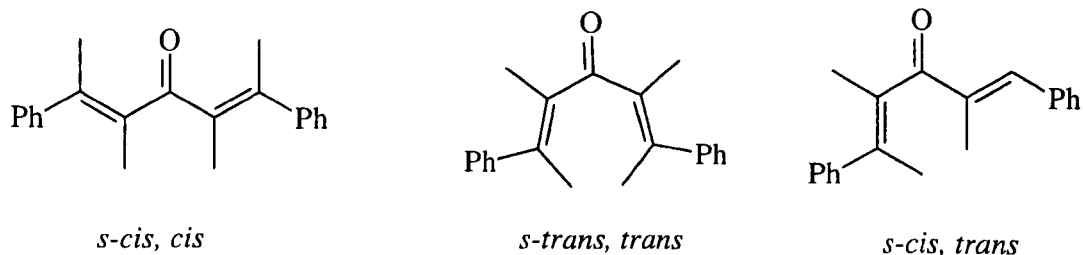


### 2.3. Dynamic NMR studies of [Pt(d<sup>4</sup>bpx)(dba)], 1

Synthetic, structural and dynamic NMR studies of [Pd(<sup>i</sup>Pr<sub>2</sub>PCH<sub>2</sub>CH<sub>2</sub>P<sup>i</sup>Pr<sub>2</sub>)(dba)] have been reported recently.<sup>21</sup> The X-ray crystallographic structure of [Pd(d<sup>1</sup>ppe)(dba)] shows that the coordinated dba ligand adopts a *s-trans, s-trans* conformation in which the palladium is coordinated to one C=C bond in a  $\eta^2$ -conformation. In the dba ligand, two degrees of rotational freedom are due to the two single bonds and this means that, as found for free dba, coordinated dba can exist as three different and easily interconvertible conformers: *s-cis, cis*; *s-trans, trans* and *s-cis, trans* forms, where *s-cis* and *s-trans* refers to the orientation of the olefin with respect to the keto group (see Scheme 2.1).<sup>22</sup> Actually, variable temperature NMR studies of coordinated dba indicate that two distinct processes must be taken into account. The first process considers the exchange between coordinated and free double bond of dba. For this process, an intramolecular mechanism has been proposed and it involves different conformers where the two phosphorus nuclei remain inequivalent and dba ligand assumes one of the three different conformers described earlier.<sup>21</sup> (Scheme 2.2)

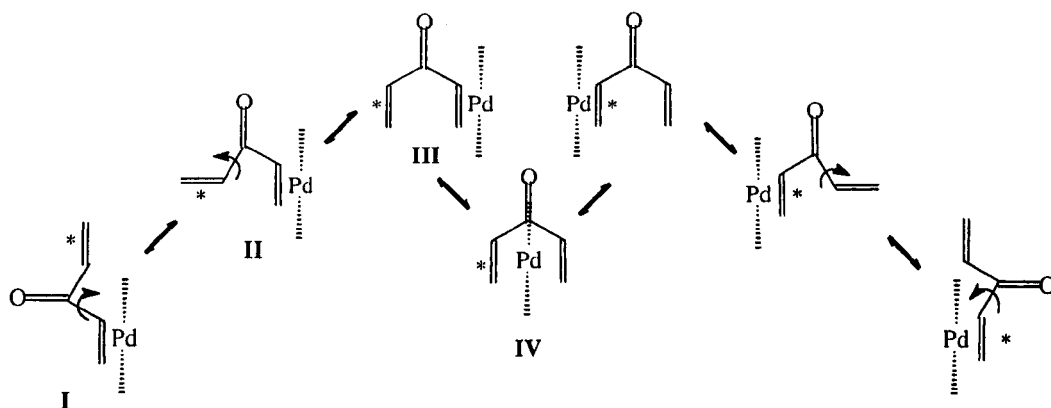
#### Scheme 2.1

##### *Three different conformers of the dba ligand*



## Scheme 2.2

Proposed intermolecular exchange of coordinated and uncoordinated double bonds in [Pd(*d*'ppe)(dba)]



The *s*-*trans*, *trans* conformer **I** can give the *s*-*cis*, *trans* conformer **II** by successive rotation by 180° about each CO-C(H)C(Ph) single bond, followed by formation of the *s*-*cis*, *cis* conformer **III**. The exchange of the coordinated and uncoordinated double bond occurs from the conformer **III** via the transition state **IV**, where the palladium assumes a pseudo-tetrahedral geometry. The mechanism proposed is analogous to that proposed for trigonal planar complexes of the type [Pd(R<sub>2</sub>PCH<sub>2</sub>CH<sub>2</sub>PR<sub>2</sub>)(η<sup>2</sup>-C<sub>4</sub>H<sub>6</sub>)] in which intramolecular exchange of coordinated and uncoordinated butadiene double bond was observed.<sup>23,24</sup> The same mechanism was used to explain similar double bond exchange in [Ni(<sup>*i*</sup>Bu<sub>2</sub>PCH<sub>2</sub>CH<sub>2</sub>P<sup>*i*</sup>Bu)<sub>2</sub>(C<sub>4</sub>H<sub>6</sub>)] and [Pd(R<sub>2</sub>PCH<sub>2</sub>CH<sub>2</sub>PR<sub>2</sub>)(1,5-C<sub>6</sub>H<sub>10</sub>)] (R = <sup>*i*</sup>Pr, <sup>*i*</sup>Bu).<sup>25,26</sup>

The second process involves interconversion of the conformers of dba shown in Scheme 2.1 and Scheme 2.2 and in both the processes the rotation around the metal-ligand axis is not involved.

There are no X-ray crystallographic data of the structure of [Pt(d<sup>t</sup>bpx)(dba)], **1**, and no NMR studies of the dynamic behavior of the platinum complex have been reported in the literature. The <sup>31</sup>P{<sup>1</sup>H} and <sup>195</sup>Pt{<sup>1</sup>H} NMR spectra of **1** at 193 K show the presence of two main conformers in the ratio 2:1 (see Figure 2.1b). The major abundance of the conformer **1A** is due to much more facile isomer interconversion. Both conformers show an AB pattern where the two phosphorus nuclei remain inequivalent over the temperature range 193-293 K. It is impossible from these NMR measurements to unambiguously assign the exact conformation of the dba ligand which gives rise to these different resonances. Probably, the most favorable conformers of the dba chain coordinated to the metal are *s-trans*, *trans* and *s-cis*, *trans*, considering that the dba and d<sup>t</sup>bpx are quite bulky ligands. In this case, at 293 K the two conformers exchange and the <sup>31</sup>P{<sup>1</sup>H} NMR spectrum shows that the two phosphorus of **1A** and the two phosphorus of **1B** appear equivalent and coalesce. Whereas, at low temperature this exchange can be 'frozen'.

## 2.4. References

- (1) R.S. Paonessa; A.L. Prignano; W.C. Trogler *Organometallics*, **1985**, *4*, 647.
- (2) A. Sen and J. Halpern *Inorg. Chem.*, **1980**, *19*, 1073.
- (3) B.E. Mann and A. Musco *J. Chem. Soc. Dalton Trans.*, **1980**, 776.
- (4) R.S. Paonessa and W.C. Trogler *J. Am. Chem. Soc.*, **1982**, *104*, 1138.
- (5) U. Nagel *Chem. Ber.* **1982**, *115*, 1998.
- (6) R.A. Head *Inorg. Synth.*, **1985**, *24*, 213.
- (7) R.A. Head *Inorg. Synth.*, **1990**, *28*, 132.
- (8) M. Camalli; F. Caruso; S. Chaloupka; E. M. Leber; H. Rimm; L.M. Veneziani *Helv. Chim. Acta*, **1990**, *73*, 2263.
- (9) R.G. Nuzzo; T.J. McCarthy; G.M. Whitesides *Inorg. Chem.*, **1981**, *20*, 1312.
- (10) W.E. Watts 'Organometallic Chemistry', *Specialistic Periodical Report*, R.S.C., London, **1982**, *10*, 283.
- (11) N. Carr; B. J. Dunne; L.Mole; A. Guy Orpen; J. L. Spencer *J.Chem.Soc.Dalton Trans*, **1991**, 863.
- (12) G.B. Stackhouse IV and L.L. Wright *Inorg. Chim. Acta* **1988**, *150*, 5.
- (13) L.E. Crascall and J.L. Spencer *Inorg. Synth.*, **1990**, *28*, 126.
- (14) J.A.K. Howard *Acta. Crystallogr., Sect. B*, **1982**, *38*, 2896.
- (15) K. Moseley and P. M. Maitlis *Chem.Comm.*, **1971**, 982.
- (16) M.C.Mazza and C.G Pierpont *Inorg. Chem.* **1973**, *12*, 2955.
- (17) L.N.Lewis; T.A.Krafft; J.C. Huffman *Inorg. Chem.* **1992**, *31*, 3555.
- (18) W. J. Cherwinski; B. F. G. Johnson; J. Lewis *J.Chem.Soc.Dalton*, **1974**, 1405.

- (19) J. Fawcett; R. D. W. Kemmitt; D. R. Russell; O. Serindag *J. Organomet. Chem.*, **1995**, 486, 171.
- (20) C. Amatore and A. Jutand *Coord. Chem. Rev.*, **1998**, 178-180, 511.
- (21) S. M. Reid; J.T. Mague; M. J. Fink *J. Organomet. Chem.*, **2000**, 616, 10.
- (22) F.A. Jalon; B.R. Manzano; F.Gomez-de la Torre; A.M. Lopez-Agenjo *J. Chem. Soc., Dalton Trans.*, **2001**, 2417.
- (23) R. Benn; P.W. Jolly; T. Joswing; R. Mynott; K.-P. Schick *Z. Naturforsch. Teil*, **1986**, B 41, 680.
- (24) R. Benn; P. Betz; R. Goddard; P.W. Jolly; N. Kokel; C. Kruger; I. Topalovic *Z. Naturforsch. Teil*, **1991**, B 46.
- (25) K.R. Porschke; C. Pluta; B. Proft; F. Lutz *Z. Naturforsch. Teil*, **1993**, B 48.
- (26) J. Krause; W. Bonrath; K.R. Porschke *Organometallics*, **1992**, 11.

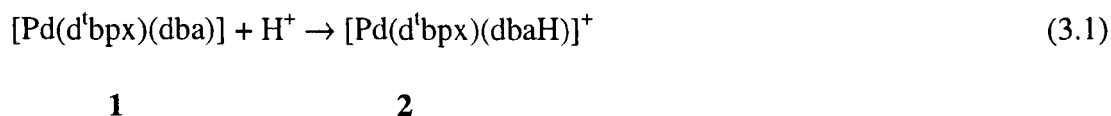
# **Chapter Three**

### 3. Reactivity of [Pt(d<sup>t</sup>bpx)(dba)] with acids

#### 3.1. The CF<sub>3</sub>SO<sub>3</sub>H-system

##### 3.1.1. Protonation of [Pt(d<sup>t</sup>bpx)(dba)], **1**

In the case of palladium, [Pd(d<sup>t</sup>bpx)(dba)] reacts with RSO<sub>3</sub>H (R = CF<sub>3</sub>SO<sub>3</sub>H or CH<sub>3</sub>SO<sub>3</sub>H) to give initially a complex containing the protonated dba ligand and this complex exists as two conformers in solution.<sup>1</sup> It has been shown by X-ray diffraction and by IR and NMR spectroscopy that protonation occurs on the oxygen atom of the C=O bond, as found for α,β-unsaturated ketones (see Equation 3.1).<sup>2</sup>



It is possible to assume a similar behaviour in the case of platinum, since there is a clear similarity in the palladium and platinum <sup>31</sup>P{<sup>1</sup>H} NMR spectra of both complexes at low temperature (see Figure 3.1). Also, in this case two conformers **A** and **B** are formed, due to the different conformations of the dba ligand (see Section 2.3). The only difference is that in the palladium spectrum four doublets are present, whereas in the platinum spectrum it is possible to see only four singlets. Probably the phosphorus-phosphorus coupling constant is too small to be resolved for the [Pt(d<sup>t</sup>bpx)(dbaH)][CF<sub>3</sub>SO<sub>3</sub>], **2a**, complex. Spencer<sup>3</sup> has reported examples in which protonation of [Pt(P-P)(olefin)] containing non substituted olefins (*e.g.* ethene,

styrene, norborn-2-ene) gives  $[\text{Pt}(\overline{\text{P-P}})(\text{CH}_2\text{CH}_3)]^+$  which contains a  $\beta$ -agostic Pt-H interaction as a result of the protonation of the C=C bond. This contrasts with the protonation of  $\alpha,\beta$ -unsaturated ketones, such as benzoquinone ligand in Pd(cod)(benzoquinone),<sup>4</sup> which results in the protonation of the oxygen. Hence, it seems that when the ligand is a substituted olefin, protonation does not occur on the C=C bond. In agreement with this conclusion, the complex formed during the protonation of [Pt(d<sup>t</sup>bpx)(dba)], **1**, is actually [Pt(d<sup>t</sup>bpx)(dbaH)][CF<sub>3</sub>SO<sub>3</sub>], **2a**.

The reaction between [Pt(d<sup>t</sup>bpx)(dba)], **1**, and CF<sub>3</sub>SO<sub>3</sub>H has been carried out in MeOH by addition of incremental amounts of acid and monitoring the <sup>31</sup>P{<sup>1</sup>H} NMR spectrum immediately at 193 K. All the phosphorus NMR spectra show that the two conformers are formed and reach a maximum after the addition of one mole of acid per mole of metal complex; further addition of acid (10 equivalents) has no effect on the phosphorus spectrum. All the NMR data for **2a** are reported in Table 3.1.

**Table 3.1**

*NMR data for the two conformers of [Pt(d<sup>t</sup>bpx)(dbaH)][CF<sub>3</sub>SO<sub>3</sub>], **2a**, at 193 K*

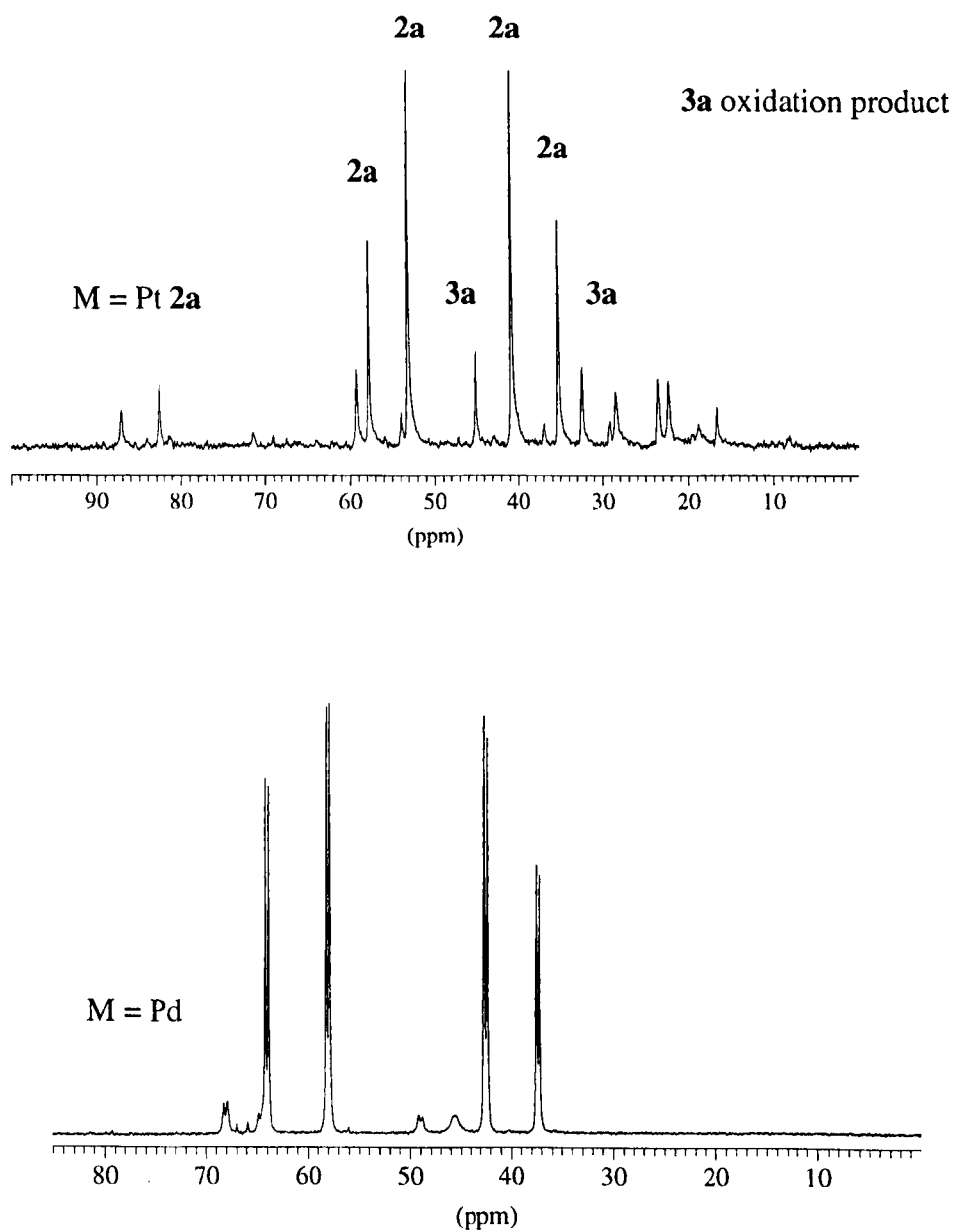
	$\delta\text{P}_1(\text{ppm})$	$\delta\text{P}_2(\text{ppm})$	$^1J(\text{P}_1\text{-Pt})(\text{Hz})$	$^1J(\text{P}_2\text{-Pt})(\text{Hz})$
<b>conformer A</b>	53.0	40.8	4733	2965
<b>conformer B</b>	57.7	35.5	4700	2994

As in the case of [Pd(d<sup>t</sup>bpx)(dba)], the platinum complex **1** is not very soluble in MeOH and forms a yellow solution with undissolved yellow solid. On addition of

acid, as found for palladium, the yellow solid completely dissolves to give a deep red solution due to the formation of **2a**.

**Figure 3.1**

$^{31}\text{P}\{^1\text{H}\}$  NMR spectra of  $[\text{M}(\text{d}^i\text{bpx})(\text{dbaH})][\text{CF}_3\text{SO}_3]$  in MeOH at 193 K

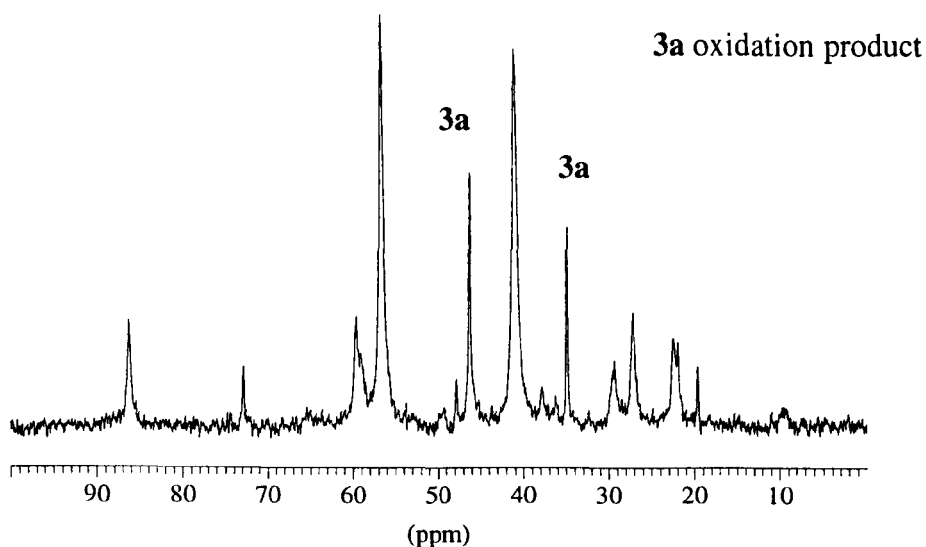


The protonated compound is very unstable and characterization proved to be very difficult. In fact, after some time even at low temperature the solution slowly changes from deep red to pale yellow and the  $^{31}\text{P}\{^1\text{H}\}$  NMR spectrum changes completely.

In all cases, it has also been possible to measure the  $^{31}\text{P}\{^1\text{H}\}$  NMR spectrum at room temperature (see Figure 3.2).

**Figure 3.2**

$^{31}\text{P}\{^1\text{H}\}$  NMR spectra of  $[\text{Pt}(\text{d}^1\text{bpx})(\text{dbaH})][\text{CF}_3\text{SO}_3]$ , **2a**, in MeOH at 290 K



As in the case of the analogous palladium complex, an exchange process between the two conformers occurs at room temperature: in fact only two broad resonances ( $\delta\text{P}_1 = 56.7$  ppm and  $\delta\text{P}_2 = 41.1$  ppm,  $^1J(\text{P}_1\text{-Pt}) = 4783$  Hz and  $^1J(\text{P}_2\text{-Pt}) = 3000$  Hz) are present. In the  $^{31}\text{P}\{^1\text{H}\}$  NMR spectrum reported in Figure 3.2, the two resonances at 46.3 ppm and 34.9 ppm are due to a partial oxidation (see Section 3.1.2). As described for  $[\text{Pt}(\text{d}^1\text{bpx})(\text{dba})]$ , **1**, this behaviour at room temperature suggests that

the exchange consists of the relative movement of the dba chain where the two phosphorus atoms always remain inequivalent (see Section 2.3).

### 3.1.2. Oxidation of [Pt(d<sup>1</sup>bpx)(dbaH)][CF<sub>3</sub>SO<sub>3</sub>], **2a**

Oxidation of [Pt(d<sup>1</sup>bpx)(dbaH)][CF<sub>3</sub>SO<sub>3</sub>], **2a**, can occur by bubbling oxygen through the solution as well as by the reaction of the platinum complex with benzoquinone in MeOH. The reaction with benzoquinone is quantitative and immediate (1 equivalent); on bubbling oxygen, the reaction is complete after about 30 minutes. Clearly, in the <sup>31</sup>P{<sup>1</sup>H} NMR spectrum at room temperature two main resonances with their satellites are present (see Figure 3.3 a). It is possible to resolve the phosphorus-phosphorus coupling constant which is about 6 Hz. Hence, we can conclude that the two main resonances are in fact two doublets with  $^2J(\text{P}_1\text{-P}_2) = 6$  Hz and the complex formed must contain two inequivalent phosphorus atoms. We propose that a metal hydride complex [Pt(d<sup>1</sup>bpx)H(MeOH)][CF<sub>3</sub>SO<sub>3</sub>H], **3a**, is formed, analogous to that found for the same reaction of the palladium complex. In fact, in the <sup>31</sup>P spectrum at room temperature (see Figure 3.3 b) the resonance at 34.6 ppm becomes a doublet with P-H coupling constant of 176 Hz. This is a typical value for a P-atom *trans* to a H-atom; the signal at lower field is always a singlet since  $^2J(\text{P-H})_{cis}$  is much smaller and is not resolved. In agreement with these hypotheses, the proton spectrum at room temperature in CD<sub>3</sub>OD shows a doublet of doublets at – 7.3 ppm (see Figure 3.4), the typical hydride region for this kind of compound. From this spectrum, the value of  $^2J(\text{P-H})_{trans}$  is found to be the same as in the <sup>31</sup>P NMR spectrum and these data are summarised in Table 3.2.

The same reaction has been repeated at 193 K and the formation of the hydride platinum complex occurs as at room temperature. There is no evidence for any inter- or intra-exchange processes and the system is not fluxional in the temperature range (193 K- 213 K).

**Figure 3.3**

$^{31}\text{P}\{^1\text{H}\}$  (a) and  $^{31}\text{P}$  (b) NMR spectra of  $[\text{Pt}(\text{d}^i\text{bpx})\text{H}(\text{MeOH})][\text{CF}_3\text{SO}_3]$ , **3a**, in MeOH at 290 K

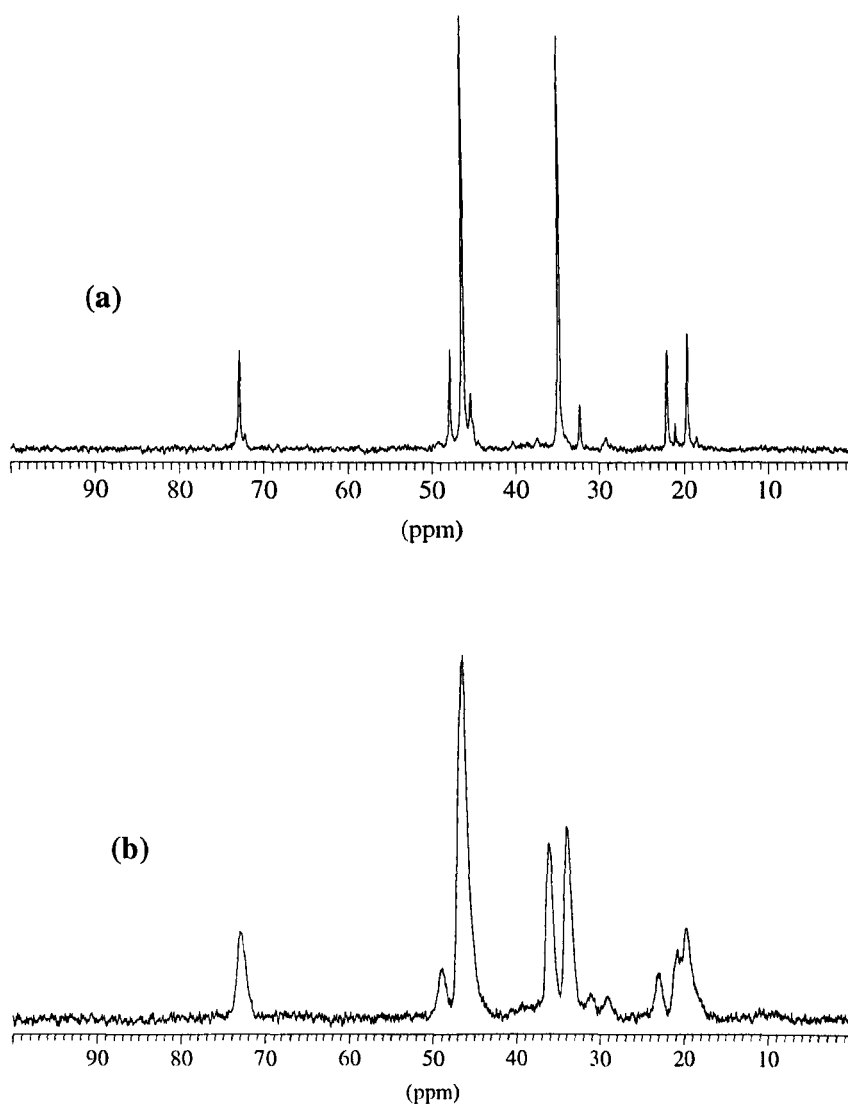
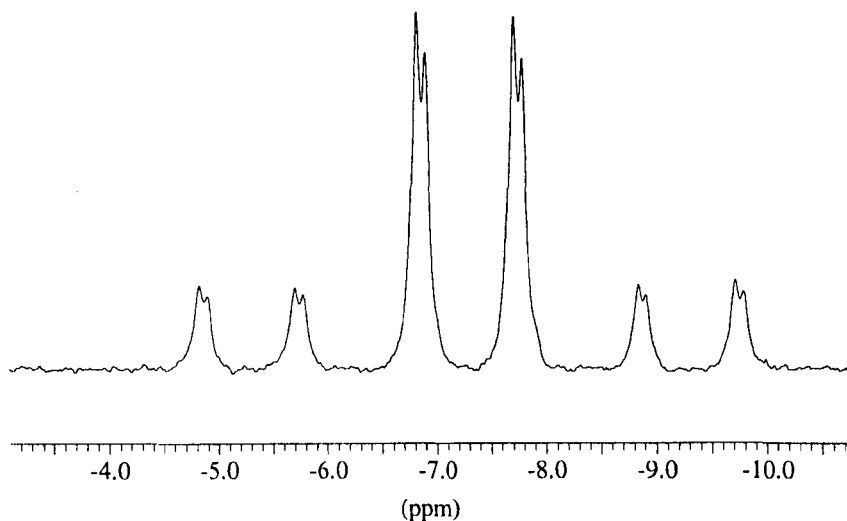


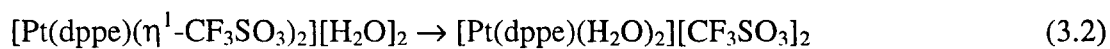
**Figure 3.4**

*<sup>1</sup>H NMR spectrum of [Pt(d<sup>1</sup>bpx)H(MeOH)][CF<sub>3</sub>SO<sub>3</sub>], **3a**, in MeOH at 290 K*



It has been observed that in tertiary alcohols or non-alcoholic media (*e.g.* <sup>1</sup>BuOH, THF, CH<sub>2</sub>Cl<sub>2</sub>, acetone) a platinum-hydride complex is not formed. For spectroscopic studies in these solvents, the hydride should first be synthesised in MeOH followed by removal of MeOH in vacuum and dissolution of the residue in the new solvent. The problem with this procedure is that the stability of the hydride in non-alcoholic solvents decreases in the presence of free acid, hence, it has been difficult to observe the complex **3a** using five equivalents of the acid. In fact, when Pt-hydride **3a** has been formed in MeOH and successively dried and redissolved in THF or CH<sub>2</sub>Cl<sub>2</sub>, the resonances due to **3a** almost disappear and new resonances appear, which are probably due to the formation of [Pt(d<sup>1</sup>bpx)(η<sup>1</sup>-CF<sub>3</sub>SO<sub>3</sub>)<sub>2</sub>] and [Pt(d<sup>1</sup>bpx)(sol<sub>v</sub>)<sub>2</sub>]<sup>2+</sup>. In the <sup>31</sup>P{<sup>1</sup>H} NMR spectrum in THF and CH<sub>2</sub>Cl<sub>2</sub>, a singlet at 16.8 ppm with <sup>1</sup>J(P-Pt) = 3774 Hz indicates the formation of [Pt(d<sup>1</sup>bpx)(H<sub>2</sub>O)<sub>2</sub>]<sup>2+</sup>. It has been reported that

when the analogous bis(triflate) products are treated with water or simply exposed to air, they readily form stable bis-aquo complexes:<sup>4,5</sup>



Some water could have been present in the acid.

There are not many platinum-hydride complexes containing monodentate phosphines with the two phosphorus atoms *cis* reported in the literature and the examples reported so far only contain chelating diphosphine ligands. The first example of a platinum hydride complex containing a bidentate phosphine was reported in 1976 by Shaw and co-workers;<sup>6</sup> the dichloride complex [Pt(d<sup>4</sup>bpx)Cl<sub>2</sub>] was reduced smoothly by sodium tetrahydroborate in ethanol to form the dihydride complex [Pt(d<sup>4</sup>bpx)H<sub>2</sub>], which from the reaction with HCl in Et<sub>2</sub>O formed the hydride complex [Pt(d<sup>4</sup>bpx)HCl] ( $\delta\text{H} = -7.69$  ppm,  $^2J(\text{P-H})_{\text{cis}} = 14$  Hz,  $^2J(\text{P-H})_{\text{trans}} = 190$  Hz,  $^1J(\text{H-Pt}) = 696$  Hz).

A platinum hydride complex has been observed as an intermediate during the catalytic hydroformylation of olefins.<sup>7</sup> [Pt(dcpp)HCl] results from the  $\beta$ -elimination reaction of the platinum ethyl complex [Pt(dcpp)(C<sub>2</sub>H<sub>5</sub>)Cl] ( $\delta\text{H} = -11.3$  ppm,  $^2J(\text{P-H})_{\text{cis}} = 11$  Hz,  $^2J(\text{P-H})_{\text{trans}} = 146$  Hz). All these NMR data agree with those reported in Table 3.2 for [Pt(d<sup>4</sup>bpx)H(MeOH)][CF<sub>3</sub>SO<sub>3</sub>], **3a**.

The main difference in the chemistry of analogous platinum and palladium complexes is apparent from the different stability of the hydride complex. Unlike the palladium hydride, the platinum analogue is very stable in MeOH and it does not decompose even after one week at room temperature. Further addition of oxygen or CF<sub>3</sub>SO<sub>3</sub>H has no effect on the phosphorus NMR spectrum. Generally, the platinum

compounds formed are more stable, the Pt-H bond is stronger than the Pd-H bond and in many cases the reactions of platinum hydrides are kinetically slower than for palladium.

**Table 3.2**

*NMR data for [Pt(*d*<sup>1</sup>bpx)H(MeOH)][CF<sub>3</sub>SO<sub>3</sub>], **3a**, in MeOH*

	@ 293 K	@ 193 K
$\delta P_1$ (ppm)	46.2	45.3
$\delta P_2$ (ppm)	34.6	32.6
$\delta H$ (ppm)	-7.3	-
$^2J(P_1-P_2)$ (Hz)	6.1	6.1
$^1J(P_1-Pt)$ (Hz)	4312	4255
$^1J(P_2-Pt)$ (Hz)	2095	2063
$^2J(P_1-H)_{cis}$ (Hz)	17.9	-
$^2J(P_2-H)_{trans}$ (Hz)	176	175
$^1J(Pt-H)$ (Hz)	805	-

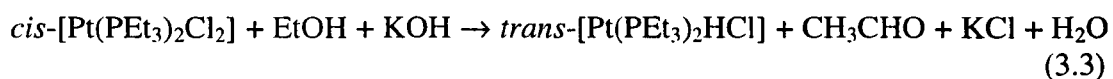
### 3.1.3. On the formation of the platinum hydride complex

Platinum(II) hydrides are usually obtained by reduction with hydrazine or alcohols in the presence of base,<sup>8,9</sup> or oxidative addition to Pt(0) complexes. Other methods include  $\beta$ -elimination reactions of platinum-alkyls, resulting in the

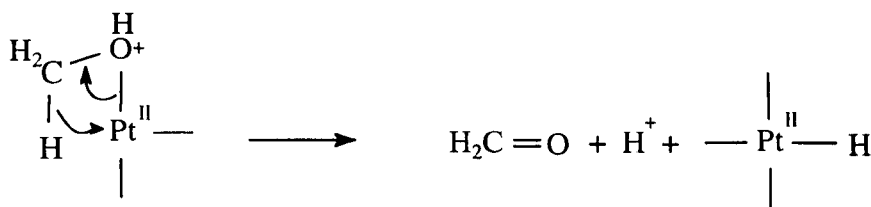
formation of metal-hydride and an olefin, ligand exchange and addition of H<sub>2</sub> to Pt(II).<sup>8</sup>

The formation of [Pt(d<sup>t</sup>bpx)H(MeOH)]<sup>+</sup>, **3a**, is not a case of oxidative addition. In fact, addition of CF<sub>3</sub>SO<sub>3</sub>H to [Pt(d<sup>t</sup>bpx)(dba)], **1**, results in the formation of [Pt(d<sup>t</sup>bpx)(dbaH)]<sup>+</sup>, **2a**, and not the hydride complex **3a**. The fact that protonation and not oxidation is observed is due to steric and electronic factors. Oxidative addition of acids to Pt(0) complexes is usually reported to occur more easily in the case of co-ordinatively unsaturated complexes. **1** is coordinatively unsaturated, but both d<sup>t</sup>bpx and dba ligands are very bulky ligands. **1** contains two basic sites, *i.e.* the Pt(0) centre and the oxygen atom; since H<sup>+</sup> is the hardest acid of all, it shows more affinity towards the hard basic centre (*i.e.* the oxygen atom) rather than the softer metal centre. These data suggest that the acid and the oxidant are used for the oxidation of the starting Pt(0) complex **1** to form a Pt(II) compound. It is evident that the hydridic reagent is the solvent, as suggested by the fact that **3a** is not formed in non alcoholic solvents. Hence, the metal hydride complex [Pt(d<sup>t</sup>bpx)H(MeOH)]<sup>+</sup>, **3a**, is formed, first by the oxidation of [Pt(d<sup>t</sup>bpx)(dbaH)]<sup>+</sup>, **2a**, followed by a redox process involving a β-hydride transfer from MeOH. It has been proposed that the reaction proceeds through the bis solvento platinum complex [Pt(d<sup>t</sup>bpx)(MeOH)<sub>2</sub>]<sup>2+</sup>, which rearranges to give the hydride (see Scheme 3.1).

This mechanism was first proposed in 1962, where *cis*-[Pt(PEt<sub>3</sub>)<sub>2</sub>Cl<sub>2</sub>] was converted to the hydride by heating with primary or secondary alcohols in the presence of base.<sup>8,10</sup> In this reaction aldehydes or ketones are formed and were identified chemically and spectroscopically.



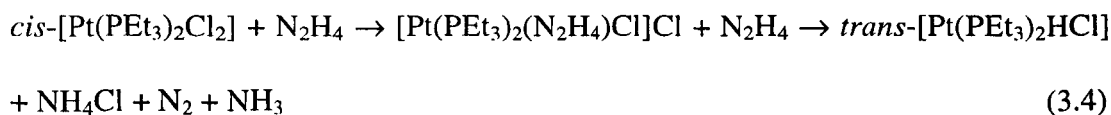
## Scheme 3.1



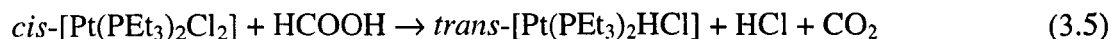
It has been observed that isopropyl alcohol reacts similarly, in this case one mole of acetone is formed during the reaction. This general reaction has also been used to prepare hydride complexes of ruthenium, rhodium, osmium and iridium.<sup>11-13</sup> It is important to note that the reaction proposed has been carried out in basic conditions, whereas the formation of the platinum hydride **3a** occurs in acid conditions. Bases are usually used in order to make the reduction of the alcohol easier. Therefore, the formation of **3a** under acid conditions suggests that in the presence of d<sup>1</sup>bpx, platinum can easily activate the solvent. It is also interesting to note that the Pt(I) hydride dimer [Pt<sub>2</sub>(dppe)<sub>2</sub>H<sub>2</sub>] (dppe = 1,2-bis(diphenylphosphino)ethane) is formed in the presence of protonic solvents such as methanol.<sup>14</sup> Probably the formation of this dimer involves the formation of an intermediate Pt(II)-hydride and a Pt(0)-complex which condenses to form the final Pt(I) complex. In our case, the bulky d<sup>1</sup>bpx ligand, steric effects probably make it difficult to form the binuclear compound and the Pt(II)-hydride is the final stable product.

Beside the use of basic alcohols, hydrazine has been the most convenient transfer agent: the most common configuration of these Pt(II)-hydrides is with the two phosphorus atoms *trans*, some examples are reported of *cis* complexes with chelating

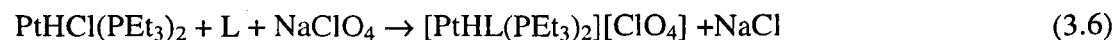
diphosphine ligands.<sup>6,7,15</sup> These syntheses start from the halides *cis*-[Pt(PR<sub>3</sub>)<sub>2</sub>X<sub>2</sub>], which are more reactive due to the greater *trans* effect of the phosphine ligands.<sup>16</sup>



Reduction by formic acid has also been used:



The synthesis of cationic complexes of general formula [PtHL(PEt<sub>3</sub>)<sub>2</sub>][ClO<sub>4</sub>] (L = py, PEt<sub>3</sub>, PPh<sub>3</sub>, P(OPh)<sub>3</sub>) has been reported.<sup>17</sup> A series of complexes can be prepared by adding the stoichiometric quantity of a ligand L and NaClO<sub>4</sub>:



In the infrared measurements, the platinum hydrides show a strong absorption due to the Pt-H stretching mode near 2000 cm<sup>-1</sup>. Usually the value of ν(Pt-H) is dependent on the *trans* ligand and decreases as the *trans* influence of the ligand increases. The chemical shift in the <sup>1</sup>H NMR spectrum is in the region at high field and the coupling constant <sup>1</sup>J(H-Pt) is very large (800-1300 Hz), which also varies with *trans* ligand.

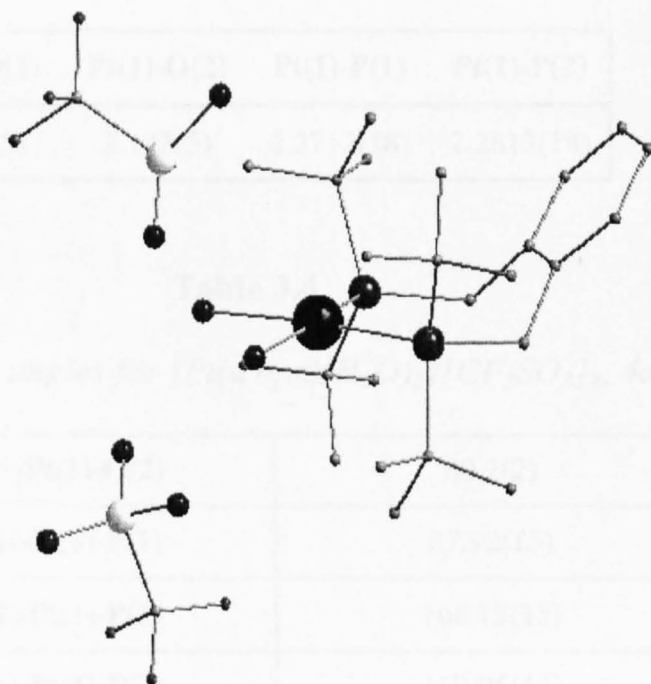
### 3.1.4. Crystal structure of [Pt(d<sup>4</sup>bpx)(H<sub>2</sub>O)<sub>2</sub>][CF<sub>3</sub>SO<sub>3</sub>]<sub>2</sub>, **4a**

Yellow crystals of [Pt(d<sup>4</sup>bpx)(H<sub>2</sub>O)<sub>2</sub>][CF<sub>3</sub>SO<sub>3</sub>]<sub>2</sub>, **4a**, crystallised when the solution of the complex [Pt(d<sup>4</sup>bpx)H(CO)][CF<sub>3</sub>SO<sub>3</sub>], **6a**, in THF was layered with n-hexane. [Pt(d<sup>4</sup>bpx)H(CO)][CF<sub>3</sub>SO<sub>3</sub>], **6a**, (see Chapter 5) is a very stable compound. Also,

after three months in solution (MeOH, THF) no decomposition is observed, storing the sample at low temperature. Its formation occurs on adding CO to the solution of  $[\text{Pt}(\text{d}^1\text{bpx})\text{H}(\text{MeOH})][\text{CF}_3\text{SO}_3]$ , **3a**, at room temperature. Probably the bisaquo compound **4a** is the first that crystallizes; in fact the acid used contains water. The  $^{31}\text{P}\{^1\text{H}\}$  NMR spectrum of the solution of crystallization shows very weak resonances due to  $[\text{Pt}(\text{d}^1\text{bpx})\text{H}(\text{CO})][\text{CF}_3\text{SO}_3]$ . The crystallization process occurs over about three days and at the end of this time, yellow crystals were obtained with some dark precipitate in the bottom of the tube, probably some Pt-metal.

**Figure 3.5**

*Crystal Structure of  $[\text{Pt}(\text{d}^1\text{bpx})(\text{H}_2\text{O})_2][\text{CF}_3\text{SO}_3]_2$ , **4a***



The dication is a square planar Pt(II) complex, with two coordination sites occupied by the phosphorus atoms of d<sup>t</sup>bpx ligand and the other sites by two molecules of water. The square planar geometry around the platinum center is almost perfect. The *trans* O-Pt-P angles are close to 180° and the four *cis* angles are very near 90°. The biggest deviation is the P(1)-Pt-P(2) angle (102°), but this can be easily explained because of the presence of a very long back bone of the diphosphine ligand. The two Pt-P bond lengths are almost identical, as are the two Pt-O distances. Finally, the two oxygen atoms, the two phosphine atoms and the platinum atom lie on the same plane.

**Table 3.3**

*Main bond distances for [Pt(d<sup>t</sup>bpx)(H<sub>2</sub>O)<sub>2</sub>][CF<sub>3</sub>SO<sub>3</sub>]<sub>2</sub>, 4a*

Pt(1)-O(1)	Pt(1)-O(2)	Pt(1)-P(1)	Pt(1)-P(2)
2.119(5)	2.123(5)	2.2712(18)	2.2813(18)

**Table 3.4**

*Main bond angles for [Pt(d<sup>t</sup>bpx)(H<sub>2</sub>O)<sub>2</sub>][CF<sub>3</sub>SO<sub>3</sub>]<sub>2</sub>, 4a*

O(1)-Pt(1)-O(2)	80.2(2)
O(1)-Pt(1)-P(1)	87.92(15)
O(2)-Pt(1)-P(1)	168.15(15)
O(1)-Pt(1)-P(2)	169.06(14)
O(2)-Pt(1)-P(2)	89.44(15)
P(1)-Pt(1)-P(2)	102.39(6)

In the palladium system, it has been shown that the reaction of [Pd(d<sup>t</sup>bpx)(dba)] with CH<sub>3</sub>SO<sub>3</sub>H in THF, followed by layering the resulting solution with n-hexane gives yellow crystals of [Pd(d<sup>t</sup>bpx)(H<sub>2</sub>O)<sub>2</sub>][CH<sub>3</sub>SO<sub>3</sub>]<sub>2</sub>, which has a very similar structure to [Pt(d<sup>t</sup>bpx)(H<sub>2</sub>O)<sub>2</sub>][CF<sub>3</sub>SO<sub>3</sub>]<sub>2</sub>, **4a**.

Different bisaquo platinum complexes have been reported in the literature and they are usually obtained on attempting to crystallise complexes containing the fragment Pt-(η<sup>1</sup>-CF<sub>3</sub>SO<sub>3</sub>)<sub>2</sub>.

The first crystallographically reported complex containing two monodentate phosphine ligands and two water molecules was [Pt(PR<sub>3</sub>)<sub>2</sub>(H<sub>2</sub>O)<sub>2</sub>][CF<sub>3</sub>SO<sub>3</sub>]<sub>2</sub> (R = PEt<sub>3</sub>, PPh<sub>3</sub>).<sup>18</sup> The crystal structure of [Pt(dppe)(H<sub>2</sub>O)<sub>2</sub>][CF<sub>3</sub>SO<sub>3</sub>]<sub>2</sub> (dppe = 1,2-bis(diphenylphosphino)-ethane) shows a planar coordination around the platinum. The P-Pt-O angles are slightly greater than 180° and the P-Pt-P and O-Pt-O angles are less than 90°; the Pt-P distances are almost identical.<sup>4</sup> In the crystal structure of [Pt(dppf)(H<sub>2</sub>O)<sub>2</sub>][CF<sub>3</sub>SO<sub>3</sub>]<sub>2</sub> (dppf = 1,1'-bis(diphenylphosphino)ferrocene) the centroids of the ferrocene unit are located in the Pt(II) coordination plane. In this structure the P-Pt-P angle is 97.3° and the O-Pt-O angle is 86°.<sup>5</sup> This last structure is most similar to that of [Pt(d<sup>t</sup>bpx)(H<sub>2</sub>O)<sub>2</sub>][CF<sub>3</sub>SO<sub>3</sub>]<sub>2</sub>, **4a**.

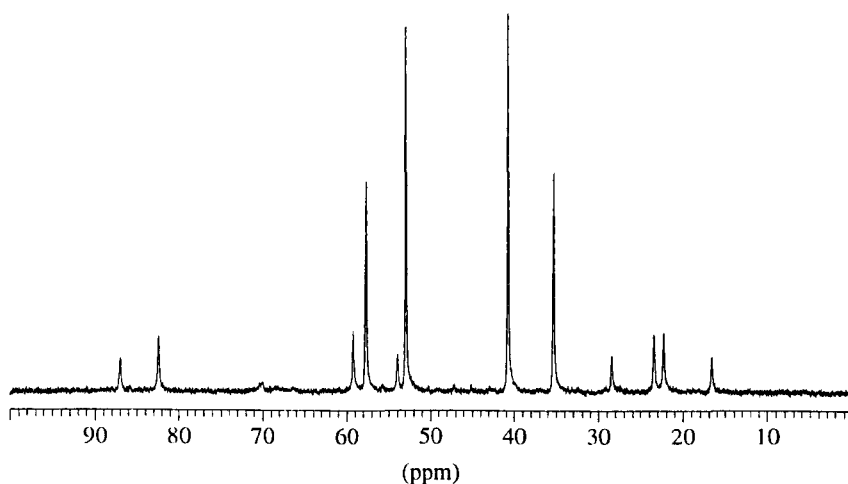
## 3.2. The CH<sub>3</sub>SO<sub>3</sub>H-system

### 3.2.1. Protonation of [Pt(d<sup>1</sup>bpx)(dba)], **1**

The reaction of [Pt(d<sup>1</sup>bpx)(dba)], **1**, with acids seems to be completely independent of the nature of the acid used. In fact, the reaction between [Pt(d<sup>1</sup>bpx)(dba)], **1**, and CH<sub>3</sub>SO<sub>3</sub>H shows four resonances (see Figure 3.6) with the same chemical shifts, coupling constants and intensities as found with CF<sub>3</sub>SO<sub>3</sub>H (see Figure 3.1).

**Figure 3.6**

*<sup>31</sup>P{<sup>1</sup>H} NMR spectra of [Pt(d<sup>1</sup>bpx)(dbaH)][CH<sub>3</sub>SO<sub>3</sub>], **2b**, in MeOH at 193 K*

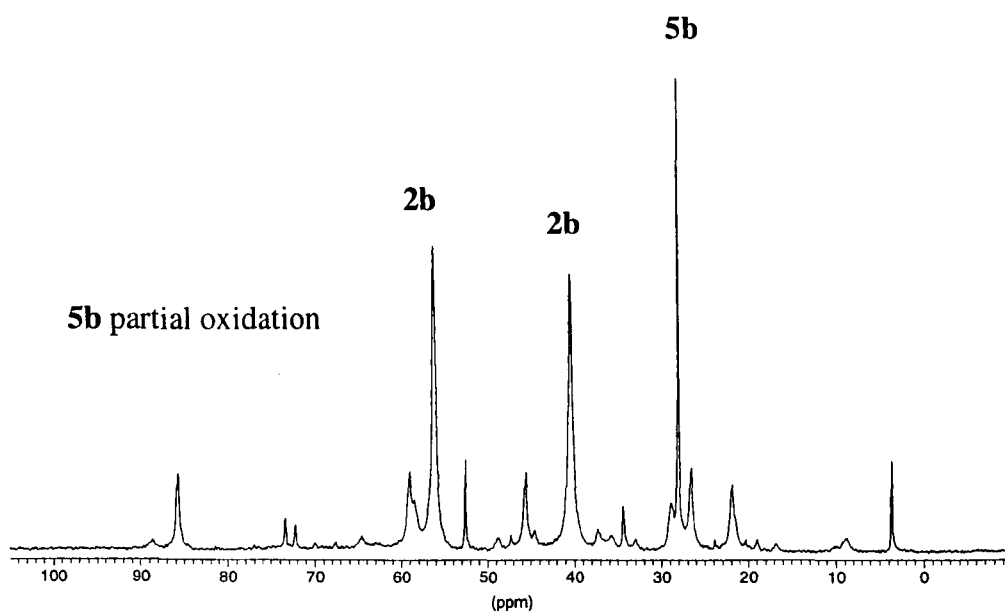


As found in the CF<sub>3</sub>SO<sub>3</sub>H-system, an exchange process is present, in fact only two resonances are present in the <sup>31</sup>P{<sup>1</sup>H} NMR spectrum at room temperature (see Figure 3.7), as found in the CF<sub>3</sub>SO<sub>3</sub>H-system (see Figure 3.2). The only difference between the <sup>31</sup>P{<sup>1</sup>H} NMR spectra of [Pt(d<sup>1</sup>bpx)(dbaH)][CF<sub>3</sub>SO<sub>3</sub>], **2a**, and

$[\text{Pt}(\text{d}^4\text{bpx})(\text{dbaH})][\text{CH}_3\text{SO}_3]$ , **2b**, are the resonances due to products resulting from different degrees of partial oxidation (**5b**). In the case of **2b** a singlet at 28.0 ppm appears with its platinum satellites (see Figure 3.7), instead of the two resonances at 46.3 ppm and 34.9 ppm due to **3a** observed in the NMR spectrum of **2a** (see Figure 3.2).

**Figure 3.7**

$^{31}\text{P}\{^1\text{H}\}$  NMR spectra of  $[\text{Pt}(\text{d}^4\text{bpx})(\text{dbaH})][\text{CH}_3\text{SO}_3]$ , **2b**, in MeOH at 290 K



### 3.2.2. Oxidation of $[\text{Pt}(\text{d}^4\text{bpx})(\text{dbaH})][\text{CH}_3\text{SO}_3]$ , **2b**

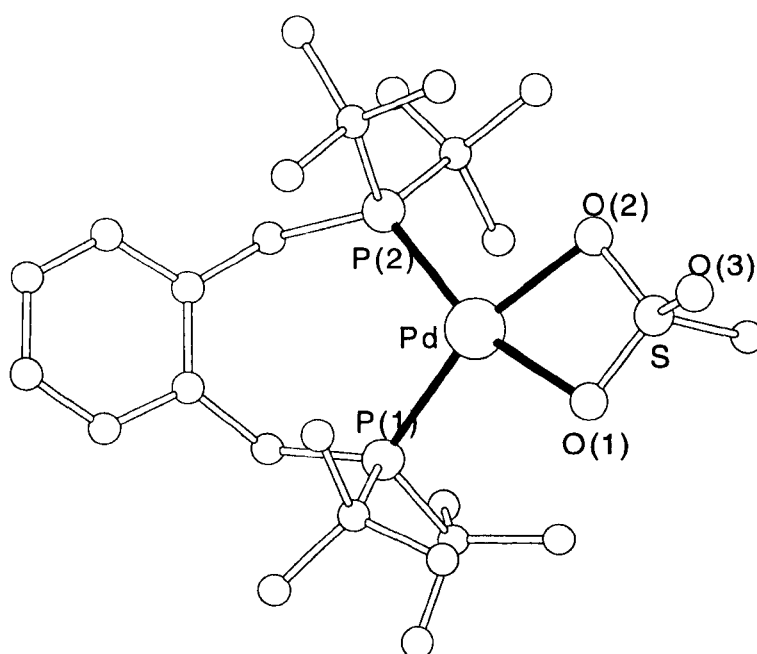
As in the  $\text{CF}_3\text{SO}_3\text{H}$ -system, the oxidation of  $[\text{Pt}(\text{d}^4\text{bpx})(\text{dbaH})][\text{CH}_3\text{SO}_3]$ , **2b**, can occur by bubbling oxygen through the solution as well as by the reaction of the platinum complex **2b** with benzoquinone. The reaction with benzoquinone is

quantitative and immediate; on bubbling oxygen, the reaction is complete after about 30 minutes. However, this work has shown that the oxidation reaction is extremely sensitive to the nature of the acid used for the protonation.

In the case of palladium, the oxidation of  $[\text{Pd}(\text{d}^t\text{bpx})(\text{dbaH})][\text{CH}_3\text{SO}_3]$  results in the formation of  $[\text{Pd}(\text{d}^t\text{bpx})(\eta^2\text{-CH}_3\text{SO}_3)]^+$  (see Figure 3.8).<sup>19</sup>

**Figure 3.8**

*Crystal Structure of  $[\text{Pd}(\text{L-L})(\eta^2\text{-CH}_3\text{SO}_3)][\text{CH}_3\text{SO}_3]$*



This structure shows two interesting features: the anion is a dimer in which a methylsulfonate anion interacts through a hydrogen bond with a molecule of methylsulfonic acid and the cation contains a rare example of a methylsulfonate anion bonding as a chelating ligand.

The room temperature  $^{31}\text{P}\{^1\text{H}\}$  NMR spectrum of the oxidised platinum complex shows only one resonance (see Figure 3.9) and at 193 K two resonances (see Figure 3.10). Previous studies of the behaviour of the analogous palladium compound in solution demonstrate that the two resonances at low temperature are really two singlets due to two different conformers present in solution. In fact, these two resonances never integrate 1:1 and the ratio changes with both solvent and temperature. It is reasonable to conclude that oxidation of the platinum complex results in the formation of  $[\text{Pt}(\text{d}^1\text{bpX})(\eta^2\text{-CH}_3\text{SO}_3)]^+$ , **5b**, as found for the palladium analogue. Also in the platinum case, bubbling oxygen or adding benzoquinone, results in a colour change from deep red to pale yellow. The fact that the protonated complex is easily oxidised by oxygen accounts for the difficulties experienced in the characterisation of  $[\text{Pt}(\text{d}^1\text{bpX})(\text{dbaH})]^+$  **2**. The NMR data at room temperature and 193 K of  $[\text{Pt}(\text{d}^1\text{bpX})(\eta^2\text{-MeSO}_3)]^+$ , **5b**, are reported in Table 3.5.

**Table 3.5**

*NMR data of  $[\text{Pt}(\text{d}^1\text{bpX})(\eta^2\text{-MeSO}_3)]^+[\text{CH}_3\text{SO}_3]$ , **5b**, at 293 K and 193 K in MeOH*

	$\delta\text{P}$ (ppm)	$^1\text{J}(\text{P-Pt})$ (Hz)
@ 293 K	28.9	3924
conf. A @ 193 K	27.6	3932
conf. B @ 193 K	27.0	3952

**Figure 3.9**

$^{31}\text{P}\{^1\text{H}\}$  NMR spectra of  $[\text{M}(\text{d}^1\text{bpx})(\eta^2\text{-MeSO}_3)][\text{CH}_3\text{SO}_3]$  in MeOH at 290 K

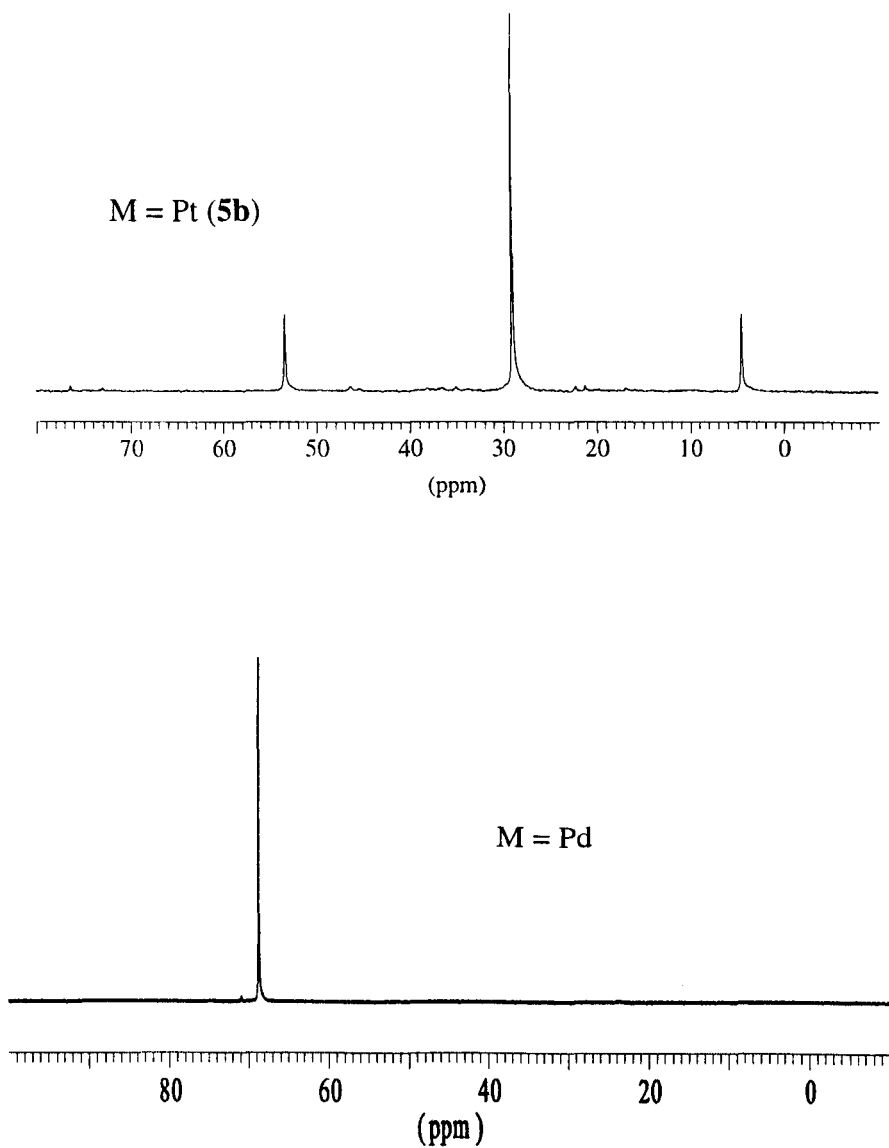
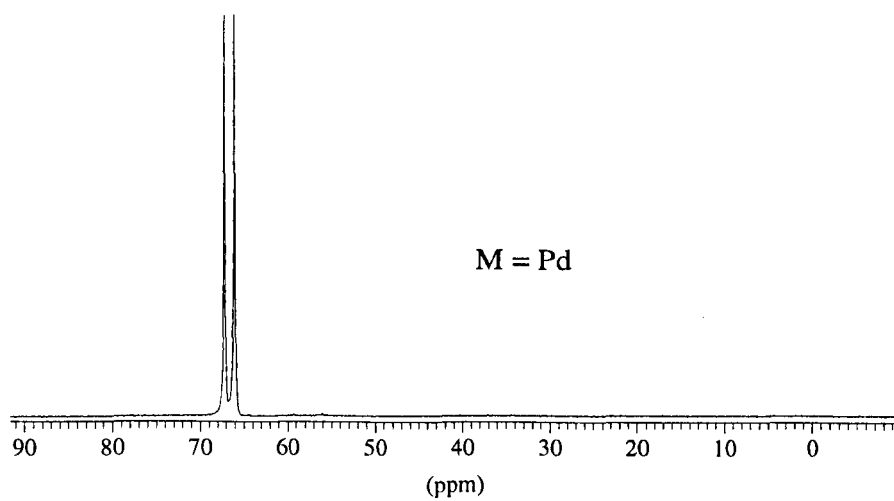
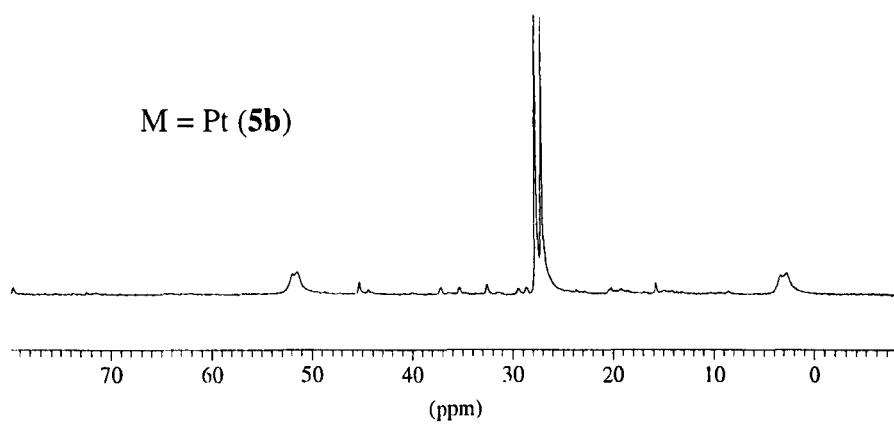


**Figure 3.10**

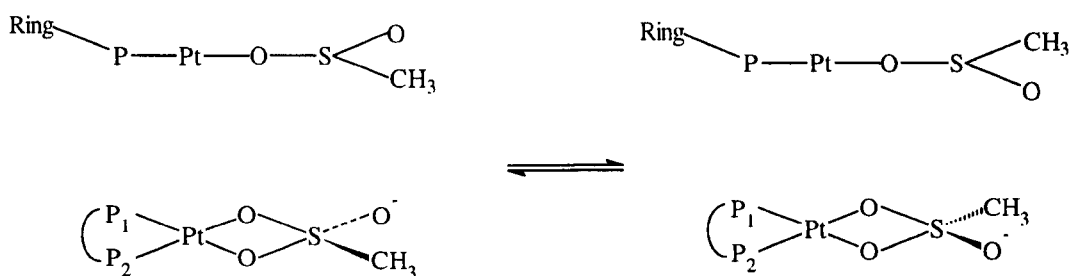
$^{31}\text{P}\{^1\text{H}\}$  NMR spectra of  $[\text{M}(\text{d}^t\text{bpx})(\eta^2\text{-MeSO}_3)][\text{CH}_3\text{SO}_3]$  in MeOH at 193 K



The two conformers of  $[\text{Pt}(\text{d}^1\text{bpx})(\eta^2\text{-CH}_3\text{SO}_3)][\text{CH}_3\text{SO}_3]$ , **5b**, differ in the orientation of the benzene ring of the  $\text{d}^1\text{bpx}$  ligand with respect to the  $\text{CH}_3$ -group of the chelating  $\text{CH}_3\text{SO}_3^-$  anion relative to the plane determined by platinum, the two phosphorus and the two co-ordinated oxygen atoms (see Scheme 3.2). These two conformers can exchange and, hence, at higher temperature only one resonance is present.

### Scheme 3.2

Representation of the conformers of  $[\text{Pt}(\text{d}^1\text{bpx})(\eta^2\text{-MeSO}_3)][\text{CH}_3\text{SO}_3]$

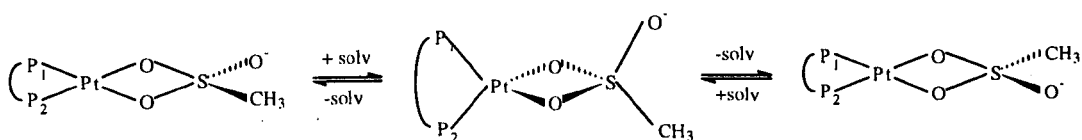


The problem is to understand the mechanism involved during the exchange. Two hypotheses are possible to explain the exchange between the *cis* and *trans* conformers of  $[\text{Pt}(\text{d}^1\text{bpx})(\eta^2\text{-CH}_3\text{SO}_3)][\text{CH}_3\text{SO}_3]$ , **5b**.

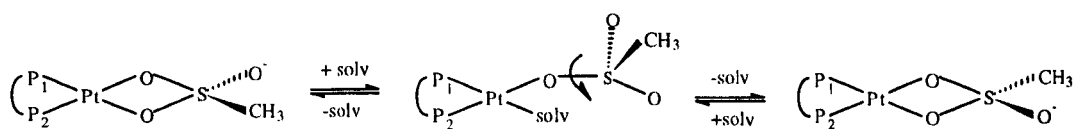
- The exchange could involve the rotation of some bonds inside the molecule, without any bond dissociation. For this mechanism, an isomerisation through a tetrahedral intermediate must be involved (see Scheme 3.3).
- It is possible that the exchange between the conformers takes place *via* a direct interaction of the metal and the solvent (see Scheme 3.4). In this case, solvent coordinates to the metal and the coordination mode of  $\text{CH}_3\text{SO}_3^-$

changes from  $\eta^2$  to  $\eta^1$  followed by rotation of the ligand  $\eta^1\text{-CH}_3\text{SO}_3^-$  and replacement of the solvent by re-coordination of the  $\text{CH}_3\text{SO}_3^-$  in an  $\eta^2$ -mode.

Scheme 3.3



Scheme 3.4

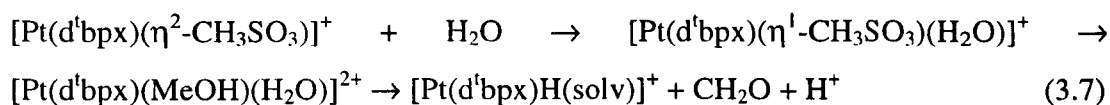


Although in the present case, it is impossible to distinguish between the two mechanism shown in Scheme 3.3 and 3.4, related work on the palladium system, suggests that the mechanism in Scheme 3.3 is the most probable, since there is no direct relationship between the rate of the exchange and the polarity of the solvent. For the mechanism shown in Scheme 3.4, the coalescence temperature should increase with the polarity of the solvent and this effect has not been observed.

### 3.2.3. Reactivity of [Pt(d<sup>1</sup>bpx)(η<sup>2</sup>-CH<sub>3</sub>SO<sub>3</sub>)] [CH<sub>3</sub>SO<sub>3</sub>], **5b**, with water

It has been observed that the oxidation of [Pt(d<sup>1</sup>bpx)(dbaH)]<sup>+</sup>, **2**, is extremely sensitive to the nature of the acid used for the protonation. In both CF<sub>3</sub>SO<sub>3</sub>H and CH<sub>3</sub>SO<sub>3</sub>H systems the compound formed is [Pt(d<sup>1</sup>bpx)(η<sup>2</sup>-RSO<sub>3</sub>)]<sup>+</sup>, **5**, (R = CF<sub>3</sub>, CH<sub>3</sub>) and depending on the co-ordination ability of the sulfonate anion, it can partially or completely dissociate to give a dicationic species. The oxidation of [Pt(d<sup>1</sup>bpx)(dbaH)] [CH<sub>3</sub>SO<sub>3</sub>], **2b**, results in the formation of [Pt(d<sup>1</sup>bpx)(η<sup>2</sup>-CH<sub>3</sub>SO<sub>3</sub>)]<sup>+</sup>, **5b**, whereas the oxidation of [Pt(d<sup>1</sup>bpx)(dbaH)] [CF<sub>3</sub>SO<sub>3</sub>], **2a**, results in the formation of Pt(d<sup>1</sup>bpx)H(MeOH)]<sup>+</sup>, **3a**. In the case of CF<sub>3</sub>SO<sub>3</sub>H, the coordination ability of the sulfonate anion is not very good, so that it dissociates to give a dicationic species, which can then react easily with MeOH, or other alcohols containing a α-hydrogen. In this reaction, the β-carbon of the alcohol is oxidized to give a carbonyl group and the proton is reduced with formation of the hydride (see Scheme 3.1). Indeed, the coordination ability of the sulfonate anion is fundamental in determining the final product of the oxidation of the [Pt(d<sup>1</sup>bpx)(dbaH)]<sup>+</sup>, **2**. The fact that dissociation of the anion RSO<sub>3</sub><sup>-</sup> (R = CF<sub>3</sub>, CH<sub>3</sub>) is required in order to form the hydride, suggests that addition of an appropriate ligand should be able to induce the elimination of CH<sub>3</sub>SO<sub>3</sub><sup>-</sup>. Indeed, this has been confirmed by addition of water. It has been experimentally shown that it is possible to obtain the hydride complex by reacting [Pt(d<sup>1</sup>bpx)(η<sup>2</sup>-CH<sub>3</sub>SO<sub>3</sub>)]<sup>+</sup>, **5b**, with water in MeOH. In this case, water can, basically, assist with the dissociation of the sulfonate anion by co-ordinating to the metal, forcing the sulfonate anion to act as a monodentate ligand. In this way, the extra stability of the complex due to the chelating effect is lost and the anion can

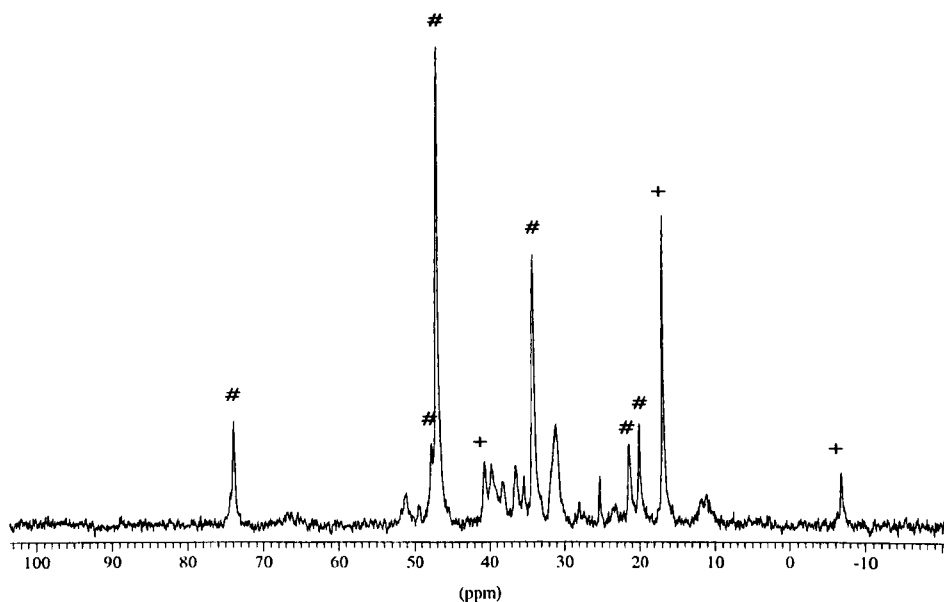
completely dissociate to give  $[\text{Pt}(\text{d}^1\text{bpx})(\text{MeOH})(\text{H}_2\text{O})]^{2+}$ . The dicationic species should be very reactive and as described above, the carbon of the  $\text{CH}_3\text{OH}$  is oxidized to give a carbonyl group and the proton is reduced with formation of the hydride.



The problem with this last reaction is the high affinity of the platinum for water. Thus, addition of 0.2 ml of  $\text{H}_2\text{O}$  to a solution of  $[\text{Pt}(\text{d}^1\text{bpx})(\eta^2\text{-CH}_3\text{SO}_3)]^+$ , **5b**, in MeOH, the  $^{31}\text{P}\{^1\text{H}\}$  NMR spectrum shows the appearance of resonances due to  $[\text{Pt}(\text{d}^1\text{bpx})\text{H}(\text{solv})]^+$ , **3b**, together with a singlet at 16 ppm due to the formation of  $[\text{Pt}(\text{d}^1\text{bpx})(\text{H}_2\text{O})_2]^{2+}$ , **4b**, (see Figure 3.11).

**Figure 3.11**

$^{31}\text{P}\{^1\text{H}\}$  NMR spectrum of  $[\text{Pt}(\text{d}^1\text{bpx})\text{H}(\text{solv})][\text{CH}_3\text{SO}_3]$  **3b** (#) and  $[\text{Pt}(\text{d}^1\text{bpx})(\text{H}_2\text{O})_2][\text{CH}_3\text{SO}_3]_2$  **4b** (+) in MeOH @ 293 K



### 3.3. Conclusions

The results outlined in this chapter show that the platinum system is quite similar to the palladium system, when the reactions under nitrogen are considered.

In fact, there is spectroscopic evidence for the initial formation of the compound [Pt(d<sup>4</sup>bpx)(dbaH)]<sup>+</sup>, **2**, which is formed with acids containing weakly coordinating anions and **2** has been shown to exist in solution as two conformers, as found for the palladium analogue; these two conformers undergo exchange at room temperature and the exchange involves the relative movement of the dba chain. This compound is very unstable to oxidising agents, and the oxidised product formed depends on the nature of the acid used for the protonation, as found in the palladium system. Oxidation of [Pt(d<sup>4</sup>bpx)(dbaH)][CH<sub>3</sub>SO<sub>3</sub>], **2b**, gives [Pt(d<sup>4</sup>bpx)(η<sup>2</sup>-MeSO<sub>3</sub>)] [CH<sub>3</sub>SO<sub>3</sub>], **5b**, whereas oxidation of [Pt(d<sup>4</sup>bpx)(dbaH)][CF<sub>3</sub>SO<sub>3</sub>], **2a**, gives the hydride complex, [Pt(d<sup>4</sup>bpx)H(MeOH)][CF<sub>3</sub>SO<sub>3</sub>], **3a**.

The mechanism for the formation of **3a** is almost the same as in the palladium system. First, [Pt(d<sup>4</sup>bpx)(dba)], **1**, is protonated to give [Pt(d<sup>4</sup>bpx)(dbaH)]<sup>+</sup>, **2a**, which is then oxidised to form **3a**. The last step probably involves the intermediate [Pt(d<sup>4</sup>bpx)(η<sup>2</sup>-CF<sub>3</sub>SO<sub>3</sub>)]<sup>+</sup>, **5a**, (detected in the palladium but not in the platinum system), in which the CF<sub>3</sub>SO<sub>3</sub><sup>-</sup> group can easily be displaced from the metal by the solvent in a polar medium to give [Pt(d<sup>4</sup>bpx)(MeOH)<sub>2</sub>]<sup>2+</sup>. The bis-solvento complex in the presence of an alcohol with an α-hydrogen, activates the alcohol, which is oxidised to give a carbonyl-containing species and a proton is reduced to form the hydride.



In the  $\text{CH}_3\text{SO}_3\text{H}$ -system the platinum hydride **3b** can be formed by reaction involving water. In this case the anion can be dissociated from the metal and MeOH or water can coordinate before the hydride is formed. The problem of this reaction is the affinity of platinum for water. From the experiments done it seems that there is a competition between the two bis-solvento complexes  $[\text{Pt}(\text{d}^t\text{bpx})(\text{MeOH})_2]^{2+}$  and  $[\text{Pt}(\text{d}^t\text{bpx})(\text{H}_2\text{O})_2]^{2+}$ , **4b**, in fact the bis-aquo complex **4b** is present in solution when the hydride is formed. It is interesting to observe the stability of the chelating sulfonate anion **5b**, which is not displaced by solvents such as THF, acetone and  $\text{CH}_2\text{Cl}_2$ .

### 3.4. References

- (1) W. Clegg; G.R. Eastham; M.R.J. Elsegood; B.T. Heaton; J.A. Iggo; R.P. Tooze; R. Whyman; S. Zacchini *Organometallics*, **2002**, *21*, 1832.
- (2) H. Grennberg; A. Gogoll; J.E. Backvall *Organometallics*, **1993**, *12*, 1790.
- (3) N. Carr; B. J. Dunne; L.Mole; A. Guy Orpen; J. L. Spencer *J.Chem.Soc.Dalton Trans*, **1991**, 863.
- (4) S. Fallis; G.K. Anderson; N.P. Rath *Organometallics* **1991**, *10*, 3180.
- (5) P. J. Stang; B. Olenyuk; J. Fun; A. M. Arif *Organometallics* **1996**, *15*, 904.
- (6) C.J. Moulton and B.L. Shaw *J.C.S. Chem. Comm.*, **1976**, 365.
- (7) A. Scrivanti; C. Botteghini; L. Toniolo; A. Berton *J. Organomet. Chem.*, **1988**, *344*, 261.
- (8) J. Chatt and B.L. Shaw *J. Chem. Soc.*, **1962**, 5075.
- (9) W. R. Meyer and L. M. Venanzi *Angew. Chem. Int. Ed. Engl.*, **1984**, *23*, 529.
- (10) J. Chatt; L.A. Duncanson; B.L. Shaw *Proc. Chem. Soc.*, **1957**, 343.
- (11) J. Chatt and B.L. Shaw *Chem. and Ind.*, **1960**, 931.
- (12) J. Chatt and B.L. Shaw *Chem. and Ind.*, **1961**, 290.
- (13) Vaska *J. Am. Chem. Soc.*, **1961**, *83*, 756.
- (14) D. Carmichael; P.B. Hitchcock; J.F. Nixon; A. Pidcock *J. Chem. Soc., Chem. Commun*, **1988**, 1554.
- (15) G.K. Anderson and G.J. Lumetta *Inorg. Chem.*, **1987**, 1518.
- (16) F. Basolo and R.G. Pierson *Progress in Inorganic Chemistry, Vol.4, New York*, **1962**.
- (17) M.J. Church and M.J. Mays *J. Chem. Soc. (A)*, **1968**, 3074.

- (18) K. Siegmann; P.S. Pregosin; L.M. Venanzi *Organometallics* **1989**, 8, 2659.
- (19) W. Clegg; G. R. Eastham; M. R. J. Elsegood; B.T. Heaton; J.A. Iggo; R. P. Tooze; R. Whyman; S. Zacchini *J. Chem. Soc., Dalton Trans.*, **2002**, 3300.

# Chapter Four

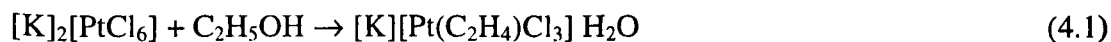
## 4. Reactivity of $[\text{Pt}(\text{d}^t\text{bpx})\text{H}(\text{solv})][\text{RSO}_3]$ with $\text{C}_2\text{H}_4$

### 4.1. Introduction

Olefin complexes are the oldest class of organometallic complexes known; the first complex  $[\text{Pt}(\text{C}_2\text{H}_4)\text{Cl}_3]\text{K}\cdot\text{H}_2\text{O}$ , known as Zeise's salt, was reported in 1830,<sup>1</sup> and they have been now extensively studied. It has been observed that they are kinetically more stable than their palladium analogue, which because of their lower stability are catalytically more useful.<sup>2</sup> Complexes in which the platinum atom is formally in the zerovalent state differ substantially from those in which the metal is formally in the divalent oxidation state. However, in this section the olefin platinum complexes where the metal is in the oxidation state II will be mostly considered.

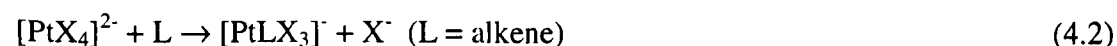
These complexes are part of a more general class of  $\pi$ -complexes; where the  $\text{L}\rightarrow\text{M}$  donor as well as the  $\text{L}\leftarrow\text{M}$  acceptor interactions utilise ligand orbitals which have a  $\pi$ -symmetry. The bonding in metal-olefin complexes<sup>3,4</sup> was first proposed from the studies of Dewar-Chatt-Duncanson.<sup>5,6</sup> In this configuration, two different interactions can be taken into account: a  $\sigma$  (olefin to platinum) bond formed by donation of charge from the full  $\pi$ -orbital on the olefin to the empty  $\text{dsp}^2$  hybrid orbital on platinum and a  $\pi$  (platinum to olefin) bond being formed by back-donation of charge from the  $5\text{d}6\text{p}$  hybrid orbital on platinum to the empty  $\pi^*$  (anti-bonding) orbital on the olefin.

Different preparations have been published for the synthesis of platinum(II)-olefin complexes. Zeise prepared the first platinum(II)-ethylene complex by boiling a solution of  $\text{K}_2\text{PtCl}_6$  in ethanol:<sup>1</sup>



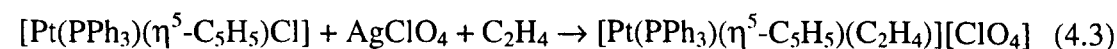
The mechanism of this reaction has not been fully understood. It is probable that the reduction of platinum(IV) to platinum(II) is due to the ethanol which is oxidised to acetaldehyde. A related procedure involves shaking a platinum(II) salt like  $\text{Na}_2\text{PtCl}_4$  in primary alcohols at room temperature. In this reaction, slow dehydration of the alcohol takes place with the formation of a platinum(II)-olefin complex together with platinum metal.<sup>7</sup>

Platinum(II)-ethyl complexes can be formed by the reaction of a platinum(II) salt with an olefin in water. These may be with water soluble olefins (allylamine),<sup>8</sup> with water insoluble olefins (cyclooctatetraene)<sup>9</sup> or with gaseous olefins (ethylene) with<sup>10</sup> or without<sup>11</sup> pressure.

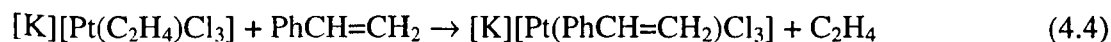


The above reaction with ethylene usually takes a number of days to go to completion but it can be accelerated by addition of a trace of tin(II) chloride.<sup>10</sup>

Cationic platinum(II)-olefin complexes can be prepared by treating a chloroplatinum(II) salt with a silver(I) salt in the presence of an olefin:<sup>12,13</sup>



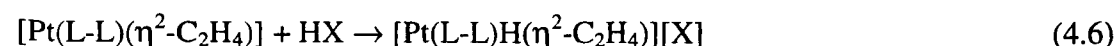
Platinum(II)-olefin complexes also can be formed by displacement of a different olefin from its complex. Usually, ethylene complexes have been used as starting materials because the volatility of ethylene helps its displacement.<sup>13</sup>



A series of cationic platinum(II)-ethyl complexes have been formed starting from  $[\text{Pt}(\text{L-L})(\eta^2\text{-C}_2\text{H}_4)]$  (L-L = dcpe, dbpe, dcpp, dbpp, dbpx). First, the Pt(0) complex is formed by reaction of  $[\text{Pt}(\text{cod})_2]$  with the diphosphine ligand in an ethene-saturated hexane solution at 273 K.<sup>14</sup>



Treatment of a solution of the platinum(0)-ethene complex with an equimolar amount of acid in diethyl ether solution at 273 K gives  $[\text{Pt}(\text{L-L})\text{H}(\eta^2\text{-C}_2\text{H}_4)][\text{X}]$  (X =  $\text{BF}_4$ ,  $\text{PF}_6$ ,  $\text{CF}_3\text{SO}_3$ ) (equation 4.6).

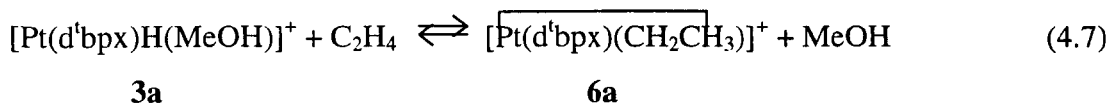


However, the reaction between metal-hydrides and olefins is one of the classic routes for the synthesis of metal-alkyl complexes.<sup>15</sup> In the next section of this chapter this reaction will be fully described.

## 4.2. Reactivity of $[\text{Pt}(\text{d}^t\text{bpx})\text{H}(\text{solv})][\text{CF}_3\text{SO}_3]$ , **3a**, with $\text{C}_2\text{H}_4$

The reaction between  $[\text{Pt}(\text{d}^t\text{bpx})\text{H}(\text{MeOH})][\text{CF}_3\text{SO}_3]$ , **3a**, and ethene has been performed in MeOH. Under one atmosphere of ethene at 293 K and 273 K, the main

resonances are due to the platinum hydride complex **3a**. On bubbling ethene for ca. 30 minutes at 273 K, quantitative conversion to the ethyl complex occurs. Indeed, on increasing the temperature both species, the hydride and the ethyl complex are present in solution, probably because there is an equilibrium correlated to the solubility of ethene in solution:

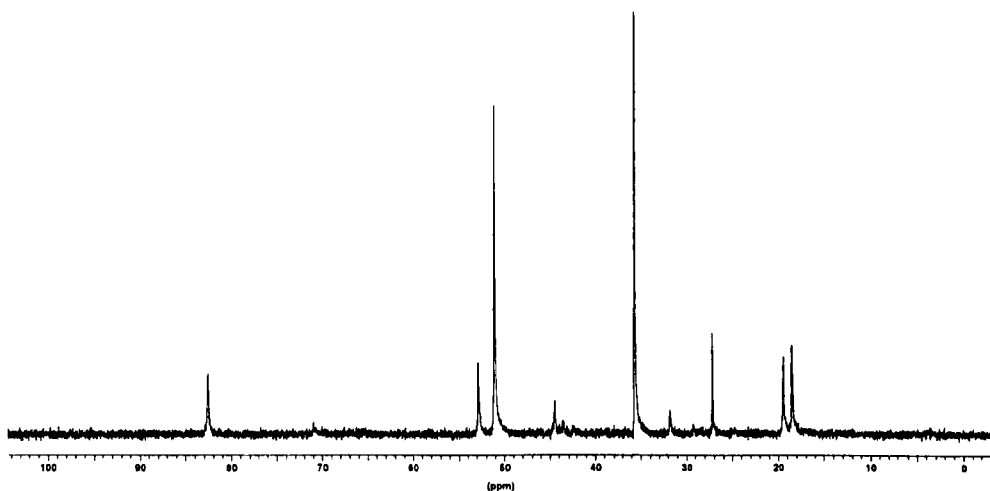


The <sup>31</sup>P{<sup>1</sup>H} NMR data for the platinum ethyl complex **6a** are available in the literature and agree well with those reported for [Pt(d<sup>t</sup>bpx)(CH<sub>2</sub>CH<sub>3</sub>)](CF<sub>3</sub>SO<sub>3</sub>) (dbpx = o-Bu<sup>t</sup><sub>2</sub>PCH<sub>2</sub>C<sub>6</sub>H<sub>4</sub>CH<sub>2</sub>PBu<sup>t</sup><sub>2</sub>) where the ethyl ligand binds to platinum through both the σ-alkyl and β-agostic C-H-Pt bonds.<sup>14</sup> The <sup>31</sup>P{<sup>1</sup>H} NMR spectrum at low temperature shows two main resonances at 50.9 ppm and 35.6 ppm with their platinum satellites (see Figure 4.1); it should be noted the phosphorus-phosphorus coupling constant from the two inequivalent phosphorus atoms is not resolved. At room temperature, the phosphorus spectrum shows two resonances due to the platinum hydride complex **3a** and, moreover, the resonances due to the platinum ethyl complex **6a** broaden (see Figure 4.2), due to an exchange process but the platinum-phosphorus couplings are still clearly present (see Section 4.3).

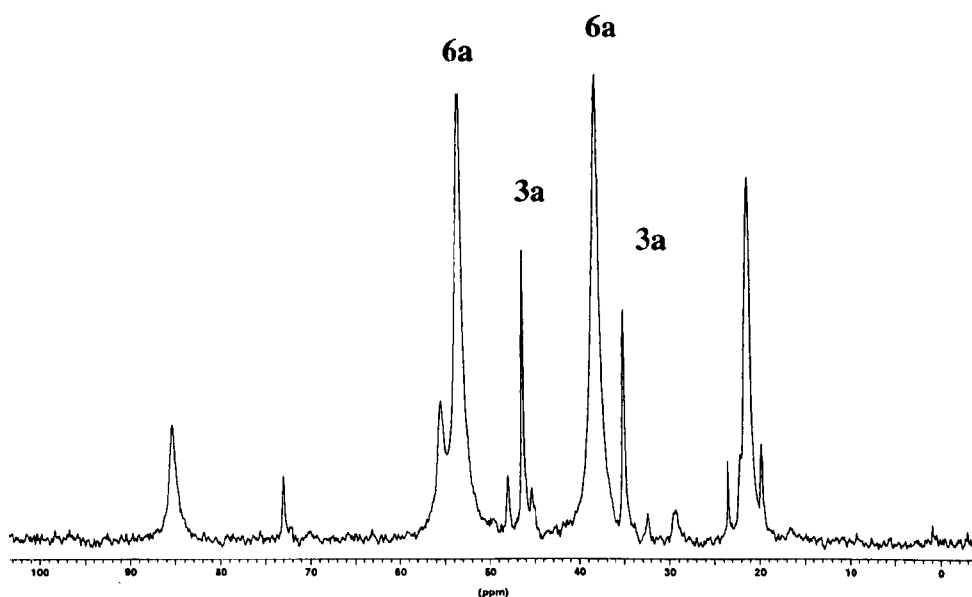
It is clear that the equilibrium between the hydride complex **3a** and the ethyl complex **6a** is shifted in favour of the formation of the complex **3a** and it is necessary to use high ethene pressure to favour the complex **6a**. An alternative synthesis has been used, in order to form the complex **6a**, without using high ethene pressure.

**Figure 4.1**

$^{31}\text{P}\{^1\text{H}\}$  NMR spectrum of  $[\text{Pt}(d^4\text{bpx})(\text{CH}_2\text{CH}_3)]^+$ , **6a**, at 193 K in MeOH

**Figure 4.2**

$^{31}\text{P}\{^1\text{H}\}$  NMR spectrum of  $[\text{Pt}(d^4\text{bpx})\text{H}(\text{MeOH})]^+$ , **3a**, and  $[\text{Pt}(d^4\text{bpx})(\text{CH}_2\text{CH}_3)]^+$ , **6a**, at 293 K in MeOH



It has been reported by Spencer that the complex  $[\text{Pt}(\text{d}^t\text{bpx})(\eta^2\text{-C}_2\text{H}_4)]$ , **7**, can be formed from the reaction of  $[\text{Pt}(\text{cod})_2]$  with diphosphine  $\text{d}^t\text{bpx}$  in the presence of  $\text{C}_2\text{H}_4$  in hexane.<sup>14</sup>

The  $^{31}\text{P}\{^1\text{H}\}$  NMR spectrum at room temperature shows a singlet at 49.7 ppm with  $^1J(\text{Pt-P}) = 3497$  Hz. Protonation of  $[\text{Pt}(\text{d}^t\text{bpx})(\eta^2\text{-C}_2\text{H}_4)]$ , **7**, by  $\text{CF}_3\text{SO}_3\text{H}$  in diethyl ether at 273 K results in the formation of  $[\text{Pt}(\text{d}^t\text{bpx})(\text{CH}_2\text{CH}_3)]^+$ , **6a**, (see Scheme 4.1). Spectroscopic characterisation has been carried out in  $\text{CH}_2\text{Cl}_2$  and the NMR data are the same as those in MeOH (see Table 4.1).

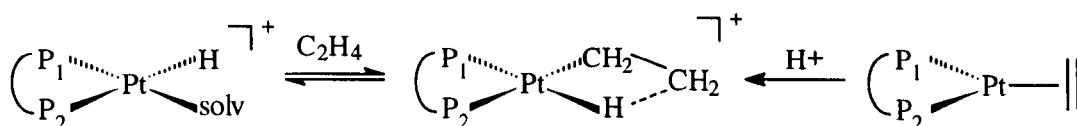
**Table 4.1**

$^{31}\text{P}$  NMR data of  $[\text{Pt}(\text{d}^t\text{bpx})(\text{CH}_2\text{CH}_3)]^+$ , **6a**, at 193 and 293 K in MeOH

	$\delta\text{P}_1$ (ppm)	$\delta\text{P}_2$ (ppm)	$^1J(\text{P}_1\text{-Pt})(\text{Hz})$	$^1J(\text{P}_2\text{-Pt})(\text{Hz})$
at 293 K	52.4	37.0	5108	2759
at 193 K	50.9	35.6	5114	2785

**Scheme 4.1**

Formation of  $[\text{Pt}(\text{d}^t\text{bpx})(\text{CH}_2\text{CH}_3)]^+$ , **6a**

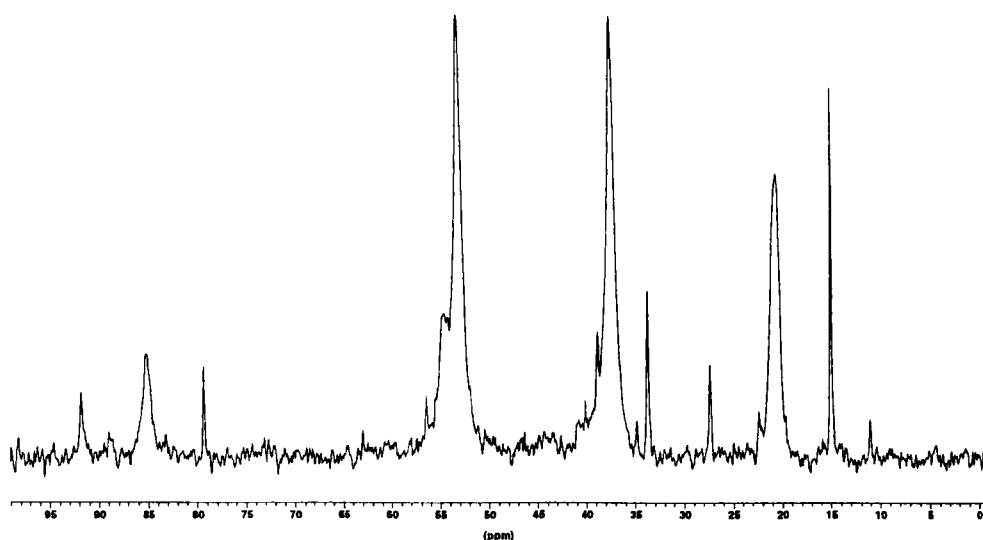


Previously, it has been observed that the  $^{31}\text{P}\{^1\text{H}\}$  NMR spectrum at 293 K in MeOH also contains resonances due to the hydride complex **3a**. If we consider the

same sample in  $\text{CH}_2\text{Cl}_2$  at room temperature, it is possible to observe only two broad resonances due to the ethyl complex (see Figure 4.3). This solvent effect is in agreement with what has been reported in the previous chapter. In fact, the platinum hydride complex **3** is formed only in alcoholic solvents and under the same conditions in other solvents the platinum hydride complex **3** is not formed.

**Figure 4.3**

$^{31}\text{P}\{^1\text{H}\}$  NMR spectrum of  $[\text{Pt}(\text{d}^t\text{bpx})(\text{CH}_2\text{CH}_3)]^+$ , **6a**, at 293 K in  $\text{CH}_2\text{Cl}_2$



#### 4.3. The dynamic behaviour of $[\text{Pt}(\text{d}^t\text{bpx})(\text{CH}_2\text{CH}_3)]^+$ , **6a**

It is possible to conclude that an exchange process occurs in the platinum ethyl complex **6a** at 293 K; in fact in the  $^{31}\text{P}\{^1\text{H}\}$  NMR spectrum at 293 K the half widths of the resonances are bigger than in the  $^{31}\text{P}\{^1\text{H}\}$  NMR spectrum at 193 K.

In order to understand which atoms are involved in the exchange process and which mechanism accounts for this exchange, two experiments have been performed.

The first experiment describes the dynamic studies of the platinum ethyl complex **6a** at high temperature (293 – 353 K) (Section 4.3.1), whereas the second experiment will consider the dynamic behaviour of **6a** at low temperature (293 - 193 K) (Section 4.3.2).

### 4.3.1 Dynamic behaviour of **6a** at high temperature (293-353 K)

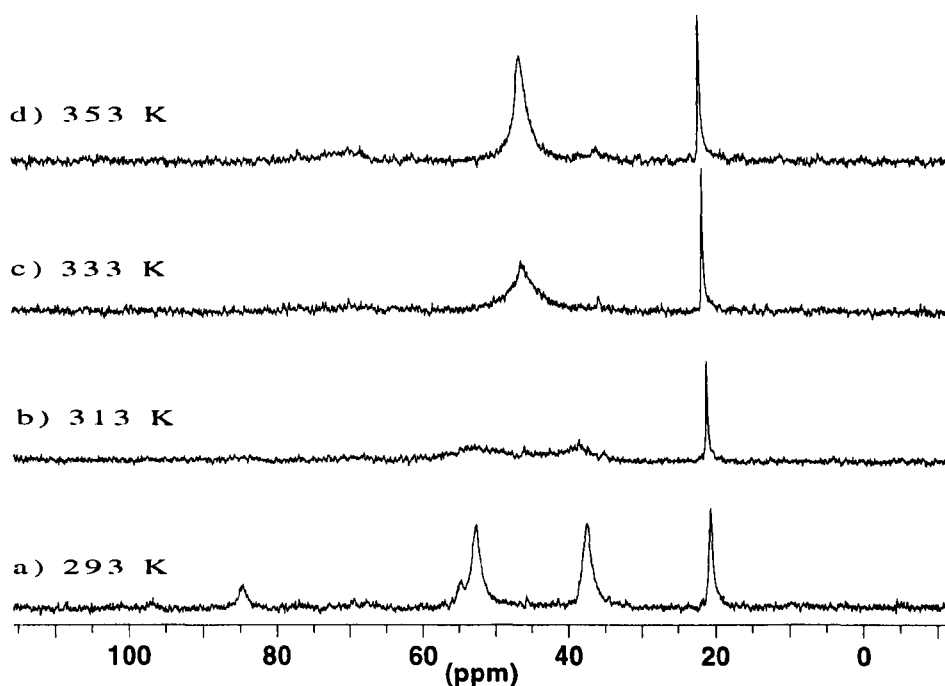
It has been observed above that an exchange process between the two phosphorus atoms occurs at 293 K. In fact, in the  $^{31}\text{P}\{^1\text{H}\}$  NMR spectrum the two resonances of the two phosphorus atoms of  $[\text{Pt}(\text{d}^t\text{bpx})(\text{CH}_2\text{CH}_3)]^+$ , **6a**, broaden on increasing the temperature (see Paragraph 4.2). In order to understand which mechanism is involved in the exchange process, first, the behaviour of the platinum ethyl complex **6a** has been investigated at temperatures higher than 293 K.

In this experiment a solution of  $[\text{Pt}(\text{d}^t\text{bpx})\text{H}(\text{MeOH})][\text{CF}_3\text{SO}_3]$ , **3a**, in MeOH has been degassed and put under 10 bar of  $\text{C}_2\text{H}_4$  in a sapphire tube and the  $^{31}\text{P}\{^1\text{H}\}$  NMR spectra have been recorded from 293 K to 353 K. The  $^{31}\text{P}\{^1\text{H}\}$  NMR spectrum of this solution at 293 K (see Figure 4.4 a) shows only the presence of the platinum ethyl complex **6a** with no evidence for the platinum hydride complex **3a** under these conditions. This confirms that it is necessary to put the solution of  $[\text{Pt}(\text{d}^t\text{bpx})(\text{CH}_2\text{CH}_3)]^+$ , **6a**, under a pressure of  $\text{C}_2\text{H}_4$  to shift the equilibrium between the two complexes in favour of the formation of the ethyl complex **6a**. On increasing the temperature to 213 K, the resonances due to the ethyl complex **6a** broaden, until they coalesce at 333 K to form only one resonance at 46.6 ppm (see Figure 4.4 c). However, no other resonances due to other compounds are present in the NMR

spectrum (apart a sharp resonance at 20 ppm which is always present, also at room temperature). These spectra are completely reproducible both on heating and cooling the solution of **6a**.

**Figure 4.4**

*VT  $^{31}\text{P}\{^1\text{H}\}$  NMR spectra of  $[\text{Pt}(\text{d}^1\text{bpx})(\text{CH}_2\text{CH}_3)]^+$ , **6a**, in MeOH under 10 bar of  $\text{C}_2\text{H}_4$*

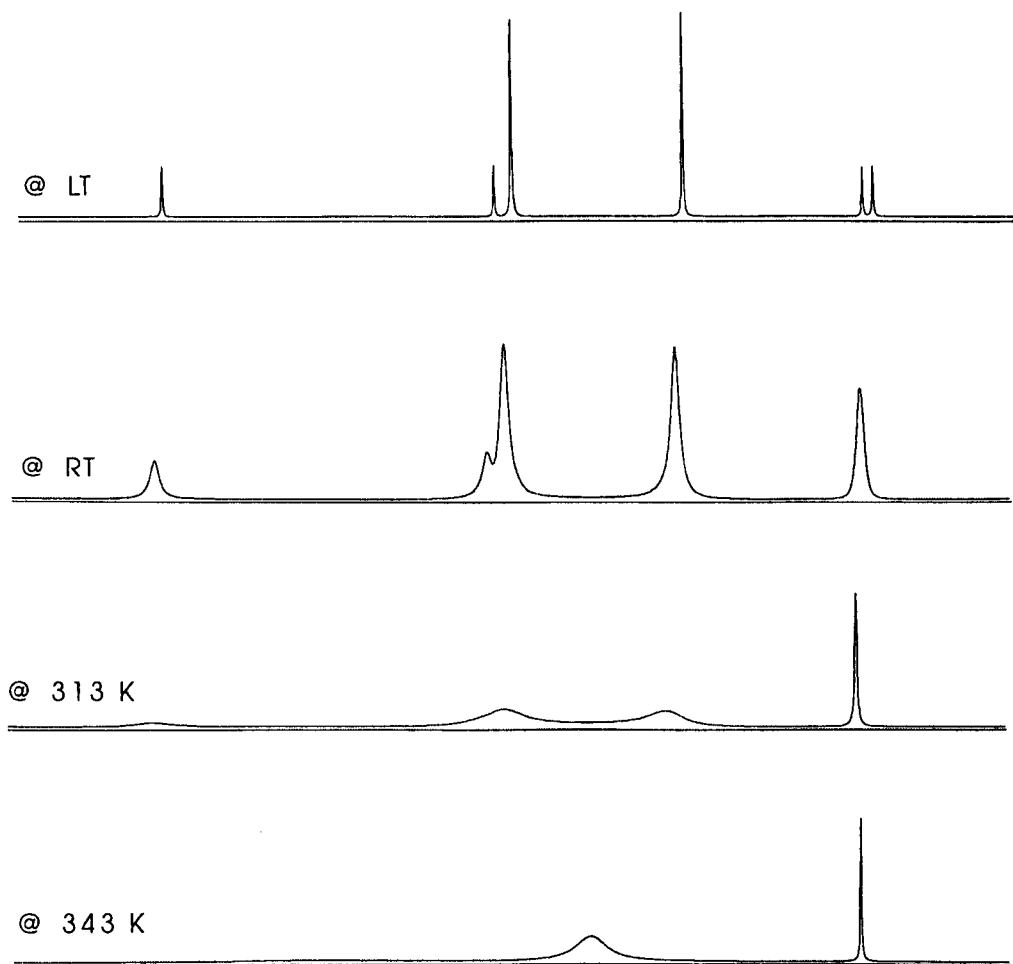
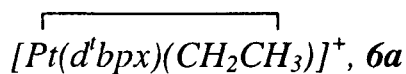


It is interesting to observe the behaviour of the resonance at *ca.* 20 ppm. In the  $^{31}\text{P}\{^1\text{H}\}$  NMR spectrum at room temperature of **6a** in Figure 4.2 and 4.4a, this resonance is quite broad. It becomes sharper on increasing the temperature (see Figure 4.4). We have shown that this must be due to an overlap of the two satellites of the two main resonances of the platinum ethyl complex **6a**. In fact, in the  $^{31}\text{P}\{^1\text{H}\}$

NMR spectrum at low temperature (see Figure 4.1) the two platinum satellites at *ca.* 20 ppm are very close to each other but clearly separated.

**Figure 4.5**

*Computer simulation of the VT  $^{31}\text{P}\{^1\text{H}\}$  NMR spectra of*

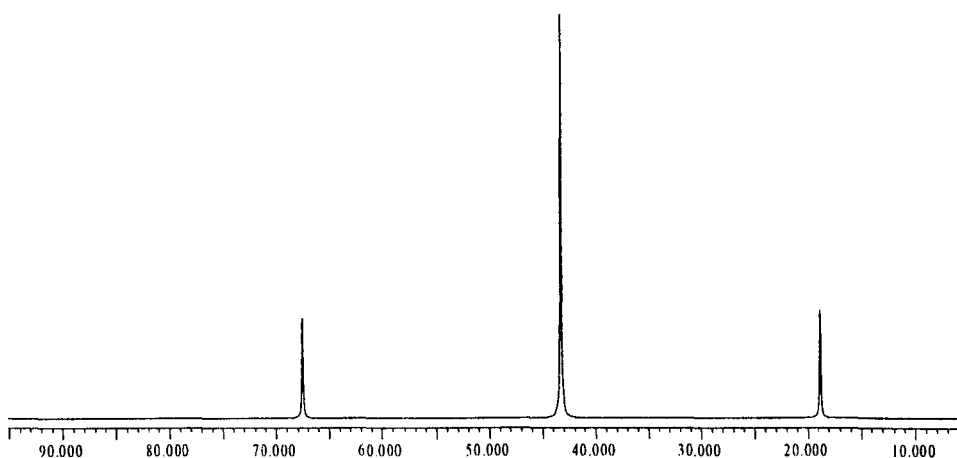
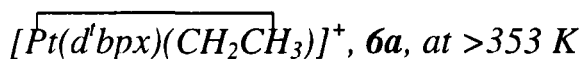


The unusual behaviour of the resonance at *ca.* 20 ppm is due to an exchange process, which has the effect of making the two phosphorus atoms equivalent. This explanation is confirmed by the computer simulation made with the program gNMR

(see Figure 4.5). In this simulation, the two phosphorus atoms exchange at different rates in a magnetic field of 200 MHz. On increasing the rate by increasing the temperature the two main resonances coalesce and the resonance at higher field (20 ppm) becomes sharper. The computer simulation of the  $^{31}\text{P}\{^1\text{H}\}$  NMR spectrum in Figure 4.6 shows only one singlet with its satellites due to the platinum ethyl complex **6a**. The temperature reached in this example is higher than 353 K and the rate of exchange between the two phosphorus atoms is so high that they behave as though they are equivalent.

**Figure 4.6**

Computer simulation of the  $^{31}\text{P}\{^1\text{H}\}$  NMR spectrum of

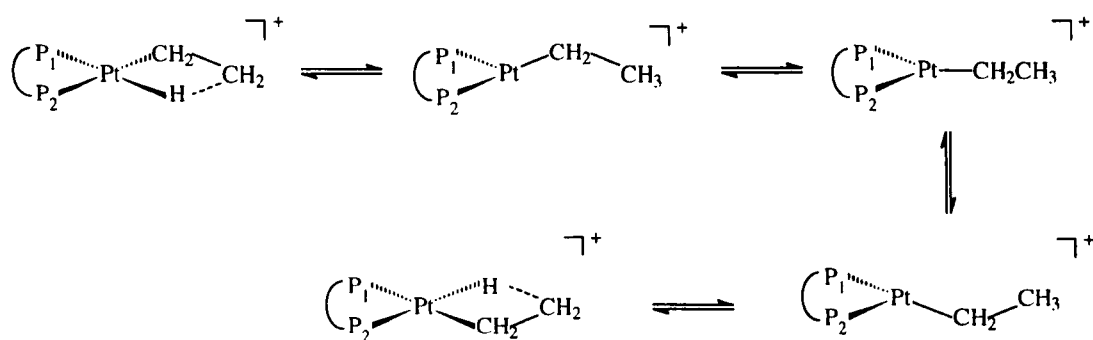


Two different mechanisms can be proposed in order to explain the equivalence of the two phosphorus atoms of **6a** at high temperature. The first mechanism involves an *inter-molecular* rearrangement of **6a**, where bond-breaking and making is

involved (see Scheme 4.2). Indeed, this mechanism involves dissociation of the agostic interaction with formation of a 14 electron T-shaped intermediate which can then, become Y-shaped, allowing the change of the relative positions of the ethyl group and phosphorus atoms. Spencer has proposed this mechanism in order to explain the same process in complexes like **6a** (i.e.  $[\text{Pt}(\text{L-L})(\text{CH}_2\text{CH}_3)]^+$  where L-L = dbpe and dbpp).<sup>16</sup>

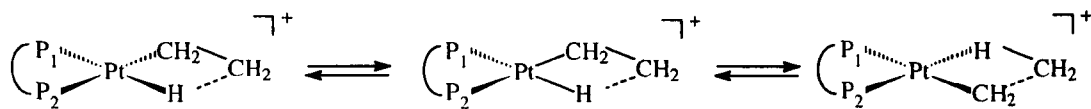
### Scheme 4.2

#### *Inter-molecular mechanism*



The second mechanism involves an *intra-molecular* rearrangement of **6a** via a tetrahedral intermediate (see Scheme 4.3). This mechanism has been proposed previously to explain other rearrangements occurring in four co-ordinate square planar complexes, such as *cis-trans* isomerisation.<sup>17</sup> Usually, the energy separation between tetrahedral and planar forms is very large; but in some cases, when the central atom has partially-filled d orbitals, the energy of tetrahedral and planar forms often become similar for the lighter transition elements. Tetrahedral and planar forms can coexist in solution for  $\text{Ni}^{2+}$  ( $d^8$ ), i.e.  $[(\text{R}_3\text{P})_2\text{NiX}_2]$  and  $[(\text{dppfO}_2)\text{NiCl}_2]$ .<sup>18,19,20</sup>

## Scheme 4.3

*Intra-molecular mechanism*

Unfortunately, from the data available it is not possible in our case to understand which mechanism is involved in making the two phosphorus atoms equivalent. One experiment which could help in distinguishing between these alternative mechanisms is to follow the  $^1\text{H}$  NMR spectra at different temperatures and observe if the phosphorus-proton or platinum-proton couplings are retained; in this case, if the dissociation of the bonds is not involved, the intra-molecular mechanism would then be confirmed. However, this experiment has not been performed because above 240 K the equivalence of the two carbons and all five protons has been previously observed by Spencer and only average signals are shown in the  $^1\text{H}$  and  $^{13}\text{C}$  NMR spectra.

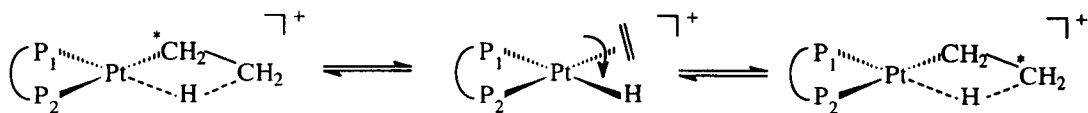
#### 4.3.2 Dynamic behaviour of **6a** at low temperature (293–145 K)

Initially, the aim of this experiment was to repeat the same procedure at high temperature as in the experiment described in the previous paragraph, studying the  $^{13}\text{C}\{^1\text{H}\}$  and  $^1\text{H}$  NMR spectra. Spencer reported in the literature the  $^{13}\text{C}$  and  $^1\text{H}$  NMR data of  $[\text{Pt}(\text{d}^t\text{bpx})(\text{CH}_2\text{CH}_3)]^+$ , **6a**, at RT, 203 K and 145 K.<sup>14</sup> He observed that at room temperature the  $^{13}\text{C}\{^1\text{H}\}$  NMR spectrum in  $\text{CH}_2\text{Cl}_2$  shows a single resonance at

16.5 ppm, coupled to one phosphorus atom with  ${}^2J(\text{C-P}) = 18$  Hz and  ${}^1J(\text{Pt-C}) = 91$  Hz. At the same temperature, the  ${}^1\text{H}$  NMR spectrum shows only one resonance at 0.74 ppm with  ${}^2J(\text{C-P}) = 12$  Hz, and no platinum proton coupling is observed. It is evident that the two carbons and the five protons exchange already at room temperature. At 203 K Spencer does not report any  ${}^{13}\text{C}\{^1\text{H}\}$  NMR data and he observes that the  ${}^1\text{H}$  NMR spectrum at this temperature shows a resonance at -2.8 ppm, which indicates the presence of a hydride coordinated to platinum. Unfortunately, the phosphorus-carbon and platinum-carbon coupling constants were not observed. Only at 145 K are the two inequivalent carbons and all five protons of the platinum ethyl complex **6a** clearly distinguished. In the  ${}^{13}\text{C}$  NMR spectrum at 145 K in  $\text{CH}_2\text{Cl}_2/\text{THF}$ , two main resonances are present at high field: one at 22.0 ppm due to the  $-\text{CH}_2$ -group ( ${}^1J(\text{C}_\alpha\text{-H}) = 155$  Hz,  ${}^2J(\text{C}_\alpha\text{-P}) = 39$  Hz and  ${}^1J(\text{C}_\alpha\text{-Pt}) = 218$  Hz) and the other at 9.0 ppm due to  $-\text{CH}_3$  group ( ${}^1J(\text{C}_\beta\text{-H}_{\text{ag}}) = 75$  Hz and  ${}^1J(\text{C}_\beta\text{-H}_\text{t}) = 155$  Hz). These data are consistent with the ethyl ligand bonded to platinum through both  $\sigma$ -alkyl and  $\beta$ -agostic C-H-Pt bonds. Indeed, the resonance at 22.0 ppm is a triplet and the resonance at 9.0 ppm is a triplet of doublets.

From the NMR data reported by Spencer, the comparison of the  ${}^{13}\text{C}$  NMR spectra of **6a** at 293 K and 142 K, indicates a facile scrambling of the  $\text{C}_2\text{H}_5$  group at 293 K, which results in the equivalence of all five protons and the two carbons. These observations are consistent with a rapid intra-molecular process involving the formation of the ethene hydride complex, where the ethene rotation is rapid (see Scheme 4.4).

## Scheme 4.4

*Mechanism for the rearrangement of the  $\beta$ -agostic ethyl in 6a*

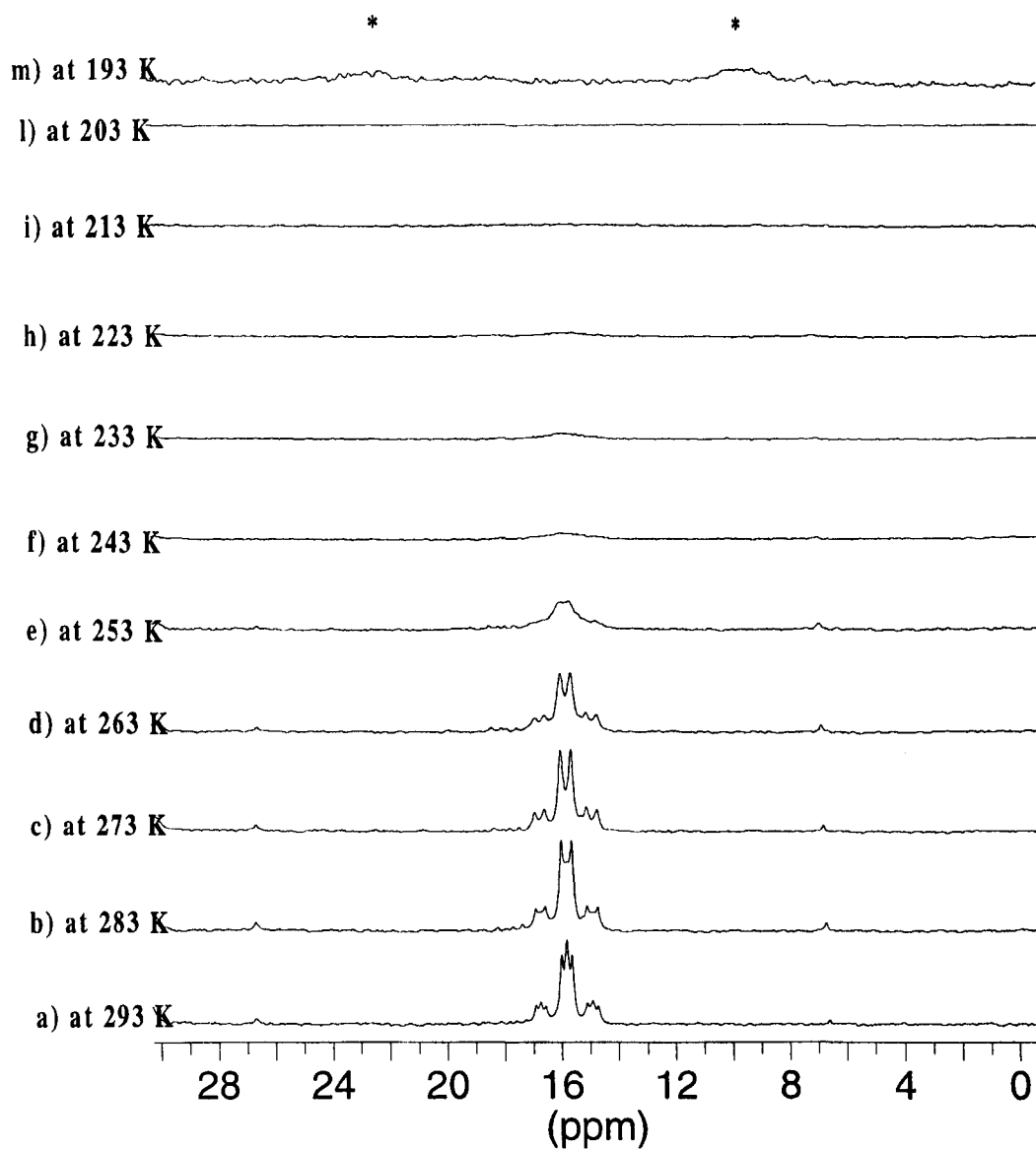
At room temperature, the two carbons are equivalent and give rise to one resonance at 16.4 ppm, which is the average value of the two resonances observed at 145 K ( $\delta\text{C}_\alpha = 22.0$  ppm and  $\delta\text{C}_\beta = 9.0$  ppm). This resonance is a doublet because the two carbon atoms are coupled to only one phosphorus atom (*trans* to the ethene group). The presence of the ethene hydride intermediate is confirmed by Spencer in the  $^1\text{H}$  NMR spectrum at 203 K where a chemical shift at  $-2.8$  ppm indicates the presence of the hydride but no platinum-proton or phosphorus-proton couplings are observed.<sup>14</sup>

Spencer did not report any  $^{13}\text{C}\{^1\text{H}\}$  NMR data for **6a** at intermediate temperatures between 293 and 145 K. In order to understand better the dynamic behaviour of the platinum ethyl complex **6a** in solution and to understand if it is possible to correlate the mechanism observed by Spencer with the mechanisms proposed in Scheme 4.2 and 4.4, variable temperature measurements (293 K–193 K) have been carried out. The doubly  $^{13}\text{C}$ -labelled sample of  $[\text{Pt}(\text{d}^t\text{bpx})(\overline{\text{CH}_2\text{CH}_3})]^+$ , **6a**, has been prepared from a solution of the unenriched ethyl complex **6a** in  $\text{CH}_2\text{Cl}_2$  and exchange reaches equilibrium after 30 minutes at room temperature. The  $^{31}\text{P}\{^1\text{H}\}$  spectrum at room temperature in  $\text{CH}_2\text{Cl}_2$  shows two broad resonances ( $\delta\text{P}_1 = 53.2$  ppm  $\delta\text{P}_2 = 37.5$  ppm; as in the Figure 4.3) due to the two inequivalent phosphorus

atoms and phosphorus-phosphorus or phosphorus-carbon coupling constants are not observed, as found in the spectrum of the unenriched compound because the two  $^{31}\text{P}$  resonances are very broad. The  $^{13}\text{C}\{^1\text{H}\}$  NMR spectrum at 293 K in  $\text{CH}_2\text{Cl}_2$  shows a second order NMR spectrum, where a single resonance at 16.4 ppm is due to two magnetically inequivalent carbon atoms with  $^2J(\text{C-P}) = 9.3$  Hz and  $^1J(\text{C-Pt}) = 91.5$  Hz, (see Figure 4.7a). On cooling the solution to 273 K, the resonance at 16.4 ppm becomes a doublet ( $^2J(\text{C-P}) = 18$  Hz and  $^1J(\text{Pt-C}) = 91.5$  Hz) as reported by Spencer (see Figure 4.7c).<sup>14</sup> On cooling the solution further, the resonance at 16.4 ppm due to the two equivalent carbons broadens until it disappears at 203 K. At 193 K in the  $^{13}\text{C}\{^1\text{H}\}$  NMR spectrum two broad resonances appear at *ca.* 22 ppm and 9 ppm. It has been observed above that only at 145 K is it possible to distinguish clearly the two carbons in  $[\text{Pt}(\text{d}^1\text{bpx})(\text{CH}_2\text{CH}_3)]^+$ , **6a**. All these data are consistent with the data reported by Spencer; the only difference is the spectrum at 293 K (see Figure 4.7a), where the carbon resonance is a pseudo triplet due to a second order NMR spectrum and not a doublet as previously reported.<sup>14</sup> During our experiment, the  $^{13}\text{C}\{^1\text{H}\}$  NMR spectrum at 293 K can indicate another intermediate involved in the process. Since the  $^{13}\text{C}\{^1\text{H}\}$  NMR spectrum at 293 K shows a second order NMR spectrum, this indicates that the two chemically equivalent carbon atoms are magnetically inequivalent. It is possible to conclude that three different intermediates are present in the temperature range 145–293 K (see Scheme 4.5).

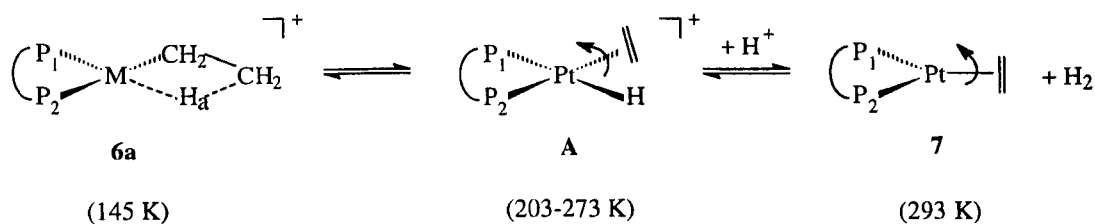
**Figure 4.7**

*VT*  $^{13}\text{C}\{^1\text{H}\}$  NMR spectra of  $[\text{Pt}(\text{d}^t\text{bpx})(\text{CH}_2\text{CH}_3)]^+$ , **6a**, in  $\text{CH}_2\text{Cl}_2$



## Scheme 4.5

*Dynamic behaviour of  $[\text{Pt}(\text{d}^t\text{bpx})(\text{CH}_2\text{CH}_3)]^+$ , **6a**, and the dominant species present at different temperatures*



At 145 K, the NMR spectra of the platinum ethyl complex **6a** are all entirely consistent with the ethyl being bonded to platinum *via*  $\sigma$ -alkyl and  $\beta$ -agostic C-H-Pt bonds as reported by Spencer. From 203-273 K, the platinum ethene-hydride **A** complex is the predominant species in solution. At 293 K, we propose that the dominant species in solution is the 16-electron  $[\text{Pt}(\text{d}^t\text{bpx})(\eta^2\text{-C}_2\text{H}_4)]$ , **7**, intermediate is present in solution too. This intermediate has been reported in the literature to explain the *cis-trans* isomerisation of a platinum(II) complex, *cis*- $[\text{Pt}(\text{PEt}_3)_2(\text{neopentyl})\text{Cl}]$ ,<sup>21</sup> and its configurational stability has been supported by MO calculations.<sup>22</sup>

Spencer excluded the presence of the 16-electron species  $[\text{Pt}(\text{d}^t\text{bpx})(\eta^2\text{-C}_2\text{H}_4)]$ , **7**, over the temperature range (293-145 K) he used, because here the two phosphorus resonances remain distinct. However, the large difference in the values of  $^1J(\text{P-Pt})$  for the phosphorus nuclei *cis* and *trans* to the agostic bond is in accord with an agostic interaction but not with the presence of the platinum ethene-hydride complex or the 16-electron complex that we now propose. Thus, there is good evidence for the different species shown in Scheme 4.5 at the temperatures indicated: specie **A** allows

the two carbons of the  $\beta$ -agostic ethyl to become equivalent while coupling to only one *trans*-phosphorus and complex **7** also allows the two carbons to become equivalent and couple to two phosphorus. Nevertheless, it is surprising that there is no difference in the chemical shift for platinum(II) (species **A**) and platinum(0) complex **7**.

**Table 4.2**

*$^{13}\text{C}$  NMR data of  $[\text{Pt}(\text{d}^i\text{bpx})(\text{CH}_2\text{CH}_3)]^+$ , **6a**, at low temperature in  $\text{CH}_2\text{Cl}_2$*

	$\delta\text{C}_\alpha$ (ppm)	$^2J(\text{C}_\alpha\text{-P})$ (Hz)	$^1J(\text{C}_\alpha\text{-Pt})$ (Hz)	$\delta\text{C}_\beta$ (ppm)
<b>at 293 K</b>	16.4	18	92	16.4
<b>at 273 K</b>	16.4	9.3	92	16.4
<b>at 145 K<sup>(a)</sup></b>	22.0	39	218	9.0

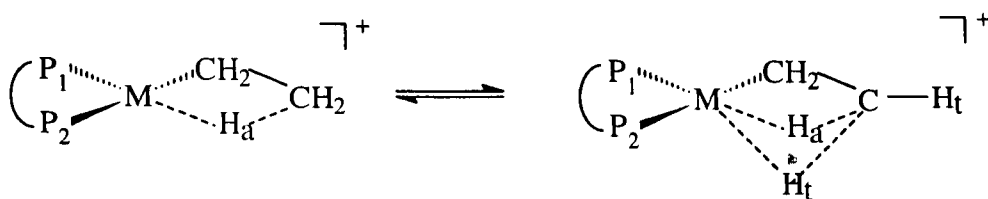
<sup>(a)</sup> NMR data from the reference 14

Different mechanisms have been proposed to allow the five protons in the ethyl group in **6a** to become equivalent. The rotation of the ethene group in the ethene-hydride platinum complex makes the protons equivalent. The rotation can occur also without full dissociation of the agostic interaction, as described by Green and Wong.<sup>23</sup> They have demonstrated that scrambling of  $\beta$ -hydrogens of the agostic ethyl group in some molybdenum and cobalt complexes occurs *via* a mechanism analogous to that described in Scheme 4.4. This process requires a gradual weakening of  $\text{M-H}_\alpha$  bond and strengthening of  $\text{M-H}_\beta$  agostic interaction and,

therefore, the dissociative mechanism can be considered to be the limiting case. From the data reported by Spencer it suggests that the dissociative mechanism shown in Scheme 4.2 is preferable to that one in Scheme 4.4, where the agostic interaction is not completely lost.

### Scheme 4.4

*Rotation mechanism without dissociation of the agostic interaction*



It is interesting to observe that the two phosphorus resonances in the  $^{31}\text{P}\{^1\text{H}\}$  NMR spectrum at 293 K always remain inequivalent in the temperature range 145–293 K; this indicates that the integrity of the square-planar geometry is not affected. For this reason, it is possible to conclude that the two processes, one which makes the two carbons equivalent in the temperature range 293–145 K and the other which makes the two phosphorus atoms equivalent in the temperature range 293–353 K are not correlated, even if the exchange process of the two phosphorus atoms present at 293 K affects the  $^{13}\text{C}\{^1\text{H}\}$  NMR spectrum at this temperature.

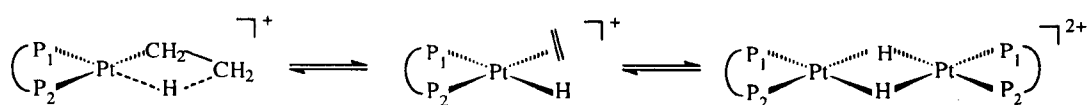
#### 4.4. The $\beta$ -agostic interaction

It has been observed above that one classic route for the formation of metal ethyl complexes is the reaction of a metal-hydride with ethene. One of the problems

associated with the compounds obtained from this reaction is that they contain a  $\beta$ -hydrogen, which can react with the metal *via*  $\beta$ -H-elimination. In all cases,  $\beta$ -H-elimination is one of the main reasons for the decomposition of metal-alkyl complexes.<sup>15</sup> The most obvious solution is to use alkyl groups without a  $\beta$ -hydrogen.

A completely different strategy has been used by Spencer, who has formed new nickel, palladium and platinum ethyl complexes, stabilised by bulky diphosphine ligands and an agostic interaction between the metal and one of the  $\beta$ -hydrogens of the ethyl ligand.<sup>24</sup> These complexes are very interesting because they represent a stable form of one of the possible intermediates in the  $\beta$ -H-elimination process. Spencer has shown clearly that these complexes are in equilibrium with the ethene-hydride complex, which can then lose ethene resulting in the formation of a binuclear di-hydride species (see Scheme 4.6).<sup>25</sup>

### Scheme 4.6



It has been shown that the formation of one of these complexes reported in Scheme 4.6 is completely controlled by the diphosphine used. Bulky and basic diphosphines (*e.g.*  $\text{d}^{\text{t}}\text{bpx}$  and  $\text{d}^{\text{t}}\text{bpp}$ ) favour the  $\beta$ -agostic ethyl compound, whereas, decreasing the size of the ligand, results in the formation of the ethene hydride complex which loses ethene resulting in dimer formation.<sup>24</sup> Spencer has also reported some effects of bulky alkyl substituents on the stability of the platinum

complexes with a  $\beta$ -agostic interaction.<sup>26</sup> He observed that the energetic balance between agostic and alkene-hydride isomers does not appear to be particularly sensitive to the introduction of bulky substituents, such as the <sup>t</sup>Bu group.

In Table 4.3 are reported some data of platinum ethyl with or without a  $\beta$ -H-agostic interactions. In all the complexes that show an agostic interaction, <sup>13</sup>C NMR studies show that the  $\text{CH}_2$  group resonates at lower field than the  $\text{CH}_3$  group. The  $^1J(\text{C}_\beta\text{-H}_\alpha)$  assumes a lower value (60-80 Hz) than in the classic ethyl complexes (120-130 Hz), due to the reduced  $\text{C}_\beta\text{-H}_\alpha$  bond order in the  $\beta$ -H-agostic system and the resultant elongated  $\text{C}_\beta\text{-H}_\alpha$  bond.<sup>27</sup>

**Table 4.3**

*NMR data for platinum ethyl complexes*

Complex	$\delta(\text{C}_\alpha)$ (ppm)	$^1J(\text{C}_\alpha\text{-H})$ (Hz)	$\delta(\text{C}_\beta)$ (ppm)	$^1J(\text{C}_\beta\text{-H})^c$ (Hz)
$[\text{Pt}(\text{d}^t\text{bpp})(\text{C}_2\text{H}_5)_2]^a$	11.1	-	17.2	-
$[\text{Pt}(\text{d}^t\text{bpp})(\text{CH}_2\text{CH}_3)]^{+b}$	22.0	158	8.2	60/153
$[\text{Pt}(\text{d}^t\text{bpx})(\text{CH}_2\text{CH}_3)]^{+b}$	22.0	155	9.0	75/155

<sup>a</sup> At 298 K in  $\text{C}_6\text{D}_6$ , see ref. 16. <sup>b</sup> at 145 K in  $\text{CD}_2\text{Cl}_2/\text{THF}$ , see ref. 16.

<sup>c</sup> The low values are due to the Pt-H-C agostic interaction and the high value are due to the  $\text{C}_\beta\text{-H}$  interaction.

As observed above (see Section 4.2), many agostic compounds are fluxional and undergo rapid exchange of the agostic hydrogen with other hydrogens, normally those attached to the same carbon. These fluxional compounds give time averaged spectra, as observed for the platinum ethyl complex **6a**. This can be explained assuming a very low barrier for the rotation of the methyl group. The static spectra

can sometimes be obtained at very low temperature and sometimes it is possible to observe the coupling between the carbon and the two different protons,  $\text{H}_t$  and  $\text{H}_a$ .

#### 4.5. Formation of $[\text{Pt}(\text{d}^1\text{bpx})(\text{CH}_2\text{CH}_3)][\text{CH}_3\text{SO}_3]$ , **4b**

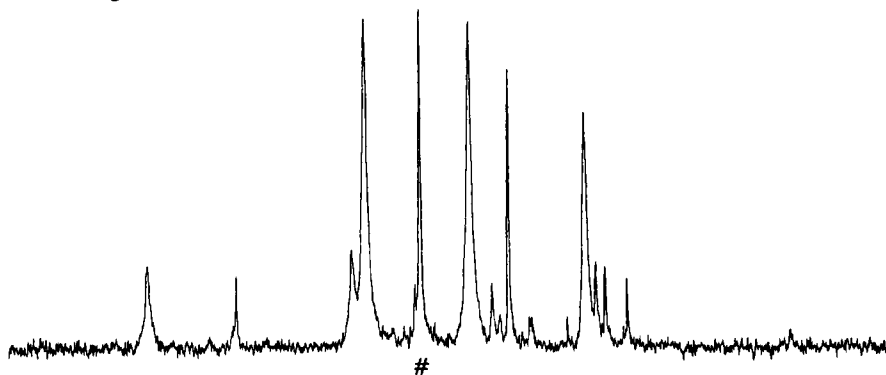
As in the case of  $[\text{Pt}(\text{d}^1\text{bpx})\text{H}(\text{MeOH})][\text{CF}_3\text{SO}_3]$ , **3a**, the reactivity of  $[\text{Pt}(\text{d}^1\text{bpx})\text{H}(\text{MeOH})][\text{CH}_3\text{SO}_3]$ , **3b**, with ethene has been studied in MeOH at room temperature. Also in this case, the reaction between the hydride complex **3b** and ethene is not immediate. Under one atmosphere of ethene at room temperature both species, the platinum hydride **3b** and the platinum ethyl complex  $[\text{Pt}(\text{d}^1\text{bpx})(\text{CH}_2\text{CH}_3)][\text{CH}_3\text{SO}_3]$ , **6b**, are present. On bubbling ethene for 30 minutes, the resonances due to the ethyl complex **6b** slightly increase, but the Pt-hydride complex is still present (see Figure 4.8).

It is possible to conclude that the Pt-hydride complex is very stable and its reactivity with ethene is slow as observed in the  $\text{CF}_3\text{SO}_3\text{H}$ -system. This experiment has not been done at low temperature but it seems that also in this case there is an equilibrium correlated to the solubility of ethene in solution, that increases at low temperature. All the NMR data of  $[\text{Pt}(\text{d}^1\text{bpx})(\text{CH}_2\text{CH}_3)][\text{CH}_3\text{SO}_3]$ , **6b**, are exactly the same as those reported for  $[\text{Pt}(\text{d}^1\text{bpx})(\text{CH}_2\text{CH}_3)][\text{CF}_3\text{SO}_3]$ , **6a**, (see Table 4.1). This behaviour indicates that the chemical shifts of the two inequivalent phosphorus atoms of **6** are not affected by changing the anion.

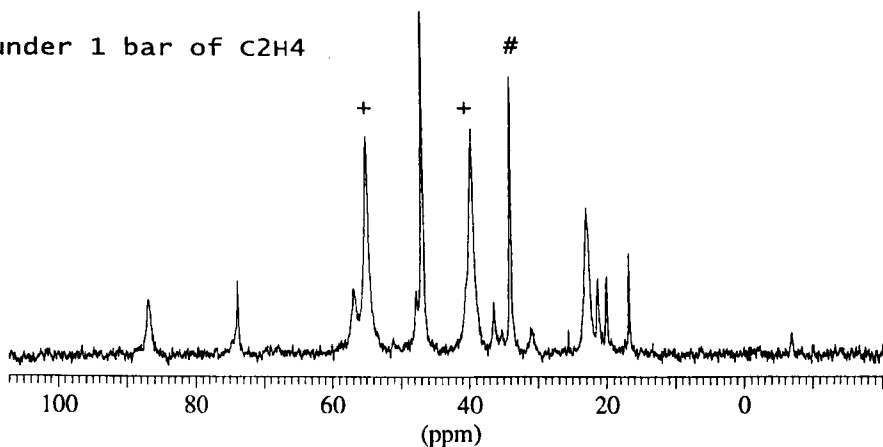
**Figure 4.8**

$^{31}\text{P}\{^1\text{H}\}$  NMR spectra of  $[\text{Pt}(\text{d}^{\text{t}}\text{bpx})(\text{CH}_2\text{CH}_3)][\text{CH}_3\text{SO}_3](+)$ , **6b**, and  $[\text{Pt}(\text{d}^{\text{t}}\text{bpx})\text{H}(\text{solv})][\text{CH}_3\text{SO}_3](\#)$ , **3b**, at 293 K in MeOH

bubbling  $\text{C}_2\text{H}_4$  for 30 min



under 1 bar of  $\text{C}_2\text{H}_4$



## 4.6. Conclusions

In the previous chapter, it has been shown that the platinum system is quite similar to the palladium system. In fact, there is spectroscopic evidence for the formation of  $[\text{Pt}(\text{d}^{\text{t}}\text{bpx})(\text{dbaH})][\text{CF}_3\text{SO}_3]$ , **2a**, and  $[\text{Pt}(\text{d}^{\text{t}}\text{bpx})(\text{dbaH})][\text{CH}_3\text{SO}_3]$ , **2b**. Oxidation of **2b** gives  $[\text{Pt}(\text{d}^{\text{t}}\text{bpx})(\eta^2\text{-CH}_3\text{SO}_3)]^+$ , **5b**, whereas oxidation of the **2a** gives  $[\text{Pt}(\text{d}^{\text{t}}\text{bpx})\text{H}(\text{MeOH})]^+$ , **3a**, as in the case of palladium.

Indirectly, it has been observed, in this chapter, that the platinum hydride complex **3a** is not formed in non-alcoholic solvents. The  $^{31}\text{P}\{^1\text{H}\}$  NMR spectrum at 293 K of the platinum ethyl complex **6a** in MeOH shows also resonances due to the platinum hydride complex **3a**. Whereas, the compound **6a** in  $\text{CH}_2\text{Cl}_2$  at room temperature does not convert into the hydride **3a**, because the platinum hydride is not stable in these conditions. In the case of palladium, the role of the solvent in the formation of  $[\text{Pd}(\text{d}^{\text{t}}\text{bpx})\text{H}(\text{MeOH})]^+$  has been investigated and the same conclusion has been obtained.

The first difference between the platinum and the palladium systems appears to be the stability of the hydride complexes and their reactivity with ethene. The formation of  $[\text{Pt}(\text{d}^{\text{t}}\text{bpx})\text{H}(\text{MeOH})]^+$ , **3a**, occurs quite quickly and its stability is evident during different NMR investigations made with the same sample.  $[\text{Pd}(\text{d}^{\text{t}}\text{bpx})\text{H}(\text{MeOH})]^+$  converts into the ethyl complex immediately after the addition of one equivalent of ethene, whereas, the platinum-hydride **3a** needs more ethene and more time to form the analogous complex. Generally, the platinum compounds formed are more stable, the Pt-H bond is stronger than the Pd-H bond and in many cases, analogous reactions of platinum compounds are kinetically slower than for palladium. It is rather difficult to understand if the formation of the ethyl complex is a kinetic or a thermodynamic problem. From the results it seems that both are involved: the stability of the hydride and its slowness in the reaction with ethene.

## 4.7. References

- (1) W.C. Zeise *Mag. Pharm.*, **1830**, 35, 105.
- (2) F.R. Hartley *Chem. Rev.*, **1969**, 69, 799.
- (3) F.R. Hartley *Angew. Chem. Int. Ed. Engl.*, **1972**, 11, 596.
- (4) S.D. Ittel and J.A. Ibers *Adv. Organomet. Chem.*, **1976**, 14, 33.
- (5) M.J.S. Dewar *Bull. Soc. Chim. Fr.*, **1951**, 18, C79.
- (6) J. Chatt and L.A. Duncanson *J. Chem. Soc.*, **1953**, 2939.
- (7) F.R. Hartley *Inorg. Chim. Acta*, **1971**, 5, 197.
- (8) R.G. Denning and L.M. Venanzi *J. Chem. Soc.*, **1963**, 3241.
- (9) K.A. Jensen *Acta Chem. Scand.*, **1953**, 7, 866.
- (10) R.D. Cramer; E.L. Jenner; R.V. Lindsey; U.G. Stolberg *J. Am. Chem. Soc.*, **1963**, 85, 1691.
- (11) J. Chatt and M.L. Searle *Inorg. Synth.* **1957**, 5, 210.
- (12) D.A. White *Synth. Inorg. Metal-Org. Chem.*, **1972**, 1, 133.
- (13) P.P. Ponti; J.C. Baldwin; W.C. Kaska *Inorg. Chem.*, **1979**, 18, 873.
- (14) N. Carr; L. Mole; A. Guy Orpen; J. L. Spencer *J. Chem. Soc., Dalton Trans.*, **1992**, 2653.
- (15) C. Elschenbroich and A. Salzer *Organometallics- A Concise Introduction*, **1992**, 195.
- (16) N. Carr; L. Mole; A. Guy Orpen; J. L. Spencer *Organometallics* **1991**, 10, 49.
- (17) B.E. Mann *Comprehensive Organometallic Chemistry*, ed. G. Wilkinson, Pergamon Press, **1982**, 3, 89.

- (18) L.H. Pignolet; W.D. Horrocks; R.H. Holm *J. Am. Chem. Soc.*, **1970**, *92*, 1855.
- (19) N.N. Greenwood and A. Earnshaw *Chemistry of the Elements*, Pergamon Press, New York, **1984**, ch. 27, 1347.
- (20) J.S.L. Yeo; J.J. Vittal; T.S. Hor *Chem. Comm.*, **1999**, 1477.
- (21) G. Alibrandi; L.M. Scolaro; R. Romeo *Inorg. Chem.*, **1991**, *30*, 4007.
- (22) T.J. McCarthy; R.J. Nuzzo; G.M. Whitesides *J. Am. Chem. Soc.*, **1981**, *103*, 1676.
- (23) M.L.H. Green and L.-L. Wong *J. Chem. Soc., Chem. Comm.*, **1988**, 677.
- (24) N. Carr; B. J. Dunne; L.Mole; A. Guy Orpen; J. L. Spencer *J.Chem.Soc.Dalton Trans*, **1991**, 863.
- (25) L. Mole; J.L. Spencer; S.A. Litster; A.D. Redhouse; N. Carr; A.G. Orpen *J. Chem. Soc.,Dalton Trans.*, **1996**, 2315.
- (26) J. L. Spencer and G. S. Mhinzi *J.Chem.Soc.Dalton Trans*, **1995**, 3818.
- (27) M. Brookhart; M.L.H. Green; L.-L. Wong *Prog. Inorg. Chem.*, **1988**, *36*, 1.

# **Chapter Five**

## 5. Reactivity of $[\text{Pt}(\text{d}^t\text{bpx})(\text{CH}_2\text{CH}_3)][\text{RSO}_3]$ with CO

### 5.1. Introduction

The first carbonyl platinum complex was made, by the French chemist P. Schutzenberger in 1868-1870 and it was a carbonyl halide of platinum. The structures of the carbonyl halides are now well established:<sup>1</sup>



When CO is passed into a solution of  $[\text{Pt}(\text{PEt}_3)_2\text{Cl}_2]$  containing excess sodium perchlorate under ambient conditions, the CO displaces a chloride to give:<sup>2</sup>



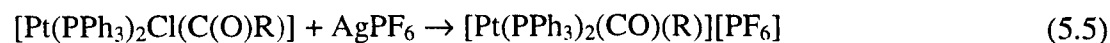
Carbon monoxide can displace olefins and acetylenes from their platinum(II) complexes:<sup>3,4</sup>



Other ligands can also be displaced by CO ( $X = \text{Cl}, \text{Br}, \text{I}, \text{CF}_3\text{CO}_2$ ):<sup>5</sup>



Elimination of CO also occurs on heating acyl complexes to give alkyl complexes, but, sometimes (see eq. 5.5) the CO may be retained:<sup>6</sup>



The metal carbon bond consists of a  $\sigma$ -bond formed by overlap of a filled  $sp$  hybrid orbital on the carbon atom with a vacant hybrid orbital on platinum, complemented by  $\pi$  back-donation of electron density from filled platinum  $d$  orbitals to empty  $\pi^*$  (antibonding) orbitals on the CO. The presence of electrons in the  $\pi^*$  orbitals of CO weakens the C-O bond and hence lowers the C-O stretching frequency which in free CO occurs at  $2145\text{ cm}^{-1}$ . In the  $^{13}\text{C}\{^1\text{H}\}$  NMR spectra of  $^{13}\text{CO}$ -enriched  $[\text{PtX}(^{13}\text{CO})\text{LL}']$  complexes, the chemical shift shows a strong dependence on the nature of the *trans* ligand, the more powerful  $\sigma$ -donors pushing it towards the value in free  $^{13}\text{CO}$ .<sup>7</sup> X-ray diffraction studies of different compounds have established that the *trans* influence of carbonyl ligand is very small but that the Pt-CO bond is itself susceptible to a strong *trans* influence, being lengthened by powerful  $\sigma$ -donors in *trans* position.<sup>8</sup>

The Pt-C bond is stronger than the corresponding Pd-C bond and this is due in large measure to much greater degree of  $\pi$  back-donation from platinum than palladium and this greater  $\pi$  back-donation is increased by stronger  $\sigma$ -bond between platinum and carbon than between palladium and carbon.<sup>9</sup>

## 5.2. Reactivity of $[\text{Pt}(\overline{\text{d}^t\text{bpx}})(\text{CH}_2\text{CH}_3)][\text{CF}_3\text{SO}_3]$ , **6a**, with CO in MeOH at 293 K

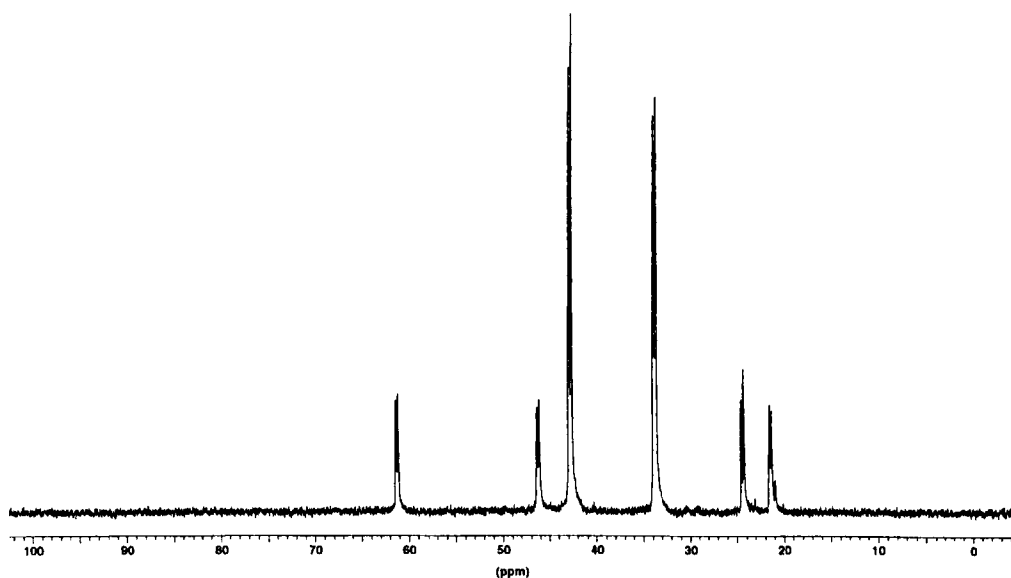
In this chapter the insertion of CO into a metal-carbon bond will be discussed, since this reaction is one of the most important steps in homogeneous catalysis.

The reaction of the platinum ethyl complex **6a** with CO has been studied, first, in MeOH at 293 K. Under one atmosphere of CO, the ethyl complex **6a** reacts in a few

minutes to give a new compound. The  $^{31}\text{P}\{^1\text{H}\}$  NMR spectrum at 293 K shows two doublets with associated platinum satellites and this means that the new complex contains two *cis* inequivalent phosphorus atoms with  $^2J(\text{P}_1\text{-P}_2) = 18.6$  Hz (see Figure 5.1); the  $^{31}\text{P}$  NMR spectrum (see Figure 5.2) shows that the resonance at 33.2 ppm becomes a doublet with  $^2J(\text{P}_2\text{-H}) = 145$  Hz, indicating the presence of a *trans*-hydride ligand. In agreement with this hypothesis, the proton NMR spectrum at 293 K in  $\text{CD}_3\text{OD}$  shows a doublet of doublets at  $-4$  ppm (see Figure 5.3), the typical hydride region for this kind of compound. From this spectrum, it is possible to obtain all the coupling constants, which are reported in Table 5.1.

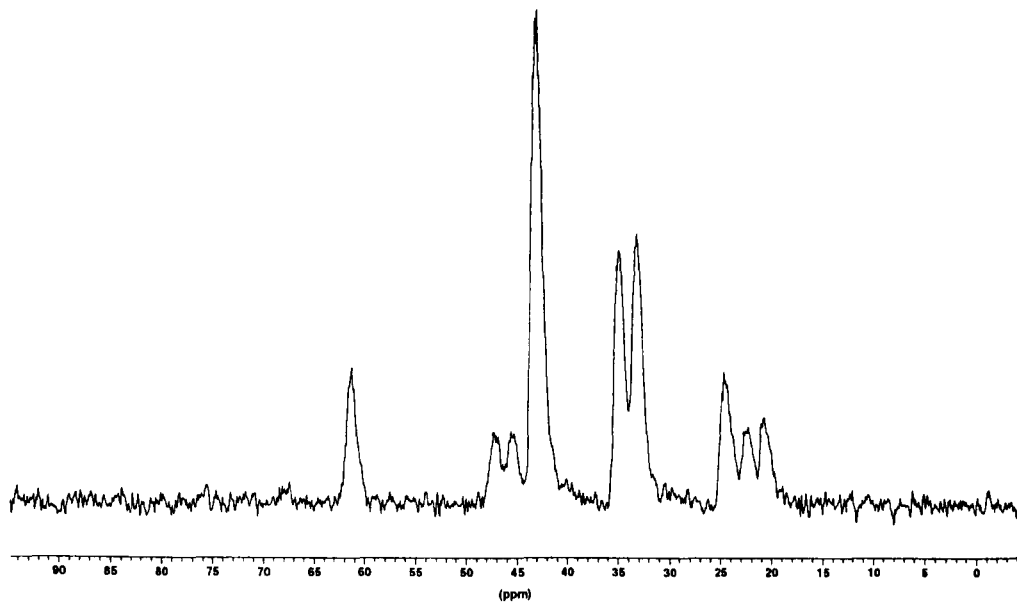
**Figure 5.1**

$^{31}\text{P}\{^1\text{H}\}$  NMR spectrum of  $[\text{Pt}(\text{d}^t\text{bpx})\text{H}(\text{CO})]^+$ , **8a**, in MeOH at 293 K

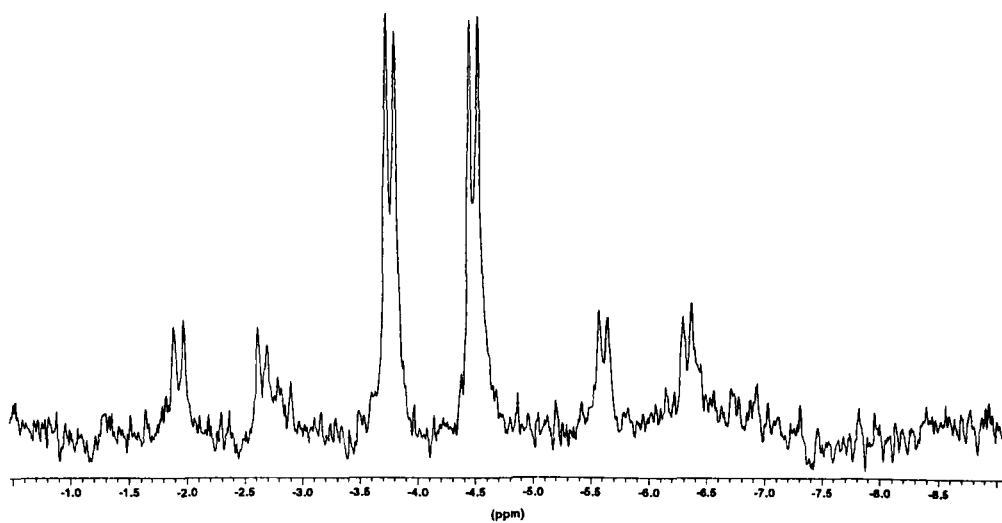


**Figure 5.2**

$^{31}\text{P}$  NMR spectrum of  $[\text{Pt}(\text{d}^t\text{bpx})\text{H}(\text{CO})]^+$ , **8a**, in MeOH at 293 K

**Figure 5.3**

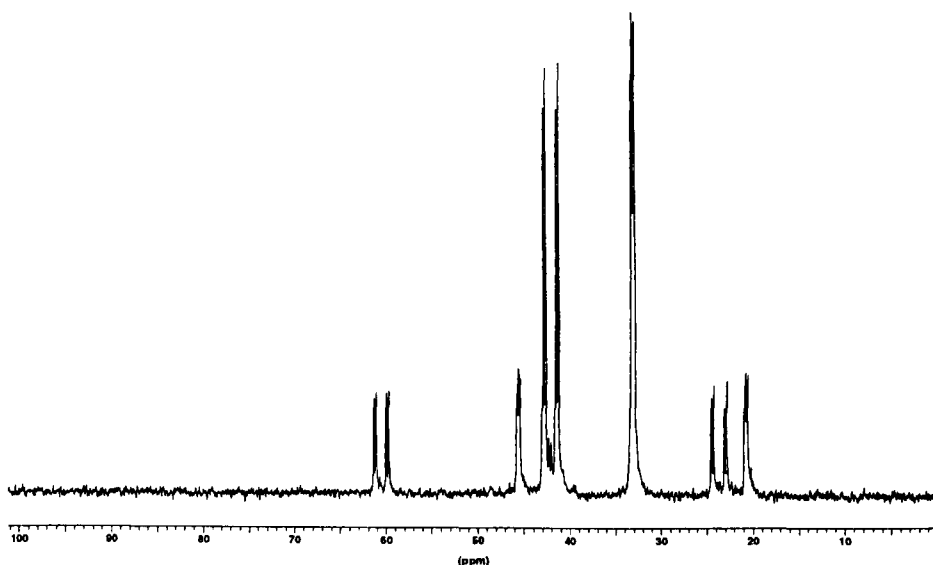
$^1\text{H}$  NMR spectrum of  $[\text{Pt}(\text{d}^t\text{bpx})\text{H}(\text{CO})]^+$ , **8a**, in MeOH at 293 K



In order to understand the nature of the product formed, the reaction has been repeated in a glass tube pressurised with *ca.* 2 bar of  $^{13}\text{CO}$ ; in the  $^{31}\text{P}\{^1\text{H}\}$  NMR spectrum in MeOH/CD<sub>3</sub>OD at 293 K, the two resonances at 42 and 33 ppm appear as doublets of doublets (see Figure 5.4) due to  $J(\text{P}_1\text{-P}_2) = 18.6$  Hz; the resonance at 33 ppm clearly shows additional coupling, which is due to  $^2J(\text{P}_2\text{-C})_{\text{cis}} = 8$  Hz and the resonance at 42 ppm shows a  $^2J(\text{P}_1\text{-C})_{\text{trans}} = 113$  Hz.

**Figure 5.4**

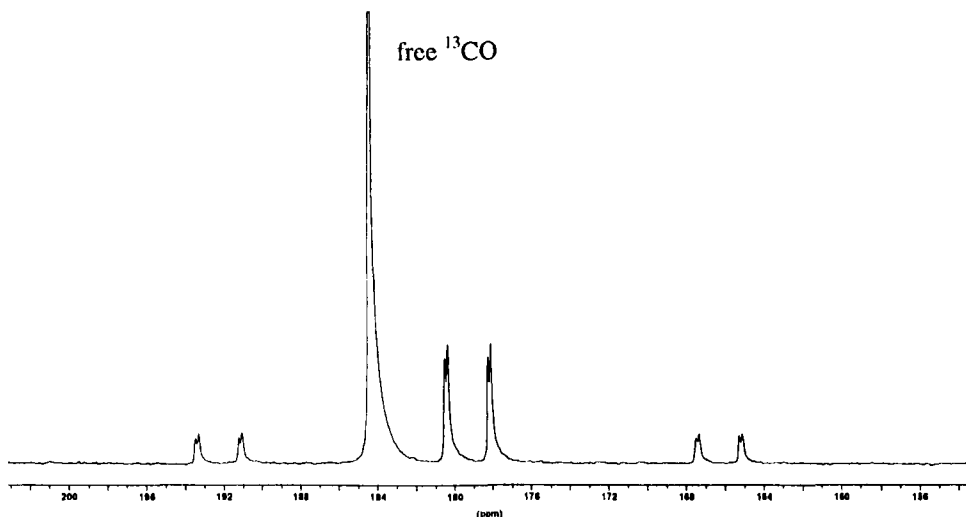
$^{31}\text{P}\{^1\text{H}\}$  NMR spectrum of  $[\text{Pt}(\text{d}^1\text{bpx})\text{H}(^{13}\text{CO})]^+$ , **8a**, in MeOH at 293 K



The  $^{13}\text{C}\{^1\text{H}\}$  NMR spectrum (see Figure 5.5) shows a doublet of doublets at 179 ppm with the same values of the phosphorus-carbon coupling constants measured in the  $^{31}\text{P}\{^1\text{H}\}$  NMR spectrum in MeOH/CD<sub>3</sub>OD at 293 K (Table 5.1). From these results it is possible to conclude that the complex formed is  $[\text{Pt}(\text{d}^1\text{bpx})\text{H}(\text{CO})][\text{CF}_3\text{SO}_3]$ , **8a**, where the hydride and the carbonyl are bonded directly to the platinum in a square planar configuration.

**Figure 5.5**

$^{13}\text{C}\{^1\text{H}\}$  NMR spectrum of  $[\text{Pt}(\text{d}^t\text{bpx})\text{H}(^{13}\text{CO})]^+$ , **8a**, in MeOH at 293 K

**Table 5.1**

NMR data of  $[\text{Pt}(\text{d}^t\text{bpx})\text{H}(^{13}\text{CO})]^+$ , **8a**, in MeOH at 293 K

	$\delta$	$J(\text{P}_1-)$	$J(\text{P}_2-)$	$J(\text{Pt}-)$	$J(\underline{\text{C}}\text{O}-)$
<b>P<sub>1</sub></b>	42.2 ppm		19 Hz	2985 Hz	113 Hz
<b>P<sub>2</sub></b>	33.2 ppm	19 Hz		2011 Hz	8 Hz
<b><u>C</u>O</b>	179.3 ppm	113 Hz	8 Hz	1299 Hz	
<b>H</b>	-4.2 Hz	15 Hz	145 Hz	740 Hz	-

In agreement with this formula, the IR spectrum of the platinum carbonyl hydride complex **8a** in MeOH shows two bands at 2238 and 2045  $\text{cm}^{-1}$ , respectively; however, without isotopic labelling, it is difficult to assign the two bands of  $[\text{Pt}(\text{d}^t\text{bpx})\text{H}(\text{CO})]^+$ , **8a**, but one is clearly due to  $\nu(\text{Pt-H})$  and the other to  $\nu(\text{C-O})$ .

In the case of palladium,  $[\text{Pd}(\text{d}^1\text{bpx})(\text{CH}_2\text{CH}_3)]^+[\text{CF}_3\text{SO}_3]^-$  reacts with one equivalent of CO in MeOH at 293 K to give MeP and  $[\text{Pd}(\text{d}^1\text{bpx})\text{H}(\text{solv})]^+[\text{CF}_3\text{SO}_3]^-$ . It has been supposed that the palladium acyl complex  $[\text{Pd}(\text{d}^1\text{bpx})(\text{C}(\text{O})\text{C}_2\text{H}_5)(\text{solv})]^+[\text{CF}_3\text{SO}_3]^-$  is first formed by insertion of CO into the Pd-ethyl bond, followed by methanolysis of the acyl intermediate.<sup>10</sup> Under the same conditions as in the palladium system, in MeOH at 293 K, the reaction of the platinum ethyl complex **6a** with CO results in the formation of  $[\text{Pt}(\text{d}^1\text{bpx})\text{H}(\text{CO})]^+$ , **8a**, and in the  $^{13}\text{C}\{^1\text{H}\}$  NMR spectrum the resonance at *ca.* 184 ppm indicates the presence of free  $^{13}\text{CO}$  in solution but formation of MeP is not observed.

In order to understand the reasons why the platinum hydride complex **3a** is not reformed after the reaction of  $[\text{Pt}(\text{d}^1\text{bpx})(\text{CH}_2\text{CH}_3)]^+$ , **6a** with CO in MeOH at 293 K and why the formation of MeP is not observed, the reaction of  $[\text{Pt}(\text{d}^1\text{bpx})(\text{CH}_2\text{CH}_3)]^+$ , **6a** with CO has been carried out in a non-alcoholic solvent at 193 K (see Section 5.4).

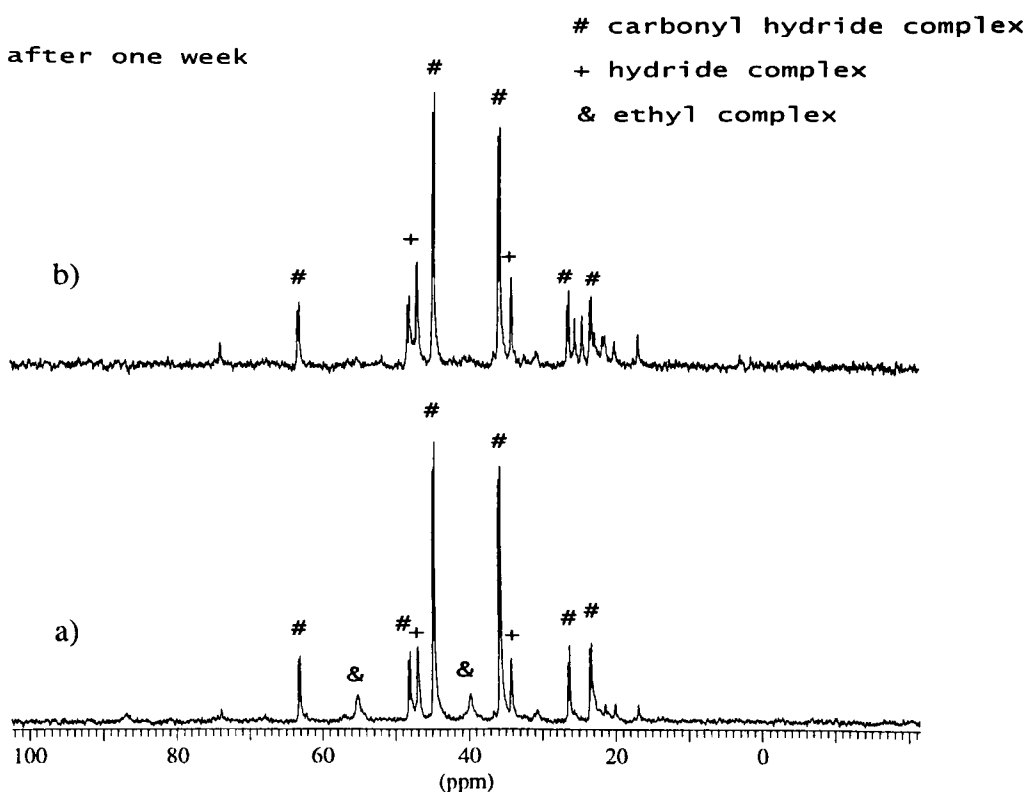
### 5.3. Reactivity of $[\text{Pt}(\text{d}^1\text{bpx})(\text{CH}_2\text{CH}_3)]^+[\text{CH}_3\text{SO}_3]^-$ , **6b**, with CO in MeOH at 293 K

As described in Section 4.5,  $[\text{Pt}(\text{d}^1\text{bpx})(\text{CH}_2\text{CH}_3)]^+$ , **6b**, is formed on bubbling ethene through a solution of  $[\text{Pt}(\text{d}^1\text{bpx})\text{H}(\text{solv})]^+$ , **3b**, and at 293 K in MeOH/H<sub>2</sub>O the ethyl complex **6b** and the hydride complex **3b** are both present in solution. Under one atmosphere of CO in MeOH/H<sub>2</sub>O at 293 K,  $[\text{Pt}(\text{d}^1\text{bpx})\text{H}(\text{CO})][\text{CH}_3\text{SO}_3]$ , **8b**, is formed after a few minutes and in the  $^{31}\text{P}\{^1\text{H}\}$  NMR spectrum the resonances due to the platinum hydride **3b** and to the platinum ethyl complex **6b** are still present (see

Figure 5.6a). It seems that the presence of the platinum hydride complex **3b** and the platinum ethyl complex **6b** in solution after reaction with CO is due to the reaction with CO in MeOH at 293 K being incomplete. After one week under CO atmosphere, no decomposition is observed; the hydride and the carbonyl-hydride complexes are both present but the ethyl complex has disappeared (see Figure 5.6b). The intensity of the resonances due to  $[\text{Pt}(\text{d}^1\text{bpx})\text{H}(\text{solv})][\text{CH}_3\text{SO}_3]$ , **3b**, increase slightly, suggesting that the ethyl complex has been converted into the hydride complex with elimination of ethene, although this was not detected spectroscopically.

**Figure 5.6**

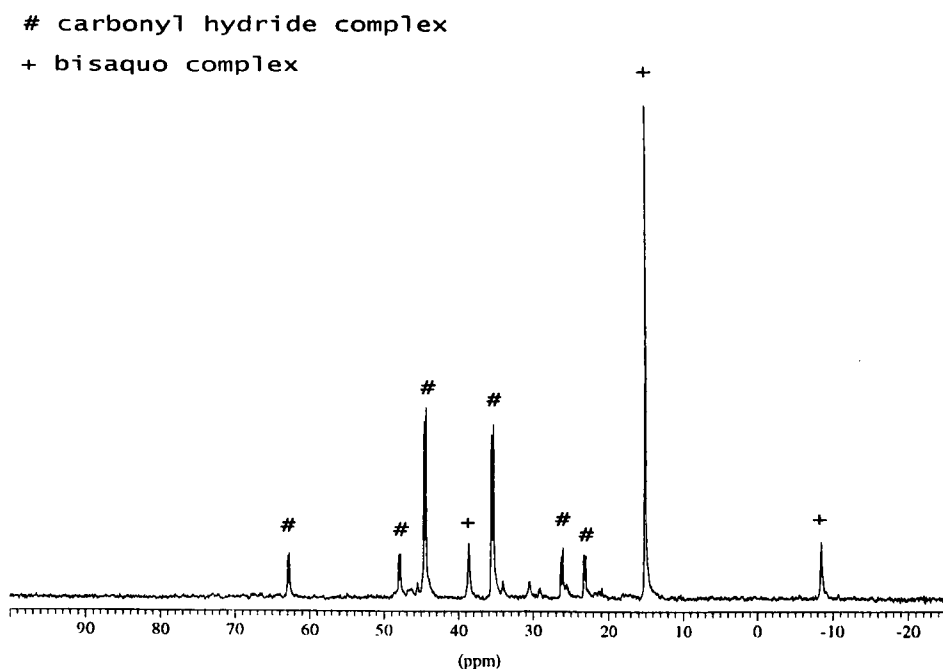
$^{31}\text{P}\{^1\text{H}\}$  NMR spectrum of  $[\text{Pt}(\text{d}^1\text{bpx})\text{H}(^{13}\text{CO})]^+$ , **8b**, in MeOH at 293 K



When the sample is dried in vacuum and redissolved in THF, the platinum carbonyl hydride complex is still present but the main resonance is due to  $[\text{Pt}(\text{d}^t\text{bpx})(\text{H}_2\text{O})_2]^{2+}$ , **4b**, formed because of the presence of water (see Figure 5.7). This reaction has been carried out using  $^{12}\text{CO}$  and there is no evidence for the formation of MeP.

**Figure 5.7**

$^{31}\text{P}\{^1\text{H}\}$  NMR spectrum of  $[\text{Pt}(\text{d}^t\text{bpx})\text{H}(^{13}\text{CO})]^+$ , **8b**, in THF at 293 K



Thus both in  $\text{CF}_3\text{SO}_3\text{H}$  and  $\text{CH}_3\text{SO}_3\text{H}$  the platinum system is more stable under CO atmosphere than was found for the palladium system; indeed,  $[\text{Pt}(\text{d}^t\text{bpx})\text{H}(\text{CO})][\text{CH}_3\text{SO}_3]$ , **8b**, is still present and no decomposition is observed even after some weeks under an atmosphere of CO.

#### 5.4. Reactivity of $[\text{Pt}(\text{d}^t\text{bpx})(\text{CH}_2\text{CH}_3)][\text{CF}_3\text{SO}_3]$ , **6a**, with CO in $\text{CH}_2\text{Cl}_2$ and THF

As reported in the palladium catalytic cycle for the methoxycarbonylation of ethene,  $[\text{Pd}(\text{d}^t\text{bpx})(\text{CH}_2\text{CH}_3)][\text{CF}_3\text{SO}_3]$  reacts immediately with CO and the formation of MeP and  $[\text{Pd}(\text{d}^t\text{bpx})\text{H}(\text{MeOH})][\text{CF}_3\text{SO}_3]$  occurs in methanol solution.<sup>10</sup> In order to avoid the immediate methoxycarbonylation of ethene and to understand the intermediate steps of the process, the reaction was repeated using THF, where the formation of palladium acyl complex  $[\text{Pd}(\text{d}^t\text{bpx})(\text{C}(\text{O})\text{C}_2\text{H}_5)(\text{solv})][\text{CF}_3\text{SO}_3]$  was observed. Different studies recognized that the acyl transition metal complex is a key intermediate in the homogeneously catalysed hydroformylation reaction and that the insertion of carbon monoxide into a metal-carbon bond is a crucial step.<sup>11</sup>

In this section the mechanism of the insertion of CO into  $[\text{Pt}(\text{d}^t\text{bpx})(\text{CH}_2\text{CH}_3)][\text{CF}_3\text{SO}_3]$ , **6a**, will be studied in  $\text{CH}_2\text{Cl}_2$  and THF following the experimental procedure for the palladium system.

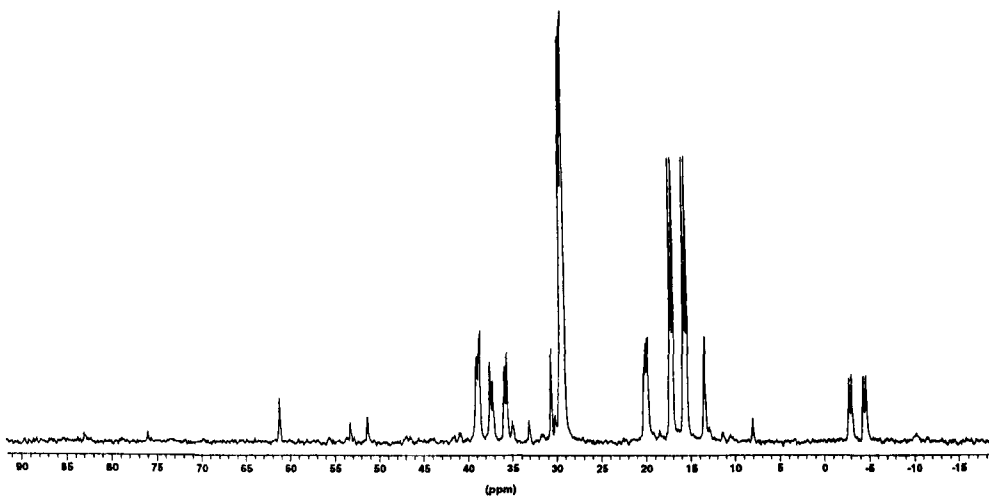
##### 5.4.1 Reactivity of **6a** with CO in $\text{CH}_2\text{Cl}_2$ at 193 K and 293 K

The reaction of  $[\text{Pt}(\text{d}^t\text{bpx})(\text{CH}_2\text{CH}_3)][\text{CF}_3\text{SO}_3]$ , **6a**, with one equivalent of  $^{13}\text{CO}$  has been carried out in  $\text{CH}_2\text{Cl}_2$  at 193 K and gives a new compound  $[\text{Pt}(\text{d}^t\text{bpx})(\text{C}_2\text{H}_5)(^{13}\text{CO})]^+$ , **9a**. The  $^{31}\text{P}\{^1\text{H}\}$  NMR spectrum of **9a** consists of two doublets of doublets at 29.4 ppm and 16.4 ppm (see Figure 5.8). These chemical shifts are quite different to those found for  $[\text{Pt}(\text{d}^t\text{bpx})\text{H}(^{13}\text{CO})][\text{CF}_3\text{SO}_3]$ , **8a**, (see Table 5.1). Unlike the previous complex **8a**, the phosphorus at higher field is coupled

to the *trans*-carbon, whereas the phosphorus at lower field exhibits coupling to *cis*-carbon.

**Figure 5.8**

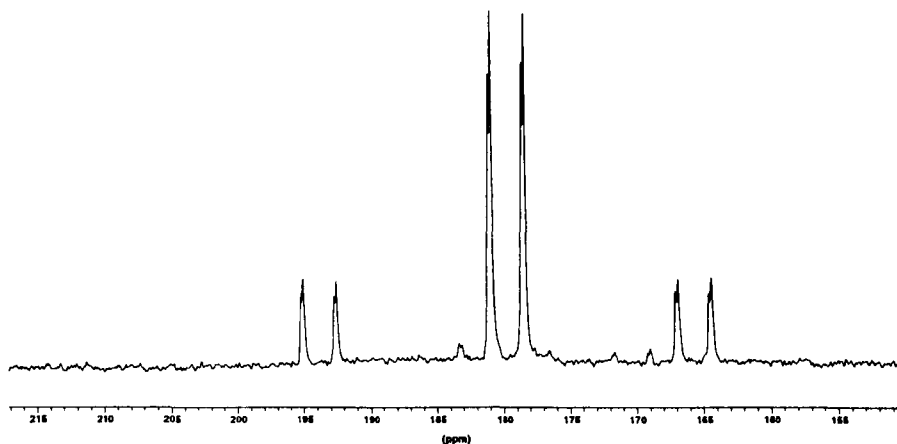
$^{31}\text{P}\{^1\text{H}\}$  NMR spectrum of  $[\text{Pt}(\text{d}^t\text{bpx})(\text{C}_2\text{H}_5)(^{13}\text{CO})]^+$ , **9a**, in  $\text{CH}_2\text{Cl}_2$  at 193 K



The  $^{13}\text{C}\{^1\text{H}\}$  NMR spectrum of **9a** (100%  $^{13}\text{CO}$ ) at 193 K in  $\text{CH}_2\text{Cl}_2$  is a doublet of doublets at 179.8 ppm with phosphorus and carbon coupling constants which are the same as those observed in the  $^{31}\text{P}\{^1\text{H}\}$  NMR spectrum (Figure 5.9). It is evident that the new complex contains two inequivalent *cis* phosphorus atoms and a carbonyl group which is bonded directly to platinum. The  $^{31}\text{P}$  NMR spectrum shows no further splitting of the two main resonances and, as a result, hydride cannot be directly bonded to the platinum.

**Figure 5.9**

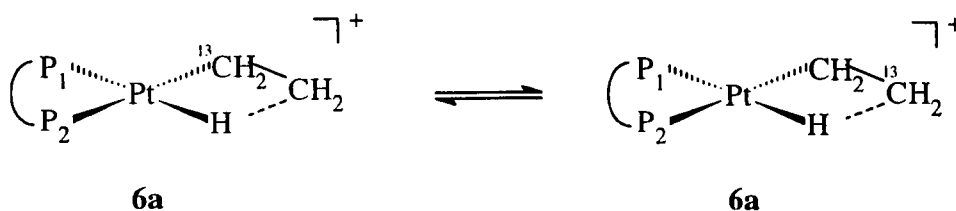
$^{13}\text{C}\{^1\text{H}\}$  NMR spectrum of  $[\text{Pt}(\text{d}^t\text{bpx})(\text{C}_2\text{H}_5)(^{13}\text{CO})]^+$ , **9a**, in  $\text{CH}_2\text{Cl}_2$  at 193 K



In order to understand the nature of the compound formed at 193 K in  $\text{CH}_2\text{Cl}_2$ , the reaction has been repeated using  $^{13}\text{CH}_2=\text{CH}_2$  and  $[\text{Pt}(\text{d}^t\text{bpx})(\text{CH}_2\text{CH}_3)]^+$ , **6a**. As discussed previously, there is rapid incorporation of  $^{13}\text{CH}_2=\text{CH}_2$  into **6a**, presumably *via* the hydride/alkene intermediate. However, because we could not observe  $^2J(\text{P}-\text{C})$  we could not establish the exact position of the equilibrium which gives rise to two isotopomers (see Scheme 5.1).

**Scheme 5.1**

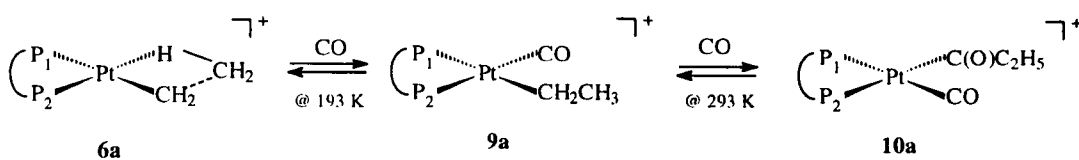
Isotopomers of **6a** ( $\text{Et} = 50\% \text{ } ^{13}\text{C}$ )



Nevertheless, we observed no further enhancements in the  $^{13}\text{C}$  spectrum after mixing equimolar amounts of reactants after 30 minutes and we therefore assume that there is complete equilibration to give both isotopomers of **6a** with 50%  $^{13}\text{C}$  in both the  $\alpha$ - and  $\beta$ -position of  $\text{C}_2\text{H}_5$ -group. Future work will thus refer to either  $\text{Et} = 50\% \text{ }^{13}\text{C}$  or when  $^{13}\text{C}_2\text{H}_4$  has been used,  $\text{Et} = 100\% \text{ }^{13}\text{C}$ .

The  $^{13}\text{C}$ -labelled sample of  $[\text{Pt}(\text{d}^t\text{bpx})(\text{CH}_2\text{CH}_3)]^+$ , **6a**, (50%  $^{13}\text{C}$ ) has been prepared from a solution of the unlabelled platinum ethyl complex in  $\text{CH}_2\text{Cl}_2$  as described in Section 4.3.2. The  $^{13}\text{C}\{^1\text{H}\}$  NMR spectrum at 293 K shows a single resonance at 16.4 ppm as reported in the literature (see Figure 5.10a). At this point one equivalent of  $^{13}\text{CO}$  has been added to the frozen and degassed solution of  $[\text{Pt}(\text{d}^t\text{bpx})(\text{CH}_2\text{CH}_3)]^+$ , **6a**, ( $\text{Et}=50\% \text{ }^{13}\text{C}$ ) in  $\text{CH}_2\text{Cl}_2$  and the sealed tube has been stored at 193 K during the first part of the experiment. From the analysis of the  $^{13}\text{C}$  NMR spectrum, it is possible to conclude that  $[\text{Pt}(\text{d}^t\text{bpx})(\text{C}_2\text{H}_5)(^{13}\text{CO})]^+$ , **9a**, ( $\text{Et}=50\% \text{ }^{13}\text{C}$ ) is formed at 193 K and both CO and the ethyl groups are coordinated to the platinum (see Scheme 5.2).

Scheme 5.2

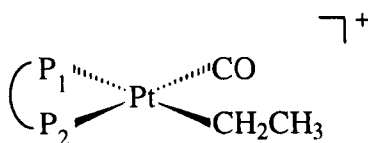


The  $^{13}\text{CO}$  ligand resonates at 179.8 ppm and appears as a doublet of doublets with associated platinum satellites (see Figure 5.11b and Figure 5.9). For the ethyl ligand, the  $\text{CH}_2$  group resonates at 4 ppm and appears as a doublet with  $^2J(\text{P}-\text{C}_\alpha) =$

53.6 Hz, whereas the  $\text{CH}_3$  group occurs at 18.3 ppm as a singlet (see figure 5.10b). In the  $^{13}\text{C}$  NMR spectrum, the resonance at 4 ppm becomes a triplet of doublets with  $^1J(\text{C}_\alpha\text{-H}) = 130$  Hz, and the resonance at 18.3 ppm becomes a quartet with  $^1J(\text{C}_\beta\text{-H}) = 125.8$  Hz. All the data are reported in Table 5.2.

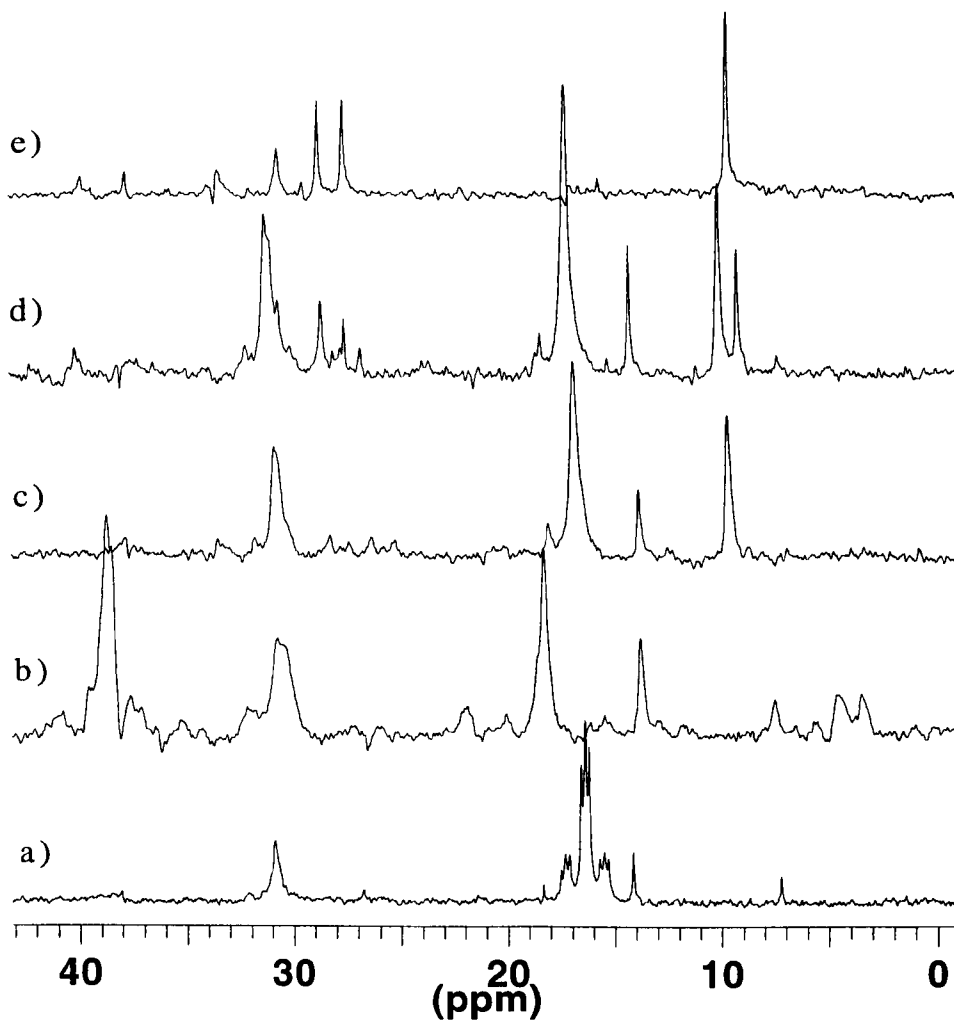
**Table 5.2**

*NMR data for  $[\text{Pt}(\text{d}^1\text{bpx})(\text{C}_2\text{H}_5)(^{13}\text{CO})]^+$ , **9a**, (Et = 50%  $^{13}\text{C}$ )  
in  $\text{CH}_2\text{Cl}_2$  at 193 K*



	$\delta$	$J(\text{P}_1\text{-})$	$J(\text{P}_2\text{-})$	$J(\text{Pt-})$	$J(\underline{\text{C}}\text{O-})$	$J(\text{C}_\alpha\text{-})$	$J(\text{H-})$
<b>P<sub>1</sub></b>	29.4 ppm		24 Hz	1531 Hz	24 Hz	54 Hz	
<b>P<sub>2</sub></b>	16.4 ppm	24 Hz		3259 Hz	10 Hz	-	
<b><u>C</u>O</b>	179.8 ppm	10 Hz	126 Hz	1416 Hz			
<b>C<sub>α</sub></b>	4 ppm	54 Hz	-		-	-	130 Hz
<b>C<sub>β</sub></b>	18.3 ppm	-	-		-		126 Hz

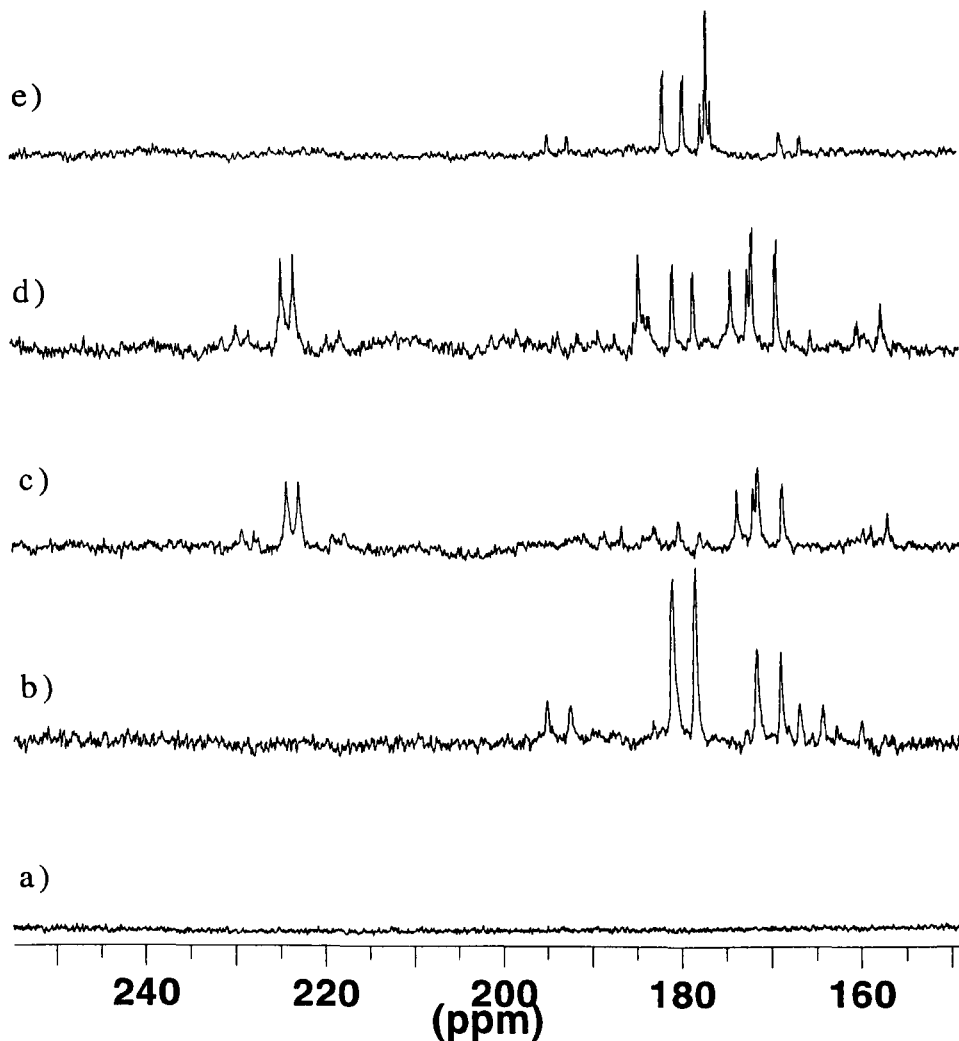
Figure 5.10

 $^{13}\text{C}\{^1\text{H}\}$  NMR spectra(alkyl region) at 193 K and 293 K

- a)  $[\text{Pt}(\text{d}^1\text{bpx})(\text{C}_2\text{H}_5)]^+ \mathbf{6a}$  (Et = 50%  $^{13}\text{C}$ ) in  $\text{CH}_2\text{Cl}_2$  @ 293 K  
 b)  $[\text{Pt}(\text{d}^1\text{bpx})(\text{C}_2\text{H}_5)(^{13}\text{CO})]^+ \mathbf{9a}$  (Et = 50%  $^{13}\text{C}$ ) in  $\text{CH}_2\text{Cl}_2$  @ 193  
 c)  $[\text{Pt}(\text{d}^1\text{bpx})(^{13}\text{C}(\text{O})\text{C}_2\text{H}_5)(^{13}\text{CO})]^+ \mathbf{10a}$  (Et = 50%  $^{13}\text{C}$ ) in  $\text{CH}_2\text{Cl}_2$  @ 293 K  
 d)  $[\text{Pt}(\text{d}^1\text{bpx})(^{13}\text{C}(\text{O})\text{C}_2\text{H}_5)(^{13}\text{CO})]^+ \mathbf{10a}$  (Et = 50%  $^{13}\text{C}$ ) +  $[\text{Pt}(\text{d}^1\text{bpx})\text{H}(\text{CO})]^+ \mathbf{8a}$  in  $\text{CH}_2\text{Cl}_2$  @ 293 K (after one week)  
 e)  $[\text{Pt}(\text{d}^1\text{bpx})\text{H}(\text{CO})]^+ \mathbf{8a}$  + EtCOOMe in MeOH @ 293 K

Figure 5.11

$^{13}\text{C}\{^1\text{H}\}$  NMR spectra(carbonyl region) at 193 K and 293 K



- a)  $[\text{Pt}(\text{d}^t\text{bpx})(\text{C}_2\text{H}_5)]^+ \mathbf{6a}$  (Et = 50%  $^{13}\text{C}$ ) in  $\text{CH}_2\text{Cl}_2$  @ 293 K  
 b)  $[\text{Pt}(\text{d}^t\text{bpx})(\text{C}_2\text{H}_5)(^{13}\text{CO})]^+ \mathbf{9a}$  (Et = 50%  $^{13}\text{C}$ ) in  $\text{CH}_2\text{Cl}_2$  @ 193  
 c)  $[\text{Pt}(\text{d}^t\text{bpx})(^{13}\text{C}(\text{O})\text{C}_2\text{H}_5)(^{13}\text{CO})]^+ \mathbf{10a}$  (Et = 50%  $^{13}\text{C}$ ) in  $\text{CH}_2\text{Cl}_2$  @ 293 K  
 d)  $[\text{Pt}(\text{d}^t\text{bpx})(^{13}\text{C}(\text{O})\text{C}_2\text{H}_5)(^{13}\text{CO})]^+ \mathbf{10a}$  (Et = 50%  $^{13}\text{C}$ ) +  $[\text{Pt}(\text{d}^t\text{bpx})\text{H}(\text{CO})]^+ \mathbf{8a}$  in  $\text{CH}_2\text{Cl}_2$  @ 293 K (after one week)  
 e)  $[\text{Pt}(\text{d}^t\text{bpx})\text{H}(\text{CO})]^+ \mathbf{8a}$  + EtCOOMe in MeOH @ 293 K

The NMR data of the complex **9a** are in agreement with those reported for  $[\text{Pt}(\text{dppe})(\text{CH}_3)(\text{CO})][\text{BF}_4]$ .<sup>12</sup> Also in this platinum complex the value of  $^1J(\text{P}_1\text{-Pt}) = 1606$  Hz is assigned to the phosphorus atom *trans* to the group  $-\text{CH}_3$ , whereas the value of  $^1J(\text{P}_2\text{-Pt}) = 3212$  Hz is more typical of a phosphorus *trans* to CO.

Under these conditions, there is no evidence for the formation of the platinum acyl complex. However, upon warming to room temperature, it is evident that further reaction occurs. The  $^{31}\text{P}\{^1\text{H}\}$  NMR spectrum, run immediately after reaching room temperature, does not show any well defined resonances and it seems that the system is undergoing further reaction. In the  $^{13}\text{C}\{^1\text{H}\}$  NMR spectrum, the two peaks at 18.3 ppm and 4.1 ppm disappear and two new peaks at 16.8 ppm and 9.6 ppm appear (see Figure 5.10c). The resonance at 179.8 ppm, due to  $[\text{Pt}(\text{d}^1\text{bpx})(\text{C}_2\text{H}_5)(^{13}\text{CO})]^+$ , **9a**, (Et=50%  $^{13}\text{C}$ ), disappears and two doublets at 223.9 ppm and at 173.2 ppm appear, due to the formation of a new platinum complex,  $[\text{Pt}(\text{d}^1\text{bpx})(^{13}\text{C}(\text{O})\text{C}_2\text{H}_5)(^{13}\text{CO})]^+$ , **10a**, (Et = 50%  $^{13}\text{C}$ ) (see Figure 5.11c). After one week, the alkyl region of the  $^{13}\text{C}\{^1\text{H}\}$  NMR spectrum does not show any new resonances (see Figure 5.10d). In the carbonyl region, **10a** is still present and the doublet of doublets due to the platinum carbonyl hydride complex **8a** appears (see Figure 5.11d). In order to understand if the new platinum complex **10a** formed at 293 K in  $\text{CH}_2\text{Cl}_2$  is the platinum acyl complex, the solvent has been evaporated under vacuum and the residue dissolved in MeOH at 293 K. The  $^{31}\text{P}\{^1\text{H}\}$  NMR spectrum shows principally resonances due to  $[\text{Pt}(\text{d}^1\text{bpx})\text{H}(^{13}\text{CO})]^+$ , **8a**, and other impurities. In the carbonyl region, the  $^{13}\text{C}\{^1\text{H}\}$  NMR spectrum shows that the platinum complex **10a** has disappeared; the resonances due to the carbonyl hydride complex **8a** are still present and a resonance at 176.8 ppm consisting of a superimposed singlet and doublet with

$^1J(\underline{\text{CO}}-\underline{\text{C}}_\alpha) = 58$  Hz is observed, due to the presence of a  $^{13}\text{C}(\text{O})\text{Et}$  group (Et=50%  $^{13}\text{C}$ ) (see Figure 5.11e). The singlet at 9.54 ppm and the doublet at 28.1 ppm with  $^1J(\underline{\text{CO}}-\underline{\text{C}}_\alpha) = 58$  Hz confirm the formation of  $\text{Et}^{13}\text{COOMe}$  (Et=50%  $^{13}\text{C}$ ) (see Figure 5.10e). In the  $^{13}\text{C}$  NMR spectrum, the peak at 9.54 ppm becomes a quartet with  $^1J(\text{C}_\beta\text{-H}) = 128.5$  Hz, whereas the doublet at 28.1 ppm becomes a triplet of doublets with  $^1J(\text{C}_\alpha\text{-H}) = 127.6$  Hz. We can conclude that the complex formed in  $\text{CH}_2\text{Cl}_2$  at 293 K is a platinum acyl complex but in the platinum complex **10a** one coordination site is occupied by CO, this is demonstrated by the resonance at 173.2 ppm in the  $^{13}\text{C}\{^1\text{H}\}$  NMR spectrum at 293 K in  $\text{CH}_2\text{Cl}_2$ . Then,  $[\text{Pt}(\text{d}^t\text{bpx})(\text{C}(\text{O})\text{Et})(\text{CO})]^+$ , **10a**, is formed on warming the solution of  $[\text{Pt}(\text{d}^t\text{bpx})(\text{C}_2\text{H}_5)(^{13}\text{CO})]^+$ , **9a**, to 293 K in  $\text{CH}_2\text{Cl}_2$  under a CO atmosphere and methoxycarbonylation occurs on addition of MeOH at 293 K. The amount of MeP is very small; in fact it was not detected in any of the experiments when non  $^{13}\text{C}$ -labelled materials were used.

Different experiments have shown that the formation of  $[\text{Pt}(\text{d}^t\text{bpx})(\text{C}(\text{O})\text{Et})(\text{CO})]^+$ , **10a**, is favoured when an excess of CO is present. Thus the  $^{13}\text{C}\{^1\text{H}\}$  NMR spectrum shows clearly that pressurising a solution of the platinum ethyl complex **6a**, with 2 atm of  $^{13}\text{CO}$  in  $\text{CH}_2\text{Cl}_2$  at 293 K in a glass tube gives **10a** (see Figure 5.12). The  $^{31}\text{P}\{^1\text{H}\}$  NMR spectrum shows clearly an AB second order NMR spectrum (see Figure 5.13) and some of the  $^{31}\text{P}$  NMR data for the platinum acyl carbonyl complex **10a** reported in Table 5.3 have been obtained by computer iteration, because of the difficulty in the analysis of the spectrum.

**Table 5.3**

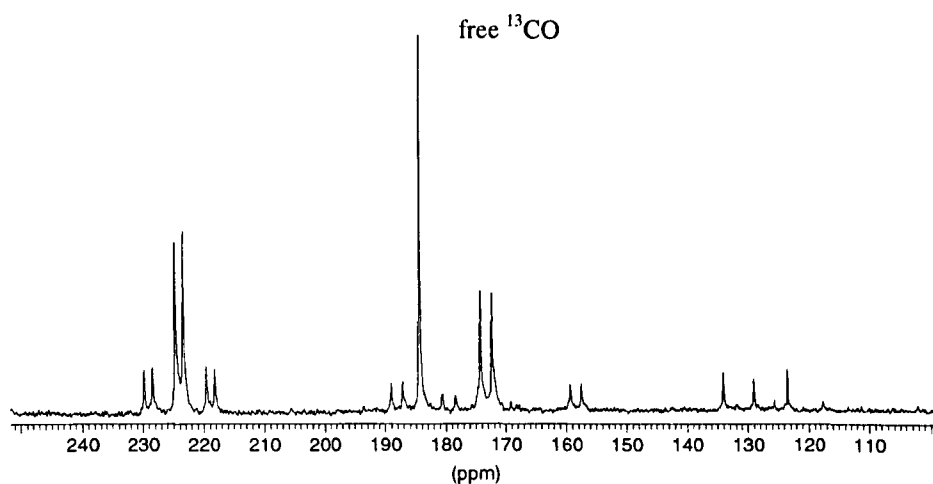
*NMR data for  $[\text{Pt}(\text{d}^i\text{bpx})(^{13}\text{C}(\text{O})\text{C}_2\text{H}_5)(^{13}\text{CO})]^+$ , 10a, in  $\text{CH}_2\text{Cl}_2$  at 293 K*

		$J(\text{P}_1-)$	$J(\text{P}_2-)$	$J(\text{Pt}-)$	$J(\underline{\text{C}}\text{O}-)$	$J(\underline{\text{C}}(\text{O})-)$
$\delta\text{P}_1$	23.0 ppm	-				
$\delta\text{P}_2$	23.1 ppm	26 Hz	-			
$\delta\text{Pt}$	-	3616 Hz	<i>1397 Hz</i>	-		
$\delta\underline{\text{C}}\text{O}$	173.2 ppm	93 Hz	-	1487 Hz		
$\delta\underline{\text{C}}(\text{O})$	223.9 ppm	-	69 Hz	514 Hz	4 Hz	-

The numbers in *italics* have been adjusted by the computer iteration.

**Figure 5.12**

*$^{13}\text{C}\{^1\text{H}\}$  NMR spectrum of  $[\text{Pt}(\text{d}^i\text{bpx})(^{13}\text{C}(\text{O})\text{C}_2\text{H}_5)(^{13}\text{CO})]^+$ , 10a, in  $\text{CH}_2\text{Cl}_2$  at 293 K*





There is a good agreement between the NMR data reported in Table 5.2 and 5.3 and the NMR data reported by Horvath *et al* for the complexes in Scheme 5.3. In complex **I**,  $^1J(\text{P-Pt}) = 1564$  Hz, which is a typical value for a phosphorus *trans* to the methyl group. In complex **II**,  $^1J(\text{P-Pt}) = 3265$  Hz, which is typical for phosphorus *trans* to CO. In complex **III**,  $^1J(\text{P-Pt}) = 1342$  Hz; this coupling constant is very close to that observed for  $^1J(\text{P}_2\text{-Pt}) = 1397$  Hz for  $[\text{Pt}(\overline{\text{d}^1\text{bpx}})(\text{C}(\text{O})\text{Et})(\text{CO})]^+$ , **10a**, in Table 5.3. Different platinum acyl complexes have been reported in the literature, mainly isolated as precursors of catalytic processes.<sup>11,14-16</sup> In all these platinum acyl complexes, the phosphorus platinum coupling constants are strongly influenced by the ligand in the *trans* position and are about 1300-1500 Hz for phosphorus *trans* to the acyl group, similar to what was already observed for analogous complexes reported by Appleton and Bennett.<sup>12</sup>

#### 5.4.2 Reactivity of **6a** with CO in THF at 193 K and 293 K

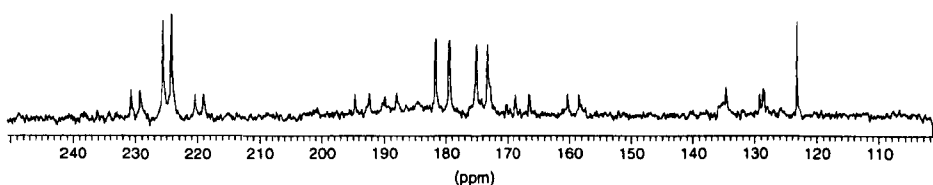
It has been observed in the previous section that the only platinum acyl complex isolated from the reaction of  $[\text{Pt}(\overline{\text{d}^1\text{bpx}})(\text{CH}_2\text{CH}_3)]^+$ , **6a**, with CO at room temperature is  $[\text{Pt}(\overline{\text{d}^1\text{bpx}})(\text{C}(\text{O})\text{Et})(\text{CO})]^+$ , **10a**. It has not been possible to detect the formation of the platinum acyl solvento complex  $[\text{Pt}(\overline{\text{d}^1\text{bpx}})(\text{C}(\text{O})\text{Et})(\text{solv})]^+$ , which is the main product in the palladium system.

The same reaction between platinum ethyl complex **6a** and CO has been repeated in THF, first at 193 K and then at 293 K, in order to understand if it would be possible to form the platinum acyl solvento complex  $[\text{Pt}(\overline{\text{d}^1\text{bpx}})(\text{COEt})(\text{solv})]^+$  using the more strongly coordinating solvent THF. Initially, CO has been bubbled through

a solution of **6a** for ten minutes at 193 K and the  $^{31}\text{P}\{^1\text{H}\}$  NMR spectrum shows that the main products are  $[\text{Pt}(\text{d}^1\text{bpx})(\text{CO})(\text{C}_2\text{H}_5)]^+$ , **9a**, and  $[\text{Pt}(\text{d}^1\text{bpx})\text{H}(\text{CO})]^+$ , **8a**. On warming the solution to 293 K the resonances due to the complex **9a** disappear and **8a** is the only complex present in solution. In the second experiment, the complex  $[\text{Pt}(\text{d}^1\text{bpx})(^{13}\text{C}(\text{O})\text{Et})(^{13}\text{CO})]^+$ , **10a**, has been prepared in  $\text{CH}_2\text{Cl}_2$ , followed by evaporation and dissolution of the precipitate in THF under a  $\text{N}_2$  atmosphere. The  $^{13}\text{C}\{^1\text{H}\}$  NMR spectrum in THF of this solution at 293 K shows the formation of  $[\text{Pt}(\text{d}^1\text{bpx})(^{13}\text{C}(\text{O})\text{Et})(^{13}\text{CO})]^+$ , **10a**, and  $[\text{Pt}(\text{d}^1\text{bpx})\text{H}(^{13}\text{CO})]^+$ , **8a**; there is no evidence for the presence of other complexes, thus, even in THF, it has not been possible to isolate the platinum acyl solvento complex,  $[\text{Pt}(\text{d}^1\text{bpx})(\text{C}(\text{O})\text{Et})(\text{THF})]^+$  (Figure 5.14).

**Figure 5.14**

$^{13}\text{C}\{^1\text{H}\}$  NMR spectrum of  $[\text{Pt}(\text{d}^1\text{bpx})(^{13}\text{C}(\text{O})\text{C}_2\text{H}_5)(^{13}\text{CO})]^+$ , **10a**, in  $\text{CH}_2\text{Cl}_2$  at 293 K



It is possible to conclude that the reactivity of  $[\text{Pt}(\text{d}^1\text{bpx})(\text{CH}_2\text{CH}_3)]^+$ , **6a**, with CO is not affected by using different solvents, such as  $\text{CH}_2\text{Cl}_2$  and THF, and in both

solvents  $[\text{Pt}(\text{d}^t\text{bpx})(\text{CO})(\text{C}_2\text{H}_5)]^+$ , **9a**, is formed at 193 K and  $[\text{Pt}(\text{d}^t\text{bpx})(\text{C}(\text{O})\text{Et})(\text{CO})]^+$ , **10a**, at 293 K, emphasising the great affinity of platinum for CO. The formation of  $[\text{Pt}(\text{d}^t\text{bpx})\text{H}(\text{CO})]^+$ , **8a**, has been observed at 193 K and 293 K, *vide infra*.

### 5.5. Reactivity of **9a** and **10a** with $\text{PPh}_3$

Because of the high affinity of the platinum complexes discussed in this thesis for CO, it was of interest to investigate the affinity of these platinum complexes for  $\text{PPh}_3$ . If such triphenylphosphine complexes can be made, it would be of interest for the following reasons:

- Current ideas suggest that these complexes only give monomers rather than polymers because of steric constraints.
- The occupancy of the fourth vacant site in the acyl complex may enable a distinction between inter- and intra-methanolysis of the acyl complex in the final step in the formation of MeP.

There is no reaction of one equivalent of  $\text{PPh}_3$  with  $[\text{Pt}(\text{d}^t\text{bpx})(\text{C}_2\text{H}_5)(\text{CO})]^+$ , **9a**, in  $\text{CH}_2\text{Cl}_2$  at 193 K over one hour. However, on increasing the temperature to 293 K there is an immediate reaction; the platinum acyl carbonyl complex **10a** is present and new resonances appear in the  $^{31}\text{P}\{^1\text{H}\}$  and  $^{13}\text{C}\{^1\text{H}\}$  NMR spectra. The  $^{13}\text{C}\{^1\text{H}\}$  NMR spectrum in  $\text{CH}_2\text{Cl}_2$  shows the disappearance of the acyl resonance due to **10a** and the appearance of a new doublet at 230.4 ppm due to  $[\text{Pt}(\text{d}^t\text{bpx})(\text{C}(\text{O})\text{C}_2\text{H}_5)(\text{PPh}_3)]^+$ , **11a**; this new acyl platinum complex does not contain

a CO coordinated to the platinum (see Figure 5.15b). The NMR data due to  $[\text{Pt}(\text{d}^1\text{bpx})(\text{C}(\text{O})\text{C}_2\text{H}_5)(\text{PPh}_3)]^+$ , **11a**, are summarised in Table 5.4.

**Figure 5.15**

$^{13}\text{C}\{^1\text{H}\}$  NMR spectra of  $[\text{Pt}(\text{d}^1\text{bpx})(^{13}\text{C}(\text{O})\text{C}_2\text{H}_5)(^{13}\text{CO})]^+$ , **10a**, and  $[\text{Pt}(\text{d}^1\text{bpx})(^{13}\text{C}(\text{O})\text{C}_2\text{H}_5)(^{13}\text{CO})]^+$ , **11a**, in  $\text{CH}_2\text{Cl}_2$  at 293 K

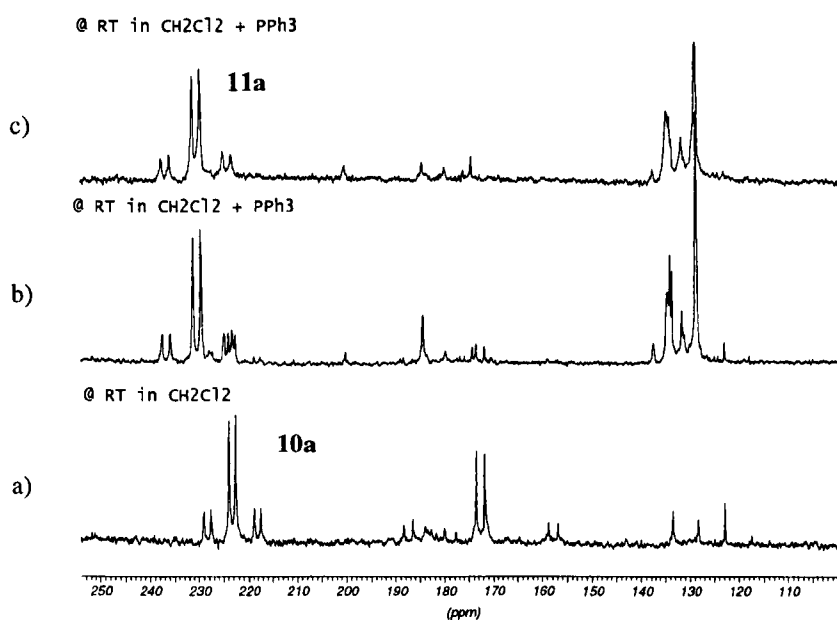


**Table 5.4**

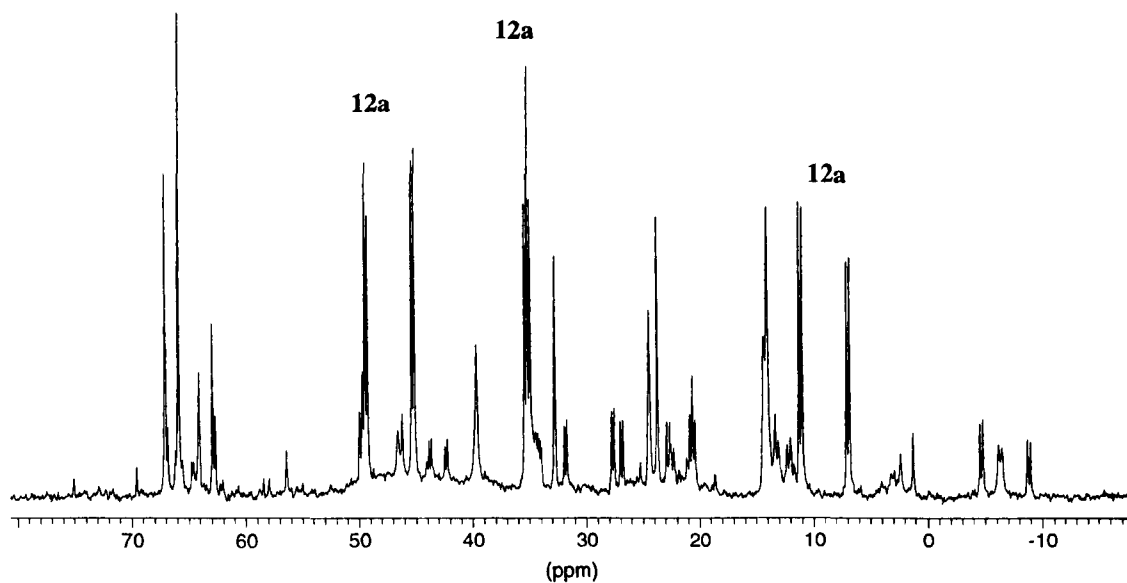
$^{13}\text{C}$  NMR data of  $[\text{Pt}(\text{d}^1\text{bpx})(^{13}\text{C}(\text{O})\text{C}_2\text{H}_5)(\text{PPh}_3)]^+$ , **11a**, in  $\text{CH}_2\text{Cl}_2$  at 293 K

$\delta\text{C}(\text{O})$ (ppm)	$^1J(\text{C}(\text{O})\text{-Pt})(\text{Hz})$	$^2J(\text{C}(\text{O})\text{-P})(\text{Hz})$
230.4	632	79

Unfortunately, it is very difficult to confirm the formation of this complex in the  $^{31}\text{P}\{^1\text{H}\}$  NMR spectrum because the presence of resonances due to already known and new platinum complexes hide the resonances of the complex **11a**. In this spectrum the resonance due to free  $\text{PPh}_3$  has disappeared, which indicates that  $\text{PPh}_3$  present in solution has all reacted. The main resonances are due to  $[\text{Pt}(\text{d}^t\text{bpx})\text{H}(\text{PPh}_3)]^+$ , **12a**; which contains three inequivalent phosphorus resonances at 9.2 dd, at 35.2 *pseudo* triplet due to the coupling with two *cis*-phosphorus and 47.2 dd (see Figure 5.16).

**Figure 5.16**

$^{31}\text{P}\{^1\text{H}\}$  NMR spectrum of  $[\text{Pt}(\text{d}^t\text{bpx})\text{H}(\text{PPh}_3)]^+$ , **12a**, in  $\text{CH}_2\text{Cl}_2$  at 293 K



The  $^1\text{H}$  NMR spectrum of the above solution in  $\text{CH}_2\text{Cl}_2$  at 293 K consists of a doublet of doublets of doublets at -7.9 ppm with  $^1J(\text{Pt}-\text{H}) = 613$  Hz (see Figure 5.17). All the NMR data for the complex **12a** are reported in Table 5.5. The complex **12a** is

formed from the platinum carbonyl hydride complex **8a**, whose formation is always observed in the presence of CO. During the reaction with  $\text{PPh}_3$ , the CO coordinated to the platinum in **8a** is replaced by  $\text{PPh}_3$  as observed for  $[\text{Pt}(\text{d}^t\text{bpx})(\text{C}(\text{O})\text{C}_2\text{H}_5)(\text{PPh}_3)]^+$ , **11a**.

**Figure 5.17**

$^1\text{H}$  NMR spectrum of  $[\text{Pt}(\text{d}^t\text{bpx})\text{H}(\text{PPh}_3)]^+$ , **12a**, in  $\text{CH}_2\text{Cl}_2$  at 293 K

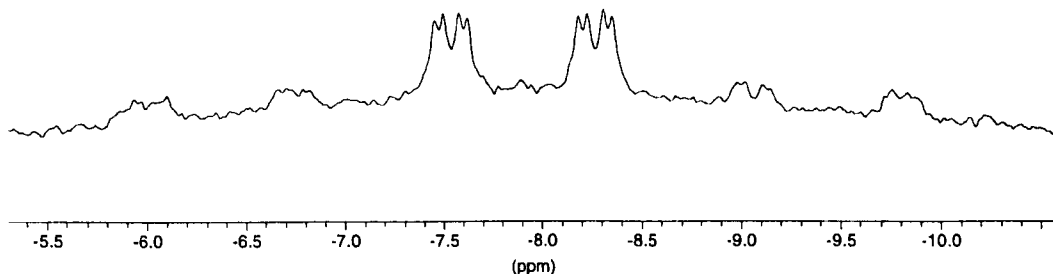


**Table 5.5**

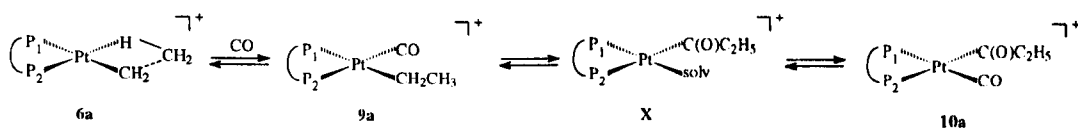
NMR data for  $[\text{Pt}(\text{d}^t\text{bpx})\text{H}(\text{PPh}_3)]^+$ , **12a**, in  $\text{CH}_2\text{Cl}_2$  at 293 K

	$\delta$	$J(\text{P}_1-)$	$J(\text{P}_2-)$	$J(\text{PPh}_3-)$	$J(\text{Pt}-)$
<b>P<sub>1</sub></b>	47.2 ppm	-			2847 Hz
<b>P<sub>2</sub></b>	35.2 ppm	18 Hz	-		2356 Hz
<b>PPh<sub>3</sub></b>	9.2 ppm	334 Hz	22 Hz	-	2558 Hz
<b>H</b>	-7.9 ppm	26 Hz	146 Hz	9 Hz	613 Hz

### 5.6. Formation and decomposition of $[\text{Pt}(\text{d}^t\text{bpx})(\text{C}(\text{O})\text{Et})(\text{CO})]^+$ , **10a**

The formation of the platinum carbonyl acyl complex **10a** occurs by the steps described in Scheme 5.4. In the first step the insertion of CO into the platinum ethyl complex **6a** and the formation of  $[\text{Pt}(\text{d}^t\text{bpx})(\text{C}_2\text{H}_5)(\text{CO})]^+$ , **9a**, occurs, then the  $\text{C}_2\text{H}_5$ -group migrates<sup>17</sup> with the formation of  $[\text{Pt}(\text{d}^t\text{bpx})(\text{C}(\text{O})\text{Et})(\text{solv})]^+$ . It is possible to suppose that the formation of **10a** takes place through the formation of the platinum solvento-acyl complex **X**, which has not been observed in the platinum system because the CO present in solution coordinates to the platinum in the fourth position.

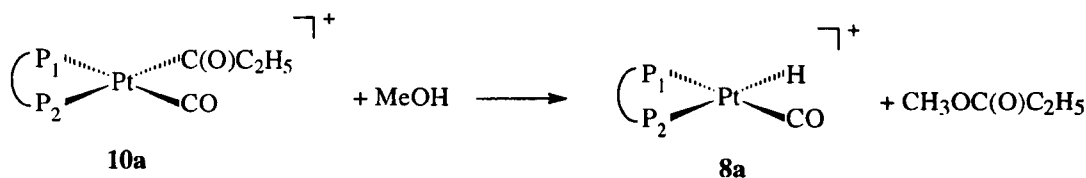
**Scheme 5.4**



In many cases it has been observed that  $[\text{Pt}(\text{d}^t\text{bpx})\text{H}(\text{C}^{13}\text{CO})]^+$ , **8a**, and  $[\text{Pt}(\text{d}^t\text{bpx})(\text{C}(\text{O})\text{Et})(\text{CO})]^+$ , **10a**, are both present in solution at 293 K after the reaction of CO with the platinum ethyl complex **6a** and after time the complex **10a** disappears. This process has been observed in  $\text{CH}_2\text{Cl}_2$  and THF, whether before drying and dissolving the precipitate in MeOH or after the addition of MeOH and formation of MeP. It seems that the stability of the complex **10a** is correlated to the presence of CO in solution, in fact the complex is not very stable when there is not sufficient CO to coordinate and stabilize the platinum acyl complex **10a**. Two



## Scheme 5.6



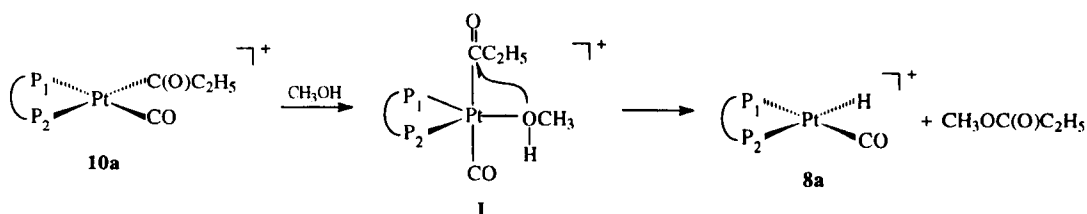
## 5.7. Alcoholysis-step

It has been observed in Section 5.3.1 that the reaction between  $[\text{Pt}(\text{d}^t\text{bpx})(\text{C}(\text{O})\text{C}_2\text{H}_5)(\text{CO})]^+$ , **10a**, and  $\text{MeOH}$  results in the formation of  $\text{MeP}$  and  $[\text{Pt}(\text{d}^t\text{bpx})(\text{H})(\text{CO})]^+$ , **8a**. The formation of the platinum carbonyl hydride complex **8a** has been discussed in the previous section and here the methanolysis of the platinum acyl complex **10a** will be analysed.

Two principal mechanisms can be proposed in order to explain how  $\text{MeOH}$  interacts with the platinum complex **10a** to form  $\text{MeP}$ .

The first process considers the formation of a five coordinate intermediate **I**, followed by an intra-molecular nucleophilic attack by  $-\text{OCH}_3$  (see Scheme 5.7).

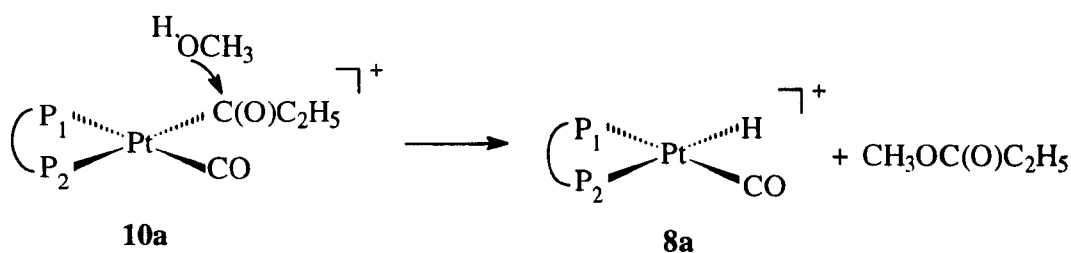
## Scheme 5.7



Because of the high affinity of platinum for CO it is unlikely that CO dissociation occurs and methanolysis *via* an intra-molecular route must involve a five coordinate intermediate.

The second process considers a direct nucleophilic attack of MeOH on the acyl group in the platinum acyl complex **10a** (see Scheme 5.8).

Scheme 5.8



Yamamoto reported some similar mechanistic studies of the alcoholysis process of an acyl halide of palladium in the presence of a base.<sup>18</sup> In his studies the base can deprotonate the nucleophile MeO-H, which can then coordinate to the palladium. Also Moser proposed a mechanism that involves the formation of a methoxide anion that attacks the acyl palladium complex.<sup>19</sup>

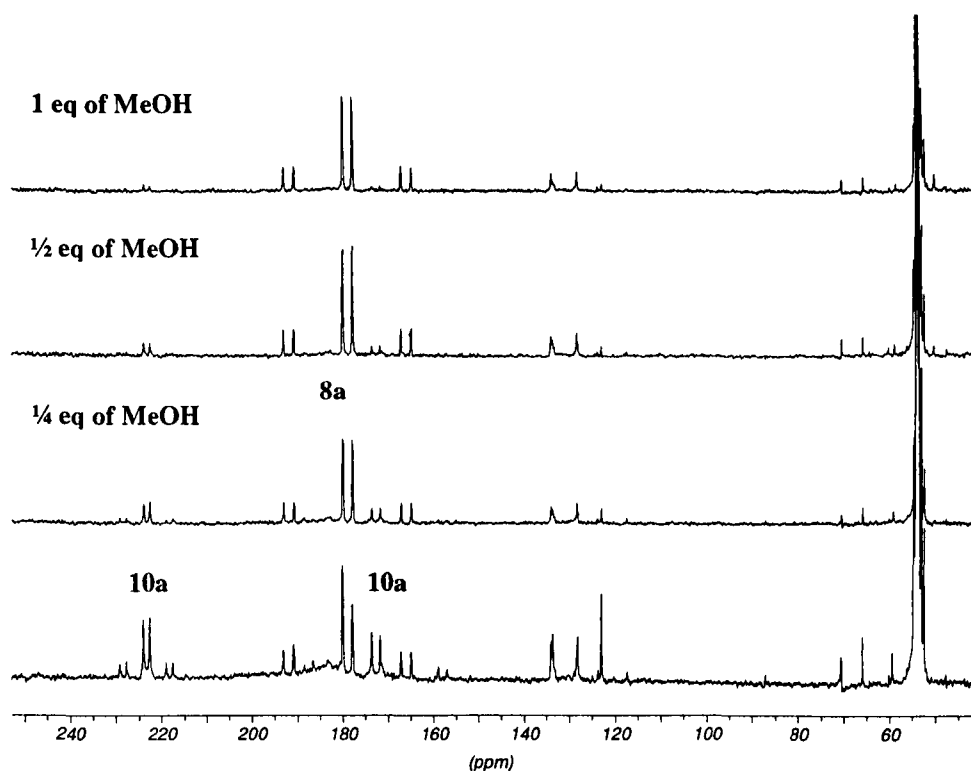
Recently Cole-Hamilton reported some studies dealing with the methoxy-process in the palladium acyl complex  $[\text{Pd}(\text{d}^t\text{bpx})(\text{C}(\text{O})\text{C}_2\text{H}_5)(\text{CO})]^+$ . He suggests an external attack by MeOH but he underlines that the very high electron density on the metal would disfavour the nucleophilic attack of methanol.<sup>20</sup> He proposes that the diphosphine becomes unidentate, forming a three coordinated intermediate with dissociation of the phosphorus atom *trans* to the acyl group (see Scheme 5.8), which has a very high *trans* effect in dissociative processes.<sup>21</sup> He suggests that the evidence



MeOH to the solution of  $[\text{Pt}(\text{d}^1\text{bpx})(^{13}\text{C}(\text{O})\text{C}_2\text{H}_5)(^{13}\text{CO})]^+$ , **10a**, the formation of MeP is not observed and the only complex formed is  $[\text{Pt}(\text{d}^1\text{bpx})\text{H}(^{13}\text{CO})]^+$ , **8a**, and the resonance at *ca.* 50 ppm is due to un-reacted MeOH (see Figure 5.18).

**Figure 5.18**

$^{13}\text{C}\{^1\text{H}\}$  NMR spectra of  $[\text{Pt}(\text{d}^1\text{bpx})\text{H}(\text{CO})]^+$ , **8a**, and  $[\text{Pt}(\text{d}^1\text{bpx})(\text{C}(\text{O})\text{C}_2\text{H}_5)(\text{CO})]^+$ , **10a**, + MeOH in  $\text{CH}_2\text{Cl}_2$  at 293 K



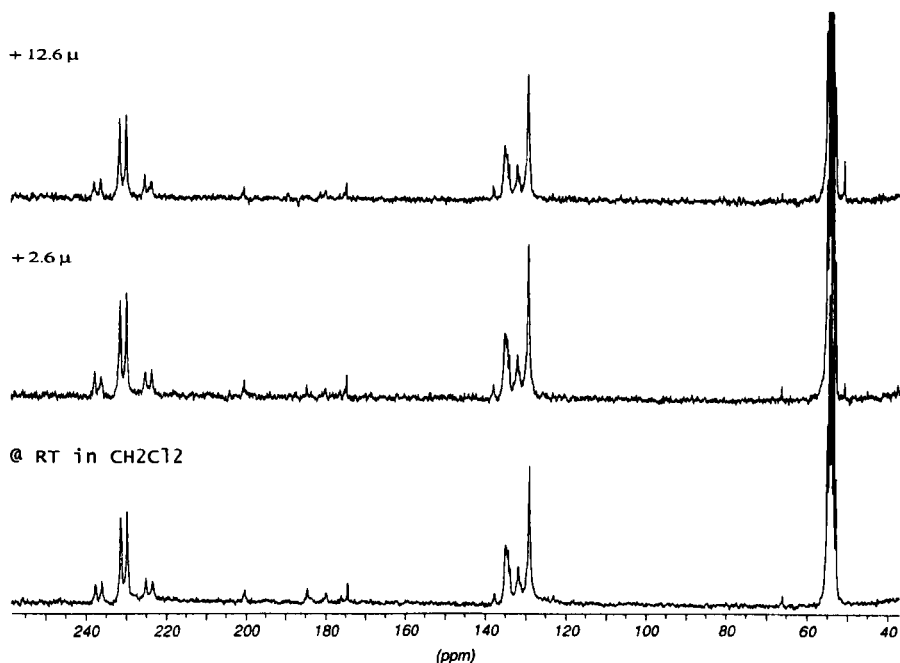
After each addition of MeOH, the resonances due to  $[\text{Pt}(\text{d}^1\text{bpx})(^{13}\text{C}(\text{O})\text{C}_2\text{H}_5)(^{13}\text{CO})]^+$ , **10a**, decrease with formation of the platinum complex **8a**. This occurs in MeOH and all other solvent studied under an atmosphere of  $\text{N}_2$  because of the decomposition of the platinum acyl complex **10a** and release

$^{13}\text{C}$  which is observed on opening the NMR tube to add further MeOH; under  $\text{N}_2$ , the decomposition of the platinum complex **10a** is mainly due to the lack of CO in solution (see Section 5.5).

When MeOH is added to a solution of  $[\text{Pt}(\text{d}^1\text{bpx})(^{13}\text{C}(\text{O})\text{C}_2\text{H}_5)(\text{PPh}_3)]^+$ , **11a**, in  $\text{CH}_2\text{Cl}_2$  at 293 K, no reaction occurs. The  $^{13}\text{C}\{^1\text{H}\}$  NMR spectrum in  $\text{CH}_2\text{Cl}_2$  shows the presence of the complex **11a** and the resonance at *ca.* 50 ppm is due to the unreacted MeOH (see Figure 5.19).

**Figure 5.19**

$^{13}\text{C}\{^1\text{H}\}$  NMR spectra of  $[\text{Pt}(\text{d}^1\text{bpx})(\text{C}(\text{O})\text{C}_2\text{H}_5)(\text{PPh}_3)]^+$ , **11a**, + MeOH in  $\text{CH}_2\text{Cl}_2$  at 293 K



In this experiment, the reaction of MeOH with the platinum complex **11a** could be disfavoured by the high electron density on the platinum due to the presence of a chelating diphosphine and the triphenylphosphine.

These experiments do not help in distinguishing between the two alternative mechanisms involved in the methanolysis step. The mechanism shown in Scheme 5.7 would appear to be disfavoured both by electronic and steric effects, although presently this appears to be the favoured mechanism for the palladium acyl complex. The external nucleophilic attack of MeOH on the acyl group (see Scheme 5.8) seems more probable than the mechanism shown in Scheme 5.7. It should be noted that we have no evidence for the dissociation of the chelating ligand to allow the mechanism proposed by Cole Hamilton.

## 5.8. References

- (1) D. Belli Dell'Amico; F. Calderazzo; C. A. Veracini; N. Zandona' *Inorg. Chem.* **1984**, *23*, 3030.
- (2) M.J. Church and M.J. Mays *Chem. Comm.*, **1968**, 435.
- (3) T. Theophanides and P.C. Kong *Inorg. Chim. Acta*, **1971**, *5*, 485.
- (4) L. Spaulding; B.A. Reinhardt; M. Orchin *Inorg. Chem.*, **1972**, *11*, 2092.
- (5) R.G. Goel; W.O. Ogini; R.G. Scrivastava *Organometallics* **1982**, *1*, 819.
- (6) M. Kubota; R.K. Rothrock; J. Geibel *J. Chem. Soc., Dalton Trans.*, **1973**, 1267.
- (7) J. Browning; P.L. Goggin; R.J. Goodfellow; M.G. Norton; A.J.M. Rattray; B.F. Taylor; S.J. Mink *J. Chem. Soc., Dalton Trans.*, **1977**, 2061.
- (8) J.D. Oliver and P.E. Rush *J. Organomet. Chem.*, **1976**, *104*, 117.
- (9) F. Calderazzo and D.B. Dell'Amico *Inorg. Chem.* **1981**, *20*, 1310.
- (10) W. Clegg; G.R. Eastham; M.R.J. Elsegood; B.T. Heaton; J.A. Iggo; R.P. Tooze; R. Whyman; S. Zacchini *Organometallics*, **2002**, *21*, 1832.
- (11) C. Anklin; F. Bachechi; P. Mura; P.S. Pregosin; L. Zambonelli *J. Organometal. Chem.*, **1981**, *222*, 175.
- (12) T. G. Appleton and M. A. Bennett *Inorg. Chem.* **1978**, *17*, 738.
- (13) K. Nozaki; T. Hiyama; S. Kacker; I. T. Horvath *Organometallics*, **2000**, *19*, 2031.
- (14) A. Gusso; C. Baccin; F. Pinna; G. Strukul *Organometallics* **1994**, *13*, 3442.
- (15) S. Reinartz; M. Brookhart; J. L. Templeton *Organometallics*, **2002**, *21*, 247.
- (16) O. Fujimura *J. Am. Chem. Soc.*, **1998**, *120*, 10032.

- (17) P.W.N.M. van Leeuwen; C.F. Roobeek; H.J. van der Heijden *J. Am. Chem. Soc.*, **1994**, *116*, 12117.
- (18) Y.S. Lin and A. Yamamoto *Organometallics* **1998**, *17*, 3466.
- (19) W.R. Moser; A.W. Wang; N.K. Kjeldahal *J. Am. Chem. Soc.*, **1988**, *110*, 2816.
- (20) D.J. Cole-Hamilton and R.A.M. Robertson *in press* **2002**.
- (21) T. G. Appleton; H.C. Clark; L. Manzer *Coord. Chem. Rev.*, **1973**, *10*, 335.

# Chapter Six

## 6. Studies at high temperature and high pressure

### 6.1. Introduction

The previous chapters described the behaviour of platinum complexes during the reaction with acids, ethene and CO at 193 K and 293 K, using atmospheric pressure. It has been possible to isolate and fully characterise most of the complexes involved and their stability and their reactivity has been fully described under these conditions.

The aim of this chapter is to describe the experiments carried out at  $> 293$  K and  $> 1$  atm, using a NMR sapphire tube and a conventional autoclave, in order to understand if it is possible to increase the reactivity of platinum complexes, using higher gas pressures and higher temperatures. Some experiments carried out using a mixture of gases (CO/C<sub>2</sub>H<sub>4</sub>) repeated the industrial procedure carried out previously for the palladium system.

### 6.2. CF<sub>3</sub>SO<sub>3</sub>H-system

First, the stability of the complexes characterised in the CF<sub>3</sub>SO<sub>3</sub>H-system was analysed under high pressure and high temperature.

#### 6.2.1 Stability of [Pt(d<sup>4</sup>bpx)H(solvent)][CF<sub>3</sub>SO<sub>3</sub>], 3a, under N<sub>2</sub> pressure

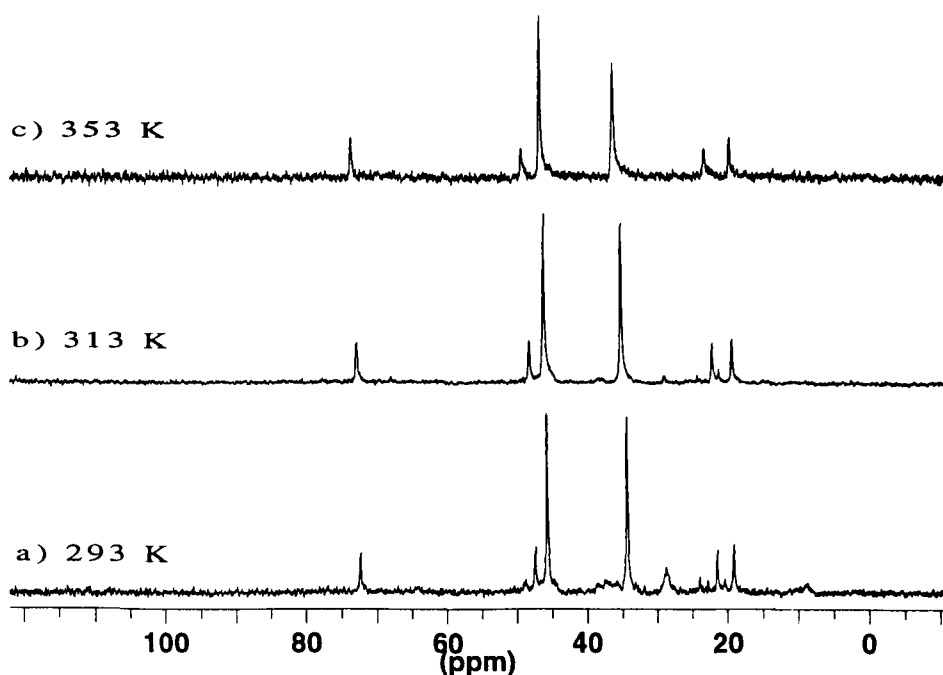
In order to carry out NMR measurements on the reaction between [Pt(d<sup>4</sup>bpx)(dba)], **1**, BQ and CF<sub>3</sub>SO<sub>3</sub>H in MeOH at high temperature, it was necessary

to use a sapphire tube and to pressurise with 7 bar of  $N_2$  in order to prevent the evaporation of the solvent.

The  $^{31}P\{^1H\}$  NMR spectrum of  $[Pt(d^4bpx)H(MeOH)]^+$ , **3a**, (under 7 bar of  $N_2$ ) has been recorded at different temperatures in MeOH. The spectra are reported in Figure 6.1, which show that there are no exchange processes  $\leq 353$  K. Thus, all the resonances remain basically unchanged and there is no evidence of decomposition. This behaviour confirms the stability of the platinum hydride complex **3a** which remains unchanged in solution after one week at room temperature.

**Figure 6.1**

*VT  $^{31}P\{^1H\}$  NMR spectra of  $[Pt(d^4bpx)H(MeOH)]^+$ , **3a**, in MeOH under 7 bar of  $N_2$*



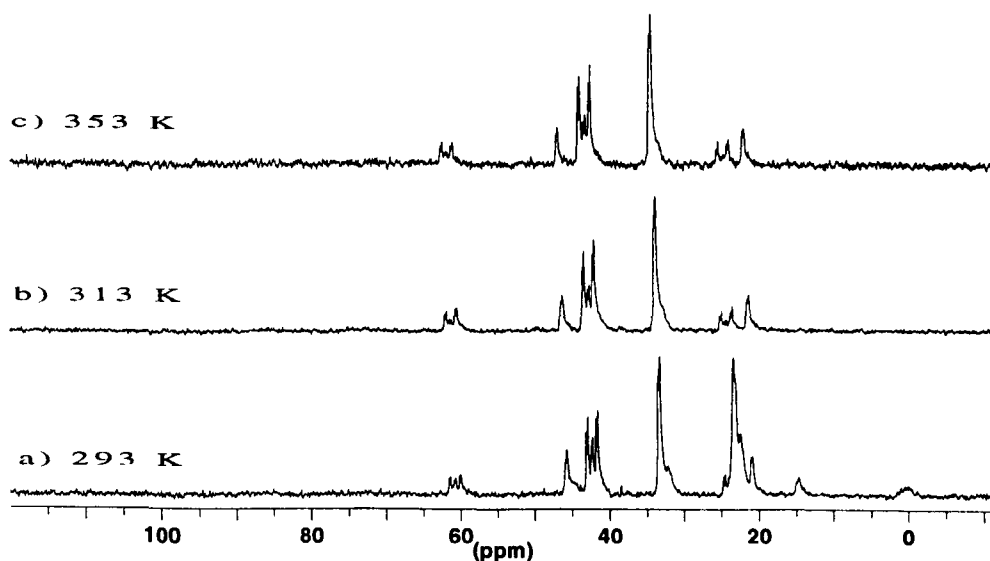
### 6.2.2 Stability of $[\text{Pt}(\text{d}^4\text{bpx})\text{H}(\text{}^{13}\text{CO})][\text{CF}_3\text{SO}_3]$ , **3a**, under $^{13}\text{CO}$ and $\text{C}_2\text{H}_4$ pressure

The stability of  $[\text{Pt}(\text{d}^4\text{bpx})(\text{CH}_2\text{CH}_3)]^+$ , **6a**, at high temperature under ethylene pressure has been fully discussed previously (see Section 4.3.1).

Instead, when the solution of the platinum ethyl complex **6a** is depressurised to 1 bar of  $\text{C}_2\text{H}_4$  and then put under 3 bar of  $^{12}\text{CO}$ , the formation of  $[\text{Pt}(\text{d}^4\text{bpx})\text{H}(\text{CO})]^+$ , **8a**, is immediate in MeOH. In order to understand the behaviour of the compound from the  $^{13}\text{C}$  NMR spectra at different temperatures, the sample has been depressurised to 1 bar again and put under 6 bar of  $^{13}\text{CO}$ . The  $^{31}\text{P}\{^1\text{H}\}$  NMR spectra of **8a** under 6 bar of  $^{13}\text{CO}$  do not show any changes at different temperatures; at each temperature, the only species present is  $[\text{Pt}(\text{d}^4\text{bpx})\text{H}(\text{CO})]^+$ , **8a**, (see Figure 6.2).

**Figure 6.2**

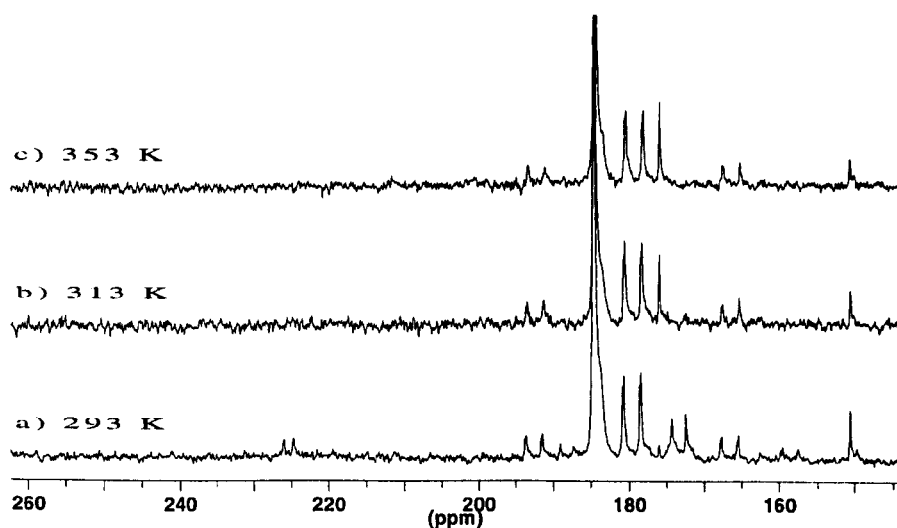
*VT  $^{31}\text{P}\{^1\text{H}\}$  NMR spectra of  $[\text{Pt}(\text{d}^4\text{bpx})\text{H}(\text{}^{13}\text{CO})]^+$ , **8a**, in MeOH under 6 bar of  $^{13}\text{CO}$*



The  $^{13}\text{C}\{^1\text{H}\}$  NMR spectrum of the above solution at 293 K shows that the main doublet of doublets is due to the platinum carbonyl hydride complex **8a**. Much weaker doublets at 225 ppm and at 174 ppm are also observed and they are due to the platinum acyl complex **10a**, despite using MeOH as solvent (see Figure 6.3a). On increasing the temperature to 313 K, the resonance in the acyl region disappears and a singlet at 176 ppm appears due to the formation of MeP; at 333 K, the resonance at 176 ppm slightly increases, but there are no other obvious changes (see Figure 6.3c).

**Figure 6.3**

*VT  $^{13}\text{C}\{^1\text{H}\}$  NMR spectra of  $[\text{Pt}(d^4\text{bpx})\text{H}(^{13}\text{CO})]^+$ , **8a**, in MeOH under 6 bar of  $^{13}\text{CO}$*

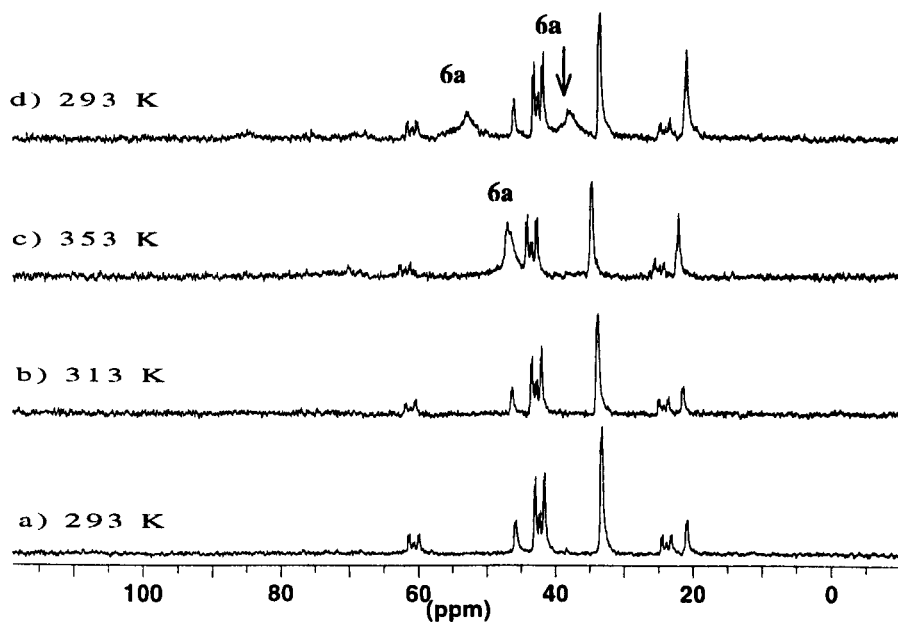


At this point, the sample was cooled to room temperature and degassed, followed by addition of 10 bar of  $\text{C}_2\text{H}_4$ . The  $^{31}\text{P}\{^1\text{H}\}$  NMR spectrum at room temperature shows the resonances due to  $[\text{Pt}(d^4\text{bpx})\text{H}(\text{CO})]^+$ , **8a**, (see Figure 6.4a). On increasing the temperature to 333 K (see Figure 6.4c), a broad resonance appears at ca. 46.6

ppm as found in the  $^{31}\text{P}\{^1\text{H}\}$  NMR spectrum of the platinum ethyl complex **6a** at this temperature (see Figure 4.4). Cooling this solution to room temperature results in the appearance of two resonances at 52.9 and 38.2 ppm and it is possible to conclude that the reformation of  $[\text{Pt}(\text{d}^1\text{bpx})(\text{CH}_2\text{CH}_3)]^+$ , **6a**, has occurred (see Figure 6.4d). From the  $^{13}\text{C}\{^1\text{H}\}$  NMR spectra it is evident that on increasing the temperature the amount of MeP increases (see Figure 6.5).

**Figure 6.4**

*VT  $^{31}\text{P}\{^1\text{H}\}$  NMR spectra of  $[\text{Pt}(\text{d}^1\text{bpx})\text{H}(^{13}\text{CO})]^+$ , **8a**, in MeOH under 10 bar of  $\text{C}_2\text{H}_4$*

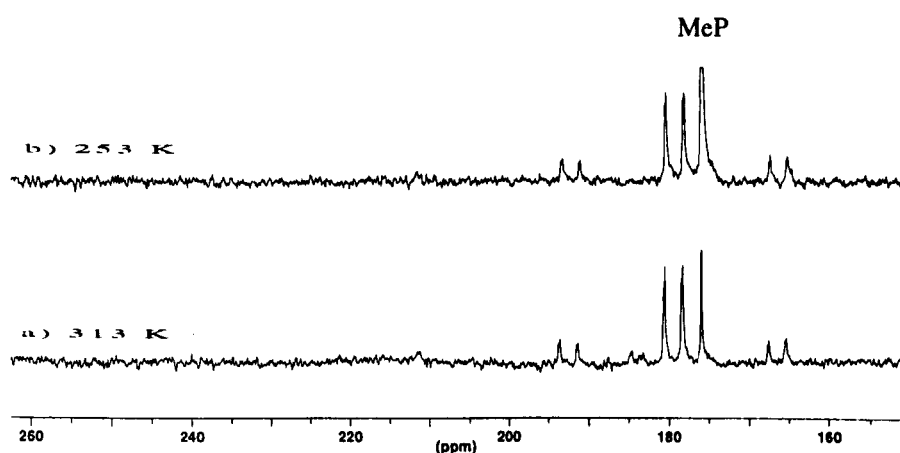


From these results, it is evident that methoxycarbonylation occurs in the platinum system but the conditions required are much more drastic than in the palladium system, because of the greater stability of the platinum hydride and the platinum carbonyl hydride complexes. The stability of these compounds is also evident, under the conditions reported above, and there is only evidence for slight traces of

decomposition. Moreover, the formation of the ethyl complex is very difficult, and this seems to be the main reason for the lower activity of the Pt-catalyst compared to the Pd-catalyst.

**Figure 6.5**

*VT  $^{13}\text{C}\{^1\text{H}\}$  NMR spectra of  $[\text{Pt}(\text{d}^4\text{bpx})\text{H}(^{13}\text{CO})]^+$ , **8a**, in MeOH under 10 bar of  $\text{C}_2\text{H}_4$*



### 6.3. $\text{CH}_3\text{SO}_3\text{H}$ -system with addition of $\text{H}_2\text{O}$

This section deals with the study of the reaction of  $[\text{Pt}(\text{d}^4\text{bpx})(\text{dba})]$ , **1**, with  $\text{CH}_3\text{SO}_3\text{H}$  and BQ, in the presence of water at high temperature and high pressure.

The behavior of  $[\text{Pt}(\text{d}^4\text{bpx})\text{H}(\text{solv})][\text{CH}_3\text{SO}_3]$ , **3b**, and  $[\text{Pt}(\text{d}^4\text{bpx})(\text{H}_2\text{O})_2][\text{CH}_3\text{SO}_3]_2$ , **4b**, was studied at different temperatures (293-343 K) in a sapphire tube under a pressure of  $\text{N}_2$ ,  $\text{C}_2\text{H}_4$  and  $^{13}\text{CO}$ . The same reaction of  $[\text{Pt}(\text{d}^4\text{bpx})(\text{dba})]$ , **1**, with  $\text{CH}_3\text{SO}_3\text{H}$  and BQ, in the presence of water was studied using different gas mixtures ( $\text{CO}/\text{C}_2\text{H}_4 = 1/1$  and  $1/9$ ) at different temperatures.

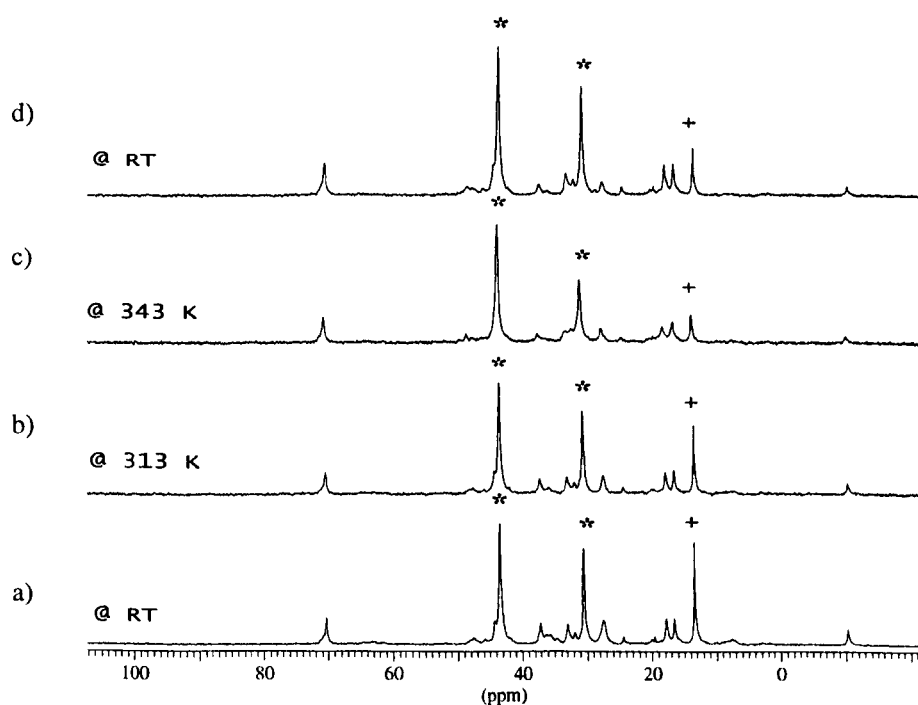
The experiments described below have been carried out sequentially.

### 6.3.1 Reactivity under 10 bar of N<sub>2</sub>

It has been shown that the reaction of [Pt(d<sup>1</sup>bpx)(dba)], **1**, with CH<sub>3</sub>SO<sub>3</sub>H and BQ results in the formation of [Pt(d<sup>1</sup>bpx)(η<sup>2</sup>-CH<sub>3</sub>SO<sub>3</sub>)]<sup>+</sup>, **5b**, in MeOH and the hydride complex **3b** is formed only on addition of water (0.2 ml) to the solution of **5b** (see Section 3.2.3). In this experiment, first, [Pt(d<sup>1</sup>bpx)(η<sup>2</sup>-CH<sub>3</sub>SO<sub>3</sub>)]<sup>+</sup>, **5b**, was formed and then 0.2 ml of water were added. The sapphire tube was closed and pressurised with 10 bar of N<sub>2</sub>. In the <sup>31</sup>P{<sup>1</sup>H} NMR spectrum at 293 K in MeOH the two compounds, [Pt(d<sup>1</sup>bpx)H(sol<sub>v</sub>)]<sup>+</sup>, **3b**, and [Pt(d<sup>1</sup>bpx)(H<sub>2</sub>O)<sub>2</sub>]<sup>2+</sup>, **4b**, are present (see Figure 6.6a).

**Figure 6.6**

*VT <sup>31</sup>P{<sup>1</sup>H} NMR spectra of [Pt(d<sup>1</sup>bpx)H(sol<sub>v</sub>)]<sup>+</sup> (\*), **3b**, and [Pt(d<sup>1</sup>bpx)(H<sub>2</sub>O)<sub>2</sub>]<sup>2+</sup> (+), **4b**, in MeOH under 10 bar of N<sub>2</sub>*



On increasing the temperature, the resonance due to the bisquo complex decreases (see Figure 6.6d). Of interest is that the intensities of the resonances due to  $[\text{Pt}(\text{d}^4\text{bpx})\text{H}(\text{solvent})]^+$ , **3b**, remain relatively unchanged despite the disappearance of  $[\text{Pt}(\text{d}^4\text{bpx})(\text{H}_2\text{O})_2]^{2+}$ , **4b**. Thus, it seems that the bisquo complex **4b** provides a route for decomposition to platinum metal. There is no change in the resonances due to the hydride compound, showing that at temperatures  $\leq 353\text{K}$  there is no exchange process as it has been observed in the  $\text{CF}_3\text{SO}_3\text{H}$ -system.

### 6.3.2 Reactivity under 10 bar of $\text{C}_2\text{H}_4$

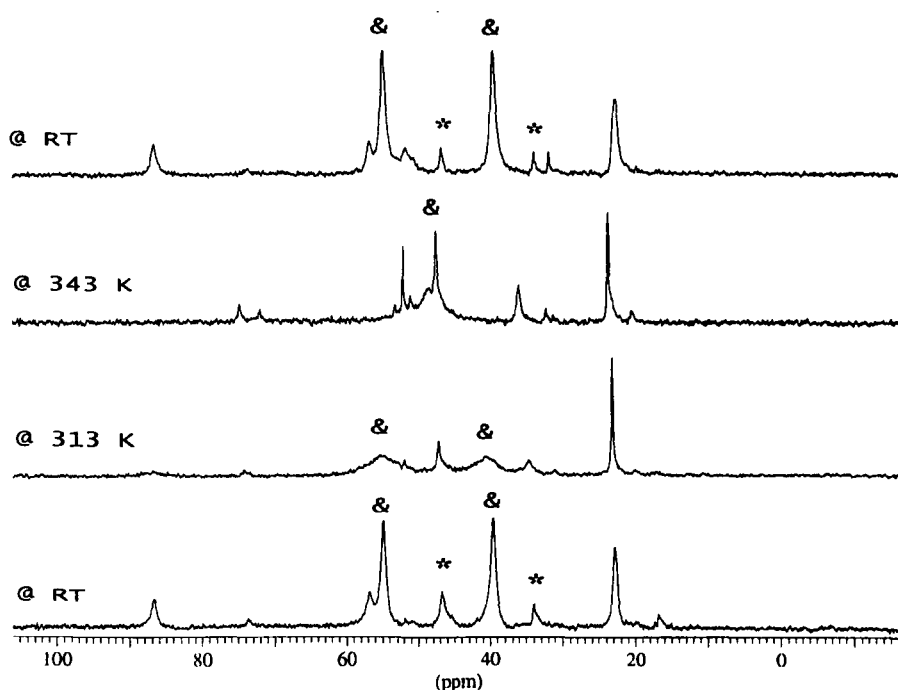
The compounds  $[\text{Pt}(\text{d}^4\text{bpx})\text{H}(\text{solvent})]^+$ , **3b**, and  $[\text{Pt}(\text{d}^4\text{bpx})(\text{H}_2\text{O})_2]^{2+}$ , **4b**, formed during the first part of the reaction (Section 6.3.1) were put under 10 bar of  $\text{C}_2\text{H}_4$ . The sapphire tube, containing this mixture under  $\text{N}_2$  pressure was simply depressurised and repressurised with ethene. The resulting  $^{31}\text{P}\{^1\text{H}\}$  NMR spectrum at 293 K shows the formation of the platinum ethyl complex **6b** and resonances due to the hydride compound are present too (see Figure 6.7a). On increasing the temperature to 313 K, the resonances due to  $[\text{Pt}(\text{d}^4\text{bpx})(\text{CH}_2\text{CH}_3)]^+$ , **6b**, broaden and coalesce at 353 K to form one resonance at about 46 ppm. The same process which makes the two phosphorus atoms equivalent at high temperature has been observed in the case of  $[\text{Pt}(\text{d}^4\text{bpx})(\text{CH}_2\text{CH}_3)][\text{CF}_3\text{SO}_3]$ , **6a**, (see Section 4.3.1).

However, there are some differences between the  $\text{CF}_3\text{SO}_3\text{H}$ -system and  $\text{CH}_3\text{SO}_3\text{H}$ -system. In the  $^{31}\text{P}\{^1\text{H}\}$  NMR spectrum at 293 K (see Figure 6.7a), the platinum hydride compound **3b** is present, even when the solution is under ethene pressure, and **3b** is still present on increasing the temperature to 353 K. This means

that in the  $\text{CH}_3\text{SO}_3\text{H}$ -system the equilibrium between the hydride complex and the ethyl complex is shifted more in favour of the hydride complex than in the  $\text{CF}_3\text{SO}_3\text{H}$ -system.

**Figure 6.7**

*VT  $^{31}\text{P}\{^1\text{H}\}$  NMR spectra of  $[\text{Pt}(\text{d}^1\text{bpx})\text{H}(\text{solv})]^+$  (\*), **3b**, and  $[\text{Pt}(\text{d}^1\text{bpx})(\text{CH}_2\text{CH}_3)]^+$  (&), **6b**, in MeOH under 10 bar of  $\text{C}_2\text{H}_4$*



Working with  $\text{CH}_3\text{SO}_3\text{H}$  and water, all the compounds formed seem less stable and decomposition to metal is observed. Also, the  $^{31}\text{P}\{^1\text{H}\}$  NMR spectrum at 343 K (see Figure 6.7c) contains a new resonance at ca. 50 ppm, which probably is due to protonation of the free ligand, formed as a result of decomposition and metal precipitation.

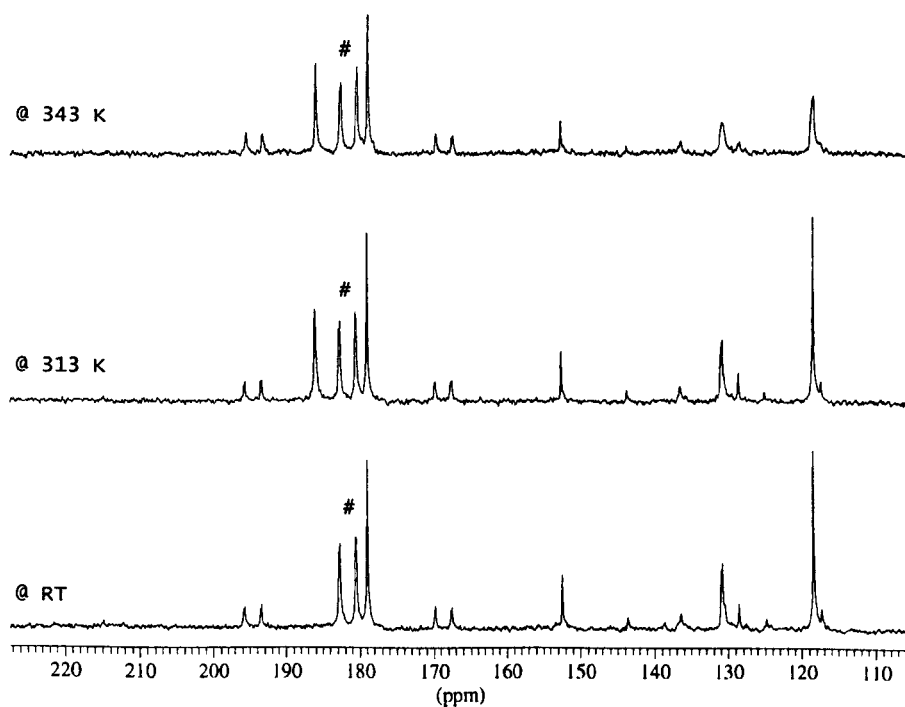
### 6.3.3 Reactivity under 7 bar of CO and 10 bar of C<sub>2</sub>H<sub>4</sub>

When the solution containing a mixture of the platinum ethyl **6b** and hydride **3b** complexes is depressurised to 1 bar of ethene and then put under 7 bar of <sup>13</sup>CO, the formation of [Pt(d<sup>4</sup>bpx)H(<sup>13</sup>CO)][CH<sub>3</sub>SO<sub>3</sub>], **8b**, is observed immediately.

The <sup>31</sup>P{<sup>1</sup>H} NMR spectra of [Pt(d<sup>4</sup>bpx)H(<sup>13</sup>CO)][CH<sub>3</sub>SO<sub>3</sub>], **8b**, do not show any changes at higher temperatures. In the <sup>13</sup>C{<sup>1</sup>H} NMR spectrum at 293 K, [Pt(d<sup>4</sup>bpx)H(<sup>13</sup>CO)][CH<sub>3</sub>SO<sub>3</sub>], **8b**, and MeP are observed, but the intensity of MeP does not increase with increasing temperature (see Figure 6.8).

**Figure 6.8**

*VT <sup>31</sup>P{<sup>1</sup>H} NMR spectra of [Pt(d<sup>4</sup>bpx)H(CO)]<sup>+</sup> (#), **8b**,  
in MeOH under 7 bar of <sup>13</sup>CO*

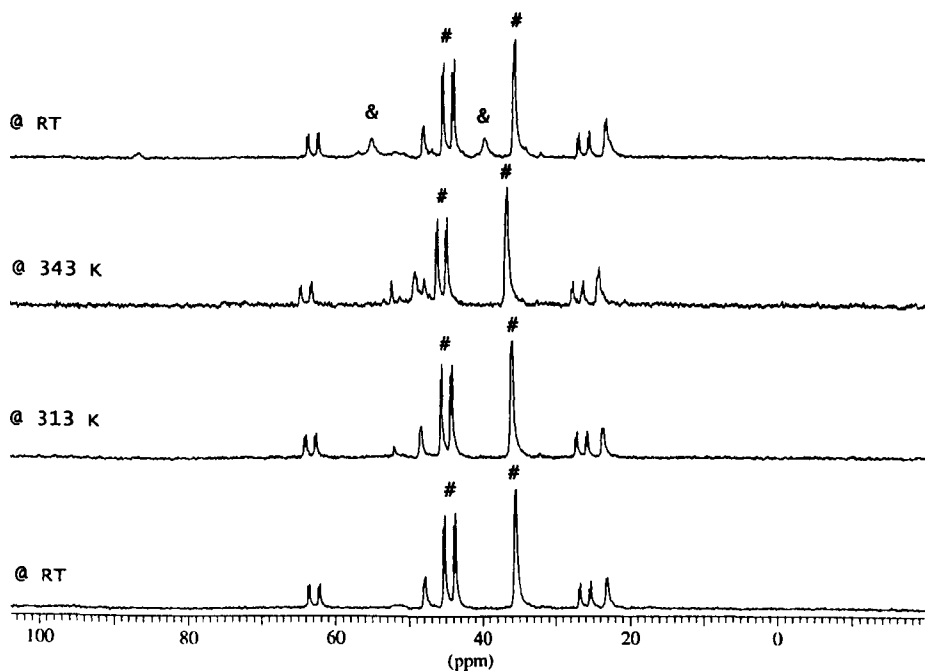


Despite the high pressure of  $^{13}\text{CO}$ , the resonance due to free  $^{13}\text{CO}$  is not observed in the  $^{13}\text{C}\{^1\text{H}\}$  NMR spectrum at 293 K. It is necessary to increase the temperature to 313 K to observe the resonance due to free  $^{13}\text{CO}$  at about 184 ppm. For the moment, it seems that the  $\text{CH}_3\text{SO}_3\text{H}$ -system is more reactive under CO than the  $\text{CF}_3\text{SO}_3\text{H}$ -system, even when the solubility of free CO is bigger in the  $\text{CF}_3\text{SO}_3\text{H}$ -system.

The sequential experiments carried out at this stage, involve cooling the sample to 293 K, followed by depressurisation and addition of 10 bar of ethene. The  $^{31}\text{P}\{^1\text{H}\}$  NMR spectrum at 293 K consists of the resonance due to  $[\text{Pt}(\text{d}^t\text{bpx})\text{H}(\text{}^{13}\text{CO})][\text{CH}_3\text{SO}_3]$ , **8b**, and on increasing the temperature to 343 K there is evidence for the formation of  $[\text{Pt}(\text{d}^t\text{bpx})(\text{CH}_2\text{CH}_3)]^+$ , **6b**, (see Figure 6.9).

**Figure 6.9**

*VT  $^{31}\text{P}\{^1\text{H}\}$  NMR spectra of  $[\text{Pt}(\text{d}^t\text{bpx})\text{H}(\text{CO})]^+$  (#), **8b**, and  $[\text{Pt}(\text{d}^t\text{bpx})(\text{CH}_2\text{CH}_3)]^+$  (&), **6b**, in MeOH under 10 bar of  $\text{C}_2\text{H}_4$*



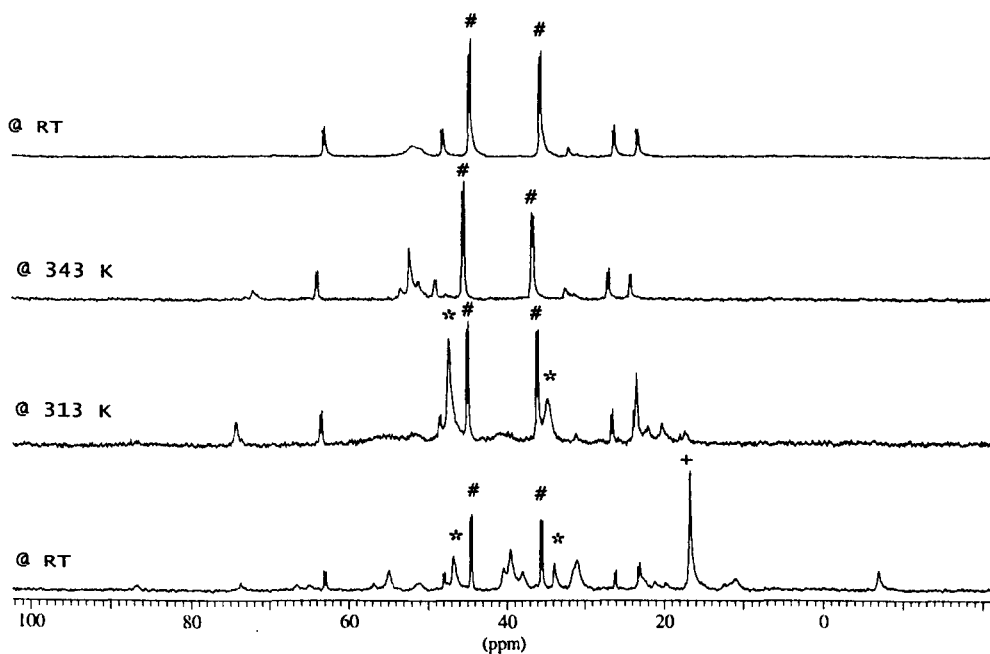
The same behaviour has been observed in the  $\text{CF}_3\text{SO}_3\text{H}$ -system. When the solution of  $[\text{Pt}(\text{d}^1\text{bpx})\text{H}(\text{}^{13}\text{CO})][\text{CF}_3\text{SO}_3]$ , **8a**, is pressurised again with  $\text{C}_2\text{H}_4$ , the platinum ethyl complex **6a** is reformed at 343 K.

#### 6.3.4 Reactivity under 10 bar of gas mixture $\text{CO}/\text{C}_2\text{H}_4$ (1/1)

Dissolution of  $[\text{Pt}(\text{d}^1\text{bpx})(\text{dba})]$ , **1**, in MeOH in the presence of BQ,  $\text{CH}_3\text{SO}_3\text{H}$  and  $\text{H}_2\text{O}$  followed by pressurisation with 10 bar of  $\text{CO}/\text{C}_2\text{H}_4$  with ratio 1/1, gives the  $^{31}\text{P}\{^1\text{H}\}$  NMR spectra shown in Figure 6.10.

**Figure 6.10**

*VT  $^{31}\text{P}\{^1\text{H}\}$  NMR spectra of  $[\text{Pt}(\text{d}^1\text{bpx})(\text{dba})]$ , **1**, +  $\text{CH}_3\text{SO}_3\text{H}$  + BQ +  $\text{H}_2\text{O}$  in MeOH under 10 bar of  $\text{CO}/\text{C}_2\text{H}_4$  (1/1)*



At 293 K,  $[\text{Pt}(\text{d}^{\text{t}}\text{bpx})(\text{H}_2\text{O})_2]^{2+}$ , **4b**,  $[\text{Pt}(\text{d}^{\text{t}}\text{bpx})\text{H}(\text{solv})]^+$ , **3b** and  $[\text{Pt}(\text{d}^{\text{t}}\text{bpx})\text{H}(\text{CO})]^+$ , **8b**, are present and, at 313 K, the platinum bisquo complex **4b** disappears. At 345 K, the platinum carbonyl hydride **8b** is the only complex present in solution, apart from some impurities and a black precipitate due to platinum metal. At this point, the solution was cooled to room temperature and the  $^{31}\text{P}\{^1\text{H}\}$  NMR spectrum shows that only the platinum carbonyl hydride complex **8b** is present in solution. Working with a 1:1 ratio of  $\text{CO}/\text{C}_2\text{H}_4$ , the formation of the platinum ethyl complex is not observed. It seems that  $[\text{Pt}(\text{d}^{\text{t}}\text{bpx})\text{H}(\text{solv})]^+$ , **3b**, reacts completely with CO because the pressure of ethene is not sufficient to form  $[\text{Pt}(\text{d}^{\text{t}}\text{bpx})(\text{CH}_2\text{CH}_3)]^+$ , **6b**, or to return inside the catalytic cycle.

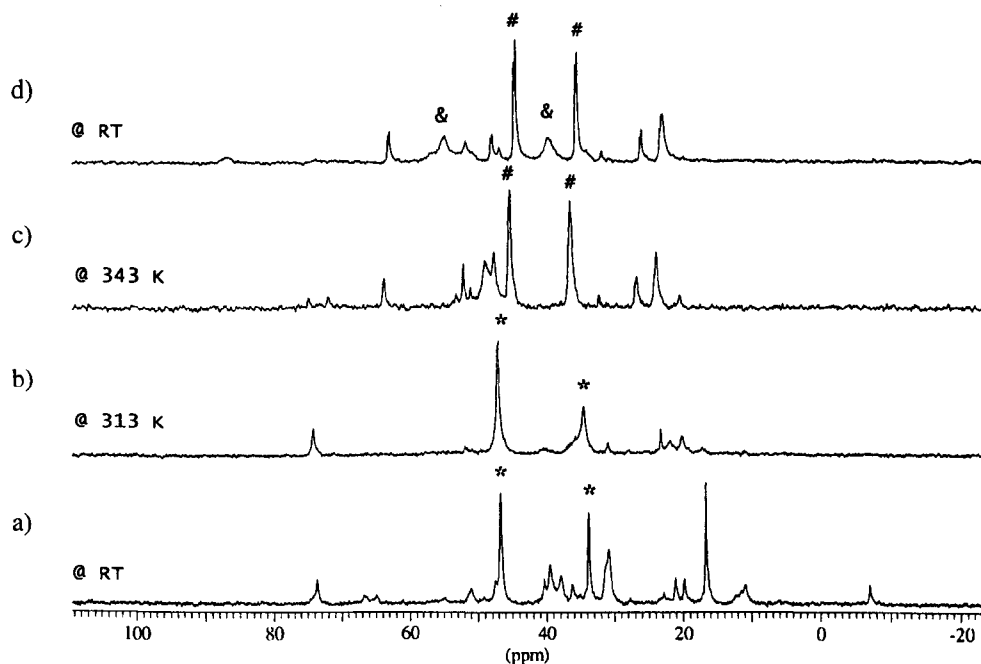
### 6.3.5 Reactivity under 10 bar of gas mixture $\text{CO}/\text{C}_2\text{H}_4$ (1/9)

The same procedure has been repeated as in the previous experiment (see Section 6.3.4), using 10 bar of  $\text{CO}:\text{C}_2\text{H}_4$  with a ratio of 1/9. The initial  $^{31}\text{P}\{^1\text{H}\}$  NMR spectrum at 293 K shows the presence of  $[\text{Pt}(\text{d}^{\text{t}}\text{bpx})(\text{H}_2\text{O})_2]^{2+}$ , **4b**, and  $[\text{Pt}(\text{d}^{\text{t}}\text{bpx})\text{H}(\text{solv})]^+$ , **3b**, and, using this gas mixture, there is no evidence for the formation of the platinum carbonyl hydride complex **8b** at 293 K. On increasing the temperature, the bisquo complex **4b** disappears and only at 345 K is the platinum carbonyl hydride complex **8b** formed, together with some impurities and metal formation. When the solution was cooled to 293 K, the  $^{31}\text{P}\{^1\text{H}\}$  NMR spectrum provides evidence for the presence of  $[\text{Pt}(\text{d}^{\text{t}}\text{bpx})\text{H}(\text{CO})]^+$ , **8b**, and the platinum ethyl complex **6b** (see Figure 6.11). This behaviour confirms the hypothesis that a big

pressure of ethene is necessary to form the ethyl complex and to carry on the catalytic cycle.

**Figure 6.11**

*VT  $^{31}\text{P}\{^1\text{H}\}$  NMR spectra of  $[\text{Pt}(\text{d}^4\text{bpx})(\text{dba})]$ , **1**, +  $\text{CH}_3\text{SO}_3\text{H}$  +  $\text{BQ}$  +  $\text{H}_2\text{O}$  in  $\text{MeOH}$  under 10 bar of  $\text{CO}/\text{C}_2\text{H}_4$  (1/9)*



#### 6.4. $\text{CH}_3\text{SO}_3\text{H}$ -system without $\text{H}_2\text{O}$

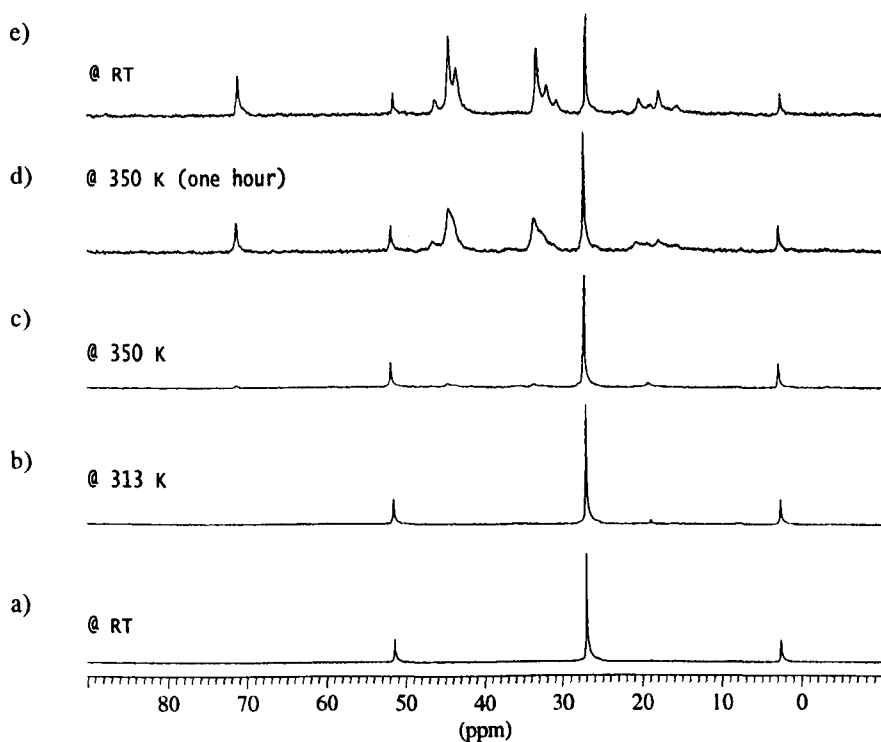
The behaviour of  $[\text{Pt}(\text{d}^4\text{bpx})(\eta^2\text{-CH}_3\text{SO}_3)]^+$ , **5b**, was studied at high temperature in  $\text{MeOH}$  without adding water, under  $\text{N}_2$ ,  $\text{C}_2\text{H}_4$  and  $\text{CO}$  pressure. It has been observed previously that it was necessary to add water to the solution of **5b** to observe the formation of  $[\text{Pt}(\text{d}^4\text{bpx})\text{H}(\text{solv})][\text{CH}_3\text{SO}_3]$ , **3b**, (see Section 3.2.3). As in the previous section, the experiments described below were carried out sequentially.

### 6.4.1 Stability of $[\text{Pt}(\text{d}^4\text{bpx})(\eta^2\text{-CH}_3\text{SO}_3)]^+$ , **5b**, under $\text{N}_2$ pressure

The  $^3\text{P}\{^1\text{H}\}$  NMR spectrum at 293 K shows the formation of  $[\text{Pt}(\text{d}^4\text{bpx})(\eta^2\text{-CH}_3\text{SO}_3)]^+$ , **5b**, after the reaction of  $[\text{Pt}(\text{d}^4\text{bpx})(\text{dba})]$ , **1**, with  $\text{CH}_3\text{SO}_3\text{H}$  and BQ at room temperature in MeOH in the absence of water under 10 bar of  $\text{N}_2$  (see Figure 6.12a).

**Figure 6.12**

*VT  $^3\text{P}\{^1\text{H}\}$  NMR spectra of  $[\text{Pt}(\text{d}^4\text{bpx})(\eta^2\text{-CH}_3\text{SO}_3)]^+$ , **4b**, and  $[\text{Pt}(\text{d}^4\text{bpx})\text{H}(\text{solv})]^+$ , **3b**, in MeOH under 10 bar of  $\text{N}_2$*



On increasing the temperature to 350 K, the resonances due to  $[\text{Pt}(\text{d}^4\text{bpx})(\eta^2\text{-CH}_3\text{SO}_3)]^+$ , **5b**, remain unchanged, but slowly (over 1 h)  $[\text{Pt}(\text{d}^4\text{bpx})\text{H}(\text{MeOH})]^+$ , **3b**,

is formed (see Figure 6.12d). The resonances due to the platinum hydride complex **3b** are very broad at high temperature. On cooling to room temperature, each of the two hydride resonances are resolved into two different resonances, probably because of the presence of different solvents (H<sub>2</sub>O/MeOH) in [Pt(d<sup>4</sup>bpx)H(solv)]<sup>+</sup>, **3b**, (see Figure 6.12e). The presence of adventitious water arises from the addition of CH<sub>3</sub>SO<sub>3</sub>H, which is difficult to obtain in the anhydrous form. At the end of the experiment, at room temperature, [Pt(d<sup>4</sup>bpx)(η<sup>2</sup>-CH<sub>3</sub>SO<sub>3</sub>)]<sup>+</sup>, **5b**, is still present, no precipitation is observed and the colour of the solution is red.

#### 6.4.2 Reactivity under 10 bar of C<sub>2</sub>H<sub>4</sub>

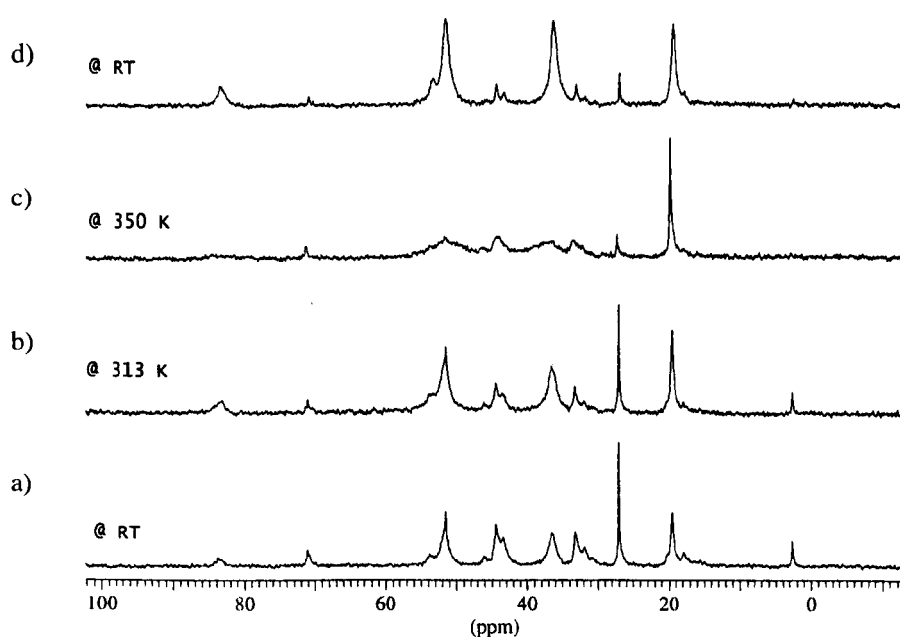
The three compounds [Pt(d<sup>4</sup>bpx)(η<sup>2</sup>-CH<sub>3</sub>SO<sub>3</sub>)]<sup>+</sup>, **5b**, [Pt(d<sup>4</sup>bpx)H(solv)]<sup>+</sup>, **3b**, (solv = H<sub>2</sub>O, MeOH) formed during the first part of the experiment (see Section 6.4.1) were put under 10 bar of C<sub>2</sub>H<sub>4</sub>. Under this ethene pressure at 293 K [Pt(d<sup>4</sup>bpx)(η<sup>2</sup>-CH<sub>3</sub>SO<sub>3</sub>)]<sup>+</sup>, **5b**, [Pt(d<sup>4</sup>bpx)H(solv)]<sup>+</sup>, **3b**, are observed and the conversion to  $\overline{[Pt(d^4bpx)(CH_2CH_3)]^+}$ , **6b**, is not complete (see Figure 6.13a). On increasing the temperature to 313 K the platinum hydride complex **3b** further reacts to give the platinum ethyl complex **6b** but at this temperature the resonances due to the ethyl complex broaden (see Figure 6.13b). When the sample is cooled to room temperature, the resonances due to [Pt(d<sup>4</sup>bpx)(η<sup>2</sup>-CH<sub>3</sub>SO<sub>3</sub>)]<sup>+</sup>, **5b**, and [Pt(d<sup>4</sup>bpx)H(solv)]<sup>+</sup>, **3b**, almost disappear and the platinum ethyl complex **6a** is the principal compound present in solution (see Figure 6.13d).

Actually, the same behaviour has been observed working with CH<sub>3</sub>SO<sub>3</sub>H/H<sub>2</sub>O in MeOH (see Section 6.3). Also, in this case, the platinum hydride complex **3b** is

present at room temperature under 10 bar of  $C_2H_4$  and does not disappear on increasing the temperature to 350 K. However, in the absence of water this system seems more stable. No metal precipitation is observed and at this stage of the experiment the colour of the solution is still red.

**Figure 6.13**

*VT  $^{31}P\{^1H\}$  NMR spectra of  $[Pt(d^4bpx)(CH_2CH_3)]^+$ , **6b**,  $[Pt(d^4bpx)(\eta^2-CH_3SO_3)]^+$ , **4b**, and  $[Pt(d^4bpx)H(solvent)]^+$ , **3b**, in MeOH under 10 bar of  $C_2H_4$*



#### 6.4.3 Reactivity under 7 bar of $^{13}CO$ and 10 bar of $C_2H_4$

Depressurisation of the solution followed by pressurisation with  $^{13}CO$  (7 bar) results in the immediate formation of  $[Pt(d^4bpx)H(^{13}CO)]^+$ , **8b**. In the  $^{31}P\{^1H\}$  NMR spectrum at 293 K, two weak resonances due to the platinum ethyl complex **6b** are

still present. On increasing the temperature they disappear and the platinum carbonyl hydride complex **8b** is the only species present (as in Figure 6.2). In the  $^{13}\text{C}\{^1\text{H}\}$  NMR spectrum at 293 K a singlet at 176 ppm confirms the immediate formation of MeP, but as found for the analogous reaction using  $\text{MeSO}_3\text{H}/\text{H}_2\text{O}$ , its intensity does not increase on increasing the temperature (as in Figure 6.18).

As in the  $\text{CH}_3\text{SO}_3\text{H}$ -system with addition of water, the resonance due to free  $^{13}\text{CO}$  is not observed at 293 K. It has been necessary to increase the temperature to 350 K to observe this resonance at about 180 ppm. In the  $\text{CH}_3\text{SO}_3\text{H}$ -system the diffusion of  $^{13}\text{CO}$  into the solution is very slow and it does not depend on addition of water. At this point, on depressurising the above solution and repressurising with  $\text{C}_2\text{H}_4$ , the  $^{31}\text{P}\{^1\text{H}\}$  NMR spectra does not show the reformation of the platinum ethyl complex at high temperature and the only complex present is  $[\text{Pt}(\text{d}^i\text{bpx})\text{H}(^{13}\text{CO})]^+$ , **8b**. The  $^{13}\text{C}\{^1\text{H}\}$  NMR spectra of **8b** at different temperatures under 10 bar of  $\text{C}_2\text{H}_4$  do not show any changes even when the sample is kept at 350 K for two hours. This underlines the stability of the platinum complexes and it should be compared with the non observation/instability of the analogous palladium complexes.

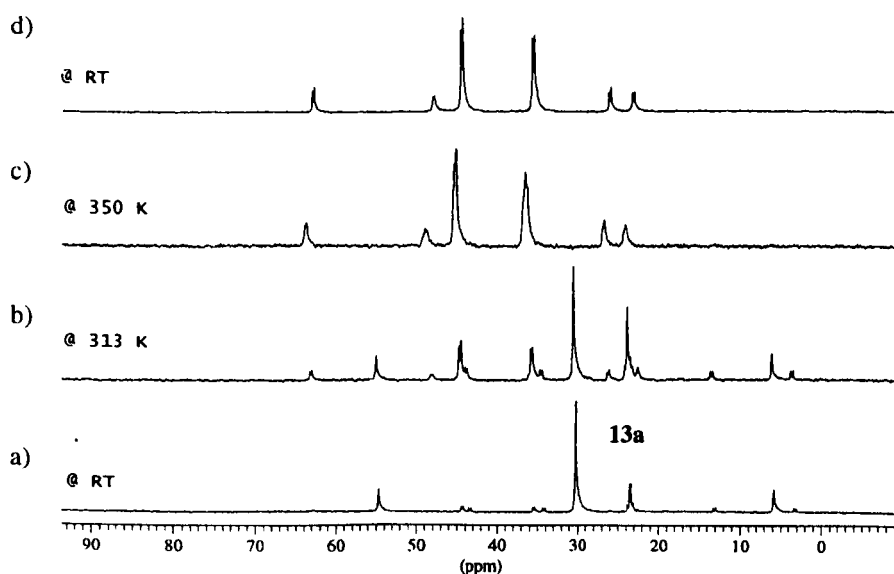
#### 6.4.4 Reactivity under 10 bar of gas mixture $\text{CO}/\text{C}_2\text{H}_4$ (1/1)

In this experiment, the reaction of  $[\text{Pt}(\text{d}^i\text{bpx})(\text{dba})]$ , **1**, with BQ and  $\text{CH}_3\text{SO}_3\text{H}$  in MeOH has been carried out in the sapphire tube under 10 bar of  $\text{CO}:\text{C}_2\text{H}_4$  (1:1). The  $^{31}\text{P}\{^1\text{H}\}$  NMR spectrum at 293 K shows the formation of  $[\text{Pt}(\text{d}^i\text{bpx})(\eta^2\text{-CH}_3\text{SO}_3)]^+$ , **5b**, and  $[\text{Pt}(\text{d}^i\text{bpx})\text{H}(\text{CO})]^+$ , **8b**, and there is evidence for the formation of a new compound **13b** (see Figure 6.14a). The new compound **13b** contains two

inequivalent phosphorus atoms and shows a second order NMR spectrum with  $\delta P$  ca 23.4 ppm. Of particular interest are the two very different coupling constants ( $^1J(\text{Pt-P}_1)=1714$  Hz and  $^1J(\text{Pt-P}_2)=3254$  Hz), despite the values of the two phosphorus chemical shifts being very similar.

**Figure 6.14**

*VT  $^{31}\text{P}\{^1\text{H}\}$  NMR spectra of  $[\text{Pt}(\text{d}^t\text{bpx})(\text{dba})]$ , **1**, +  $\text{CH}_3\text{SO}_3\text{H}$  +  $\text{BQ}$  in MeOH under 10 bar of  $\text{CO}/\text{C}_2\text{H}_4$  (1/1)*



The exact nature of this new complex **13b** is not very clear. First, it will be necessary to understand if its formation is due to the reaction of  $[\text{Pt}(\text{d}^t\text{bpx})(\eta^2\text{-CH}_3\text{SO}_3)]^+$  with CO or  $\text{C}_2\text{H}_4$ . The reaction will be repeated pressurising separately with CO and  $\text{C}_2\text{H}_4$  gas (see Section 6.4.5). On increasing the temperature the intensities of the resonances due to the platinum carbonyl hydride **8b** complex increase slightly and the new compound **13b** is still present. At 350 K,  $[\text{Pt}(\text{d}^t\text{bpx})(\eta^2\text{-$

$\text{CH}_3\text{SO}_3\text{)]}^+$ , **5b**, and the new compound **13b** disappear and  $[\text{Pt}(\text{d}^1\text{bpx})\text{H}(\text{CO})]^+$ , **8b**, is the only species present (see Figure 6.14c). At this temperature, the singlet at 46 ppm due to the platinum ethyl complex **6b** never appears. In fact, on cooling to room temperature, no new species appear and only the two doublets due to  $[\text{Pt}(\text{d}^1\text{bpx})\text{H}(\text{CO})]^+$ , **8b**, are observed (see Figure 6.14d). It is interesting to note, that even in this experiment using  $\text{CO}:\text{C}_2\text{H}_4$  (1:1),  $[\text{Pt}(\text{d}^1\text{bpx})(\text{CH}_2\text{CH}_3)]^+$ , **6b**, is not reformed, as found for the same reaction in the presence of water (see Section 6.3).

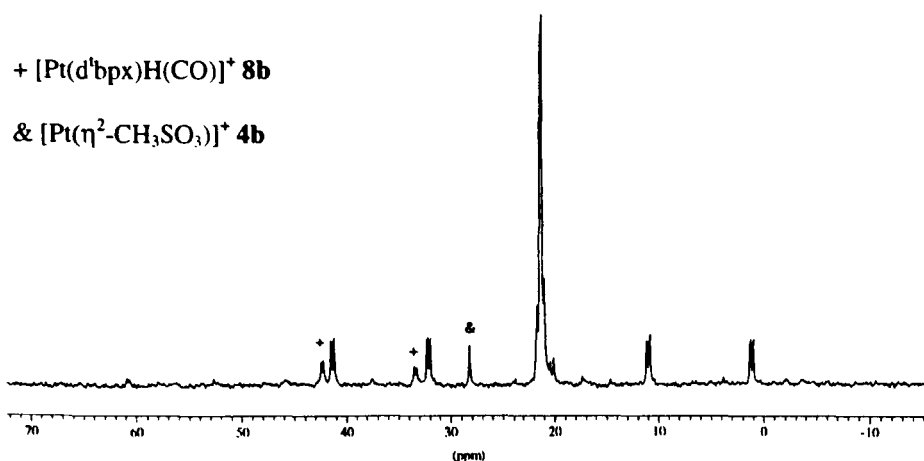
#### 6.4.5 Reaction of $[\text{Pt}(\text{d}^1\text{bpx})(\eta^2\text{-CH}_3\text{SO}_3)]^+$ **5b** with CO, formation of the complex **13b**

In the previous section (Section 6.4.4), the behaviour of  $[\text{Pt}(\text{d}^1\text{bpx})(\eta^2\text{-CH}_3\text{SO}_3)]^+$ , **5b**, has been studied in MeOH without adding water, at high temperature, under  $\text{C}_2\text{H}_4$  and CO pressure. As reported, there is evidence for the formation of a new compound **13b** when  $[\text{Pt}(\text{d}^1\text{bpx})(\eta^2\text{-CH}_3\text{SO}_3)]^+$ , **5b**, is put under 10 bar of  $\text{CO}:\text{C}_2\text{H}_4$  (1:1). The new complex contains two inequivalent phosphorus atoms and shows a second order NMR spectrum, where the two coupled and inequivalent phosphorus atoms have similar chemical shifts, with very different platinum-phosphorus coupling constants (see Section 6.4.4). The first step is to understand whether the formation of this new complex **13a** is due to the reaction of  $[\text{Pt}(\text{d}^1\text{bpx})(\eta^2\text{-CH}_3\text{SO}_3)]^+$ , **5b**, with CO or  $\text{C}_2\text{H}_4$ . When, **5b** is first formed, then pressurized with 4 bar of CO, the new compound is formed immediately (see Figure 6.15). It is not necessary to repeat the experiment by pressurizing the sapphire tube with ethylene because it is evident that the new complex is formed as a result of the

reaction of CO with  $[\text{Pt}(\text{d}^1\text{bpx})(\eta^2\text{-CH}_3\text{SO}_3)]^+$ , **5b**. The  $^{31}\text{P}$  NMR spectrum does not show any additional coupling showing that there is no Pt-H bond in the new complex.

**Figure 6.15**

$^{31}\text{P}\{^1\text{H}\}$  NMR spectra of complex **13b** in MeOH under 4 bar of CO



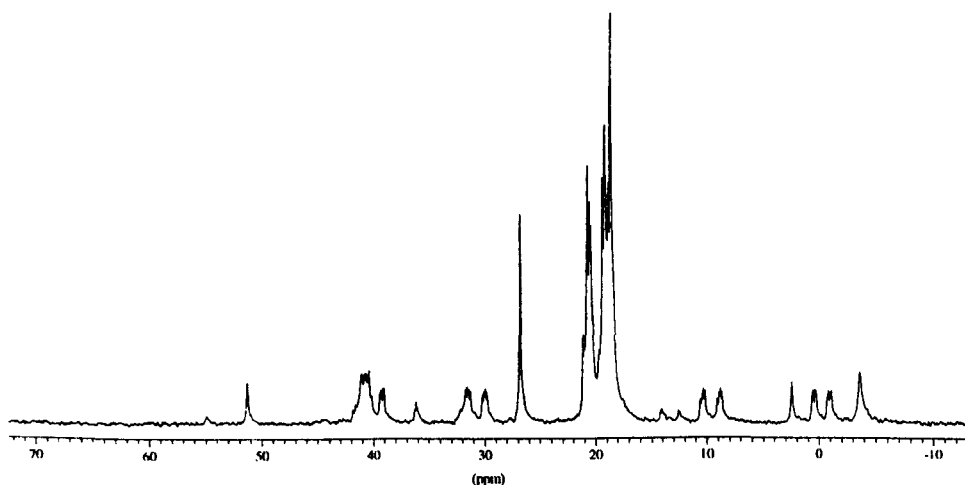
The experiment has been repeated using different pressure of CO. It seems that 4 bar is the best condition for the formation of the compound **13b**. When one bar of pressure is used or when the gas is bubbled for 20 minutes no reaction is observed. When the pressure is more than 4 bar,  $[\text{Pt}(\text{d}^1\text{bpx})\text{H}(\text{CO})]^+$ , **8b**, is the principal compound formed.

In order to understand the nature of the product formed, the reaction has been repeated by pressurizing the sapphire tube with 4 bar of  $^{13}\text{CO}$ . In the  $^{31}\text{P}\{^1\text{H}\}$  NMR spectrum the two resonances due to the two different phosphorus atoms change significantly (see Figure 6.16). The second order effect of the spectrum makes difficult the interpretation of the spectrum because none of the line separations

correspond to a coupling constant. Whereas, the four satellites clearly appear as a doublet of two doublets. This suggests that the two phosphorus atoms are coupled with two inequivalent carbon atoms (see Figure 6.16).

**Figure 6.16**

*$^{31}\text{P}\{^1\text{H}\}$  NMR spectrum of complex 13b in MeOH under 4 bar of  $^{13}\text{CO}$*



In the  $^{13}\text{C}\{^1\text{H}\}$  NMR spectrum, the interpretation is difficult too. The two carbon resonances give rise to different resonances but it is not possible to derive any meaningful coupling constants from the main resonances. As in the  $^{31}\text{P}\{^1\text{H}\}$  NMR spectrum, the four satellites of platinum are all doublets of two doublets and they confirm that each carbon is coupled with two inequivalent phosphorus atoms (see Figure 6.17).

Because of the complexity of the  $^{31}\text{P}\{^1\text{H}\}$  and  $^{13}\text{C}\{^1\text{H}\}$  NMR spectra, it is necessary to derive some data from an iteration done by the computer program gNMR. The simulation of  $^{31}\text{P}\{^1\text{H}\}$  NMR spectrum confirms the complexity of the

real spectrum due to coupling with two inequivalent carbon atoms in a second order spectrum (see Figure 6.18). From the simulation of the  $^{13}\text{C}\{^1\text{H}\}$  NMR spectrum it is possible to derive the two chemical shifts of the two carbon atoms and the coupling of each carbon atom with platinum (see Figure 6.19) (see Table 6.1).

**Figure 6.17**

$^{13}\text{C}\{^1\text{H}\}$  NMR spectrum of complex **13b** in MeOH under 4 bar of  $^{13}\text{CO}$

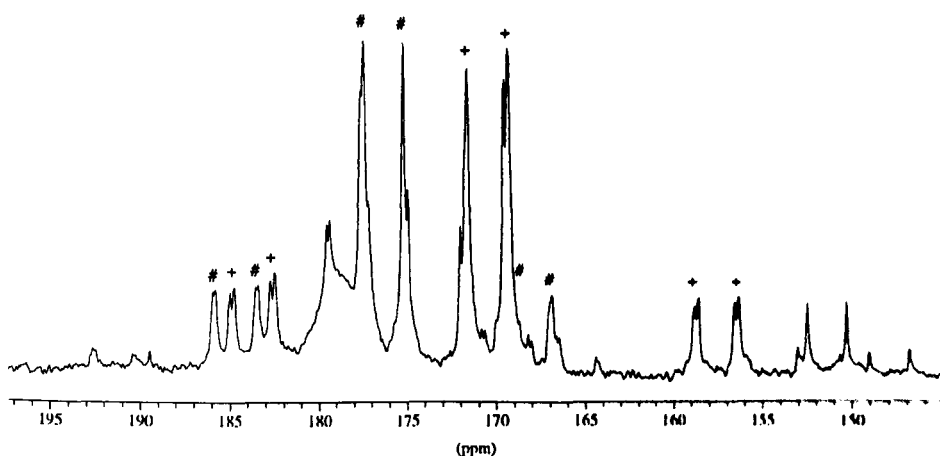


**Table 5.5**

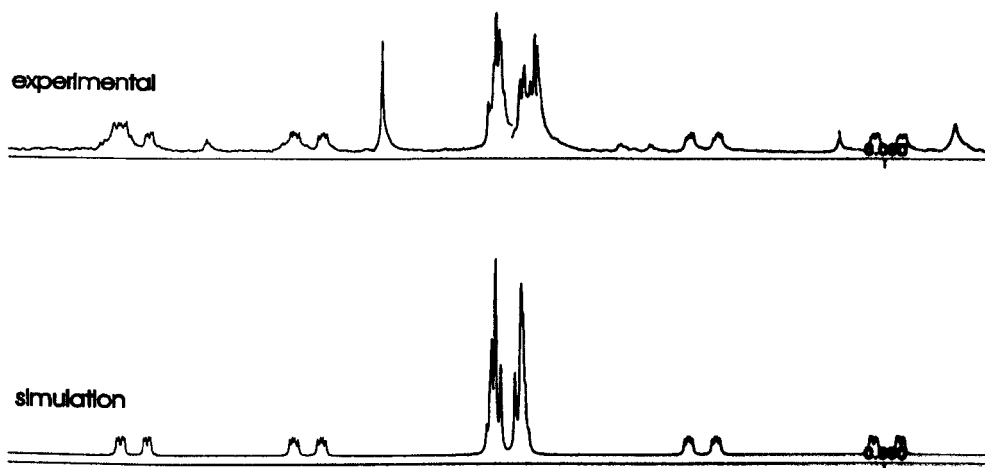
NMR data for the complex, **13a**, in MeOH at 293 K under 4 bar of  $^{13}\text{CO}$

	$\delta$	$J(\text{P}_1^-)$	$J(\text{P}_2^-)$	$J(\text{C}_1^-)$	$J(\text{Pt}^-)$
<b>P<sub>1</sub></b>	<i>20.3 ppm</i>				1714 Hz
<b>P<sub>2</sub></b>	<i>19.9 ppm</i>	22 Hz			3254 Hz
<b>C<sub>1</sub></b>	<i>176.5 ppm</i>	120 Hz	9 Hz		834 Hz
<b>C<sub>2</sub></b>	<i>170.8 ppm</i>	12 Hz	114 Hz	4 Hz	1316 Hz

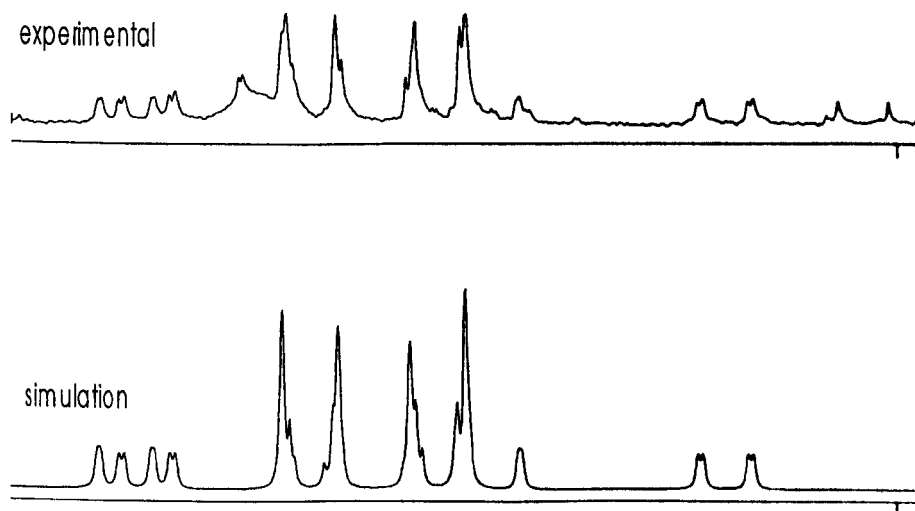
The numbers in *italics* has been adjusted by the computer iteration.

**Figure 6.18**

*Iteration of the  $^{31}\text{P}\{^1\text{H}\}$  NMR spectrum of complex 13b*

**Figure 6.19**

*Iteration of the  $^{13}\text{C}\{^1\text{H}\}$  NMR spectrum of complex 13b*



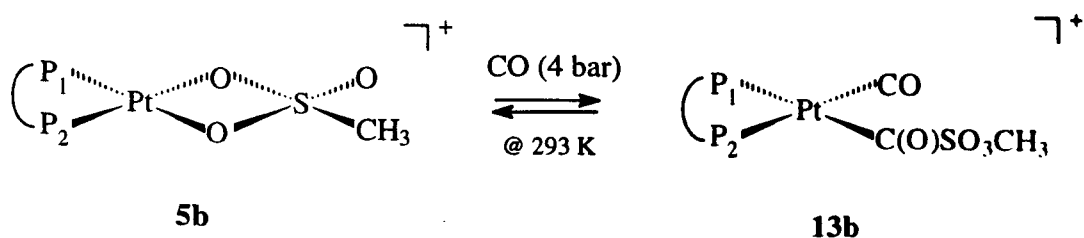
In order to better understand the nature of this new complex,  $[\text{Pt}(\text{d}^1\text{bpx})(\eta^2\text{-CH}_3\text{SO}_3)]^+$ , **5b**, has been formed in THF and acetone and pressurized with 4 bar of CO. First, **5b** is formed in THF and then pressurized with 4 bar of CO. No reaction is observed. At this point, the CO gas is bubbled through the solution for 20 minutes and the appearance of two very weak doublets indicates the formation of  $[\text{Pt}(\text{d}^1\text{bpx})\text{H}(\text{CO})]^+$ , **8b**, but the new complex **13b** is not formed.

The same solution of  $[\text{Pt}(\text{d}^1\text{bpx})(\eta^2\text{-CH}_3\text{SO}_3)]^+$ , **5b**, is dried in vacuum and dissolved in acetone. Also in this case, the new complex is not formed, whether the sample is pressurized with 4 bar of CO, or whether CO is bubbled for 20 minutes. It is necessary to dry the solution in vacuum, dissolve the precipitate in MeOH and pressurize with 4 bar of CO to observe the formation of the new complex **13b**.

It is difficult to understand what is formed when the new complex disappears. Usually, the resonances due to **8b** and **5b** are observed when the complex **13b** is formed and they both increase when the new dicarbonyl complex **13b** disappears. The hypothesis is that  $[\text{Pt}(\text{d}^1\text{bpx})(\eta^2\text{-CH}_3\text{SO}_3)]^+$ , **5b**, under 4 bar of CO in MeOH forms a square planar complex where the CO is coordinated to platinum and one of them inserts between the platinum and the oxygen of the  $\text{CH}_3\text{SO}_3$ -ligand (see Scheme 6.1).

### Scheme 6.1

#### *Proposed structure for the complex 13b*



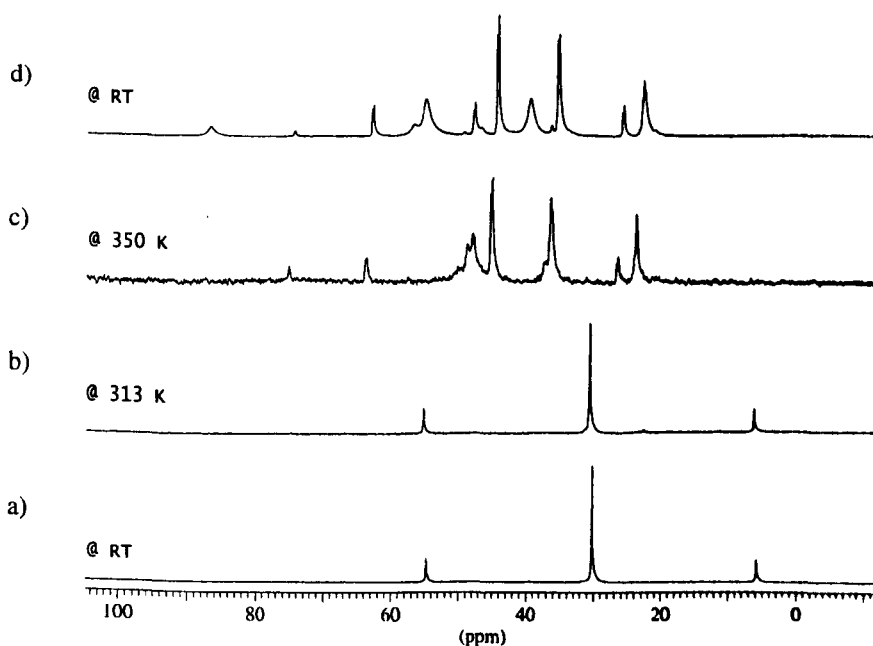
The structure proposed for the complex **13b** is in accordance with NMR data but there are still some doubts about its exact formulation.

#### 6.4.6 Reactivity under 10 bar of gas mixture CO/C<sub>2</sub>H<sub>4</sub> (1/9)

In this experiment, the reaction of [Pt(d<sup>4</sup>bpx)(dba)], **1**, with BQ and MeSO<sub>3</sub>H in MeOH has been carried out in the sapphire tube followed by the addition of 10 bar of CO:C<sub>2</sub>H<sub>4</sub> (1:9). In the <sup>31</sup>P{<sup>1</sup>H} NMR spectrum at 293 K and 313 K [Pt(d<sup>4</sup>bpx)(η<sup>2</sup>-CH<sub>3</sub>SO<sub>3</sub>)]<sup>+</sup>, **5b**, is the only complex present (see Figure 6.20a/b).

**Figure 6.20**

*VT <sup>31</sup>P{<sup>1</sup>H} NMR spectra of [Pt(d<sup>4</sup>bpx)(dba)], **1**, + CH<sub>3</sub>SO<sub>3</sub>H + BQ in MeOH under 10 bar of CO/C<sub>2</sub>H<sub>4</sub> (1/9)*



At 350 K, the system starts to change, with the appearance of new resonances and the resonance due to  $[\text{Pt}(\text{d}^t\text{bpx})(\eta^2\text{-CH}_3\text{SO}_3)]^+$ , **5b**, has disappeared (see Figure 6.20c). When the sample is cooled to room temperature, the  $^{31}\text{P}\{^1\text{H}\}$  NMR spectrum shows the presence of  $[\text{Pt}(\text{d}^t\text{bpx})(\text{CH}_2\text{CH}_3)]^+$ , **6b**, and  $[\text{Pt}(\text{d}^t\text{bpx})\text{H}(\text{CO})]^+$ , **8b**, (see Figure 6.20d). This behaviour confirms that it is necessary to have higher ethylene pressure to reform the platinum ethyl complex in order to carry on the catalytic cycle. This same behaviour has been observed during the reaction of  $[\text{Pt}(\text{d}^t\text{bpx})(\text{dba})]$ , **1**, with BQ and  $\text{CH}_3\text{SO}_3\text{H}$  in the presence of water.

## 6.5. Catalytic experiments carried out in autoclave at Ineos-Acrylics

Four catalytic tests have been carried out in a conventional autoclave, following the experimental conditions described above in sapphire tube.

### 6.5.1 $\text{CH}_3\text{SO}_3\text{H}$ , $T = 253\text{ K}$ , $P = 10\text{ bar}$ of $\text{C}_2\text{H}_4:\text{CO}$ (9:1) gas mixture

$[\text{Pt}(\text{d}^t\text{bpx})(\text{dba})]$ , **1**, and BQ were mixed under a  $\text{N}_2$  atmosphere. MeOH was added followed by  $\text{CH}_3\text{SO}_3\text{H}$ . The solution becomes red immediately after the addition of the acid but it returns to a pale yellow colour after a few seconds. Usually, in a 10 ml NMR tube the solution remains red after the addition of the acid. At this point the solution was put into the autoclave under vacuum and warmed to 60 °C. Ethene was added and the temperature increased by about 20 degrees. When the temperature was stabilized at 80 °C under *ca.* 8.1 bar of  $\text{C}_2\text{H}_4$ , the solution was left under these conditions for 30 minutes. It was not possible to check if the platinum

ethyl complex **6b** was formed because the colour of the solution was always pale yellow. After this time, the mixture  $C_2H_4:CO$  (1:1) was added to give the total pressure of *ca.* 10 bar with a gas mixture  $C_2H_4:CO = 9:1$ . After the addition of the final gas mixture, the reaction started and was left for three hours. During this time no gas absorption was observed. At the end of the experiment, the final solution was still pale yellow, indicating the presence of the catalyst in solution and no decomposition was observed. Immediately after the sample was cooled, a GC was run to understand if any MeP was formed. Considering that the retention time of MeP is 6.546 minutes, the amount of MeP formed was 0.37%.

The solution was dried in vacuum and the distilled liquid was collected for further analysis. The precipitate was dissolved in 2 ml of MeOH and transferred in a 10 ml NMR tube for an NMR spectrum. The  $^{31}P\{^1H\}$  NMR spectrum shows different resonances. The principal resonance is due to a new presently unidentified complex (A) with equivalent phosphorus atoms,  $\delta = 21.7$  ppm,  $^1J(Pt-P) = 3621$  Hz. Surprisingly, the presence of  $[Pt(d^4bpx)H(MeOH)]^+$ , **3b**, is observed too.

### 6.5.2 $CF_3SO_3H$ , $T = 353$ K, $P = 10$ bar of $C_2H_4:CO$ (9:1) gas mixture

As in the previous experiment  $[Pt(d^4bpx)(dba)]$ , **1**, and BQ were mixed under  $N_2$  in MeOH. In this case  $CF_3SO_3H$  was added. The colour of the solution became red faster than in the previous experiment and returns to yellow colour more slowly. The same procedure was used to put the solution into the autoclave and to pressurize with *ca.* 10 bar of gas mixture  $C_2H_4:CO$  (9:1). This solution was left to react at 353 K under 10 bar of gas mixture for three hours. During this time, no gas absorption was

observed, as in the previous experiment. In this experiment the amount of MeP formed was 0.06% and the colour of the solution was more orange than yellow. Also in this case the solution was dried in vacuum and the precipitate was dissolved in 2 ml of MeOH. The  $^{31}\text{P}\{^1\text{H}\}$  NMR spectrum shows the same resonance with  $\delta = 21.7$  ppm and platinum phosphorus coupling constant of 3621 Hz due to the complex (A). There are also other resonances but it is difficult to make further assignments because they are very weak.

### 6.5.3 $\text{CF}_3\text{SO}_3\text{H}$ , $T = 393$ K, $P = 10$ bar of $\text{C}_2\text{H}_4:\text{CO}$ (9:1) gas mixture

$[\text{Pt}(\text{d}^t\text{bpx})(\text{dba})]$ , **1**, and BQ were mixed under  $\text{N}_2$  in MeOH.  $\text{CF}_3\text{SO}_3\text{H}$  was added and the solution was transferred into the autoclave under vacuum. The system was warmed to 80 °C and ethylene was added. The gas mixture  $\text{C}_2\text{H}_4:\text{CO}$  (1:1) was added after leaving the solution at 393 K for 30 minutes under ethylene pressure. The reaction was left to run for three hours at 393 K under 9.8 bar of gas mixture  $\text{C}_2\text{H}_4:\text{CO}$  (9:1). During this time no gas absorption was observed, as in the previous two experiments. The amount of MeP formed was 0.20% and the colour of the solution was more orange than yellow but more pale compared with the previous experiment. No particular decomposition was observed in the autoclave. Also in this case the solution was dried in vacuum and the precipitate was dissolved in 2 ml of MeOH. The  $^{31}\text{P}\{^1\text{H}\}$  NMR spectrum shows the presence of the complex A and  $[\text{Pt}(\text{d}^t\text{bpx})\text{H}(\text{CO})]^+$ , **8a**. There are also two doublets due to the presence of a complex with inequivalent phosphorus atoms ( $\delta\text{P}_1 = 29.7$  ppm,  $\delta\text{P}_2 = 43.9$  ppm) with  $^2J(\text{P}_1-\text{P}_2) = 13.3$  Hz and  $^1J(\text{P}_1-\text{Pt}) = 3996$  Hz and  $^1J(\text{P}_2-\text{Pt}) = 3751$  Hz. The distilled solution

was collected and one part was analysed by a Gas Mass Spec Analysis. This analysis confirmed that MeP was formed.

#### 6.5.4 $\text{CH}_3\text{SO}_3\text{H}$ , $T = 393 \text{ K}$ , $P = 10 \text{ bar}$ of $\text{C}_2\text{H}_4:\text{CO}$ (9:1) gas mixture

The same method was used as in the previous experiment. The only difference was the use of  $\text{CH}_3\text{SO}_3\text{H}$  instead of  $\text{CF}_3\text{SO}_3\text{H}$ . The colour of the solution after the reaction was yellow and no particular precipitate was observed. The  $^{31}\text{P}\{^1\text{H}\}$  NMR spectrum shows one resonance due to the complex A. The amount of MeP formed was 0.07%. It is possible to conclude that the amount of MeP formed is stoichiometric and not catalytic.

All the distilled solutions of the four experiments were collected and they were used for GC analysis. First, some samples of MeP with known concentration were run. A chart was plotted and the values of MeP/standard (standard: methyl benzoate) were plotted in  $x$  and in  $y$  the different concentrations were reported (see Table 6.2 and Figure 6.21). The concentration of MeP in the solutions from the experiments were calculated from the equation of the chart (see Table 6.3).

**Table 6.2**

area MeP	area standard	MeP/standard	Conc.
1562	33681	0.046	0.010
5839	65293	0.089	0.015
7087	55373	0.13	0.020

Figure 6.21

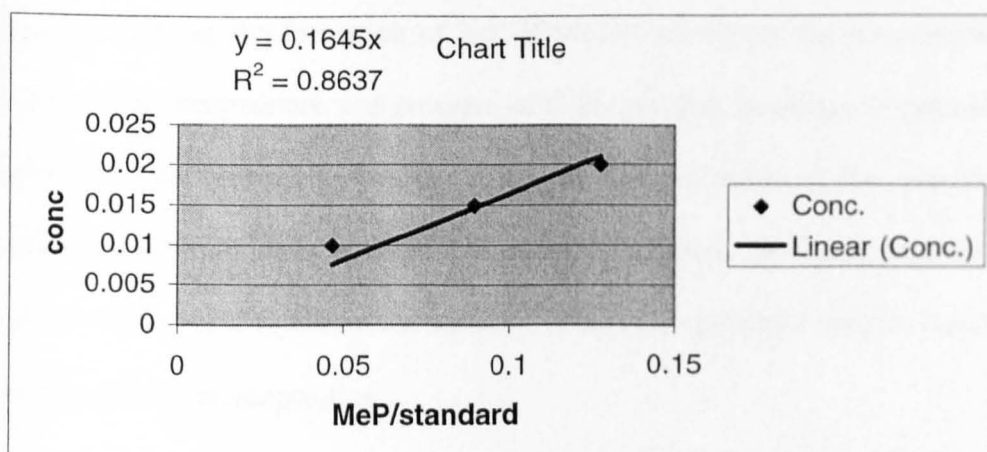


Table 6.3

	area MeP	area standard	MeP/standard	Conc
6.5.1	10145	80780	0.13	0.020
6.5.2	1944	93445	0.021	0.0034
6.5.3	3909	38776	0.10	0.017
6.5.4	1841	54282	0.034	0.0056

## 6.6. Conclusions

The experiments at high pressure and temperature underline the stability and the slow reactivity of the platinum catalyst. Under 10 bar of  $C_2H_4$ , the formation of the platinum ethyl complex **6a** is complete in MeOH and the resonances due to the platinum hydride **3a** complex are not observed. This means that it is necessary for a greater pressure than 1 bar of ethene to shift the equilibrium between the two compounds. After having added the carbon monoxide and having formed the

platinum carbonyl hydride complex **8a**, the amount of  $C_2H_4$  left in the tube is sufficient to observe the formation of EtCOOMe on increasing the temperature to 313 K. The high temperature and pressure of  $C_2H_4$  are also necessary to reform the ethyl complex **6a** from  $[Pt(d^4bpx)H(CO)]^+$ , **8a**, and to increase the amount of EtCOOMe in solution. It is evident that drastic conditions are important for the activity of this catalyst and how the stability of these compounds permits their use without significant decomposition.

In the  $CH_3SO_3H$ -system, under an atmosphere of ethene, the hydride complex **3b** is less reactive than in the  $CF_3SO_3H$ -system. The platinum ethyl complex **6b** is formed but the platinum hydride complex **3b** is still present even when the solution is under a pressure of ethene at high temperature. The  $^{13}C\{^1H\}$  NMR spectrum shows an intense resonance at about 122 ppm, due to free  $C_2H_4$  but under these conditions (high temperature and pressure) it does not react with the hydride complex **3b** which appears to be very stable. When the solution of  $[Pt(d^4bpx)H(solvent)][CH_3SO_3]$ , **3b**/ $[Pt(d^4bpx)(C_2H_5)][CH_3SO_3]$ , **6b**, was put under under 7 bar of  $^{13}CO$ , the platinum carbonyl hydride complex **8b** is immediately formed and it is the only species present in solution. Despite the high pressure of carbon monoxide, there is no evidence of free  $^{13}CO$  in solution in the  $^{13}C\{^1H\}$  NMR spectrum, but nevertheless EtCOOMe is formed even at room temperature. On increasing the temperature to 313 K, it is possible to observe the singlet due to free  $^{13}CO$ . In this case, the behavior of the reaction with CO seems opposite to that found for  $C_2H_4$ . However, the reactivity of  $[Pt(d^4bpx)H(CO)][CH_3SO_3]$ , **8b**, with ethene is similar to that observed with  $[Pt(d^4bpx)H(CO)][CF_3SO_3]$ , **8a**. In both cases, it is possible to reform the platinum ethyl complex **6** using high temperature and high pressure.

In general, the  $\text{CH}_3\text{SO}_3\text{H}$ -system seems more reactive but less stable compared to the  $\text{CF}_3\text{SO}_3\text{H}$ -system. In the  $\text{CH}_3\text{SO}_3\text{H}$ -system in presence of water, most of the reactions at high temperature result in the formation of protonated diphosphine and metal deposition. The behavior of the complexes analyzed in the  $\text{CH}_3\text{SO}_3\text{H}$ -system without adding water is quite similar to that observed when water was added. The main differences are due to the stability of  $[\text{Pt}(\text{d}^1\text{bpx})(\eta^2\text{-CH}_3\text{SO}_3)]^+$ , **4b**, and its inertia to form  $[\text{Pt}(\text{d}^1\text{bpx})\text{H}(\text{solv})]^+$ , **3b**, and the fact that the absence of water does not promote any decomposition. In fact, at the end of the experiment no precipitation was observed.

The experiments done in an autoclave show how the platinum system is stable and not particularly suitable for the formation of MeP, in particular because of its high affinity for CO and the stability of the complexes formed.

# Chapter Seven

## 7. General conclusions

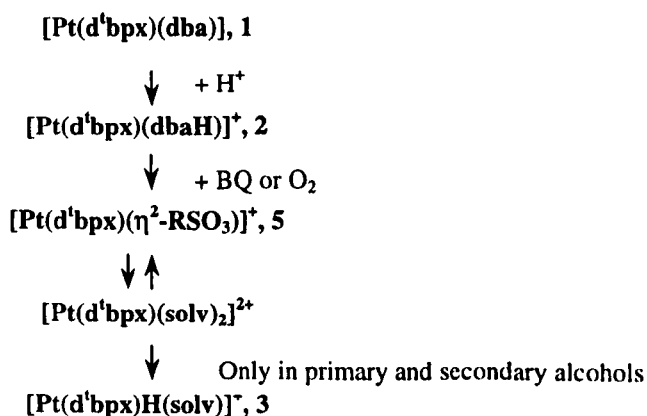
### 7.1. Platinum catalytic cycle for the methoxycarbonylation of ethene

Recently, Lucent International has announced a new process for the manufacture of methyl methacrylate *via* the palladium catalysed methoxycarbonylation of ethene to methylpropanoate (MEP).<sup>1</sup> The catalyst used is capable of converting ethene, CO and MeOH to methylpropanoate at a rate of 50,000 mol of product per mol of catalyst per hour with a selectivity of 99.98%.<sup>1,2</sup> It has been shown, *via* characterisation of all the intermediates, that this reaction follows a hydride catalytic cycle,<sup>3</sup> a result that has recently been confirmed by isotope scrambling experiments.<sup>4</sup>

What this thesis has demonstrated is that, in contrast to palladium, the catalytic performance of analogous platinum complexes is poor, typical rate 13 mol of product per mol of catalyst per hour (see Chapter 6). In order to understand if there is an intrinsic limitation associated with the 3<sup>rd</sup> row metal catalyst,<sup>5</sup> (unlike the situation with, for example, halide-promoted Rh and Ir catalysts for methanol carbonylation),<sup>6</sup> detailed mechanistic NMR investigation of the Pt system has been undertaken. Here the presence of <sup>195</sup>Pt ( $I = \frac{1}{2}$ , 33.7% abundance) has proved particularly definitive in characterising the catalytic intermediates *via* coupling between the metal and ligand nuclei. Elucidation of all the intermediates involved in the platinum cycle has revealed some unexpected differences between the chemistry of the Pd and Pt systems; particularly the ready reversibility of the alkyl migration step in the Pt system, which have allowed us to propose an explanation for the low activity of the platinum catalyst in this reaction.

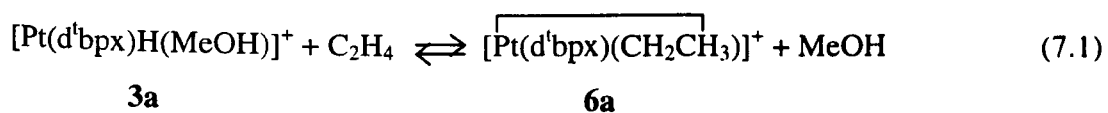
$[\text{Pt}(\text{d}^t\text{bpx})(\text{dba})]$ , **1**,  $\{\text{d}^t\text{bpx} = 1,2\text{-(CH}_2\text{P}^t\text{Bu}^t)_2\text{C}_6\text{H}_4\}$  (see Chapter 2) reacts in MeOH with  $\text{CF}_3\text{SO}_3\text{H}$  in the presence of  $\text{O}_2$  or BQ (benzoquinone) to give a new complex, characterised by  $^1\text{H}$  and  $^{31}\text{P}$  NMR spectroscopy as the metal hydride complex  $[\text{Pt}(\text{d}^t\text{bpx})\text{H}(\text{MeOH})][\text{CF}_3\text{SO}_3]$ , **3a**. Thus, the  $^{31}\text{P}\{^1\text{H}\}$  NMR spectrum of **3a** at 293 K, shows two main resonances each showing Pt satellites. The resonance at 34.0 ppm shows a further doublet splitting in the absence of  $^1\text{H}$  decoupling. The proton NMR spectrum of **3a** shows a doublet of doublets (with platinum satellites) at  $-7.3$  ppm [ $^2J(\text{P}_{\text{trans}}\text{-H}) = 176$  Hz,  $^2J(\text{P}_{\text{cis}}\text{-H}) = 18$  Hz,  $^1J(\text{Pt-H}) = 805$  Hz], values of  $\delta$  and  $J$  typical of a hydride ligand *trans* to phosphorus, in agreement with the proposed formulation of **3a**. As in the case of palladium,<sup>7</sup> the hydride is formed *via*  $[\text{Pt}(\text{d}^t\text{bpx})(\text{dbaH})][\text{CF}_3\text{SO}_3]$ , **2a**, (see Section 3.1). When  $[\text{Pt}(\text{d}^t\text{bpx})(\text{dba})]$  **1** reacts in MeOH with  $\text{CH}_3\text{SO}_3\text{H}$  in the presence of  $\text{O}_2$  or BQ (benzoquinone)  $[\text{Pt}(\text{d}^t\text{bpx})(\eta^2\text{-CH}_3\text{SO}_3)][\text{CH}_3\text{SO}_3]$ , **5b**, is formed and it is necessary to add  $\text{H}_2\text{O}$  to observe the formation of  $[\text{Pt}(\text{d}^t\text{bpx})\text{H}(\text{MeOH})][\text{CH}_3\text{SO}_3]$ , **3b**, (see Section 3.2). The formation of the platinum hydride complex **3** occurs by a multi step process like in the palladium system (see Scheme 7.1).<sup>7</sup>

### Scheme 7.1



The third step is determinant and it is the displacement of the coordinated  $\text{RSO}_3^-$  anion and formation of  $[\text{Pt}(\text{d}^1\text{bpx})(\text{solv})_2]^{2+}$ . This step is an equilibrium and its position depends on the nature of the R-group present on the anion and the solvent used. Polar solvents favour the formation of  $[\text{Pt}(\text{d}^1\text{bpx})(\text{solv})_2]^{2+}$ , which forms directly the platinum hydride complex **3**, through a redox process involving the solvent (see Scheme 3.1); whereas basic R-group shift the equilibrium towards the formation of  $[\text{Pt}(\text{d}^1\text{bpx})(\eta^2\text{-RSO}_3)]^+$ , **5**, which is the principal product.

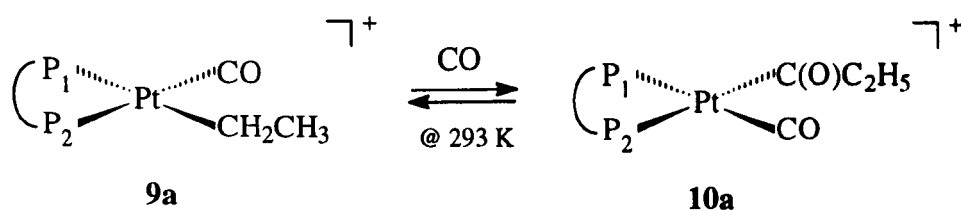
On bubbling ethene through a methanol solution of **3** for ca. 30 minutes at 193 K, quantitative conversion to  $[\text{Pt}(\overline{\text{d}^1\text{bpx}})(\text{CH}_2\text{CH}_3)][\text{CF}_3\text{SO}_3]$ , **6**, occurs. **6** has been characterised by comparison of its  $^{31}\text{P}\{^1\text{H}\}$  NMR data with those reported in literature.<sup>8</sup> As for the palladium analogue, the ethyl ligand in **6** forms a  $\beta$ -agostic interaction with the metal centre at 145 K in  $\text{CH}_2\text{Cl}_2$  (see Chapter 4). The reactivity of  $[\text{Pt}(\text{d}^1\text{bpx})\text{H}(\text{MeOH})]$ , **3**, with ethene is different compared with the analogue reaction in the palladium system. The equilibrium shown in Equation 7.1 is shifted in favour of the formation of **3** in the platinum system at room temperature, whereas during the reaction of  $[\text{Pd}(\text{d}^1\text{bpx})\text{H}(\text{MeOH})]^+$  with ethene, the formation of  $[\text{Pd}(\overline{\text{d}^1\text{bpx}})(\text{CH}_2\text{CH}_3)]^+$  is immediate under the same conditions.



Two intermediates can be observed in the reaction of **6** with  $^{13}\text{CO}$  by carrying out the reaction in  $\text{CH}_2\text{Cl}_2$  at 193 K, followed by warming to 293 K; these have been characterised as  $[\text{Pt}(\text{d}^1\text{bpx})(\text{C}_2\text{H}_5)(^{13}\text{CO})]^+$ , **9**, and  $[\text{Pt}(\text{d}^1\text{bpx})(^{13}\text{C}(\text{O})\text{Et})(^{13}\text{CO})]^+$ , **10**, by  $^{31}\text{P}\{^1\text{H}\}$  and  $^{13}\text{C}\{^1\text{H}\}$  NMR spectroscopy. **10** is only formed on warming the solution to room temperature in the presence of excess CO. Thus, at 193 K only the

resonances due to  $[\text{Pt}(\text{d}^t\text{bpx})(\text{C}_2\text{H}_5)(^{13}\text{CO})]^+$ , **9**, are seen in the  $^{13}\text{C}\{^1\text{H}\}$  NMR spectrum; these disappear on warming to 293 K to be replaced by two doublets of doublets together with associated platinum satellites at 173.2 ppm in the carbonyl and at 223.9 ppm in the acyl region. This transformation is *reversible*; cooling the solution of **10** to 193 K results in reformation of **9** (see Scheme 7.2).

Scheme 7.2



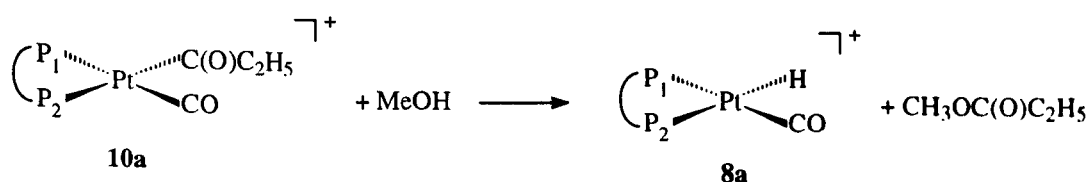
On prolonged standing of this solution at low temperature, the resonances of **9** decrease slightly in intensity and resonances due to the complex  $[\text{Pt}(\text{d}^t\text{bpx})\text{H}(\text{CO})][\text{CF}_3\text{SO}_3]$ , **8**, and ethene appear. The stability of **8** contrasts sharply with that of the palladium analogue which has a lifetime of only a few minutes at 223 K whereas solutions of **8** appear to be indefinitely stable at 293 K (see Chapter 5).

The formation of a stable carbonyl-ethyl complex **9** and the absence of alkyl migration at 193 K to give the acyl complex is in marked contrast with the reactivity pattern observed in the palladium system in which addition of CO to the ethyl complex results in immediate formation of a solvento-acyl complex **A** even at the lowest temperatures studied. A carbonyl ethyl complex must be involved, at least as a transition state in the palladium cycle, but has not been conclusively identified in the palladium system. The ready reversibility of the reaction  $\mathbf{9} \leftrightarrow \mathbf{10}$  is surprising

since the platinum ethyl-carbonyl complex only converts to the acyl complex on warming the solution to 293 K. This implies that the formation of **10** from **9** is either an endothermic process or is controlled by entropic factors. It seems unlikely that entropic factors could control this reaction since one equivalent of CO is consumed in the reaction sequence  $\mathbf{9} \rightarrow \mathbf{10}$  and, presumably, steric congestion around the metal centre will be greater for Pd in which the acyl complex is formed at 193 K. Therefore, it would appear that the position of the equilibrium is being controlled by an enthalpic preference of the platinum centre for an ethyl rather than an acyl ligand.

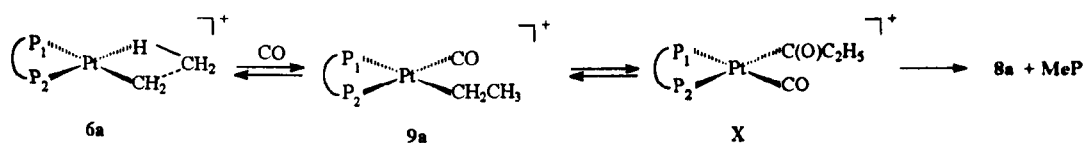
Reaction of the ethyl complex **6** with *one* equivalent of CO in MeOH at room temperature rapidly gives **8**. When this reaction is repeated in the presence of excess  $^{13}\text{CO}$ , a resonance due to MeP is observed in the  $^{13}\text{C}\{^1\text{H}\}$  NMR spectrum in addition to those of **8**. Addition of MeOH at 290 K to a sample of **3** which had been reacted first with  $^{13}\text{CH}_2=\text{CH}_2$ , then treated with excess  $^{13}\text{CO}$ , and subsequently evaporated to dryness (to remove excess carbon monoxide and ethylene), results in quantitative conversion (by  $^{31}\text{P}$  NMR) of the ethyl complex **6** to the carbonyl hydride **8**. In the  $^{13}\text{C}\{^1\text{H}\}$  NMR spectrum, resonances due to MeP and  $^{13}\text{CH}_2=\text{CH}_2$  are observed in addition to those of complex **8**. The quantitative formation of **8** implies that methanolysis probably occurs *via* the carbonyl-acyl complex **10** rather than *via* the solvento-acyl complex **A** as found in the Pd system (see Scheme 7.3).

Scheme 7.3

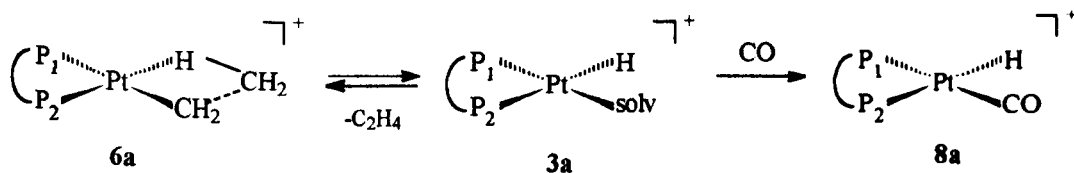


These reactions also demonstrate that, in the Pt system, only in the presence of excess CO is there significant forward reaction  $6 \rightarrow 9 \rightarrow 10 \rightarrow 8 + \text{MEP}$  (see Scheme 7.4), *ie* **8** is a thermodynamic sink and will form *via* the back reaction  $6 \rightarrow 3 \rightarrow 8$  preferentially to the forward reaction to MeP in the absence of excess CO (see Scheme 7.5).

Scheme 7.4



Scheme 7.5

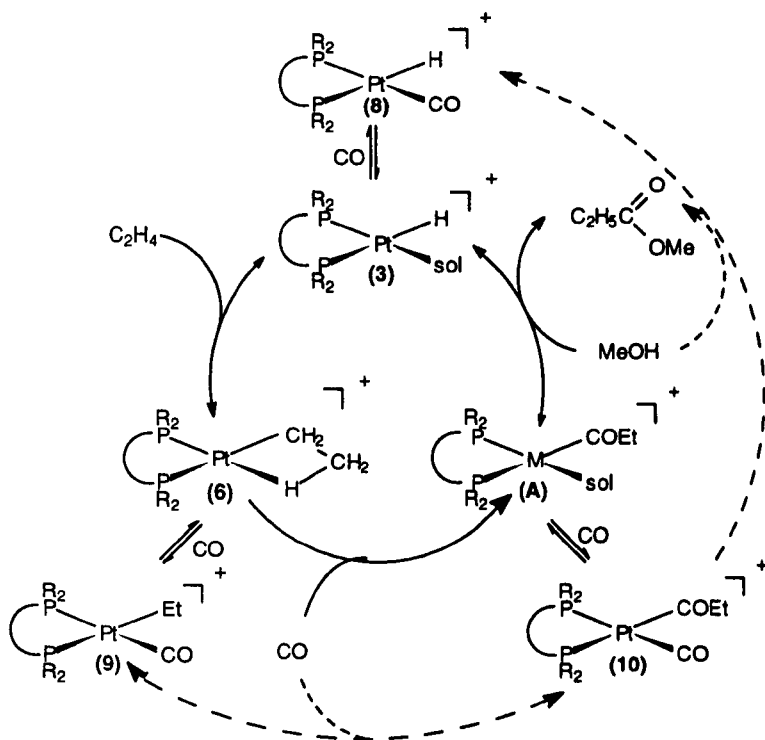


This contrasts with the chemistry of the analogous Pd-ethyl complex which gives MeP and  $[\text{Pd}(\text{d}^t\text{bpx})\text{H}(\text{MeOH})]^+$  on reaction with one equivalent of CO in MeOH and formation of MEP and protonated phosphine on reaction with excess CO.

The observed reactivity of the platinum and palladium complexes is summarized in Scheme 7.6 in terms of the proposed catalytic cycle for the methoxycarbonylation of ethene. The higher affinity of Pt for CO results in the resting states of all the intermediates switching from the solvento adducts in the palladium cycle to the analogous carbonyl complexes in the platinum cycle.

## Scheme 7.6

The Pd and Pt catalysed methoxycarbonylation of ethene,  $M = Pd$  (inner cycle dominates) or Pt (complexes in outer cycle dominate)



It is also noteworthy that in the platinum system the *reverse* reactions in the equilibria hydride ethyl acyl are readily accessible; thus we have shown that, in the absence of methanol, the carbonyl hydride **8** is formed from both **9** and **10** presumably by the back reaction, a feature not observed in the palladium system in which the momentum of the reaction appears to be in the forward direction. The carbonyl hydride complex **8** is much less reactive towards ethylene than the solvento hydride and this reaction is probably rate limiting in the Pt system although methanolysis of the carbonyl acyl complex is also slow.<sup>5</sup>

In summary, this thesis has shown that the platinum catalysed methoxycarbonylation of ethene follows an analogous pathway to the highly active palladium system. However, the formation of stable carbonyl complexes that are thermodynamic sinks for the reaction effectively removes Pt from the catalytic cycle. Coupled with easier reversibility of the product forming reactions observed in the platinum system would account for the observed low activity of platinum in the methoxycarbonylation of ethene.

## 7.2. References

- (1) W. Clegg; G. R. Eastham; M. R. J. Elsegood; R. P. Tooze; Wang, X. L.; Whiston, K. W. *Chem. Comm.* **1999**, 1877.
- (2) E. Drent and P.M.H. Budzelaar *Chem. Rev.*, **1996**, *96*, 663.
- (3) W. Clegg; G.R. Eastham; M.R.J. Elsegood; B.T. Heaton; J.A. Iggo; R.P. Tooze; R. Whyman; S. Zacchini *Organometallics*, **2002**, *21*, 1832.
- (4) G.R. Eastham; R.P. Tooze; M. Kilner; D.F. Foster; D.J. Cole-Hamilton *J. Chem. Soc., Dalton Trans.*, **2002**, 1613.
- (5) G.N. Il'inich; V.N. Zudin; A.V. Nosov; V.A. Rogov; V.A. Likholobov *J. Mol. Catal. A: Chemical*, **1995**, *101*, 221.
- (6) P.M. Maitlis; A. Haynes; G.J. Sunley; M.J. Howard *J. Chem. Soc., Dalton Trans.*, **1996**, 2187.
- (7) W. Clegg; G. R. Eastham; M. R. J. Elsegood; B.T. Heaton; J.A. Iggo; R. P. Tooze; R. Whyman; S. Zacchini *J. Chem. Soc., Dalton Trans.*, **2002**, 3300.
- (8) N. Carr; L. Mole; A. Guy Orpen; J. L. Spencer *J. Chem. Soc., Dalton Trans.*, **1992**, 2653.

# **Chapter Eight**

## 8. Experimental

### 8.1. General methods and procedures

This section summarises all the experimental procedures and syntheses of complexes described in this thesis. All the manipulation involving solutions or solids were performed under an atmosphere of nitrogen (or carbon monoxide or ethene where appropriate) using standard Schlenk line techniques. Most of the solvent were dried and distilled under nitrogen following standard literature methods; *i.e.* MeOH over Mg(OMe)<sub>2</sub>, THF over Na/benzophenone, CH<sub>2</sub>Cl<sub>2</sub> over CaH<sub>2</sub>, n-hexane over Na and acetone over B<sub>2</sub>O<sub>3</sub>. All the other solvents were degassed under *vacuum* and stored under nitrogen. Deuterated solvents were degassed under *vacuum* in a liquid nitrogen bath and stored over activated 4 Å molecular sieves under nitrogen for at least 24 hours prior to use. All the reaction were carried out in a 10 mm NMR tube, unless stated otherwise. Most of the compound have been characterised only in solution; thus, no yield nor elemental analysis is reported for them. The <sup>13</sup>CO, <sup>13</sup>CH<sub>2</sub>=CH<sub>2</sub> and <sup>13</sup>CH<sub>2</sub>=<sup>13</sup>CH<sub>2</sub> containing samples were prepared on using a high vacuum line with a mercury vapour pump.

All the reactions involving CO have been carried out in a well ventilated fume-hood. During the preparation of the samples for experiments under gas pressure, the NMR tubes have been always kept inside an appropriate metal or plastic protection. All the other experiments have been carried out following standard safety procedures.

All  $^{31}\text{P}\{^1\text{H}\}$ ,  $^{31}\text{P}$ ,  $^{13}\text{C}\{^1\text{H}\}$ ,  $^{13}\text{C}$ ,  $^1\text{H}$  and  $^{195}\text{Pt}\{^1\text{H}\}$  NMR measurements were performed on AMX200, AMX400 and WM250 instruments using commercial probes. The chemical shifts were referenced to external  $\text{H}_3\text{PO}_4$  (85% in  $\text{D}_2\text{O}$ ) for phosphorus, internal TMS for proton and carbon and external Pt-salt for platinum. Spectra of samples dissolved in non-deuterated solvents were referenced using an external deuterated solvent lock (*i.e.*  $\text{CD}_2\text{Cl}_2$  for measurements at room and low temperature).  $^1\text{H}$  NMR spectra of metal hydrides dissolved in non-deuterated solvents were recorded using the  $^1\text{H}/^{31}\text{P}$  correlations measured *via* zero and double quantum coherences,<sup>1</sup> calibrated on *trans*- $^2\text{J}(\text{P-H})$  measured in the  $^{31}\text{P}$  NMR spectra. High pressure NMR measurements were recorded using a home-built special 10 mm thick glass wall tube or a 10 mm sapphire tube.

X-ray structure of  $[\text{Pt}(\text{d}^t\text{bpx})(\text{H}_2\text{O})_2][\text{CF}_3\text{SO}_3]_2$  was determined on a STOE-IPDSimage plate diffractometer using graphite monochromated  $\text{MoK}_\alpha$  radiation ( $\lambda = 0.71073 \text{ \AA}$ ). Crystals were mounted in a glass fibre. Structures were solved by Direct Methods and structure refinements by full-matrix least-squares were based on all data using  $F^2$ .<sup>2</sup> All non-hydrogen atoms were refined anisotropically. Hydrogen positions were placed geometrically.

All the chemical products were purchased from Aldrich Chemical Co., except  $[\text{Pt}(\text{dba}_2)]$ ,  $[\text{Pt}(\text{cod})_2]$ ,<sup>3</sup>  $[\text{Pt}(\text{d}^t\text{bpx})(\eta^2\text{-C}_2\text{H}_4)]$ ,<sup>4</sup>  $[\text{Pt}(\text{d}^t\text{bpx})(\text{CH}_2\text{CH}_3)][\text{CF}_3\text{SO}_3]$ <sup>4</sup> and  $\text{d}^t\text{bpx}$ <sup>5</sup> were prepared by published methods.  $^{13}\text{CO}$  (99.8%) was purchased from Isotec Inc.,  $^{13}\text{CH}_2=\text{CH}_2$  and  $^{13}\text{CH}_2=^{13}\text{CH}_2$  from Aldrich Chemical Co.

## 8.2. Experimental for Chapter Two

### 8.2.1 Preparation of [Pt(d<sup>4</sup>bpx)(dba)], 1

The complex [Pt(d<sup>4</sup>bpx)(dba)], 1, was prepared by the reaction of Pt(dba)<sub>2</sub> with two equivalents of d<sup>4</sup>bpx ligand in THF. To a solution of d<sup>4</sup>bpx (2.90 g, 7.32 mmol) dissolved in THF (40 ml) in a two-necked round-bottomed flask equipped with a magnetic stirring bar and a gas inlet tube (N<sub>2</sub>), Pt(dba)<sub>2</sub> (2.43 g, 3.66 mmol) was added as a solution in THF (60 ml) during ten minutes time. The conversion was monitored by <sup>31</sup>P{<sup>1</sup>H} NMR spectroscopy, because the colour change on formation of product was not very obvious. After about seven days, the biggest part of the solvent was removed under vacuum. The complex was obtained by precipitation with n-hexane and by washing with cold ether (243 K). The washing were discarded and the remaining solid dried under reduced pressure to yield the product as an green-yellow powder.

Yield 1.15 g (38.1 %)

**Table 8.1**

*NMR data for the two conformers of [Pt(d<sup>4</sup>bpx)(dba)], 1, at 193 K in THF*

	$\delta P_1$ (ppm)	$\delta P_2$ (ppm)	$\delta Pt$ (ppm)	$^2J(P_1-P_2)$ (Hz)	$^1J(Pt-P_1)$ (Hz)	$^1J(Pt-P_2)$ (Hz)
conf. A	43.9	43.4	737.6	25	3808	3257
conf. B	48.2	39.8	726.7	23	3805	3270

### 8.3. Experimental for Chapter Three

#### 8.3.1 Synthesis of $[\text{Pt}(\text{d}^t\text{bpx})(\text{dbaH})][\text{RSO}_3]$ , **2**

To a solution of  $\text{Pt}(\text{d}^t\text{bpx})(\text{dba})$  (90.5 mg, 0.110 mmol) in MeOH (2 ml) the acid HX ( $\text{X} = \text{MeSO}_3^-$ ,  $\text{CF}_3\text{SO}_3^-$ ) (5 eq.) was added with a micropipette. The colour of the solution changed from yellow to deep-red, resulting in a completely different  $^{31}\text{P}\{^1\text{H}\}$  NMR spectrum. It was very important to avoid the presence of oxygen in order to prevent the oxidation of the protonated product.

**Table 8.2**

*NMR data for the two conformers of  $[\text{Pt}(\text{d}^t\text{bpx})(\text{dbaH})]^+$ , **2**  
at 193 K in MeOH*

	$\delta\text{P}_1(\text{ppm})$	$\delta\text{P}_2(\text{ppm})$	$^1J(\text{P}_1\text{-Pt})(\text{Hz})$	$^1J(\text{P}_2\text{-Pt})(\text{Hz})$
<b>conformer A</b>	53.0	40.8	4733	2965
<b>conformer B</b>	57.7	35.5	4700	2994

#### 8.3.2 Synthesis of $[\text{Pt}(\text{d}^t\text{bpx})\text{H}(\text{MeOH})][\text{CF}_3\text{SO}_3]$ , **3a**

Two different synthesis were carried out:

- Oxygen was bubbled for 30 min through a solution of  $[\text{Pt}(\text{d}^t\text{bpx})(\text{dbaH})][\text{CF}_3\text{SO}_3]$  (85.7 mg, 0.104 mmol), **2a**, in MeOH (2 ml).

Additional MeOH was periodically added in order to replace the evaporated solvent. The product formation was monitored by NMR spectroscopy.

- $[\text{Pt}(\text{d}^i\text{bpx})\text{H}(\text{MeOH})]^+$ , **3a**, was prepared directly by mixing  $\text{Pt}(\text{d}^i\text{bpx})(\text{dba})$ , **1**, (85.7 mg, 0.104 mmol) and BQ (22.8 mg, 0.210 mmol) as solids following by degassing in vacuum. This solid mixture was partially dissolved in MeOH (2 ml) under a nitrogen atmosphere, followed by addition of  $\text{CF}_3\text{SO}_3\text{H}$  (46.0  $\mu\text{l}$ , 0.520 mmol). After a few minutes the product was formed, as revealed by NMR spectroscopy.

**Table 8.3**

*NMR data for  $[\text{Pt}(\text{d}^i\text{bpx})\text{H}(\text{MeOH})][\text{CF}_3\text{SO}_3]$ , **3a**, in MeOH*

	@ 293 K	@ 193 K
$\delta\text{P}_1$ (ppm)	46.2	45.3
$\delta\text{P}_2$ (ppm)	34.6	32.6
$\delta\text{H}$ (ppm)	-7.3	-
$^2J(\text{P}_1\text{-P}_2)$ (Hz)	6.1	6.1
$^1J(\text{P}_1\text{-Pt})$ (Hz)	4312	4255
$^1J(\text{P}_2\text{-Pt})$ (Hz)	2095	2063
$^2J(\text{P}_1\text{-H})_{cis}$ (Hz)	17.9	-
$^2J(\text{P}_2\text{-H})_{trans}$ (Hz)	176	175
$^1J(\text{Pt-H})$ (Hz)	805	-

### 8.3.3 Synthesis of $[\text{Pt}(\text{d}^{\text{t}}\text{bpx})(\eta^2\text{-CH}_3\text{SO}_3)]^+[\text{CH}_3\text{SO}_3]^-$ , **5b**

The solution of  $[\text{Pt}(\text{d}^{\text{t}}\text{bpx})(\eta^2\text{-CH}_3\text{SO}_3)]^+$ , **5b**, in MeOH was prepared by bubbling oxygen for 30 min. through a solution of  $[\text{Pt}(\text{d}^{\text{t}}\text{bpx})(\text{dbaH})][\text{CH}_3\text{SO}_3]$ , **2b**, (85.7 mg, 0.104 mmol) in MeOH, together with periodic addition of solvent in order to replace the solvent which had evaporated. The solution changed from deep red to orange-yellow and the product formation was monitored by NMR spectroscopy.

The same complex **5b** was formed directly by mixing  $[\text{Pt}(\text{d}^{\text{t}}\text{bpx})(\text{dba})]$ , **1**, (85.7 mg, 0.104 mmol) and BQ (22.8 mg, 0.210 mmol) as solids following by degassing in vacuum. This solid mixture was partially dissolved in MeOH (2 ml) under a nitrogen atmosphere, followed by addition of  $\text{CH}_3\text{SO}_3\text{H}$  (33.8  $\mu\text{l}$ , 0.520 mmol). After a few minutes the product was formed, as revealed by NMR spectroscopy.

**Table 8.4**

*NMR data of  $[\text{Pt}(\text{d}^{\text{t}}\text{bpx})(\eta^2\text{-CH}_3\text{SO}_3)]^+[\text{CH}_3\text{SO}_3]^-$ , **5b**, at 293 K and 193 K in MeOH*

	$\delta\text{P}$ (ppm)	$^1\text{J}(\text{P-Pt})$ (Hz)
@ 293 K	28.9	3924
conf. A @ 193 K	27.6	3932
conf. B @ 193 K	27.0	3952

### 8.3.4 Synthesis of $[\text{Pt}(\text{d}^1\text{bpx})\text{H}(\text{solv})][\text{CH}_3\text{SO}_3]$ , **3b**

$[\text{Pt}(\text{d}^1\text{bpx})\text{H}(\text{MeOH})]^+$ , **3b**, was prepared directly by mixing  $[\text{Pt}(\text{d}^1\text{bpx})(\text{dba})]$  **1** (85.7 mg, 0.104 mmol) and BQ (22.8 mg, 0.210 mmol) as solids following by degassing in vacuum. This solid mixture was partially dissolved in MeOH (2 ml) under a nitrogen atmosphere, followed by addition of  $\text{CH}_3\text{SO}_3\text{H}$  (46.01  $\mu\text{l}$ , 0.520 mmol) and 0.2 ml of  $\text{H}_2\text{O}$ . After a few minutes the product was formed. (See Table 8.3)

### 8.3.5 Synthesis of $[\text{Pt}(\text{d}^1\text{bpx})(\text{H}_2\text{O})_2][\text{CH}_3\text{SO}_3]_2$ , **4b**

The solution of  $[\text{Pt}(\text{d}^1\text{bpx})(\text{H}_2\text{O})_2][\text{CH}_3\text{SO}_3]_2$ , **4b**, was prepared drying in vacuum the solution of  $[\text{Pt}(\text{d}^1\text{bpx})\text{H}(\text{MeOH})][\text{CH}_3\text{SO}_3]$ , **3b**, (see Section 8.3.4) and dissolving it in THF.

$^{31}\text{P}\{^1\text{H}\}$  NMR at 293 K in THF:  $\delta = 15.7$  ppm (s) and  $^1J(\text{Pt}-\text{P}) = 3827$  Hz

## 8.4. Experimental for Chapter Four

### 8.4.1 Synthesis of $[\text{Pt}(\text{d}^1\text{bpx})(\eta^2\text{-C}_2\text{H}_4)]$ , **7<sup>A</sup>**

To a stirred solution of the diphosphine  $\text{d}^1\text{bpx}$  (2.17 g, 5.49 mmol) in ethene saturated hexane (30 ml) at 273 K was added an equimolar amount of  $[\text{Pt}(\text{cod})_2]$  over a period of 10 minutes. After 30 minutes the solvent was removed in vacuum and the complex was checked by NMR spectroscopy.

$^{31}\text{P}\{^1\text{H}\}$  NMR at 293 K in  $\text{CH}_2\text{Cl}_2$ :  $\delta = 49.7$  ppm (s) and  $^1J(\text{Pt-P}) = 3497$  Hz

#### 8.4.2 Synthesis of $[\text{Pt}(\text{d}^4\text{bpx})(\text{CH}_2\text{CH}_3)]^+$ , **6a**

Different syntheses are possible

- Ethene was bubbled for 30 minutes through a solution of  $[\text{Pt}(\text{d}^4\text{bpx})\text{H}(\text{MeOH})]^+$ , **2a**, (0.104 mmol) in MeOH (2 ml), prepared as described in Section 8.3.2. The product was detected *via* NMR spectroscopy.
- In a 10 mm NMR tube,  $[\text{Pt}(\text{d}^4\text{bpx})(\text{dba})]$ , **1**, (85.7 mg, 0.104 mmol) and BQ (22.8 mg, 0.210 mmol) were mixed as solids under a  $\text{C}_2\text{H}_4$  atmosphere (1 bar). Then, MeOH (2 ml) and  $\text{CF}_3\text{SO}_3\text{H}$  (5 eq.) were added and the new complex **6a** was detected in the NMR spectrum.
- The solution of  $[\text{Pt}(\text{d}^4\text{bpx})(\eta^2\text{-C}_2\text{H}_4)]$ , **7**, (69.3 mg, 0.112 mmol) in diethyl ether (2 ml) was treated with one equivalent of  $\text{CF}_3\text{SO}_3\text{H}$  (9.9  $\mu\text{l}$ ) at 273 K resulting in the immediate precipitation of a white solid. The supernatant liquid was decanted and the precipitate was dried in vacuum. The complex was checked by NMR spectroscopy.

**Table 8.5**

$^{31}\text{P}$  NMR data of  $[\text{Pt}(\text{d}^4\text{bpx})(\text{CH}_2\text{CH}_3)]^+$ , **6**, at 193 and 293 K in MeOH

	$\delta\text{P}_1$ (ppm)	$\delta\text{P}_2$ (ppm)	$^1J(\text{P}_1\text{-Pt})(\text{Hz})$	$^1J(\text{P}_2\text{-Pt})(\text{Hz})$
at 293 K	52.4	37.0	5108	2759
at 193 K	50.9	35.6	5114	2785

### 8.4.3 Synthesis of $[\text{Pt}(\overline{\text{d}^4\text{bpx}})(\text{CH}_2\text{CH}_3)][\text{CH}_3\text{SO}_3]$ , **6b**

Ethene was bubbled for 30 minutes through a solution of  $[\text{Pt}(\overline{\text{d}^4\text{bpx}})\text{H}(\text{MeOH})][\text{CH}_3\text{SO}_3]$ , **2b**, (0.104 mmol) in MeOH (2 ml), prepared as described in Section 8.3.4. The product was detected *via* NMR spectroscopy. (See Table 8.5)

### 8.4.4 Characterisation of $[\text{Pt}(\overline{\text{d}^4\text{bpx}})(\text{CH}_2\text{CH}_3)][\text{CF}_3\text{SO}_3]$ , **6a**, *via* $^{13}\text{CH}_2=^{13}\text{CH}_2$

The complex **6a** has been formed as described in Section 8.4.2, third synthesis. After having controlled the purity of the sample *via* NMR spectroscopy, the solution was transferred to 10 mm NMR tube equipped with connection for high vacuum line. The tube was then frozen in liquid nitrogen and evacuated on a high vacuum line equipped with a mercury diffusion pump. The liquid nitrogen bath was, then, removed and the tube put immediately in a dry ice/acetone bath, in order to avoid the condensation of ethene. To this solution, two equivalents of  $^{13}\text{CH}_2=^{13}\text{CH}_2$  were added through the high vacuum line, then the tube was put again in the liquid nitrogen bath and sealed. The exchange between  $\text{C}_2\text{H}_4$  and  $^{13}\text{C}_2\text{H}_4$  reached equilibrium after 30 minutes at room temperature. This sample was used for all  $^{31}\text{P}$  and  $^{13}\text{C}$  measurements at low temperature.

## 8.5. Experimental for Chapter Five

### 8.5.1 Synthesis of $[\text{Pt}(\text{d}^1\text{bpx})\text{H}(\text{CO})]^+$ , **8**

A solution of  $[\text{Pt}(\text{d}^1\text{bpx})\text{H}(\text{MeOH})]^+$ , **3**, (0.104 mmol) was prepared as described in Section 8.3.2 or 8.3.4. CO was, then, bubbled through the solution for 5 minutes. The immediate formation of the complex **8** was checked *via* NMR spectroscopy.

### 8.5.2 Characterisation of $[\text{Pt}(\text{d}^1\text{bpx})\text{H}(\text{CO})][\text{CF}_3\text{SO}_3]$ , **8a**, *via* $^{13}\text{C}$ O

The complex **8a** has been formed as described in Section 8.5.1. After having controlled the purity of the sample *via* NMR spectroscopy, the solution was transferred to 10 mm NMR tube (thick glass tube) equipped with connection for  $^{13}\text{C}$ O gas cylinder. To this solution, 2 bar of  $^{13}\text{C}$ O were added through the gas line. This sample was used for all  $^{31}\text{P}$  and  $^{13}\text{C}$  measurements.

**Table 8.6**

*NMR data of  $[\text{Pt}(\text{d}^1\text{bpx})\text{H}(^{13}\text{C}\text{O})]^+$ , **8**, in MeOH at 293 K*

	$\delta$	$J(\text{P}_1-)$	$J(\text{P}_2-)$	$J(\text{Pt}-)$	$J(\underline{\text{C}}\text{O}-)$
<b>P<sub>1</sub></b>	42.2 ppm		19 Hz	2985 Hz	113 Hz
<b>P<sub>2</sub></b>	33.2 ppm	19 Hz		2011 Hz	8 Hz
<b><u>C</u>O</b>	179.3 ppm	113 Hz	8 Hz	1299 Hz	
<b>H</b>	-4.2 Hz	15 Hz	145 Hz	740 Hz	-

### 8.5.3 Synthesis of $[\text{Pt}(\text{d}^t\text{bpx})(\text{C}_2\text{H}_5)(\text{CO})][\text{CF}_3\text{SO}_3]$ , **9a**

A solution in  $\text{CH}_2\text{Cl}_2$  (2ml) of  $[\text{Pt}(\text{d}^t\text{bpx})(\text{CH}_2\text{CH}_3)]^+$ , **6a**, (0.112 mmol) was prepared as described in Section 8.4.2. The resulting solution was stored in dry ice/acetone bath and its purity checked *via* NMR spectroscopy. The solution was then transferred to a special 10 mm NMR tube equipped with a connection for high vacuum line. The tube was frozen in liquid nitrogen and evacuation on a high vacuum line equipped with a mercury diffusion pump. To this solution, one equivalent of CO was added through the high vacuum line and, then, the tube was sealed and stored at 193 K. The experiment has been performed with either  $^{12}\text{CO}$  and  $^{13}\text{CO}$ .

It was possible to obtain a  $^{13}\text{C}$ -double enriched complex  $[\text{Pt}(\text{d}^t\text{bpx})(\text{C}_2\text{H}_5)(^{13}\text{CO})]$ , **9a**, (Et = 50%  $^{13}\text{C}$ ) operating as follows. A solution of  $[\text{Pt}(\text{d}^t\text{bpx})(\text{CH}_2\text{CH}_3)]^+$ , **6a**, (Et = 50%  $^{13}\text{C}$ ) was prepared as described in Section 8.4.4. To this solution one equivalent of  $^{13}\text{CO}$  was added following the procedure described above.

**Table 8.7**

*NMR data for  $[\text{Pt}(\text{d}^t\text{bpx})(\text{C}_2\text{H}_5)(^{13}\text{CO})]^+$ , **9a**, (Et = 50%  $^{13}\text{C}$ )  
in  $\text{CH}_2\text{Cl}_2$  at 193 K*

	$\delta$	$J(\text{P}_1-)$	$J(\text{P}_2-)$	$J(\text{Pt}-)$	$J(\underline{\text{C}}\text{O}-)$	$J(\text{C}_\alpha-)$	$J(\text{H}-)$
<b>P<sub>1</sub></b>	29.4 ppm		24 Hz	1531 Hz	24 Hz	54 Hz	
<b>P<sub>2</sub></b>	16.4 ppm	24 Hz		3259 Hz	10 Hz	-	
<b><u>C</u>O</b>	179.8 ppm	10 Hz	126 Hz	1416 Hz			
<b>C<sub>α</sub></b>	4 ppm	54 Hz	-		-	-	130 Hz
<b>C<sub>β</sub></b>	18.3 ppm	-	-		-		126 Hz

### 8.5.4 Synthesis of $[\text{Pt}(\text{d}^1\text{bpx})(\text{C}(\text{O})\text{C}_2\text{H}_5)(\text{CO})][\text{CF}_3\text{SO}_3]$ , **10a**

The complex  $[\text{Pt}(\text{d}^1\text{bpx})(\text{C}(\text{O})\text{C}_2\text{H}_5)(\text{CO})][\text{CF}_3\text{SO}_3]$ , **10a**, was formed in  $\text{CH}_2\text{Cl}_2$  (2 ml) on warming the solution of  $[\text{Pt}(\text{d}^1\text{bpx})(\text{C}_2\text{H}_5)(\text{CO})][\text{CF}_3\text{SO}_3]$ , **9a**, (0.112 mmol), to 293 K under excess of CO.

In a different synthesis,  $[\text{Pt}(\text{d}^1\text{bpx})(\text{CH}_2\text{CH}_3)]^+$ , **6a**, was formed as described in Section 8.4.2. After having controlled the purity of the sample in  $\text{CH}_2\text{Cl}_2$  via NMR spectroscopy, the solution was transferred to 10 mm NMR tube (thick glass tube) equipped with connection for  $^{13}\text{C}$ O gas cylinder. To this solution in  $\text{CH}_2\text{Cl}_2$ , 2 bar of CO were added through the gas line at room temperature. The last experiment has been performed with either  $^{12}\text{C}$ O and  $^{13}\text{C}$ O.

**Table 8.8**

*NMR data for  $[\text{Pt}(\text{d}^1\text{bpx})(^{13}\text{C}(\text{O})\text{C}_2\text{H}_5)(^{13}\text{CO})]^+$ , **10a**, in  $\text{CH}_2\text{Cl}_2$  at 293 K*

	$\delta$	$J(\text{P}_1-)$	$J(\text{P}_2-)$	$J(\text{Pt}-)$	$J(\underline{\text{C}}\text{O}-)$
<b>P<sub>1</sub></b>	23.0 ppm	-			
<b>P<sub>2</sub></b>	23.1 ppm	26 Hz	-		
<b>Pt</b>	-	3616 Hz	<i>1397 Hz</i>	-	
<b><u>C</u>O</b>	173.2 ppm	93 Hz	-	1487 Hz	
<b><u>C</u>(O)</b>	223.9 ppm	-	69 Hz	514 Hz	4 Hz

The numbers in *italics* have been adjusted by the computer iteration.

### 8.5.5 Synthesis of $[\text{Pt}(\text{d}^4\text{bpx})(\text{C}(\text{O})\text{C}_2\text{H}_5)(\text{PPh}_3)][\text{CF}_3\text{SO}_3]$ , **11a**

To a solution of  $[\text{Pt}(\text{d}^4\text{bpx})(\text{C}(\text{O})\text{C}_2\text{H}_5)(\text{CO})]^+$ , **10a**, (0.112 mmol) in  $\text{CH}_2\text{Cl}_2$  (2 ml) one equivalent of triphenylphosphine was added at 293 K. The formation of the complex **11a** was checked by  $^{13}\text{C}\{^1\text{H}\}$  NMR spectroscopy.

$^{13}\text{C}\{^1\text{H}\}$  NMR at 293 K in  $\text{CH}_2\text{Cl}_2$ :  $\delta = 230.4$  ppm (d),  $^1J(\text{C}(\text{O})-\text{Pt}) = 632$  Hz  
 $^2J(\text{C}(\text{O})-\text{P}) = 79$  Hz

### 8.5.6 Synthesis of $[\text{Pt}(\text{d}^4\text{bpx})\text{H}(\text{PPh}_3)][\text{CF}_3\text{SO}_3]$ , **12a**

Solid  $\text{PPh}_3$  (0.030 g, 0.110 mmol) was added to a solution of  $[\text{Pt}(\text{d}^4\text{bpx})\text{H}(\text{MeOH})]^+$ , **3a**, (0.110 mmol) in MeOH (2 ml), prepared as described in Section 8.3.2. All the solid dissolved but the solution did not change colour. The formation of the complex **12a** was detected through  $^{31}\text{P}$  and  $^1\text{H}$  NMR measurements.

**Table 8.9**

*NMR data for  $[\text{Pt}(\text{d}^4\text{bpx})\text{H}(\text{PPh}_3)]^+$ , **12a**, in  $\text{CH}_2\text{Cl}_2$  at 293 K*

	$\delta$	$J(\text{P}_1-)$	$J(\text{P}_2-)$	$J(\text{PPh}_3-)$	$J(\text{Pt}-)$
<b>P<sub>1</sub></b>	47.2 ppm	-			2847 Hz
<b>P<sub>2</sub></b>	35.2 ppm	18 Hz	-		2356 Hz
<b>PPh<sub>3</sub></b>	9.2 ppm	334 Hz	22 Hz	-	2558 Hz
<b>H</b>	7.9 ppm	26 Hz	146 Hz	9 Hz	613 Hz

## 8.6. Experimental for Chapter Six

### 8.6.1 Characterisation of $[\text{Pt}(\text{d}^t\text{bpx})\text{H}(\text{MeOH})][\text{CF}_3\text{SO}_3]$ , **3**, at high temperature

A solution of  $[\text{Pt}(\text{d}^t\text{bpx})\text{H}(\text{MeOH})][\text{CF}_3\text{SO}_3]$ , **3a**, (112 mmol) in MeOH was prepared as described in Section 8.3.2 in a Schlenk tube under nitrogen pressure (1 atm). Then, this solution was transferred *via* a syringe to a 10 mm NMR sapphire tube. The tube was pressurised with 7 bar of nitrogen and the  $^{31}\text{P}\{^1\text{H}\}$  NMR spectra were recorded in the temperature range 293-353 K. The same procedure was used to study the reactivity of  $[\text{Pt}(\text{d}^t\text{bpx})\text{H}(\text{MeOH})][\text{CH}_3\text{SO}_3]$ , **3b**, under a pressure of gas mixture  $\text{C}_2\text{H}_4/\text{CO}$  with ratio 1/1 and 9/1.

### 8.6.2 Characterisation of $[\text{Pt}(\text{d}^t\text{bpx})(\text{CH}_2\text{CH}_3)]^+$ , **6**, at high temperature

A solution of  $[\text{Pt}(\text{d}^t\text{bpx})(\text{CH}_2\text{CH}_3)]^+$ , **6**, (112 mmol) in MeOH was prepared as described in Section 8.4.2 and 8.4.3 in a Schlenk tube under ethene pressure (1 atm). Then, this solution was transferred *via* a syringe to a 10 mm NMR sapphire tube. The tube was pressurised with 10 bar of ethene and the  $^{31}\text{P}\{^1\text{H}\}$  NMR spectra were recorded in the temperature range 293-353 K.

### 8.6.3 Characterisation of $[\text{Pt}(\text{d}^t\text{bpx})\text{H}(^{13}\text{CO})]^+$ , **8**, at high temperature

A solution of  $[\text{Pt}(\text{d}^t\text{bpx})\text{H}(\text{MeOH})]^+$ , **3**, (112 mmol) in MeOH was prepared as described in Section 8.3.2 and 8.3.4 in a Schlenk tube under nitrogen pressure (1

atm). Then, this solution was transferred *via* a syringe to a 10 mm NMR sapphire tube. The tube was pressurised with 7 bar of  $^{13}\text{CO}$  and the  $^{31}\text{P}\{^1\text{H}\}$  and  $^{13}\text{C}\{^1\text{H}\}$  NMR spectra were recorded in the temperature range 293-353 K.

#### 8.6.4 Characterisation of $[\text{Pt}(\text{d}^1\text{bpx})(\eta^2\text{-CH}_3\text{SO}_3)]^+$ , **5b**, at high temperature

A solution of  $[\text{Pt}(\text{d}^1\text{bpx})(\eta^2\text{-CH}_3\text{SO}_3)]^+$ , **5b**, (112 mmol) in MeOH was prepared as described in Section 8.3.3 in a Schlenk tube under nitrogen pressure (1 atm). Then, this solution was transferred *via* a syringe to a 10 mm NMR sapphire tube. The tube was pressurised with 10 bar of nitrogen and the  $^{31}\text{P}\{^1\text{H}\}$  NMR spectra were recorded in the temperature range 293-353 K. The same procedure was used to study the reactivity of  $[\text{Pt}(\text{d}^1\text{bpx})(\eta^2\text{-CH}_3\text{SO}_3)]^+$ , **5b**, under a pressure of  $\text{C}_2\text{H}_4$ , CO and of gas mixture  $\text{C}_2\text{H}_4/\text{CO}$  with ratio 1/1 and 9/1.

## 8.7. References

- (1) A. Bax; R.H. Griffey; B.L. Hawkins *J. Magn. Reson.*, **1983**, 55, 301.
- (2) G.M. Scheldrick *SHELX-97, Programs for Crystal Structure Solution and Refinement*, **1997**, University of Gottingen, Germany.
- (3) L.E. Crascall and J.L. Spencer *Inorg. Synth.*, **1990**, 28, 126.
- (4) N. Carr; L. Mole; A. Guy Orpen; J. L. Spencer *J. Chem. Soc., Dalton Trans.*, **1992**, 2653.
- (5) J. Moulton and B.L. Shaw *J. Chem. Soc., Chem. Comm.*, **1976**, 365.

## Acknowledgements

First, I would like to thank my supervisors in Liverpool, Prof. Brian T. Heaton, Dr. Jon A. Iggo and Dr Robin Whyman, and at Lucite International, Dr. Graham R. Eastham for their support and help.

A lot of thanks to Anne Flaherty for solving my bureaucratic problems and the nice chats, and all the technical staff of the Chemistry Department.

All the people that worked with me in the lab 227, Dr. C. Jacob, Kelly, Emma, Alex, Michael, Andy and Nieves. In particular I would like to thank Zac (Dr. Stefano Zacchini) for all I have learned from him and to be a special friend.

My favourite flat mates, Katy, Eva and Lavinia for making me not feel alone.

All my friends in the Chemistry Department, Mehdi, William, Sarah, Annie, Charles, Marc and Noelia.

Martina, I will come to visit you in America.

Maurizio, how could I survive in Liverpool without your fantastic dinners.

A Thousand thanks to Michela and Paul, for organising so well my private life.

Vorrei ringraziare la mia famiglia, mamma, papa', Paolo, Anna, Marcello e Benedetta, per non avermi mai fatto sentire la mancanza di casa.

Tutti i miei amici che mi sono rimasti tali considerando la lontananza, Milena, Marsia, Simona, Paolo, Daniela, Antonio, Vanessa B., Michele, Giorgia, Vanessa G, Claudia.

My last thanks go to a special person for me, Ian thank you for your support and love.